Functionalized Photochromic Scaffolds for Biological Applications

Dissertation

zur Erlangung des Doktorgrades der Naturwissenschaften

(Dr. rer. nat.)

der Fakultät für Chemie und Pharmazie

der Universität Regensburg

vorgelegt von

Daniel Wutz

aus Grafenkirchen

2017

Der experimentelle Teil der vorliegenden Arbeit wurde in der Zeit von November 2013 bis März 2017 unter der Betreuung von Prof. Dr. Burkhard König am Institut für Organische Chemie der Universität Regensburg durchgeführt. Zusätzlicher Betreuer war von Juni 2016 bis August 2016 Prof. Dr. Pau Gorostiza am Institute of Bioengineering of Catalonia, Barcelona (Spanien).

Diese Arbeit wurde angeleitet von: Prof. Dr. Burkhard König

Promotionsgesuch eingereicht am: 25.04.2017

Promotionskolloquium am: 02.06.2017

Prüfungsausschuss

     Vorsitzender: Prof. Dr. Olga García Mancheño

     1. Gutachter: Prof. Dr. Burkhard König

     2. Gutachter: PD Dr. Sabine Amslinger

     3. Prüfer: Prof. Dr. Frank-Michael Matysik

Universität Regensburg

To Claudia

&

my family

Table of Contents

1 Functionalization of Photochromic Dithienylmaleimides

1.1 Introduction

Photochromism has attracted great attention in materials science[1] and as a tool in molecular biology.[2] A variety of applications are found in molecular optoelectronics[3] and optical data storage.[4-6] In the field of life sciences, molecular switches have been used to control enzyme activity,[7-10] Watson-Crick base pairing,[11-13] the regulation of neuronal activity by photochromic ligands for ion channels and receptors,[14-20] antibiotic effects[21-22] and even the agility of a living organism[23] by light. This broad applicability is one of the reasons why photopharmacology has evolved into a vibrant field of research.[24] Various photochromic molecules, like azobenzenes,[25] spiropyrans[26], spirooxazines,[26] fulgides[27] and diarylethenes[28-29] have been developed. All these photoswitches can be reversible toggled between two isomers using light. The well investigated dithienylethenes (DTEs), including dithienylmaleimides, are characterized by a nearly quantitative photochemical conversion between the photoisomers, which are often thermally stable. Irradiation with light of a specific wavelength switches the DTEs between their open and closed photoisomer, which differ in conformational flexibility and electronic conjugation (Figure 1). Many DTEs show high fatigue resistance.[28]
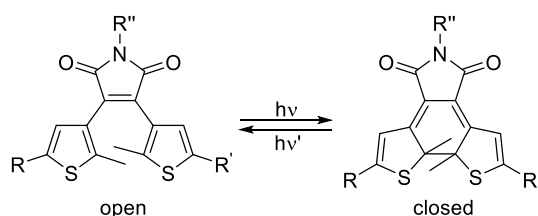
Figure 1. Reversible photochemical isomerization of a dithienylmaleimide between the open and closed photoisomer by irradiation with light of different wavelength.

Despite their outstanding photophysical properties the synthesis of DTEs, in particular of non-symmetric derivatives, is laborious.[13, 30] Different synthetic routes for the preparation of dithienylmaleimides were established. Starting from 3,4-dibromomaleimides and 3,4-diiodomaleimides, respectively, both thiophene moieties can be attached by palladium catalyzed Suzuki coupling.[31-33] However, only nitrogen protected maleimides can be used and the synthesis of non-symmetric compounds is challenging. Another route uses the reaction of a dithienylmaleic anhydride with amines to the corresponding maleimide.[34-36] The synthesis of diarylmaleimides by intramolecular Perkin condensation of two independently prepared precursors gives selective access to

non-symmetric diarylmaleimides.[10, 37-38] Compared to diarylperfluorocyclopentenes and diarylcyclopentenes, diarylmaleimides are more hydrophilic and better water soluble, which is valuable for applications in biology and pharmacy. The absorption maxima of diarylmaleimides are shifted to higher wavelengths and thus the photoisomerization can be induced by light with lower energy reducing potential cell damage.[28] Moreover, the biocompatibility of diarylmaleimides is known from bisindolylmaleimides, for instance arcyriarubins and arcyriaflavins with antibiotic activities, several other potent protein kinase and sirtuin inhibitors.[10, 39-43] However, a better synthetic access to functionalized photochromic dithienylmaleimides is desirable in order to extend their applications. Herein, we discuss the synthesis of functionalized dithienylmaleimides substituted on each thiophene moiety and the maleimide nitrogen atom.

1.2 Results and Discussion

1.2.1 Synthesis

Functionalization of the maleimide nitrogen atom

The transformation of diarylmaleic anhydrides into their corresponding diarylmaleimides provides an easy access to compounds with a functionalized maleimide nitrogen atom.[28] Complex functionalities or protecting groups can be introduced at the maleimide nitrogen by reaction with amines or hydrazines. We used the adapted synthetic approach of Scandola *et al.*[36] for the synthesis of anhydride **4** as precursor (Scheme 1).
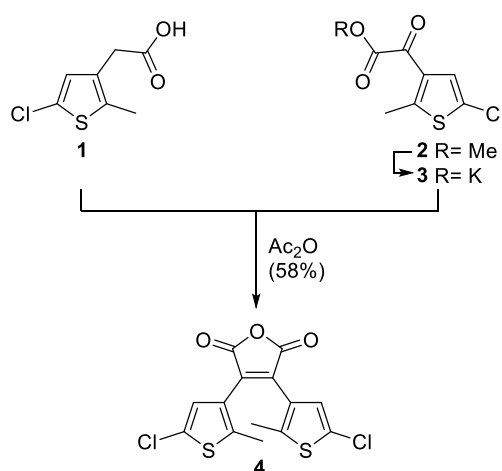
Scheme 1. Synthesis of dithienylmaleic anhydride **4**.

Methyl ester **2** was converted to its potassium salt **3** and condensed in a Perkin reaction with carboxylic acid **1** yielding the photochromic maleic anhydride **4**. The anhydride moiety allows the subsequent functionalization with hydrazines or amines (Scheme 2).
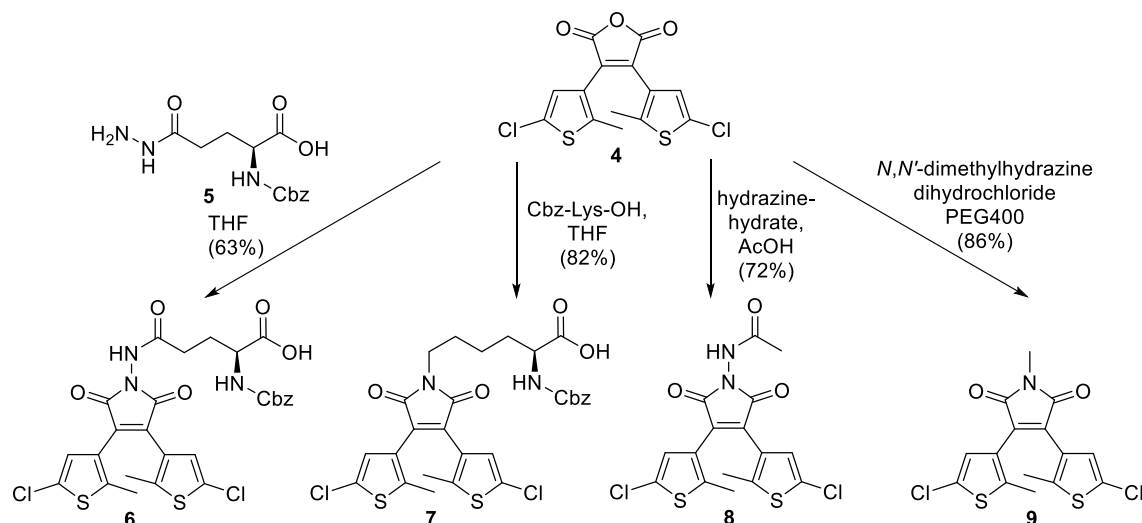
Scheme 2. Synthesis of the functionalized photochromic dithienylmaleimides **6-9** starting from maleic anhydride **4**.

Therefore, maleic anhydride **4** was treated with α-Cbz protected L-glutamic acid γ-hydrazide[44] (**5**) and α-Cbz protected L-lysine to give amino acids **6** and **7** with a photochromic dithienylmaleimide on each sidechain. Photochromic tripeptides forming hydrogels with different aggregation modes mainly depending on the switch moiety were recently reported.[45] The reaction of hydrazine hydrate in acetic acid as solvent and 1,2-dimethylhydrazine dihydrochloride, respectively, with maleic anhydride **4** afforded the maleimide nitrogen protected dithienylmaleimides **8** and **9** in good yields (Scheme 2). Remarkably, the formation of any maleic hydrazide or other tautomers was not observed. The protected maleimides **8** and **9** could be used for further functionalizations on the thiophene moieties by palladium-catalyzed cross coupling reactions or other reactions using the reactivity of the heteroaryl chlorides.

Functionalization as photochromic amino acid

Recently, DTE-based non-natural amino acids were synthesized and successfully introduced into small peptides.[46] However, their water-solubility is limited due to the diarylperfluorocyclopentene core and therefore, we developed a more polar dithienylmaleimide amino acid. Compounds **13a** and **13b** were prepared by a Perkin

condensation[10, 37-38] of the thiophene precursors **10** and **11** bearing a protected primary amino or carboxyl group, respectively (Scheme 3).
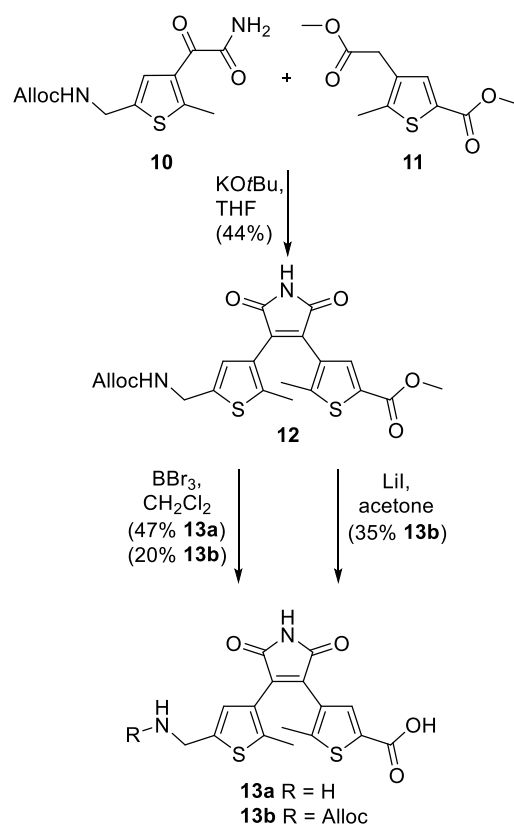
Scheme 3. Perkin condensation of thiophenes **10** and **11** yielding dithienylmaleimide **12** and after deprotection **13a** and **13b**.

The Alloc group was chosen as a suitable protection for the amine as it is stable during the synthesis of compound **12**. Diester thiophene **11** provides in 4-position the carboxylic ester giving the maleimide core in the Perkin condensation. The ester in 2-position will serve as carboxylate of the amino acid. Both carboxylic acids were protected as methyl ester. Alloc group and methyl ester of **12** were cleaved simultaneously with boron tribromide giving amino acid **13a** in 47% yield, accompanied by 20% of the Alloc amino acid **13b** as byproduct. A selective non-hydrolytic deprotection of the methyl ester of **12** is possible in low yield using lithium iodide in a polar aprotic solvent.[47-48] A large excess of lithium iodide and reflux were necessary to achieve conversion; several solvents were tested with best yields in acetone (see Supporting Information, Table S1). Standard basic hydrolytic conditions for the deprotection of the methyl ester afforded the deprotected maleic anhydride (see Supporting Information, Scheme S2). The synthesis of thiophene **10** is depicted in Scheme 4.
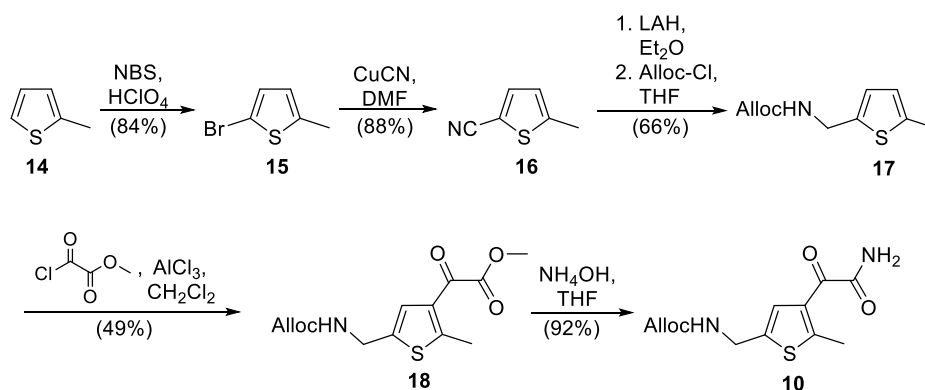
Scheme 4. Synthesis of thiophene **10**.

Bromination[49] of 2-methyl thiophene (**14**) and subsequent Rosenmund-von Braun reaction[50] giving nitrile **16** were performed according to literature procedures. The reduction of nitrile **16** with lithium aluminum hydride followed by immediate protection with allyl chloroformate afforded carbamate **17** in good yield. Using Fmoc chloride instead led to the respective Fmoc derivative in lower yields and caused the formation of side products in the subsequent Friedel-Crafts acylation. The yield of glyoxylester **18** in the Friedel-Crafts acylation depends critically on the sequence of the reagent addition. Best results were obtained by mixing **17** and methyl chlorooxoacetate before adding aluminum chloride in small portions. Quenching the reaction with saturated sodium hydrogen carbonate solution avoids the addition of hydrochloric acid to the allyl double bond. Aminolysis with aqueous ammonia converted the glyoxylester **18** in high yield into compound **10**. The overall yield for **10** after six steps is 22%.

Thiophene **11** was prepared by esterification[51] of methyl thiophene acid **19** in the presence of thionyl chloride followed by Friedel-Crafts acylation and finally a thallium trinitrate (TTN) mediated oxidative rearrangement[52] (Scheme 5). All intermediates were isolated in good to excellent yields with an overall yield of 68% for three steps. Initial moderate yields for the Friedel-Crafts acylation of around 40% significantly increased to 77% after rigorous removal of stabilizers from the solvent chloroform.
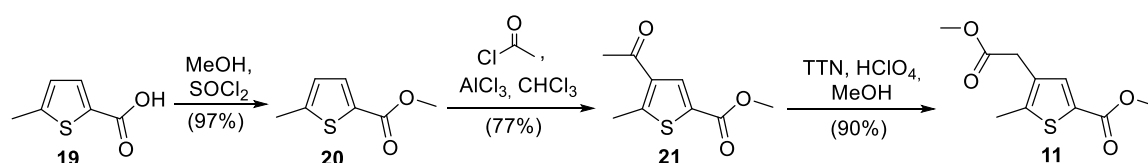
Scheme 5. Synthesis of thiophene **11**.

Functionalization by Suzuki coupling

Dithienylmaleimides are conveniently synthesized by the Perkin-type condensation. The reaction of two precursors yields the maleimide core without the need for protection of the maleimide nitrogen. Scheme 6 shows the intermolecular Perkin condensation of the two chlorosubstituted precursors **22** and **23**.
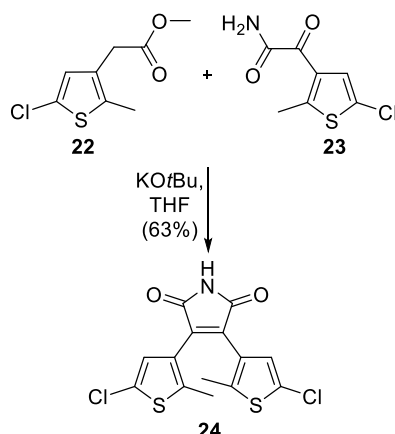
Scheme 6. Perkin condensation of **22** and **23** yielding dithienylmaleimide **24**.

Both precursors can be differently functionalized by Suzuki coupling before used in the Perkin condensation yielding non-symmetric dithienylmaleimides.

Precursor 1:

25 R^1= phenyl (52%)
26 R^1= 4-*t*Bu-phenyl (55%)
27 R^1= 3-biphenyl (72%)

Precursor 2:

29 R^2= phenyl (63%)
30 R^2= 4-*t*Bu-phenyl (48%)
31 R^2= 3-biphenyl (70%)

32 R^3= phenyl (80%)
33 R^3= 4-*t*Bu-phenyl (84%)
34 R^3= 3-biphenyl (94%)
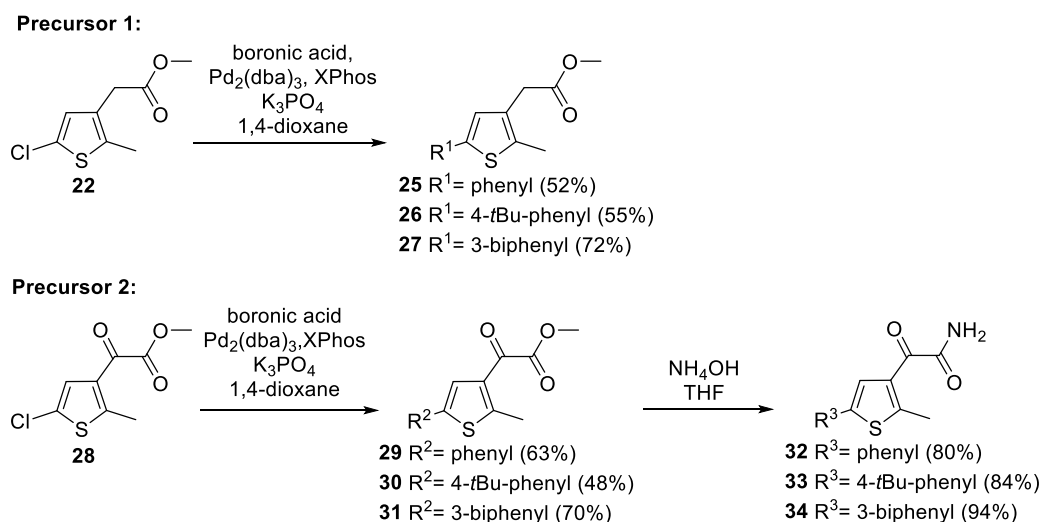
Scheme 7. Synthesis of functionalized precursors **25-27** and **32-34**.

Recently, we described the synthesis of symmetric diarylmaleimides, with thiophene moieties functionalized by palladium-catalysis prior to the condensation reaction.[10] Based on this strategy we prepared a small series of non-symmetric diarylmaleimides (Scheme 7). The Perkin condensation to the maleimide core was performed under basic

conditions combining the different thiophenes. Scheme 8 summarizes the synthesis of the non-symmetric photoswitches **35**-**37**.

26 R[1]= 4-*t*Bu-phenyl
27 R[1]= 3-biphenyl

23 R[2]= Cl
33 R[2]= 4-*t*Bu-phenyl

KO*t*Bu, THF

35 R[1]= 4-*t*Bu-phenyl, R[2]= Cl (28%)
36 R[1]= 3-biphenyl, R[2]= Cl (27%)
37 R[1]= 3-biphenyl, R[2]= 4-*t*Bu-phenyl (33%)
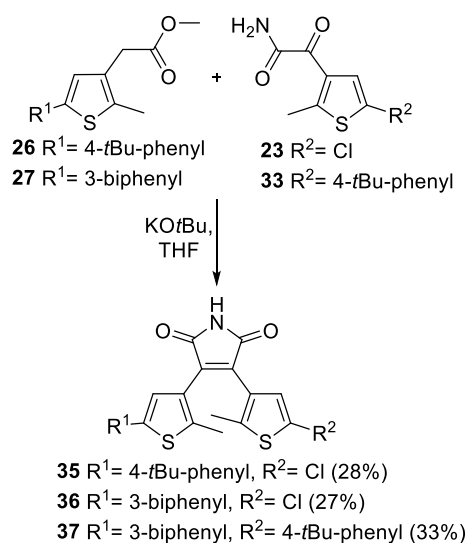
Scheme 8. Synthesis of non-symmetric substituted dithienylethenes **35**-**37** by Perkin condensation.

1.2.2 Photochromic Properties

The dithienylmaleimide core structure can be toggled reversibly between a ring-open and ring-closed photoisomer (Figure 1). The photochemical properties of photochromic compounds **4**, **6**-**9**, **12**, **13a**, **13b**, **24** and **35**-**37** were investigated by UV-Vis spectroscopy.
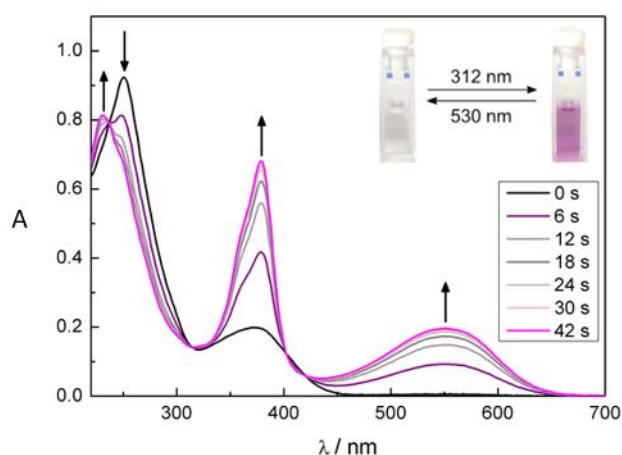
Figure 2. Changes of the UV-Vis absorption spectra of dithienylmaleimide amino acid **12** (50 µM in MeOH) upon light irradiation with 312 nm; arrows indicate the changes of the absorption maxima over 42 s irradiation in periods of 6 s (Herolab, 6 W); the cuvettes show the color of the solution before and after irradiation.

Despite of reports that diarylmaleimides are not able to undergo photoisomerization in polar solvents due to a twisted intramolecular charge transfer (TICT),[53-55] we could observe reversible photoisomerization of the dithienylmaleimides **6**-**9**, **12**, **13a**, **13b**, **24** and **35**-**37** in methanol or dimethyl sulfoxide, respectively. Figure 2 shows the changes of the UV-Vis spectra of compound **12** upon irradiation with light of 312 nm (Herolab, 6 W). Upon irradiating a methanol solution of the ring-open form of compound **12** with UV light (312 nm), the absorption band at 250 nm immediately decreases. Simultaneously, new absorption maxima at 232 nm, 378 nm and 550 nm arise (Figure 2) causing the color change of the sample from slightly yellow to purple. The isosbestic points indicate a clean conversion between two components. Compared to typical DTE-cyclopentenes the absorption maxima are red shifted. The photostationary state was reached after 42 s of irradiation (Herolab, 312 nm, 6 W) and the open form can be regained by irradiation with visible light (> 420 nm) for 5 min. The photoswitchable amino acid **12** is stable over at least seven closing/opening cycles (Figure 3).
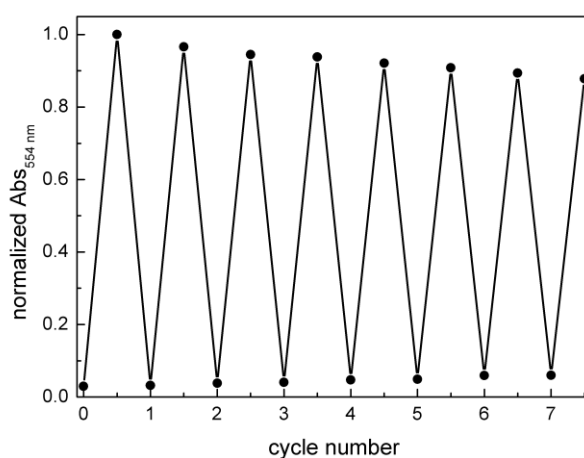
Figure 3. Cycle performance of the dithienylmaleimide amino acid **12** (50 µM in MeOH). Changes in absorption at 554 nm were measured during alternate irradiation with light of 312 nm (Herolab, 6 W) for 60 s and 530 nm (CREE-XP green, 700 mA) for 5 min.

The absorption maxima and their corresponding extinction coefficients for the open and closed form of all synthesized photochromic compounds are summarized in Table 1.

Table 1. UV-Vis spectroscopic data of the open and closed (PSS) form of the synthesized photochromic compounds.[a]

Entry	Comp.	Solvent	Conc. [μM]	λ_{max} open (ε)	λ_{max} closed (ε)
1	**4**	MeOH	100	242 (26.0), 298 (9.5)	359 (16.0), 523 (3.7)
2	**6**	DMSO	50	387 (4.6)	359 (17.4), 510 (3.2)
3	**7**	DMSO	50	381 (5.0)	355 (20.8), 500(4.1)
4	**8**	DMSO	50	386 (6.0)	359 (22.7), 508 (4.3)
5	**9**	DMSO	50	380 (3.3)	351 (12.9), 498 (2.7)
6	**12**	MeOH	50	250 (18.5)	232 (16.2), 378 (13.6), 550 (3.9)
7	**13a**	MeOH	50	252 (13.0)	231 (11.3), 375 (10.0), 537 (2.7)
8	**13b**	MeOH	50	250 (14.3)	232 (12.6), 378 (10.3), 549 (2.8)
9	**24**	MeOH	50	240 (20.2), 370 (4.5)	234 (20.6), 352 (13.8), 497 (2.5)
10	**35**	MeOH	100	264 (18.5), 292 (17.1)	369 (9.7), 543 (3.0)
11	**36**	MeOH	100	255 (28.8), 291[b] (14.3)	369 (10.1), 540 (3.7)
12	**37**	MeOH	100	262 (26.1), 297 (20.7)	391 (11.5), 586 (5.7)

[a] UV-Vis spectroscopic data are reported for solutions at 25 °C and reported in nm (λ_{max}) and 10^3 cm^{-1} M^{-1} (ε). The PSS were obtained by irradiation of solutions of the open isomer with light of 312 nm (Herolab, 6 W). [b] Shoulder.

Interestingly, the long wavelength absorption maximum of compound **13a** is blue shifted to 537 nm compared to photoswitches **12** and **13b**, which may indicate an interaction of the Alloc group with the dithienylmaleimide core. In contrast, the selective removal of the methyl ester has almost no influence on the photochromic properties. In comparison to bischloro dithienylmaleimide **24** the functionalized maleimides **35**-**37** show a bathochromic shift in their absorption maxima of the closed photoisomer. The enlarged π-system of the substituted thiophenes can explain this shift to higher wavelengths.

1.3 Conclusion

In summary, we have prepared several photochromic dithienylmaleimides. Maleimide nitrogen atom functionalized derivatives were obtained by the reaction of dithienylmaleic anhydride with different hydrazines and amines. Using a Perkin-type condensation non-symmetric dithienylmaleimides were synthesized including a photochromic amino acid and dithienylmaleimides with different aromatic substituents on each thiophene moiety. Reversible photoisomerization in dimethyl sulfoxide and methanol was observed for all synthesized photochromic compounds.

1.4 Experimental

1.4.1 General Information

Commercial reagents and starting materials were purchased from Acros Organics, Alpha-Aesar, Fluka, Sigma Aldrich or VWR and used without further purification. Solvents were used in p.a. quality and dried according to common procedures, if necessary. To purify the chloroform for Friedel-Crafts acylations, it was washed with sulfuric acid (1 M), dried over calcium chloride, filtered through silica, subsequently refluxed with phosphorous pentoxide (5-10 g L^{-1}) and distilled under nitrogen atmosphere. Compounds **1**[10], **2**[10], **5**[44], **15**[49], **16**[50], **20**[51], **22**[10], **25**[10], **28**[10], **29**[10] and **32**[10] were prepared according to previously reported procedures. Flash column chromatography was performed on a Biotage Isolera One automated flash purification system with UV/Vis detector using Sigma Aldrich MN silica gel 60 M (40-63 μm, 230-400 mesh) for normal phase or pre-packed Biotage SNAP cartridges (KP-C18-HS) for reversed phase chromatography. Reaction monitoring *via* TLC was performed on alumina plates coated with silica gel (Merck silica gel 60 F$_{254}$, 0.2 mm). Melting points were determined using a Stanford Research Systems OptiMelt MPA 100. NMR spectra were recorded on Bruker Avance 300 (^{1}H: 300 MHz, ^{13}C: 75 MHz), Bruker Avance 400 (^{1}H: 400 MHz, ^{13}C: 101 MHz) and Avance III 600 (^{1}H: 600 MHz, ^{13}C: 151 MHz) instrument. The spectra are referenced against the NMR-solvent, chemical shifts are reported in ppm and coupling constants *J* are given in Hz. Resonance multiplicity is abbreviated as: s (singlet), d (doublet), t (triplet), m (multiplet) and b (broad). Carbon NMR signals are reported with (+) for primary/tertiary, (−) for

secondary and (q) for quaternary carbons. The assignment resulted from DEPT, HSQC and HMBC experiments. Mass spectra were recorded on a Finnigan MAT95 (EI-MS), Agilent Q-TOF 6540 UHD (ESI-MS, APCI-MS), Finnigan MAT SSQ 710 A (EI-MS, CI-MS) or ThermoQuest Finnigan TSQ 7000 (ES-MS, APCI-MS) spectrometer. UV/Vis absorption spectroscopy was performed using a Varian Cary BIO 50 UV/Vis/NIR spectrometer. IR-spectra were recorded with a Specac Golden Gate Diamond Single Reflection ATR System in a Bio-Rad FT-IR-Spectrometer Excalibur FTS 3000 and peak positions are reported in wavenumbers (cm^{-1}). Standard hand-held lamps were used for visualizing TLC plates and to carry out the ring-closure reactions at 312 nm (Herolab, 312 nm, 6 W). The ring-opening reactions were performed with the light of a 200 W tungsten light bulb which was passed through a 420 nm cut-off filter to eliminate higher energy light or the light of a green LED (CREE-XP green, 530 nm, 700 mA). The power of the light is given based on the specifications supplied by the company when the lamps were purchased. A light detector was not used to measure the intensity during the irradiation experiments.

1.4.2 Synthesis and Characterization of Compounds

3,4-Bis(5-chloro-2-methylthiophen-3-yl)furan-2,5-dione (4)

To obtain the potassium salt **3**, the ester **2** was dissolved in EtOH (2.5 mL/mmol) and KOH (1.0 eq) was added. After stirring overnight, the solvent was removed and the crude product **3** was used without further purification. A mixture of the acid **1** (984 mg, 5.16 mmol), the potassium salt **3** (1.25 g, 5.16 mmol) and acetic anhydride (15 mL) was heated to 120 °C for 5 h. The reaction was cooled to room temperature and quenched by adding water (20 mL). The aqueous phase was extracted with EtOAc (3 x 15 mL). The combined organic phases were dried over $MgSO_4$, filtered and the solvent was removed under reduced pressure. The crude product was purified by automated flash column chromatography (PE/CH_2Cl_2: 30-60% CH_2Cl_2) to yield the maleic anhydride **4** (1.07 g, 58%) as gray solid; R_f: 0.45 (PE/CH_2Cl_2: 1/1); m.p.: 205 °C; ^{1}H-NMR (300 MHz, DMSO-d_6): δ = 1.94 (s, 6H, thiophene-CH_3), 7.03 (s, 2H, thiophene-H); ^{13}C-NMR (75 MHz, DMSO-d_6): δ = 14.1 (+), 125.2 (q), 125.3 (q), 127.2 (+), 134.5 (q), 141.4 (q), 164.5 (q); IR (neat) ν_{max}: 3108, 2922, 1843, 1766, 1629, 1539, 1460, 1252, 1047, 1177, 990, 919; HR-MS (ESI): calcd. for $C_{14}H_9Cl_2O_3S_2$ (M+H)$^+$ 358.9365; found 358.9362.

N^2-((Benzyloxy)carbonyl)-N^5-(3,4-bis(5-chloro-2-methylthiophen-3-yl)-2,5-dioxo-2,5-dihydro-1H-pyrrol-1-yl)-L-glutamine (6)

Maleic anhydride **4** (40 mg, 0.11 mmol) was added to a solution of acid hydrazide **5** (30 mg, 0.10 mmol) in THF (1 mL) in a crimp top vial. After heating to 85 °C for 16 h the reaction was quenched with 1 M aqueous HCl solution (1 mL) and water (1 mL). The aqueous phase was extracted with EtOAc (3 x 5 mL). The combined organic phases were dried over MgSO$_4$ and the solvent was removed under reduced pressure. Purification by automated reversed phase flash column chromatography (MeCN/H$_2$O with 0.05% TFA: 10-95% MeCN) yielded compound **6** (40 mg, 63%) as orange solid; R$_f$: 0.01 (EtOAc); m.p.: 103 °C; ^{1}H-NMR (300 MHz, DMSO-d_6): δ = 1.74 – 1.88 (m, 1H, CO-(CH_2)$_2$-CH), 1.92 (s, 6H, thiophene-CH_3), 2.00-2.10 (m, 1H, CO-(CH_2)$_2$-CH), 2.38-2.48 (m, 2H, CO-(CH_2)$_2$-CH), 4.03 (dt, J = 9.0, 4.8 Hz, 1H, CH$_2$-CH-NH), 5.05 (s, 2H, O-CH_2-Ph), 7.03 (s, 2H, thiophene-H), 7.31-7.40 (m, 5H, Ph-H), 7.68 (d, J = 8.0 Hz, 1H, CH-NH-CO), 10.63 (s, 1H, N-NH-CO), 12.70 (bs, 1H, COOH); ^{13}C-NMR (75 MHz, DMSO-d_6): δ = 14.2 (+), 26.1 (−), 29.1 (−), 53.1 (+), 65.4 (−), 125.0 (q), 125.8 (q), 127.6 (+), 127.6 (+), 127.7 (+), 128.3 (+), 131.2 (q), 136.8 (q), 140.6 (q), 156.1 (q), 166.9 (q), 170.8 (q), 173.4 (q); IR (neat) ν$_{max}$: 3250, 2924, 1789, 1727, 1522, 1462, 1434, 1215, 1175, 990; HR-MS (ESI): calcd. for C$_{27}$H$_{24}$Cl$_2$N$_3$O$_7$S$_2$ (M+H)$^+$ 636.0427; found 636.0428.

(S)-2-(((Benzyloxy)carbonyl)amino)-6-(3,4-bis(5-chloro-2-methylthiophen-3-yl)-2,5-dioxo-2,5-dihydro-1H-pyrrol-1-yl)hexanoic acid (7)

Triethylamine (131 μL, 0.95 mmol) was added to a suspension of maleic anhydride **4** (97 mg, 0.27 mmol) and Cbz-Lys-OH (83 mg, 0.30 mmol) in THF (5 mL) in a crimp top vial. After heating to 85 °C for 16 h the reaction was quenched with 1 M aqueous HCl solution (3 mL) and water (3 mL). The aqueous phase was extracted with EtOAc (3 x 15 mL). The combined organic phases were dried over MgSO$_4$ and the solvent was removed under reduced pressure. Purification by automated reversed phase flash column chromatography (MeCN/H$_2$O with 0.05% TFA: 50-100% MeCN) yielded compound **7** (138 mg, 82%) as orange solid; R$_f$: 0.09 (PE/EtOAc: 1/1); m.p.: 88 °C; ^{1}H-NMR (400 MHz, DMSO-d_6): δ = 1.29-1.43 (m, 2H, CH$_2$-(CH_2)$_3$-CH), 1.51-1.65 (m, 3H, CH$_2$-(CH_2)$_3$-CH), 1.67-1.79 (m, 1H, CH$_2$-(CH_2)$_3$-CH), 1.91 (s, 6H, thiophene-CH_3), 3.49 (t, J = 7.1 Hz, 2H, N-CH_2-

(CH$_2$)$_3$), 3.93 (dt, J = 7.9, 4.6 Hz, 1H, NH-CH-CH$_2$), 5.02 (s, 2H, O-CH_2-Ph), 7.00 (s, 2H, thiophene-H), 7.28-7.37 (m, 5H, Ph-H), 7.57 (d, J = 8.0 Hz, 1H, CO-NH-CH), 12.55 (s, 1H, COOH); ^{13}C-NMR (101 MHz, DMSO-d_6): δ = 14.1 (+), 22.8 (−), 27.4 (−), 30.2 (−), 37.7 (−), 53.5 (+), 65.3 (−), 124.6 (q), 126.4 (q), 127.6 (+), 127.7 (+), 127.7 (+), 128.2 (+), 132.3 (q), 136.9 (q), 139.8 (q), 169.6 (q), 173.8 (q); IR (neat) ν_{max}: 3351, 3095, 2932, 2870, 1698, 1526, 1438, 1404, 1211, 989; HR-MS (ESI): calcd. for C$_{28}$H$_{27}$Cl$_2$N$_2$O$_6$S$_2$ (M+H)$^+$ 621.0682; found 621.0684.

N-(3,4-Bis(5-chloro-2-methylthiophen-3-yl)-2,5-dioxo-2,5-dihydro-1H-pyrrol-1-yl)acetamide (8)

Hydrazine hydrate (39 μL, 0.81 mmol) was added to a solution of maleic anhydride **4** (97 mg, 0.27 mmol) in acetic acid (3.5 mL). The reaction mixture was heated to 100 °C for 20 h and then water (10 mL) was added. The aqueous phase was extracted with EtOAc (3 x 10 mL). The combined organic phases were dried over MgSO$_4$ and the solvent was evaporated *in vacuo*. Purification by automated phase flash column chromatography (PE/EtOAc: 15-50% EtOAc) yielded compound **8** (81 mg, 72%) as orange solid; R$_f$: 0.23 (PE/EtOAc: 2/1); m.p.: 131 °C; ^{1}H-NMR (400 MHz, DMSO-d_6): δ = 1.96 (s, 6H, thiophene-CH_3), 2.04 (s, 3H, CO-CH_3), 7.01 (s, 2H, thiophene-H), 10.58 (s, 1H, NH); ^{13}C-NMR (101 MHz, DMSO-d_6): δ = 14.2 (+), 20.0 (+), 125.0 (q), 125.8 (q), 127.6 (+), 131.3 (q), 140.6 (q), 166.9 (q), 168.5 (q); IR (neat) ν_{max}: 3328, 3088, 2924, 2359, 1717, 1702, 1510, 1429, 1255, 1193, 988; HR-MS (ESI): calcd. for C$_{16}$H$_{13}$Cl$_2$N$_2$O$_3$S$_2$ (M+H)$^+$ 414.9739; found 414.9741.

3,4-Bis(5-chloro-2-methylthiophen-3-yl)-1-methyl-1H-pyrrole-2,5-dione (9)

Maleic anhydride **4** (54 mg, 0.15 mmol) and 1,2-dimethylhydrazine dihydrochloride (60 mg, 0.45 mmol) were heated to 160 °C for 12 h in PEG400 (2 mL) in a crimp top vial. Then water (15 mL) was added and the aqueous phase was extracted with EtOAc (3 x 15 mL). The combined organic phases were washed with brine (50 mL), dried over MgSO$_4$ and the solvent was removed under reduced pressure. Purification by automated phase flash column chromatography (PE/EtOAc: 3-10% EtOAc) yielded compound **9** (48 mg, 86%) as orange foam; R$_f$: 0.32 (PE/EtOAc: 19/1); ^{1}H-NMR (300 MHz, CDCl$_3$): δ =

1.93 (s, 6H, thiophene-CH_3), 3.13 (s, 3H, N-CH_3), 6.89 (s, 2H, thiophene-H); ^{13}C-NMR (75 MHz, CDCl$_3$): δ = 14.9 (+), 24.4 (+), 126.0 (q), 127.2 (+), 127.2 (q), 132.7 (q), 140.2 (q), 170.2 (q); IR (neat) ν_{max}: 3098, 2924, 2851, 1765, 1697, 1435, 1386, 1250, 1174, 980; HR-MS (ESI): calcd. for C$_{15}$H$_{12}$Cl$_2$NO$_2$S$_2$ (M+H)$^+$ 373.9649; found 373.9652.

Allyl ((4-(2-amino-2-oxoacetyl)-5-methylthiophen-2-yl)methyl) carbamate (10)

To a solution of oxoacetate **18** (282 mg, 0.95 mmol) in THF (5 mL) was added a NH$_4$OH solution (32% in H$_2$O) (1.18 mL, 9.50 mmol) at 0 °C. The reaction was stirred for 90 min at room temperature and then quenched with water (5 mL). The aqueous phase was extracted with EtOAc (3 x 10 mL). The combined organic phases were dried over MgSO$_4$ and the solvent was removed under reduced pressure. Compound **10** (253 mg, 94%) was obtained as yellow solid and used without further purification; R$_f$: 0.21 (PE/EtOAc: 1/1); m.p.: 108 °C; ^{1}H-NMR (400 MHz, CDCl$_3$): δ = 2.70 (s, 3H, thiophene-CH_3), 4.44 (d, J = 6.1 Hz, 2H, thiophene-CH_2NH), 4.59 (d, J = 5.1 Hz, 2H, CH$_2$=CHCH_2O), 5.21 (dd, J = 10.4, 0.5 Hz, 1H, CH_2=CHCH$_2$), 5.24-5.43 (m, 2H, CH_2=CHCH$_2$ and NH), 5.90 (ddt, J = 16.2, 10.7, 5.5 Hz, 1H, CH$_2$=CHCH$_2$), 6.05 (bs, 1H, NH_2), 7.06 (bs, 1H, NH_2), 7.86 (s, 1H, thiophene-H); ^{13}C-NMR (101 MHz, CDCl$_3$): δ = 16.7 (+), 39.8 (−), 65.9 (−), 117.9 (−), 129.0 (+), 130.8 (q), 132.7 (+), 137.0 (q), 155.7 (q), 156.1 (q), 164.4 (q), 182.1 (q); IR (neat) ν_{max}: 3402, 3301, 3167, 2962, 1750, 1686, 1649, 1535, 1460, 1254, 1047, 796; HR-MS (ESI): calcd. for C$_{12}$H$_{18}$N$_3$O$_4$S (M+NH$_4$)$^+$ 300.1013; found 300.1012.

Methyl 4-(2-methoxy-2-oxoethyl)-5-methylthiophene-2-carboxylate (11)

Thallium trinitrate (850 mg, 1.91 mmol) and 70% HClO$_4$ (0.30 mL) were added to a suspension of **21** (316 mg, 1.59 mmol) in MeOH (3 mL) at room temperature. After stirring for 24 h the mixture was concentrated under vacuum and diluted with water (5 mL). The aqueous phase was extracted with EtOAc (3 x 5 mL) and the combined organic layers were dried over MgSO$_4$. The solvent was evaporated and purification of the crude product by automated flash column chromatography (PE/EtOAc: 3-15% EtOAc) yielded compound **11** (331 mg, 91%) as colorless oil; R$_f$: 0.34 (PE/EtOAc: 5/1); ^{1}H-NMR (300 MHz, CDCl$_3$): δ = 2.43 (s, 3H, thiophene-CH_3), 3.54 (s, 2H, thiophene-CH_2C(O)OCH$_3$), 3.70 (s, 3H, thiophene-CH$_2$C(O)OCH_3), 3.85 (s, 3H, C(O)OCH_3), 7.61 (s, 1H, thiophene-H); ^{13}C-NMR (75 MHz,

CDCl$_3$): δ = 13.8 (+), 33.8 (−), 52.0 (+), 52.1 (+), 129.0 (q), 130.7 (q), 135.6 (+), 144.0 (q), 162.6 (q), 170.9 (q); IR (neat) v_{max}: 2997, 2953, 2845, 1736, 1704, 1535, 1457, 1392, 1331, 1291, 1250, 1194, 1132, 1063, 1006, 927, 874, 785, 751; HR-MS (APCI): calcd. for C$_{10}$H$_{12}$O$_4$S (M+H)$^+$ 229.0529; found 229.0531.

Methyl 4-(4-(5-((((allyloxy)carbonyl)amino)methyl)-2-methyl-thiophen-3-yl)-2,5-dioxo-2,5-dihydro-1*H*-pyrrol-3-yl)-5-methylthiophene-2-carboxylate (12)

KO*t*Bu (1 M in THF, 0.88 mL, 0.88 mmol) was added to a solution of glyoxylamide **10** (206 mg, 0.73 mmol) in dry THF (5 mL) at 0 °C under nitrogen atmosphere. After stirring for 90 min at 0 °C, diester **11** (200 mg, 0.88 mmol) in THF (2 mL) was added at 0 °C and stirred for 3 d at room temperature. Then the reaction was quenched with 1 M aqueous HCl solution (3 mL) and diluted with EtOAc (10 mL). The organic phase was washed with water (2 x 10 mL), brine (10 mL) and dried over MgSO$_4$. The solvent was removed under reduced pressure and purification of the crude product by automated flash column chromatography (PE/EtOAc: 25-50% EtOAc) yielded **12** (148 mg, 44%) as yellow foam; R$_f$: 0.20 (PE/EtOAc: 2/1); ^{1}H-NMR (400 MHz, CDCl$_3$): δ = 1.90 (s, 3H, thiophene-C*H*$_3$); 1.98 (s, 3H, thiophene-C*H*$_3$), 3.87 (s, 1H, OC*H*$_3$), 4.45 (d, *J* = 6.0 Hz, 2H, thiophene-C*H*$_2$NH), 4.60 (d, *J* = 4.9 Hz, 2H, CH$_2$=CHC*H*$_2$O), 5.13-5.27 (m, 2H, C*H*$_2$=CHCH$_2$ and CH$_2$N*H*CO), 5.31 (dd, *J* = 17.2, 1.2 Hz, 1H, C*H*$_2$=CHCH$_2$), 5.92 (ddt, *J* = 16.2, 10.8, 5.5 Hz, 1H, CH$_2$=C*H*CH$_2$), 6.90 (s, 1H, thiophene-*H*), 7.74 (s, 1H, thiophene-*H*), 8.30 (bs, 1H, CON*H*CO); ^{13}C-NMR (101 MHz, CDCl$_3$): δ = 15.0 (+), 15.3 (+), 39.9 (−), 52.3 (+), 65.9 (−), 117.9 (−), 125.8 (q), 126.7 (+), 127.5 (q), 130.9 (q), 132.7 (+), 134.8 (q), 134.9 (+), 139.4 (q), 142.1 (q), 148.6 (q), 156.0 (q), 162.1 (q), 170.0 (q), 170.2 (q); IR (neat) v_{max}: 3289, 3070, 2952, 1703, 1540, 1458, 1339, 1248, 994, 909, 727; HR-MS (ESI): calcd. for C$_{21}$H$_{21}$N$_2$O$_6$S$_2$ (M+H)$^+$ 461.0838; found 461.0836.

4-(4-(5-(Aminomethyl)-2-methylthiophen-3-yl)-2,5-dioxo-2,5-dihydro-1*H*-pyrrol-3-yl)-5-methylthiophene-2-carboxylic acid (13a)

and 4-(4-(5-((((Allyloxy)carbonyl)amino)methyl)-2-methylthiophen-3-yl)-2,5-dioxo-2,5-dihydro-1*H*-pyrrol-3-yl)-5-methylthiophene-2-carboxylic acid (13b)

A solution of BBr_3 (1 M in CH_2Cl_2) (2.0 mL, 2.00 mmol) was added to a solution of compound **12** (92 mg, 0.20 mmol) in dry CH_2Cl_2 (6 mL) in a crimp top vial. The mixture was heated to 40 °C for 5 h. Then water (4 mL) was added *via* syringe and the suspension was stirred at 40 °C for additional 30 min. After cooling to room temperature the solvent was removed at the rotary evaporator. Purification by automated reversed phase flash column chromatography (MeCN/H_2O with 0.05% TFA: 3-100% MeCN) yielded compound **13a** (34 mg, 47%) as yellow solid and compound **13b** (18 mg, 20%) as another yellow solid.

Analytical data of 13a: R_f: 0.02 (PE/EtOAc: 1/1); m.p.: 173 °C; ^{1}H-NMR (600 MHz, MeOD): δ = 2.00 (s, 3H, thiophene-C*H₃*), 2.08 (s, 3H, thiophene-C*H₃*), 4.27 (s, 2H, thiophene-C*H₂*NH), 7.18 (s, 1H, thiophene-*H*), 7.64 (s, 1H, thiophene-*H*); ^{13}C-NMR (151 MHz, MeOD): δ = 14.7 (+), 15.3 (+), 38.5 (−), 128.5 (q), 129.3 (q), 132.2 (+), 132.8 (q), 133.1 (q), 135.0 (q), 135.7 (q), 136.3 (+), 144.6 (q), 149.7 (q), 164.6 (q), 172.4 (q), 172.6 (q); IR (neat) v_{max}: 3008, 2924, 1766, 1712, 1681, 1545, 1463, 1344, 1188, 1137, 1001, 839, 799, 756, 723; HR-MS (ESI): calcd. for $C_{16}H_{15}N_2O_4S_2$ (M+H)$^+$ 363.0469; found 363.0468.

Analytical data of 13b: R_f: 0.04 (PE/EtOAc: 1/1); m.p.: 94 °C; ^{1}H-NMR (300 MHz, CD_3CN): δ = 1.93 (s, 3H, thiophene-C*H₃*), 1.97 (s, 3H, thiophene-C*H₃*), 4.33 (d, *J* = 6.3 Hz, 2H, thiophene-C*H₂*NH), 4.52 (d, *J* = 5.3 Hz, 2H, CH₂=CHC*H₂*O), 5.18 (dd, *J* = 10.5, 1.4 Hz, 1H, C*H₂*=CHCH₂), 5.27 (dd, *J* = 17.3, 1.6 Hz, 1H, C*H₂*=CHCH₂), 5.74-6.05 (m, 1H, CH₂=C*H*CH₂), 6.14 (bs, 1H, CH₂N*H*CO), 6.79 (s, 1H, thiophene-*H*), 7.60 (s, 1H, thiophene-*H*), 8.80 (bs, 1H, COO*H*); ^{13}C-NMR (75 MHz, CD_3CN): δ = 14.7 (+), 15.1 (+), 40.0 (−), 65.9 (−), 117.4 (−), 127.2 (q), 127.4 (+), 129.0 (q), 131.3 (q), 134.0 (q), 134.3 (+), 136.0 (+), 136.1 (q), 141.1 (q), 141.7 (q), 149.5 (q), 157.0 (q), 162.8 (q), 171.5 (q); IR (neat) v_{max}: 2926, 1981, 1769, 1709, 1544, 1459, 1344, 1246, 1185, 1150, 1049, 991, 849, 762; HR-MS (ESI): calcd. for $C_{20}H_{18}N_2O_6S_2$ (M+H)$^+$ 447.0679; found 447.0676.

Alternative procedure to obtain 13b: Compound **12** (40 mg, 0.09 mmol) was dissolved in acetone (10 mL) and LiI (350 mg, 2.60 mmol) was added. The mixture was heated to

100 °C overnight. After cooling to room temperature it was quenched with 1 M aqueous HCl solution (5 mL) and diluted with CH_2Cl_2 (5 mL). The phases were separated and the aqueous phase was extracted with CH_2Cl_2 (3 x 5 mL). The combined organic phases were dried over Na_2SO_4 and the solvent was removed at the rotary evaporator. Automated reversed phase flash column chromatography (MeCN/H_2O with 0.05% TFA: 3-100% MeCN) yielded compound **13b** (14 mg, 35%) as yellow solid.

Allyl ((5-methylthiophen-2-yl)methyl)carbamate (17)

LAH (2.78 g, 73.2 mmol) was added in portions to a solution of nitrile **16** (3.01 g, 24.4 mmol) in dry Et_2O (250 mL) at 0 °C under nitrogen atmosphere. After stirring for 4 h at room temperature the reaction was quenched with water (80 mL) and saturated aqueous $NaHCO_3$ solution (50 mL) at 0 °C. The suspension was filtered and the aqueous phase was extracted with Et_2O (3 x 80 mL). The combined organic phases were dried over $MgSO_4$ and concentrated *in vacuo*. Then the residue was dissolved in dry THF (100 mL) and pyridine (2.47 mL, 30.50 mmol) was added at 0 °C. Within 1 h allyl chloroformate (4.02 mL, 37.82 mmol) in dry THF (5 mL) was dropped to the solution *via* a syringe pump at 0 °C. After stirring for 14 h at room temperature the reaction was quenched cautiously with water (50 mL) and extracted with EtOAc (3 x 30 mL). The combined organic phases were dried over $MgSO_4$ and the solvent was removed under reduced pressure. Purification of the crude product by automated flash column chromatography (PE/EtOAc: 8-15% EtOAc) yielded **17** (3.40 g, 66%) as yellow oil; R_f: 0.20 (PE/EtOAc: 9/1); ^{1}H-NMR (400 MHz, $CDCl_3$): δ = 2.44 (s, 3H, thiophene-CH_3), 4.44 (d, J = 5.7 Hz, 2H, thiophene-CH_2NH), 4.59 (d, J = 5.3 Hz, 2H, CH_2=CHCH_2O), 5.05 (bs, 1H, NH), 5.21 (dd, J = 10.4, 0.3 Hz, 1H, CH_2=CHCH$_2$), 5.30 (dd, J = 17.1, 1.2 Hz, 1H, CH_2=CHCH$_2$), 5.92 (ddt, J = 16.4, 10.8, 5.7 Hz, 1H, CH$_2$=CHCH$_2$), 6.57 (dd, J = 3.1, 1.0 Hz, 1H, 4-thiophene-H), 6.74 (d, J = 3.1 Hz, 1H, 3-thiophene-H); ^{13}C-NMR (101 MHz, $CDCl_3$): δ = 15.4 (+), 40.1 (−), 65.6 (−), 117.8 (−), 124.8 (+), 125.7 (+), 132.8 (+), 138.8 (q), 139.9 (q), 155.9 (q); IR (neat) ν_{max}: 3335, 3073, 2922, 1695, 1514, 1426, 1236, 982, 799; HR-MS (ESI): calcd. for $C_{10}H_{14}NO_2S$ (M+H)$^+$ 212.0740; found 212.0740.

Methyl 2-(5-((((allyloxy)carbonyl)amino)methyl)-2-methylthiophen-3-yl)-2-oxoacetate (18)

Carbamate **17** (169 mg, 0.80 mmol) and methyl chlorooxoacetate (81 µL, 0.88 mmol) were dissolved in dry CH_2Cl_2 (6 mL) under nitrogen atmosphere. Then $AlCl_3$ (427 mg, 3.20 mmol) was added in portions at 0 °C and the suspension was stirred for 20 h at room temperature. The reaction was quenched with saturated aqueous $NaHCO_3$ solution (1 mL) at 0 °C and diluted with water (5 mL). The aqueous phase was extracted with CH_2Cl_2 (3 x 5 mL), the combined organic layers were washed with brine (10 mL) and dried over $MgSO_4$. After evaporation of the solvent the crude product was purified by automated flash column chromatography (PE/EtOAc: 15-40% EtOAc) to obtain **18** (117 mg, 49%) as brown oil; R_f: 0.22 (PE/EtOAc: 3/1); ^{1}H-NMR (400 MHz, $CDCl_3$): δ = 2.70 (s, 3H, thiophene-CH_3) 3.91 (s, 3H, OCH_3), 4.42 (d, J = 6.1 Hz, 2H, thiophene-CH_2NH), 4.58 (d, J = 5.3 Hz, 2H, CH_2=CHCH_2O), 5.16-5.34 (m, 3H, CH_2=CHCH$_2$ and NH), 5.90 (ddt, J = 16.3, 10.8, 5.6 Hz, 1H, CH$_2$=CHCH$_2$), 7.32 (s, 1H, thiophene-H); ^{13}C-NMR (101 MHz, $CDCl_3$): δ = 16.3 (+), 39.7 (−), 52.8 (+), 65.9 (−), 118.0 (−), 127.5 (+), 131.0 (q), 132.6 (+), 138.0 (q), 154.8 (q), 156.1 (q), 164.0 (q), 180.0 (q); IR (neat) v_{max}: 3395, 2954, 1726, 1670, 1517, 1434, 1242, 1200, 1112, 984, 757; HR-MS (ESI): calcd. for $C_{13}H_{16}NO_5S$ (M+H)$^+$ 298.0744; found 298.0744.

Methyl 4-acetyl-5-methylthiophene-2-carboxylate (21)

Thiophene **20** (800 mg, 5.12 mmol) and acetyl chloride (550 µL, 7.68 mmol) were dissolved in purified anhydrous $CHCl_3$ (10 mL) under nitrogen atmosphere. After cooling to 0 °C $AlCl_3$ (2.05 g, 15.4 mmol) was added in small portions. The yellow suspension was heated to 45 °C overnight upon turning bright red, then the reaction was quenched with ice/water and the aqueous phase was extracted with EtOAc (3 x 10 mL). The combined organic phases were washed with a saturated aqueous solution of $NaHCO_3$ (10 mL) and brine (10 mL). The organic phase was dried over $MgSO_4$ and the solvent was evaporated. The crude product was purified by automated flash column chromatography (PE/EtOAc: 5-25% EtOAc) and compound **21** (781 mg, 77%) was obtained as colorless solid; R_f: 0.41 (PE/EtOAc: 3/1); m.p.: 84 °C; ^{1}H-NMR (300 MHz, $CDCl_3$): δ = 2.52 (s, 3H, thiophene-CH_3), 2.76 (s, 3H, acetyl-CH_3), 3.88 (s, 3H, OCH_3), 8.03 (s, 1H, thiophene-H); ^{13}C-NMR (75 MHz, $CDCl_3$): δ = 16.8 (+), 29.6 (+), 52.3 (+),128.5 (q), 135.0 (+), 136.3 (q), 155.8 (q), 162.0 (q),

193.7 (q); IR (neat) ν_{max}: 3007, 2957, 1717, 1678, 1539, 1457, 1439, 1254, 1233, 1074, 1021, 745; HR-MS (APCI): calcd. for $C_9H_{10}O_3S$ (M+H)$^+$ 199.0423; found 199.0424.

General procedure A: Suzuki coupling:

To a suspension of Pd$_2$(dba)$_3$ (5 mol%), XPhos (10 mol%), the appropriate boronic acid (1.5 eq.) and K$_3$PO$_4$ (1.5 eq.) in 1,4-dioxane (0.5 M) the appropriate ester (1.0 eq.) was added. The resulting mixture was heated to 100 °C and stirred overnight. After cooling to room temperature the reaction mixture was diluted with EtOAc and the organic phase was washed two times with water. The organic phase was dried over MgSO$_4$, filtered and the solvent was removed under reduced pressure.

General procedure B: Aminolysis

An NH$_4$OH solution (25% in H$_2$O) (10.0 eq.) was added to a solution of the appropriate oxoacetate (1.0 eq.) in THF (0.3 M) at 0 °C. The reaction was stirred for 1 h at room temperature and then quenched with water. The aqueous phase was extracted with EtOAc. The combined organic phases were dried over MgSO$_4$, filtered and the solvent was removed under reduced pressure.

General procedure C: Perkin condensation

KOtBu (1 M in THF) (1.2 eq.) was added to a solution of the appropriate amide (1.0 eq.) in THF (0.2 M) at 0 °C. After 90 min stirring at 0 °C the appropriate ester (1.0 eq.) was added at 0 °C and stirred overnight at room temperature. The reaction was quenched with 1 M HCl and diluted with EtOAc. The organic phase was washed three times with water and brine. The organic phase was dried over MgSO$_4$, filtered and the solvent was removed under reduced pressure.

2-(5-Chloro-2-methylthiophen-3-yl)-2-oxoacetamide (23)

Compound **23** was prepared from **28** (800 mg, 3.66 mmol) according to general procedure B. The amide **23** (640 mg, 85%) was obtained as light yellow solid and used without further purification. m.p.: 183 °C; ^{1}H-NMR (300 MHz, DMSO-d_6): δ = 2.64 (s, 3H, thiophene-CH_3), 7.49 (s, 1H, thiophene-H), 7.94 (bs, 1H, NH), 8.25 (bs, 1H, NH); ^{13}C-NMR (75 MHz, DMSO-d_6): δ = 15.2 (+), 123.9 (q), 128.4 (+), 131.4 (q), 150.9 (q), 166.1 (q), 184.2 (q); IR (neat)

ν_{max}: 3446, 3252, 1996, 1670, 1618, 1296, 1221, 1153; HR-MS (ESI): calcd. for $C_7H_{10}ClN_2O_2S$ (M+NH$_4$)$^+$ 221.0146; found 221.0144.

3,4-Bis(5-chloro-2-methylthiophen-3-yl)-1*H*-pyrrole-2,5-dione (24)

Compound **24** was prepared from amide **23** (600 mg, 2.95 mmol) and ester **22** (720 mg, 3.54 mmol) according to general procedure C. Purification by automated flash column chromatography (heptane/EtOAc: 5/1) yielded **24** (660 mg, 63%) as orange solid. R$_f$: 0.18 (heptane/EtOAc: 5/1); m.p.: 237 °C. ^{1}H-NMR (400 MHz, DMSO-d_6): δ = 1.87 (s, 6H, thiophene-C*H*$_3$), 6.97 (s, 2H, thiophene-*H*), 11.25 (bs, 1H, N*H*); ^{13}C-NMR (101 MHz, DMSO-d_6): δ = 14.6 (+), 125.0 (q), 127.0 (q), 128.4 (+), 133.6 (q), 140.0 (q), 171.4 (q); IR (neat) ν_{max}: 3381, 2939, 2818, 1653, 1437, 1002; HR-MS (ESI): calcd. for $C_{14}H_{10}Cl_2NO_2S_2$ (M+H)$^+$ 357.9525; found 357.9523.

Methyl 2-(5-(4-(tert-butyl)phenyl)-2-methylthiophen-3-yl)acetate (26)

Compound **26** was prepared from **22** (200 mg, 0.98 mmol) according to general procedure A. Purification by automated flash column chromatography (PE/EtOAc: 0-25% EtOAc) yielded **26** (163 mg, 55%) as yellow liquid. R$_f$: 0.63 (PE/EtOAc: 5/1); ^{1}H-NMR (300 MHz, CDCl$_3$): δ = 1.33 (s, 9H, *t*Bu), 2.41 (s, 3H, thiophene-C*H*$_3$), 3.55 (s, 2H, thiophene-C*H*$_2$C(O)OCH$_3$), 3.71 (s, 3H, thiophene-CH$_2$C(O)OC*H*$_3$), 7.08 (s, 1H, thiophene-*H*), 7.32-7.40 (m, 2H, Ph), 7.43-7.52 (m, 2H, Ph); ^{13}C-NMR (75 MHz, CDCl$_3$): δ =13.3 (+), 31.3 (+) 34.1 (−), 34.6 (q), 52.1 (+), 124.7 (+), 125.2 (+), 125.7 (+), 130.1 (q), 131.6 (q), 134.8 (q), 140.1 (q), 150.2 (q), 171.6 (q); IR (neat) ν_{max}: 2961, 1736, 1609, 1520, 1435, 1364, 1239, 1018, 825; HR-MS (ESI): calcd. for $C_{18}H_{23}O_2S$ (M+H)$^+$ 303.1413; found 303.1418.

Methyl 2-(5-([1,1'-biphenyl]-3-yl)-2-methylthiophen-3-yl)acetate (27)

Compound **27** was prepared from **22** (500 mg, 2.44 mmol) according to general procedure A. Purification by automated flash column chromatography (PE/EtOAc: 0-15% EtOAc) yielded **27** (569 mg, 72%) as yellow liquid. R$_f$: 0.50 (PE/EtOAc: 5/1); ^{1}H-NMR (300 MHz, CDCl$_3$): δ = 2.44 (s, 3H, thiophene-C*H*$_3$), 3.58 (s, 2H, thiophene-C*H*$_2$C(O)OCH$_3$), 3.72 (s, 3H, thiophene-CH$_2$C(O)OC*H*$_3$), 7.19 (s, 1H, thiophene-*H*), 7.37-7.45 (m, 3H, Ph), 7.46-7.54 (m, 3H, Ph), 7.59-7.66 (m, 2H, Ph), 7.74-7.76 (m, 1H, Ph); ^{13}C-NMR (75 MHz, CDCl$_3$): δ =2.44 (s,

3H, thiophene-CH_3), 3.58 (s, 2H, thiophene-CH_2C(O)OCH$_3$), 3.72 (s, 3H, thiophene-CH$_2$C(O)OCH_3), 7.19 (s, 1H, thiophene-H), 7.37-7.42 (m, 1H, Ph), 7.43-7.47 (m, 3H, Ph), 7.48-7.54 (m, 2H, Ph), 7.60-7.65 (m, 2H, Ph), 7.74-7.76 (m, 1H, Ph); ^{13}C-NMR (75 MHz, CDCl$_3$): δ = 13.3 (+), 34.1 (−), 52.1 (+), 124.3 (+), 124.4 (+), 125.3 (+), 126.0 (+), 127.2 (+), 127.5 (+), 128.8 (+), 129.2 (+), 130.3 (q), 134.8 (q), 135.5 (q), 139.9 (q), 140.9 (q), 141.9 (q), 171.5 (q); IR (neat) ν$_{max}$: 1707, 1597, 1449, 1262, 1174, 755, 696; HR-MS (EI): calcd. for C$_{20}$H$_{18}$O$_2$S (M$^{+•}$) 322.1028; found 322.1032.

Methyl 2-(5-(4-(tert-butyl)phenyl)-2-methylthiophen-3-yl)-2-oxoacetate (30)

Compound **30** was prepared from **28** (500 mg, 2.29 mmol) according to general procedure A. Purification by automated flash column chromatography (PE/EtOAc: 0-15% EtOAc) yielded **30** (350 mg, 48%) as dark yellow liquid. R$_f$: 0.67 (PE/EtOAc: 5/1); ^{1}H-NMR (300 MHz, CDCl$_3$): δ = 1.34 (s, 9H, tBu), 2.78 (s, 3H, thiophene-CH_3), 3.96 (s, 3H, thiophene-CH$_2$C(O)OCH_3), 7.39-7.44 (m, 2H, Ph), 7.46-7.51 (m, 2H, Ph), 7.63 (s, 1H, thiophene-H); ^{13}C-NMR (75 MHz, CDCl$_3$): δ =16.3 (+), 31.3 (+) 34.7 (q), 52.8 (+), 124.2 (+), 125.6 (+), 126.0 (+), 130.3 (q), 132.2 (q), 140.5 (q), 151.3 (q), 153.5 (q), 164.1 (q), 180.2 (q); IR (neat) ν$_{max}$: 2961, 2866, 1732, 1676, 1456, 1191, 1127, 993, 753; HR-MS (EI): calcd. for C$_{18}$H$_{20}$O$_3$S (M$^{+•}$) 316.1133; found 316.1139.

Methyl 2-(5-([1,1'-biphenyl]-3-yl)-2-methylthiophen-3-yl)-2-oxoacetate (31)

Compound **31** was prepared from **28** (500 mg, 2.29 mmol) according to general procedure A. Purification by automated flash column chromatography (PE/EtOAc: 0-15% EtOAc) yielded **31** (537 mg, 70%) as yellow oil. R$_f$: 0.40 (PE/EtOAc: 5/1); ^{1}H-NMR (300 MHz, CDCl$_3$): δ = 2.81 (s, 3H, thiophene-CH_3), 3.98 (s, 3H, thiophene-CH$_2$C(O)OCH_3), 7.36-7.43 (m, 1H, Ph), 7.45-7.49 (m, 2H, Ph), 7.50-7.57 (m, 3H, Ph), 7.60-7.65 (m, 2H, 4-H, Ph), 7.73-7.76 (m, 2H, Ph, thiophene-H); ^{13}C-NMR (75 MHz, CDCl$_3$): δ = 16.4 (+), 52.9 (+), 124.6 (+), 124.7 (+), 124.8 (+), 126.9 (+), 127.2 (+), 127.7 (+), 128.9 (+), 129.5 (+), 132.3 (q), 133.5 (q), 140.2 (q), 140.6 (q), 142.2 (q), 154.0 (q), 164.0 (q), 180.1 (q); IR (neat) ν$_{max}$: 3028, 1724, 1668, 1598, 1464, 1197, 1132, 1000, 748, 695; HR-MS (ESI): calcd. for C$_{20}$H$_{15}$O$_2$S (M+H$^+$) − (H$_2$O) 319.0787; found 319.0787.

2-(5-(4-(tert-Butyl)phenyl)-2-methylthiophen-3-yl)-2-oxoacetamide (33)

Compound **33** was prepared from **30** (312 mg, 0.99 mmol) according to general procedure B. The amide **33** (250 mg, 84%) was obtained as light yellow solid and used without further purification. m.p.: 202 °C; ^{1}H-NMR (300 MHz, DMSO-d_6): δ = 1.29 (s, 9H, tBu), 2.71 (s, 3H, thiophene-CH_3), 7.36-7.48 (m, 2H, Ph), 7.51-7.59 (m, 2H, Ph), 7.74 (s, 1H, thiophene-H), 7.91 (s, 1H, NH), 8.26 (s, 1H, NH); ^{13}C-NMR (75 MHz, DMSO-d_6): δ = 15.4 (+), 30.9 (+), 34.3 (q), 124.4 (+), 125.0 (+), 126.0 (+), 129.7 (q), 133.0 (q), 138.9 (q), 150.5 (q), 150.6 (q), 167.0 (q), 185.5 (q); IR (neat) ν$_{max}$: 3395, 2955, 1712, 1651, 1454, 1191, 575; HR-MS (ESI): calcd. for $C_{17}H_{20}NO_2S$ (M+H$^+$) 303.1240; found 303.1240.

2-(5-([1,1'-Biphenyl]-3-yl)-2-methylthiophen-3-yl)-2-oxoacetamide (34)

Compound **34** was prepared from **31** (250 mg, 0.74 mmol) according to general procedure B. The amide **34** (224 mg, 94%) was obtained as light yellow solid and used without further purification. m.p.: 151 °C; ^{1}H-NMR (300 MHz, DMSO-d_6): δ = 2.73 (s, 3H, thiophene-CH_3), 7.39-7.44 (m, 1H, Ph), 7.47-7.56 (m, 3H, Ph), 7.58-7.66 (m, 2H, Ph), 7.71-7.75 (m, 2H, Ph), 7.83-7.85 (m, 1H, NH), 7.93 (bs, 2H, Ph, thiophene-H), 8.28 (bs, 1H, NH); ^{13}C-NMR (75 MHz, DMSO-d_6): δ = 15.4 (+), 123.4 (+), 124.4 (+), 125.5 (+), 126.4 (+), 126.8 (+), 127.7 (+), 128.9 (+), 129.9 (+), 133.1 (q), 133.2 (q), 138.7 (q), 139.5 (q), 141.1 (q), 151.1 (q), 166.9 (q), 185.6 (q); IR (neat) ν$_{max}$: 3393, 3302, 3184, 1721, 1652, 1597, 1456, 1352, 1196, 747, 689, 608; HR-MS (ESI): calcd. for $C_{19}H_{16}NO_2S$ (M+H$^+$) 322.0896; found 322.0893.

3-(5-(4-(tert-Butyl)phenyl)-2-methylthiophen-3-yl)-4-(5-chloro-2-methylthiophen-3-yl)-1H-pyrrole-2,5-dione (35)

Compound **35** was prepared from amide **23** (100 mg, 0.49 mmol) and ester **26** (178 mg, 0.59 mmol) according to general procedure C. Purification by automated flash column chromatography (PE/EtOAc: 0-25% EtOAc) yielded **35** (62 mg, 28%) as dark green solid. R$_f$: 0.47 (PE/EtOAc: 5/1); m.p.: 145 °C; ^{1}H-NMR (300 MHz, DMSO-d_6): δ = 1.28 (s, 9H, tBu), 1.88 (s, 3H, thiophene-CH_3), 1.99 (s, 3H, thiophene-CH_3), 7.02 (s, 1H, thiophene-H), 7.28 (s, 1H, thiophene-H), 7.40-7.49 (m, 4H, Ph), 11.27 (s, 1H, NH); ^{13}C-NMR (75 MHz, DMSO-d_6): δ = 14.0 (+), 14.2 (+), 30.9 (+), 34.2 (q), 124.0 (+), 124.3 (q), 124.7 (+), 125.9 (+), 126.7 (q), 127.8 (q), 127.9 (+), 130.2 (q), 132.7 (q), 134.1 (q), 139.3 (q), 139.5 (q), 139.8 (q), 150.3

(q), 171.0 (q), 171.1 (q); IR (neat) ν_{max}: 3055, 2961, 1707, 1459, 1338, 1181, 1018, 987, 825; HR-MS (ESI): calcd. for $C_{24}H_{26}ClN_2O_2S_2$ $(M+NH_4)^+$ 473.1119; found 473.1116.

3-(5-([1,1'-Biphenyl]-3-yl)-2-methylthiophen-3-yl)-4-(5-chloro-2-methylthiophen-3-yl)-1*H*-pyrrole-2,5-dione (36)

Compound **36** was prepared from amide **23** (100 mg, 0.49 mmol) and ester **27** (160 mg, 0.49 mmol) according to general procedure C. Purification by automated flash column chromatography (PE/EtOAc: 0-25% EtOAc) yielded **36** (63 mg, 27%) as dark red solid. R$_f$: 0.16 (PE/EtOAc: 5/1); m.p.: 137 °C; ^{1}H-NMR (300 MHz, DMSO-d_6): δ = 1.91 (s, 3H, thiophene-CH_3), 2.01 (s, 3H, thiophene-CH_3), 7.03 (s, 1H, thiophene-*H*), 7.37-7.44 (m, 1H, Ph), 7.46-7.56 (m, 5H, thiophene-*H*, Ph), 7.58-7.63 (m, 1H, Ph), 7.69-7.75 (m, 2H, Ph), 7.77-7.79 (m, 1H, Ph), 11.30 (s, 1H, N*H*); ^{13}C-NMR (75 MHz, DMSO-d_6): δ = 14.1 (+), 14.2 (+), 123.2 (+), 124.1 (+), 124.3 (q), 125.1 (+), 126.1 (+), 126.6 (q), 126.7 (+), 127.7 (+), 127.9 (+), 128.0 (q), 128.9 (+), 129.8 (+), 132.8 (q), 133.6 (q), 134.0 (q), 139.4 (q), 139.5 (q), 139.6 (q), 140.2 (q), 141.1 (q), 171.0 (q), 171.1 (q); IR (neat) ν_{max}: 2736, 1705, 1338, 1022, 1006, 756, 700; HR-MS (ESI): calcd. for $C_{26}H_{22}ClN_2O_2S_2$ $(M+NH_4)^+$ 493.0806; found 493.0804.

3-(5-([1,1'-Biphenyl]-3-yl)-2-methylthiophen-3-yl)-4-(5-(4-(tert-butyl)phenyl)-2-methylthiophen-3-yl)-1*H*-pyrrole-2,5-dione (37)

Compound **37** was prepared from amide **33** (260 mg, 0.86 mmol) and ester **27** (277 mg, 0.86 mmol) according to general procedure C. Purification by automated flash column chromatography (PE/EtOAc: 0-15% EtOAc) yielded **37** (155 mg, 33%) as purple solid. R$_f$: 0.13 (PE/EtOAc: 5/1); m.p.: 145 °C; ^{1}H-NMR (300 MHz, DMSO-d_6): δ = 1.27 (s, 9H, *t*Bu), 2.02 (s, 6H, thiophene-CH_3, thiophene-CH_3), 7.31 (s, 1H, thiophene-*H*), 7.38-7.43 (m, 3H, Ph), 7.44-7.50 (m, 5H, thiophene-*H*, Ph), 7.50-7.52 (m, 1H, Ph), 7.54-7.56 (m, 1H, Ph), 7.58-7.61 (m, 1H, Ph), 7.68-7.71 (m, 2H, Ph), 7.76-7.78 (m, 1H, Ph), 11.27 (s, 1H, N*H*); ^{13}C-NMR (75 MHz, DMSO-d_6): δ = 14.3 (+), 31.0 (+), 34.3 (q), 123.2 (+), 124.1 (+), 124.2 (+), 124.8 (+), 125.4 (+), 126.0 (+), 126.1 (+), 126.8 (+), 127.7 (+), 128.2 (q), 128.3 (q), 128.9 (+), 129.9 (+), 130.3 (q), 133.7 (q), 133.9 (q), 134.0 (q), 139.4 (q), 139.5 (q), 139.6 (q), 139.8 (q), 140.1 (q), 141.1 (q), 150.3 (q), 171.6 (q), 171.7 (q); IR (neat) ν_{max}: 2921, 2851, 1707, 1334, 831, 756; HR-MS (ESI): calcd. for $C_{36}H_{32}NO_2S_2$ $(M+H)^+$ 576.1879; found 576.1875.

1.5 Supporting Information

Non-hydrolytic methyl ester deprotection of 12

**Table S1.** Non-hydrolytic methyl ester deprotection of **12**.

Entry	LiI [eq.]	Solvent	T [°C]	Isolated yield[a]
1	3.0	EtOAc	RT	--
2	3.0	EtOAc	reflux	--
3	30	EtOAc	reflux	26%
4	3.0	acetone	reflux	--
5	30	acetone	reflux	35%
6	30	MeCN	reflux	--
7	30	DMSO	100 °C	--

[a] If conversion was too low, the product **13b** was not isolated.

Synthesis of compounds 11S, 12S, 13S and 21S
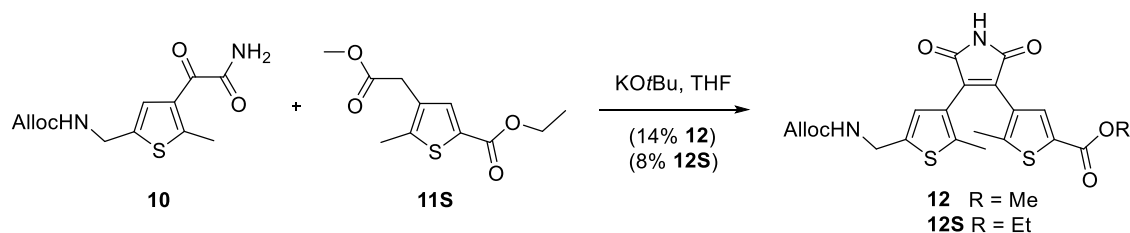
Scheme S1. Perkin condensation of **10** and **11S** yielding dithienylmaleimide **12** and **12S**.
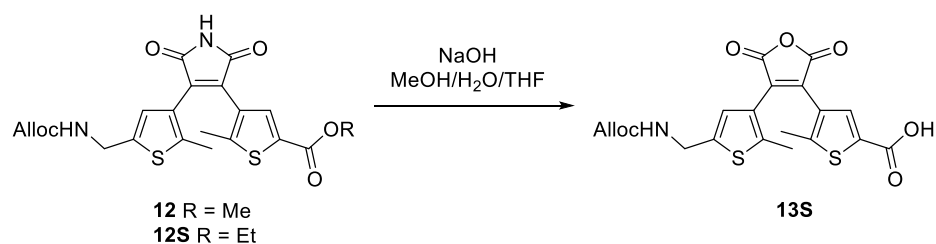
Scheme S2. Hydrolytic ester cleavage yielding maleic anhydride **13S**.
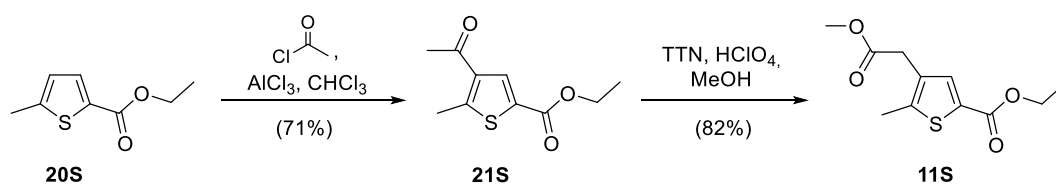
Scheme S3. Synthesis of ethyl ester **11S**.

Ethyl 4-(2-methoxy-2-oxoethyl)-5-methylthiophene-2-carboxylate (11S)

Thallium trinitrate (2.20 g, 4.94 mmol) and 70% $HClO_4$ (2 mL) were added to a suspension of **21S** (875 mg, 4.12 mmol) in MeOH (10 mL) at RT. After stirring for 24 h the mixture was concentrated under reduced pressure and diluted with water (10 mL). The aqueous phase was extracted with $CHCl_3$ (3 x 15 mL) and the combined organic layers were dried over $MgSO_4$. The solvent was evaporated and purification of the crude product by automated flash column chromatography (PE/EtOAc: 3-15% EtOAc) yielded compound **11S** (816 mg, 82%) as yellowish oil. R_f: 0.23 (PE/EtOAc: 9/1); ^{1}H-NMR (400 MHz, $CDCl_3$): δ = 1.35 (t, J = 7.1 Hz, 3H, O−CH_2−CH_3), 2.42 (s, 3H, thiophene-CH_3), 3.54 (s, 2H, C−CH_2−CO), 3.70 (s, 3H, CO−O−CH_3), 4.31 (q, J = 7.1 Hz, 2H, O−CH_2−CH$_3$), 7.60 (s, 1H, thiophene-H); ^{13}C-NMR (101 MHz, $CDCl_3$): δ = 13.8 (+), 14.4 (+), 33.8 (−), 52.2 (+), 61.0 (−), 129.6 (q), 130.6 (q), 135.4 (+), 143.8 (q), 162.2 (q), 171.0 (q); IR (neat) ν_{max}: 3081, 2987, 2922, 1730, 1705, 1460, 1254, 1201, 1172, 1061; HR-MS (ESI): calcd. for $C_{11}H_{14}NaO_4S$ (M+Na)$^+$ 265.0505; found 265.0502.

Methyl/Ethyl 4-(4-(5-((((allyloxy)carbonyl)amino)methyl)-2-methyl-thiophen-3-yl)-2,5-dioxo-2,5-dihydro-1H-pyrrol-3-yl)-5-methylthiophene-2-carboxylate (12/12S)

KOtBu (1 M in THF, 1.34 mL, 1.34 mmol) was added to a solution of **10** (316 mg, 1.12 mmol) in anhydrous THF (6 mL) at 0 °C under nitrogen atmosphere. After stirring for 90 min at 0 °C, diester **11S** (326 mg, 1.34 mmol) was added and stirred for 15 h at RT. Then the reaction was heated to 60 °C for 1 h, quenched with 1 M HCl solution (4 mL) and diluted with EtOAc (10 mL). The organic phase was washed with water (3 x 5 mL), brine (5 mL) and dried over $MgSO_4$. The solvent was removed under reduced pressure and purification of the crude product by automated reversed phase flash column chromatography (H_2O/EtOH: 20-45% EtOH) yielded **12S** (40 mg, 8%) as orange foam, **12** (74 mg, 14%) as yellow foam and a mixed fraction of both (65 mg). _Analytical data of 12S_: R_f: 0.25 (PE/EtOAc: 2/1); ^{1}H-NMR (400 MHz, $CDCl_3$): δ = 1.36 (t, J = 7.1 Hz, 3H, O−CH_2−CH_3), 1.91 (s, 3H, thiophene-CH_3), 1.97 (s, 3H, thiophene-CH_3), 4.33 (q, J = 7.1 Hz, 2H, O−CH_2−CH$_3$), 4.45 (d, J = 5.9 Hz, 2H, C−CH_2−NH), 4.60 (d, J = 4.8 Hz, 2H, O−CH_2−CH), 5.14-5.26 (m, 2H, CH_2=CH−CH$_2$ and CH$_2$−NH−CO), 5.31 (dd, J = 17.2, 1.1 Hz, 1H, CH_2=CH−CH$_2$), 5.92 (ddt, J = 16.3, 10.8, 5.6 Hz, 1H, CH$_2$=CH−CH$_2$), 6.90 (s, 1H, thiophene-H), 7.75 (s, 1H,

thiophene-*H*), 7.97 (bs, 1H, CO–N*H*–CO); ^{13}C-NMR (101 MHz, CDCl$_3$): δ = 14.3 (+), 15.0 (+), 15.3 (+), 39.9 (−), 61.4 (−), 65.9 (−), 117.9 (−), 125.8 (q), 126.7 (+), 127.4 (q), 131.4 (q), 132.7 (+), 132.8 (q), 134.7 (+), 139.4 (q), 142.1 (q), 148.4 (q), 156.0 (q), 161.7 (q), 170.0 (q), 170.1 (q); IR (neat) ν$_{max}$: 3288, 3071, 2980, 1710, 1541, 1458, 1252, 995, 916, 760; HR-MS (ESI): calcd. for C$_{22}$H$_{23}$N$_2$O$_6$S$_2$ (M+H)$^+$ 475.0993; found 475.0992; UV/Vis (50 μM in MeOH): open isomer: λ$_{max}$ = 250 nm; closed isomer: λ$_{max}$ = 232 nm, 378 nm, 554 nm.

4-(4-(5-((((Allyloxy)carbonyl)amino)methyl)-2-methylthiophen-3-yl)-2,5-dioxo-2,5-dihydrofuran-3-yl)-5-methylthiophene-2-carboxylic acid (13S)

A mixture of **12** and **12S** (62 mg) in 10 mL of H$_2$O/MeOH/THF (2:5:3, v/v/v) was stirred for 20 h with NaOH (78 mg, 1.95 mmol) at RT. After addition of water (10 mL) the reaction mixture was washed with EtOAc (2 x 10 mL) and then acidified with conc. HCl to pH 1. The aqueous phase was extracted with EtOAc (3 x 10 mL) and the combined organic phases were dried over MgSO$_4$. Evaporation of the solvent and purification of the crude product by automated reversed phase flash column chromatography (H$_2$O/MeCN: 20-55% MeCN) yielded **13S** (29 mg)^A as green solid. R$_f$: 0.02 (PE/EtOAc: 1/1); mp: 84 °C; ^{1}H-NMR (400 MHz, DMSO-*d$_6$*): δ = 1.90 (s, 3H, thiophene-C*H$_3$*), 1.96 (s, 3H, thiophene-C*H$_3$*), 4.28 (d, *J* = 6.1 Hz, 2H, thiophene-C*H$_2$*NH), 4.49 (d, *J* = 5.3 Hz, 2H, CH$_2$=CHC*H$_2$*O), 5.17 (dd, *J* = 10.5, 1.4 Hz, 1H, C*H$_2$*=CHCH$_2$), 5.27 (dd, *J* = 17.2, 1.5 Hz, 1H, C*H$_2$*=CHCH$_2$), 5.90 (ddt, *J* = 17.2, 10.6, 5.3 Hz, 1H, CH$_2$=C*H*CH$_2$), 6.86 (s, 1H, thiophene-*H*), 7.65 (s, 1H, thiophene-*H*), 7.92 (t, *J* = 6.0 Hz, 1H, CH$_2$N*H*CO), 13.30 (bs, 1H, COO*H*); ^{13}C-NMR (101 MHz, DMSO-*d$_6$*): δ = 14.1 (+), 14.5 (+), 38.8 (−), 64.4 (−), 116.9 (−), 124.9 (q), 125.5 (+), 126.8 (q), 131.6 (q), 133.5 (+), 133.9 (q), 134.1 (+), 135.6 (q), 140.8 (q), 141.4 (q), 148.6 (q), 155.9 (q), 162.2 (q), 164.9 (q), 164.9 (q); IR (neat) ν$_{max}$: 3327, 3164, 3020, 2925, 1764, 1702, 1541, 1458, 1254, 931, 750; HR-MS (ESI): calcd. for C$_{20}$H$_{18}$NO$_7$S$_2$ (M+H)$^+$ 448.0519; found 448.0516; UV/Vis (50 μM in MeOH): open isomer: λ$_{max}$ = 246 nm; closed isomer: λ$_{max}$ = 384 nm, 568 nm.

Ethyl 4-acetyl-5-methylthiophene-2-carboxylate (21S)

A solution of acetyl chloride (128 μL, 1.80 mmol) in anhydrous CHCl$_3$ (2 mL) was added to AlCl$_3$ (480 mg, 3.60 mmol) at RT under nitrogen atmosphere. After stirring for 10 min a

---

^{A} Yield could not be determined because the ratio of **12** to **12S** in the mixture was not calculated.

solution of **20S** (204 mg, 1.20 mmol) in anhydrous CHCl$_3$ (2 mL) was dropped to the suspension. The mixture was heated to 60 °C for 9 h, then the reaction was quenched with ice/water and the aqueous phase was extracted with CHCl$_3$ (2 x 30 mL). The combined organic phases were washed with saturated aqueous solution of NaHCO$_3$ (50 mL) and brine (50 mL). The organic phase was dried over MgSO$_4$ and the solvent was evaporated. The crude product was purified by automated flash column chromatography (PE/EtOAc: 8-30% EtOAc) and **21S** (180 mg, 71%) was obtained as colorless solid. R$_f$: 0.15 (PE/EtOAc: 9/1); mp: 103 °C; ^{1}H-NMR (400 MHz, CDCl$_3$): δ = 1.37 (t, J = 7.1 Hz, 3H, O−CH$_2$−CH_3), 2.52 (s, 3H, thiophene-CH_3), 2.75 (s, 3H, acetyl-CH_3), 4.34 (q, J = 7.1 Hz, 2H, O−CH_2−CH$_3$), 8.02 (s, 1H, thiophene-H); ^{13}C-NMR (101 MHz, CDCl$_3$): δ = 14.3 (+), 16.8 (+), 29.6 (+), 61.4 (−), 129.0 (q), 134.7 (+), 136.3 (q), 155.6 (q), 161.6 (q), 193.7 (q); IR (neat) ν_{max}: 3008, 2985, 2944, 1713, 1670, 1540, 1452, 1250, 1236, 1082, 1021, 747; HR-MS (ESI): calcd. for C$_{10}$H$_{13}$O$_3$S (M+H)$^+$ 213.0580; found 213.0581.
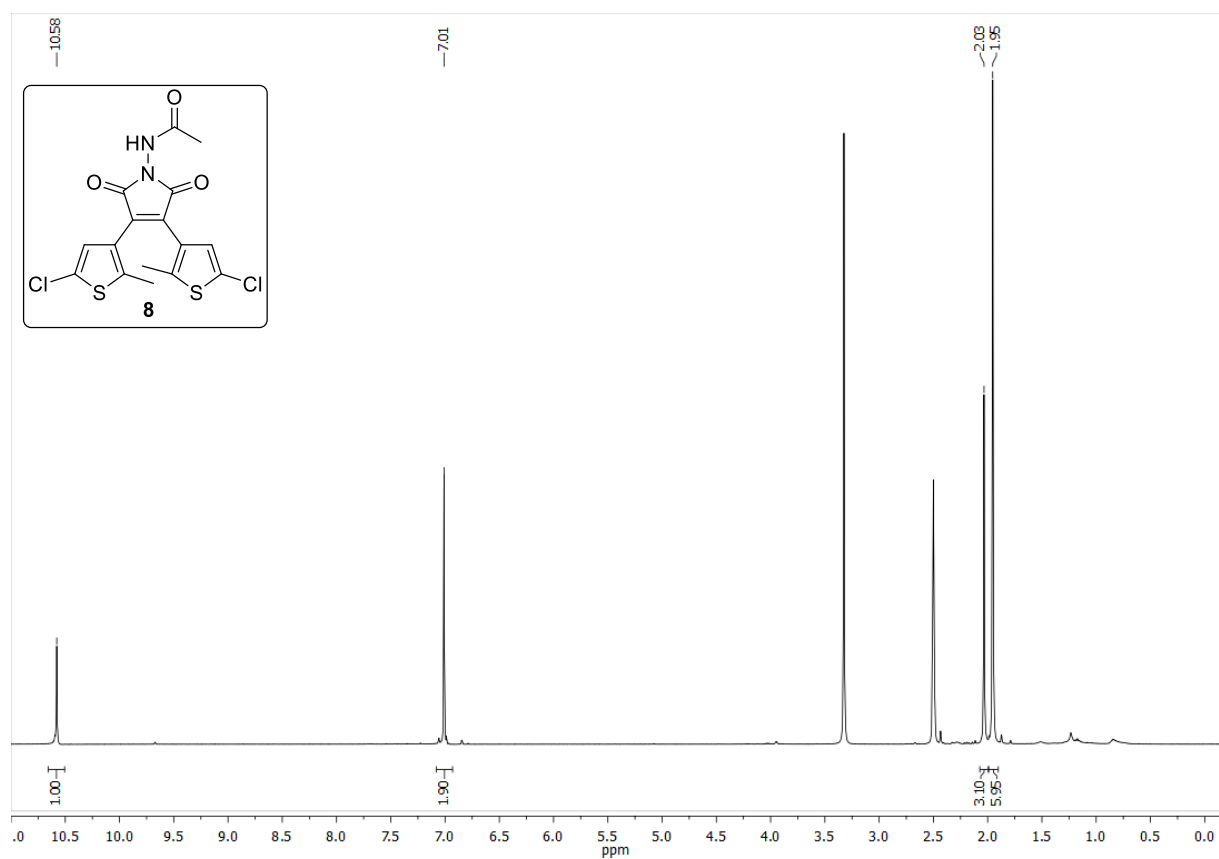
¹H- and ¹³C-NMR spectra

¹H-NMR (300 MHz, DMSO-d_6) for compound **4**:
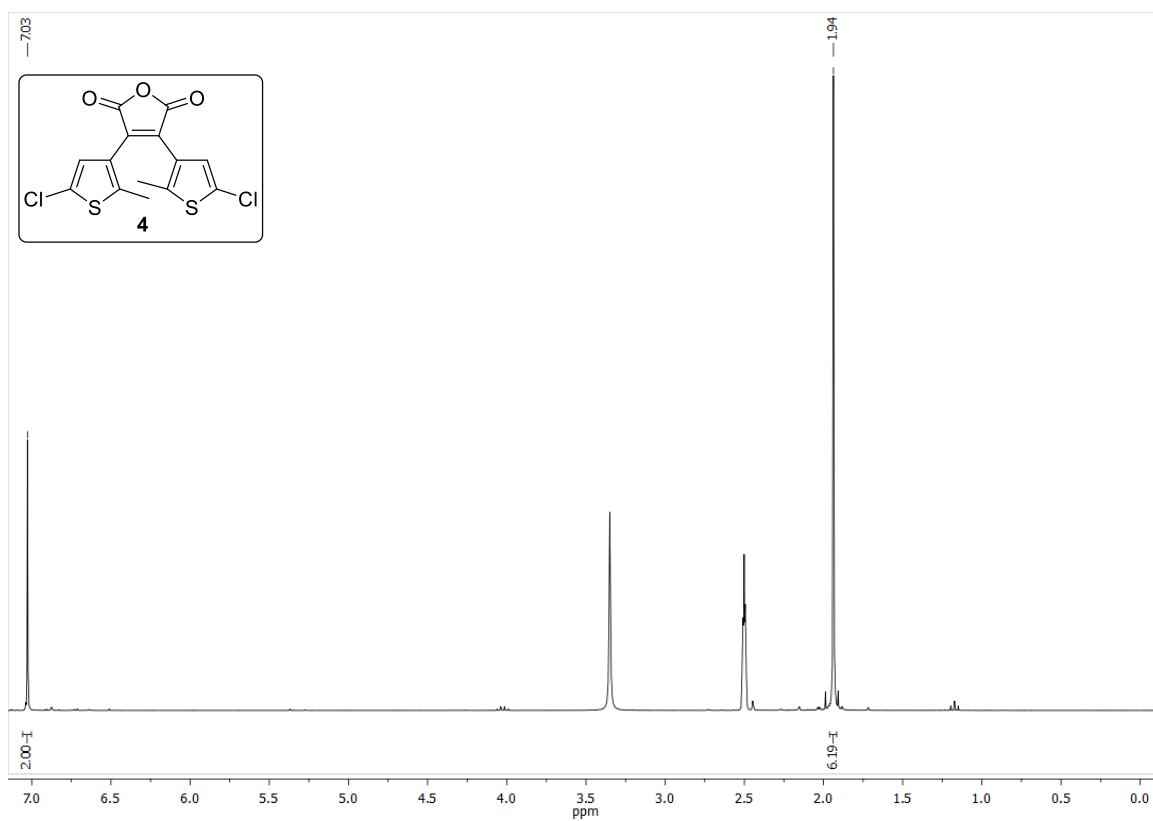
¹³C-NMR (75 MHz, DMSO-d_6) for compound **4**:
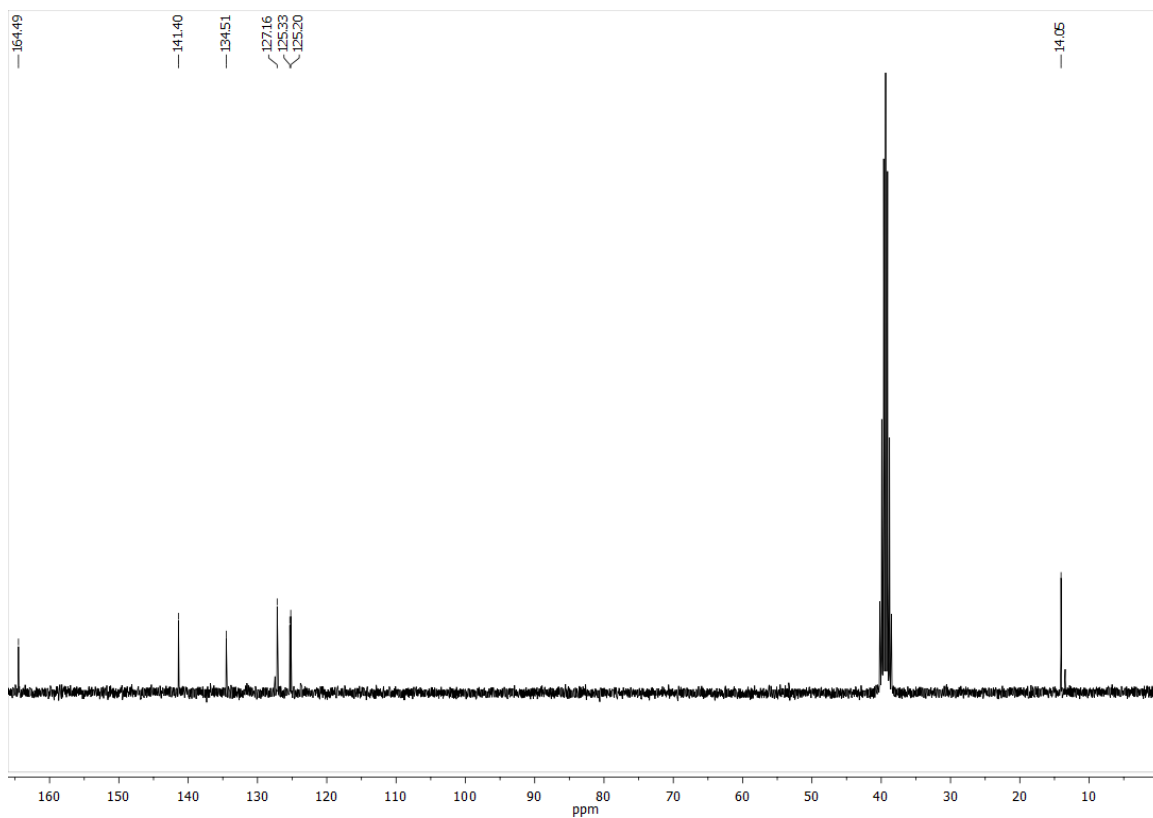
^{1}H-NMR (300 MHz, DMSO-d_6) for compound **6**:
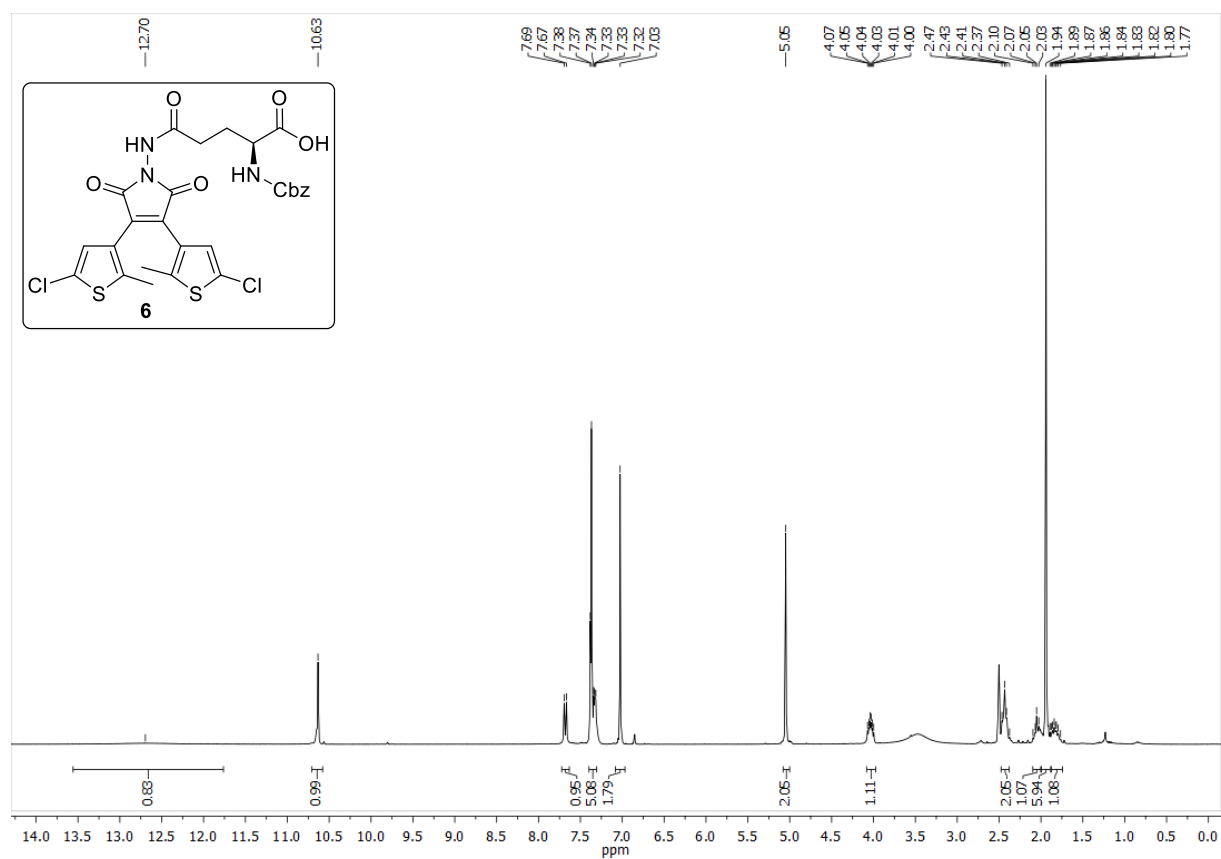
^{13}C-NMR (75 MHz, DMSO-d_6) for compound **6**:
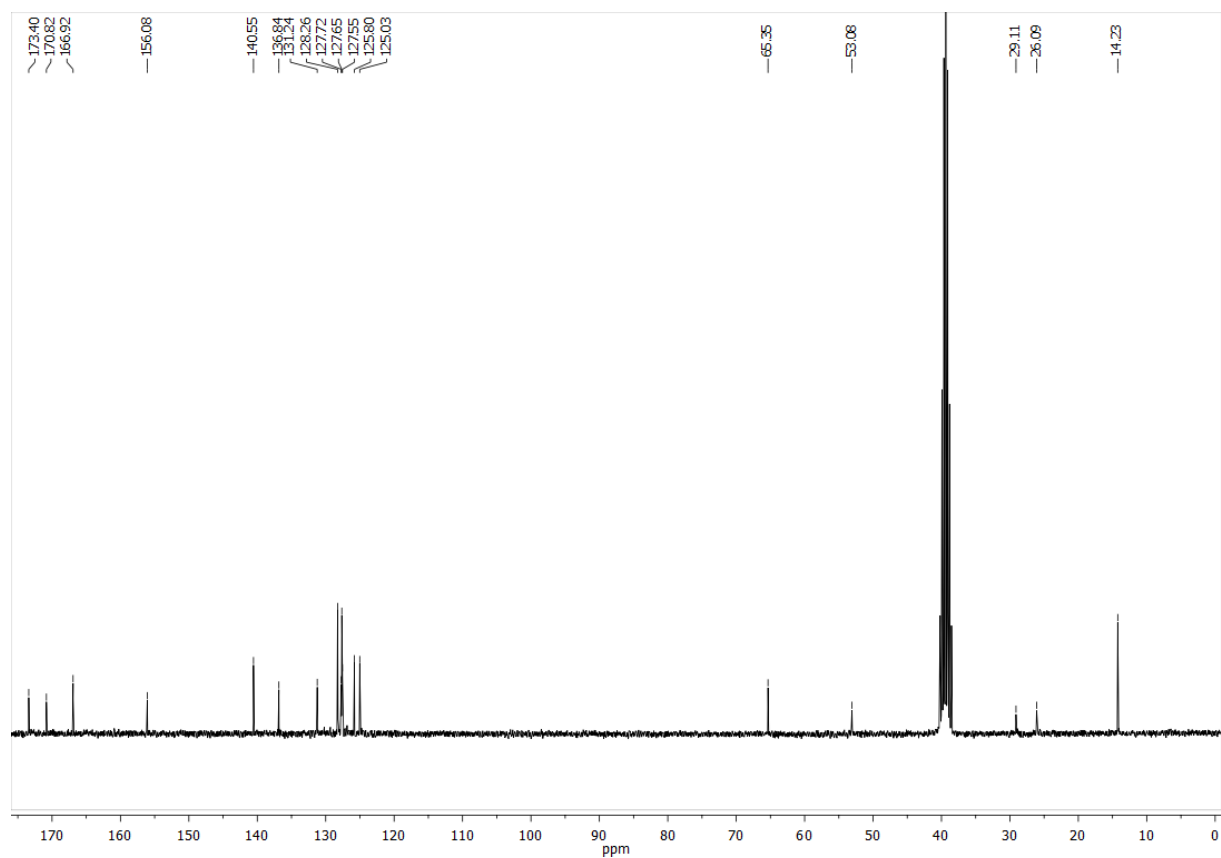
^{1}H-NMR (400 MHz, DMSO-d_6) for compound **7**:
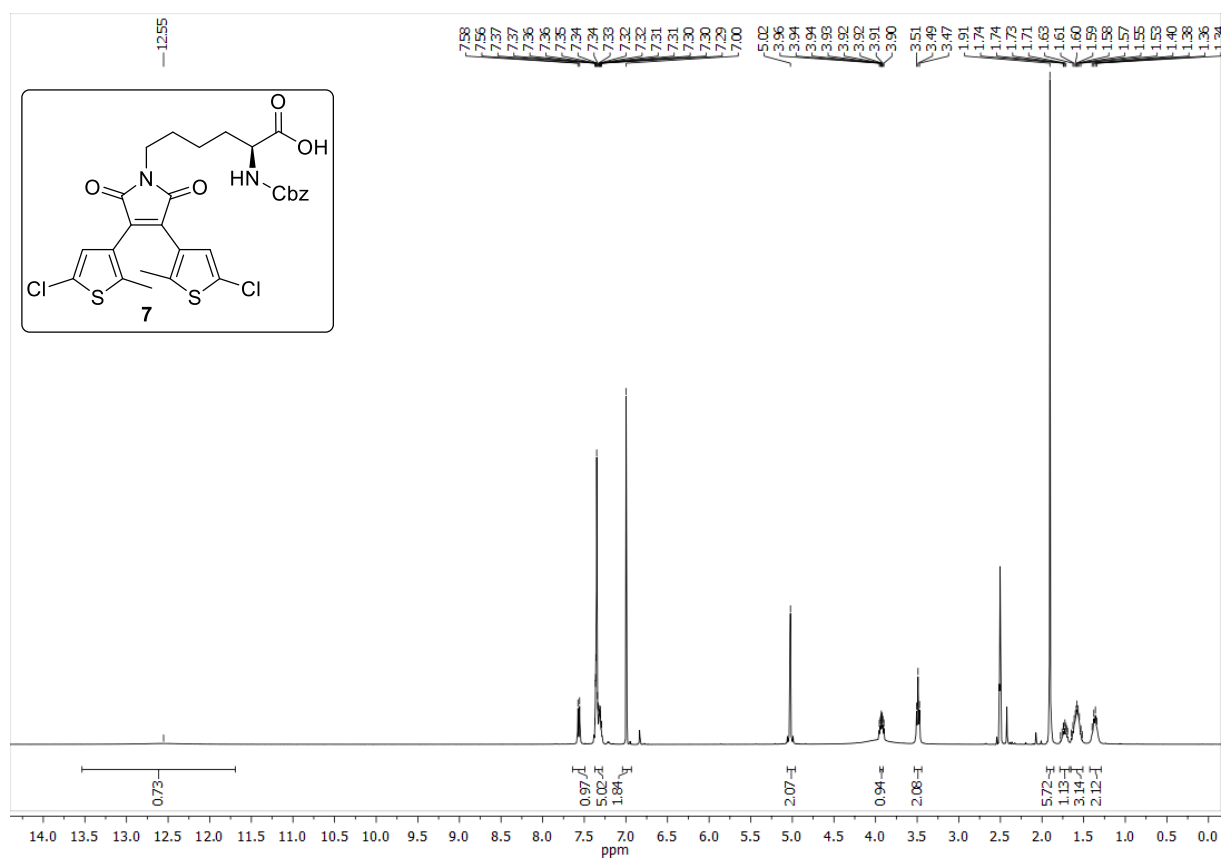
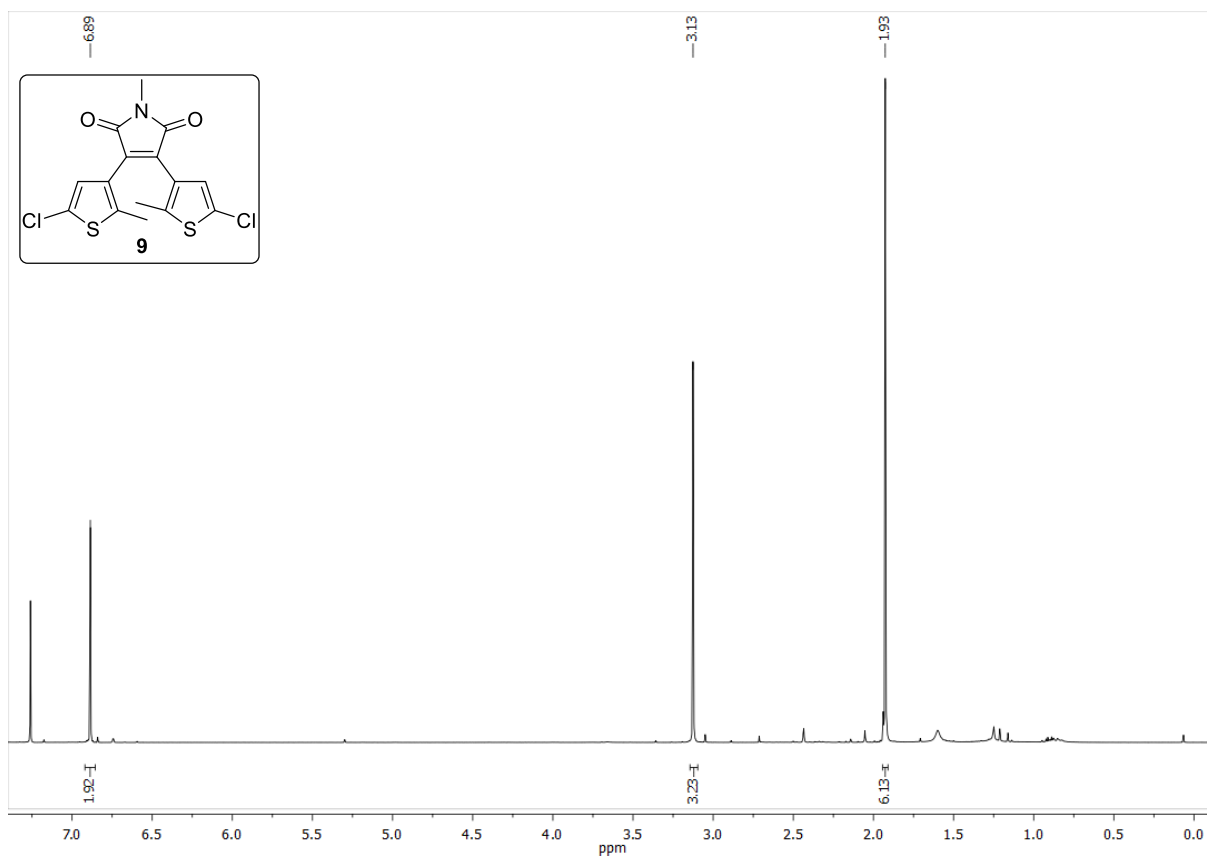## ^{13}C-NMR (101 MHz, DMSO-d_6) for compound **7**:
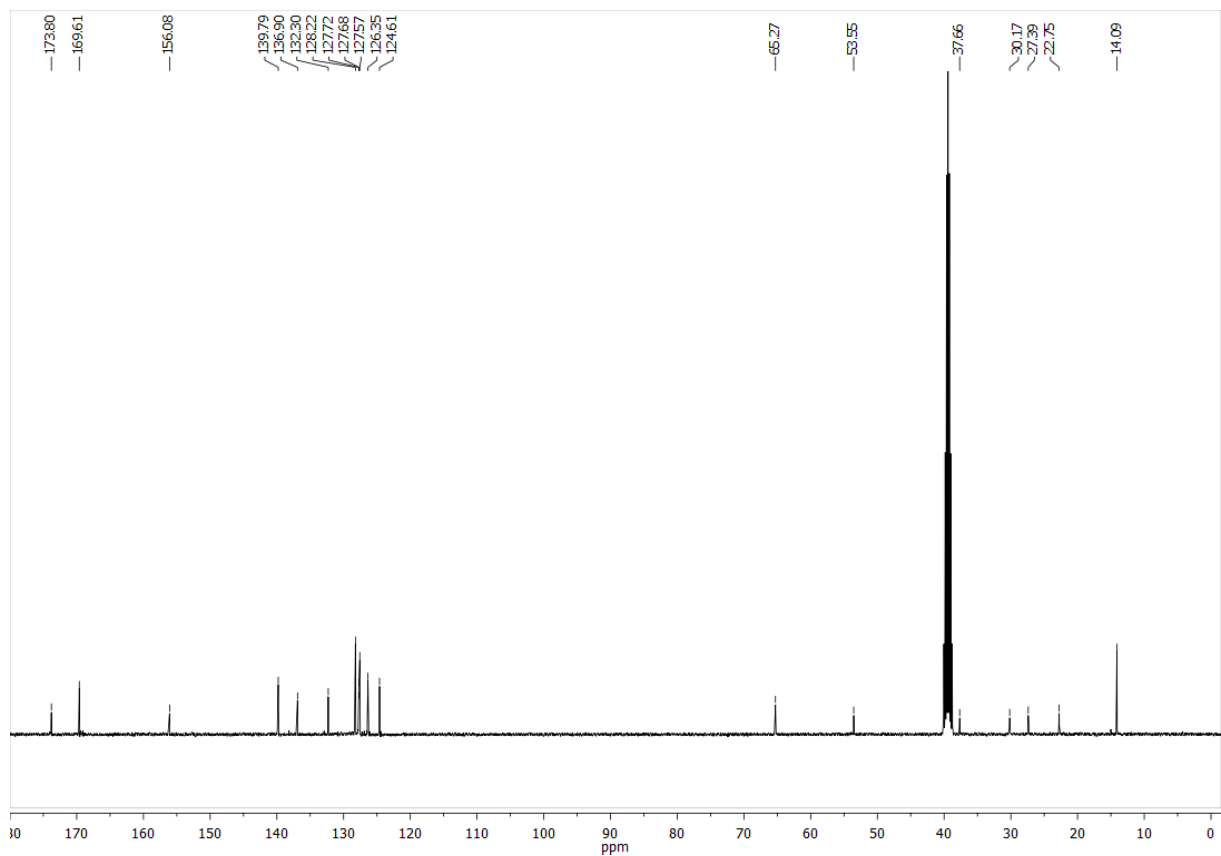
^{1}H-NMR (400 MHz, DMSO-d_6) for compound **8**:
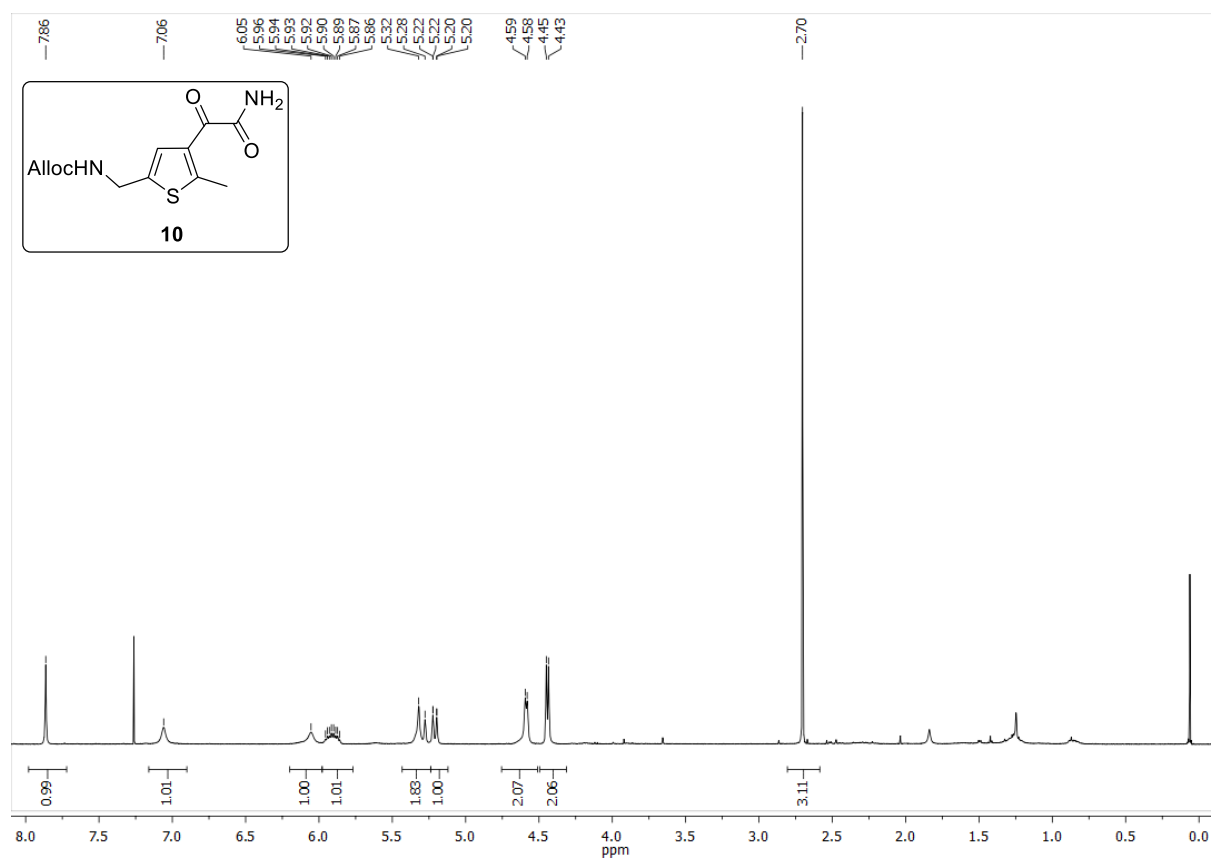

^{13}C-NMR (101 MHz, DMSO-d_6) for compound **8**:
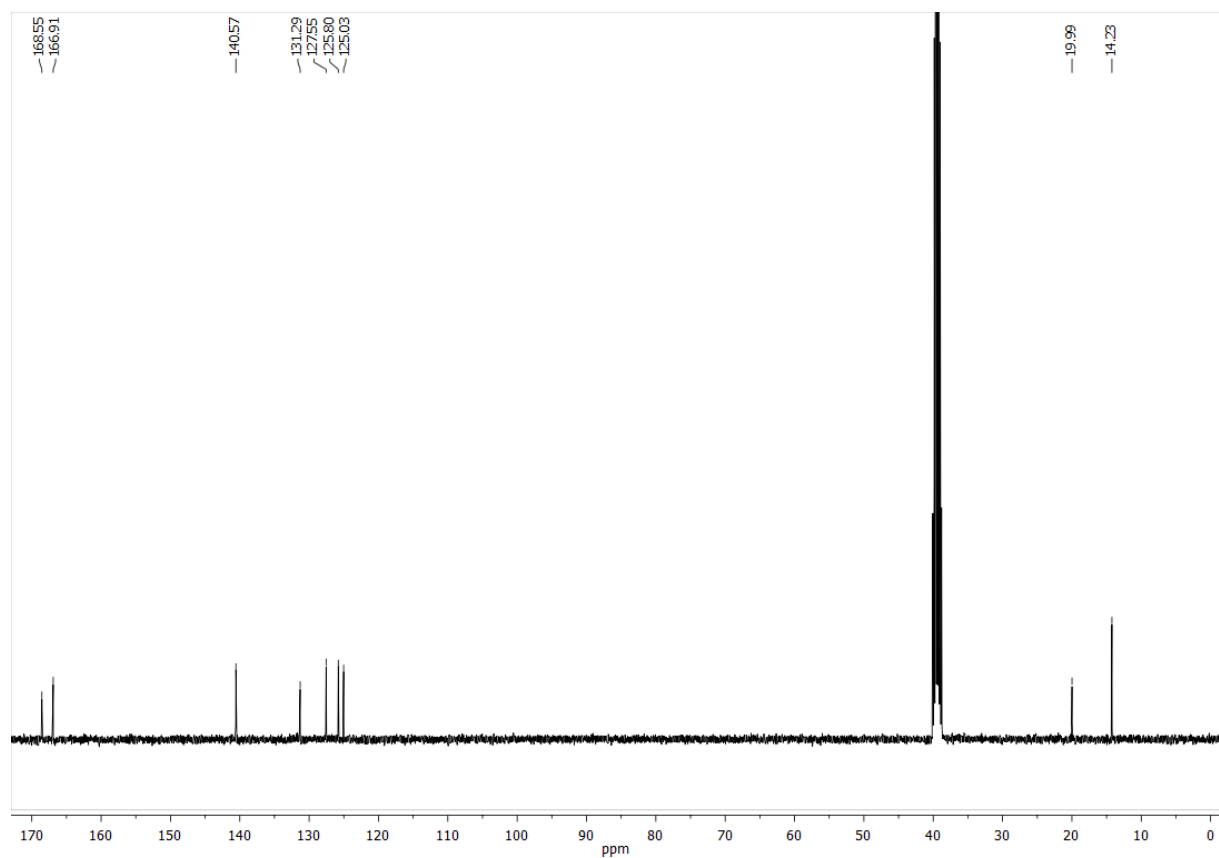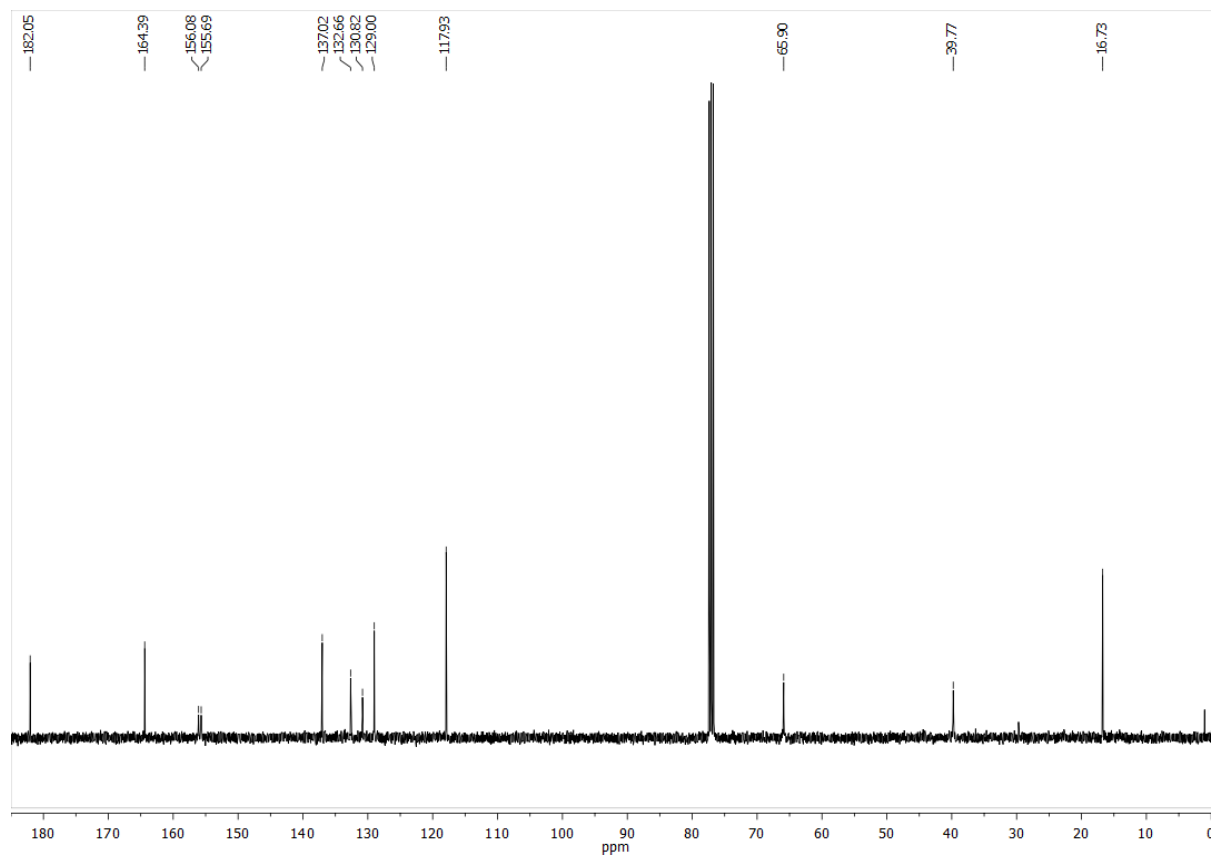
^{1}H-NMR (300 MHz, CDCl$_3$) for compound **9**:

^{13}C-NMR (75 MHz, CDCl$_3$) for compound **9**:
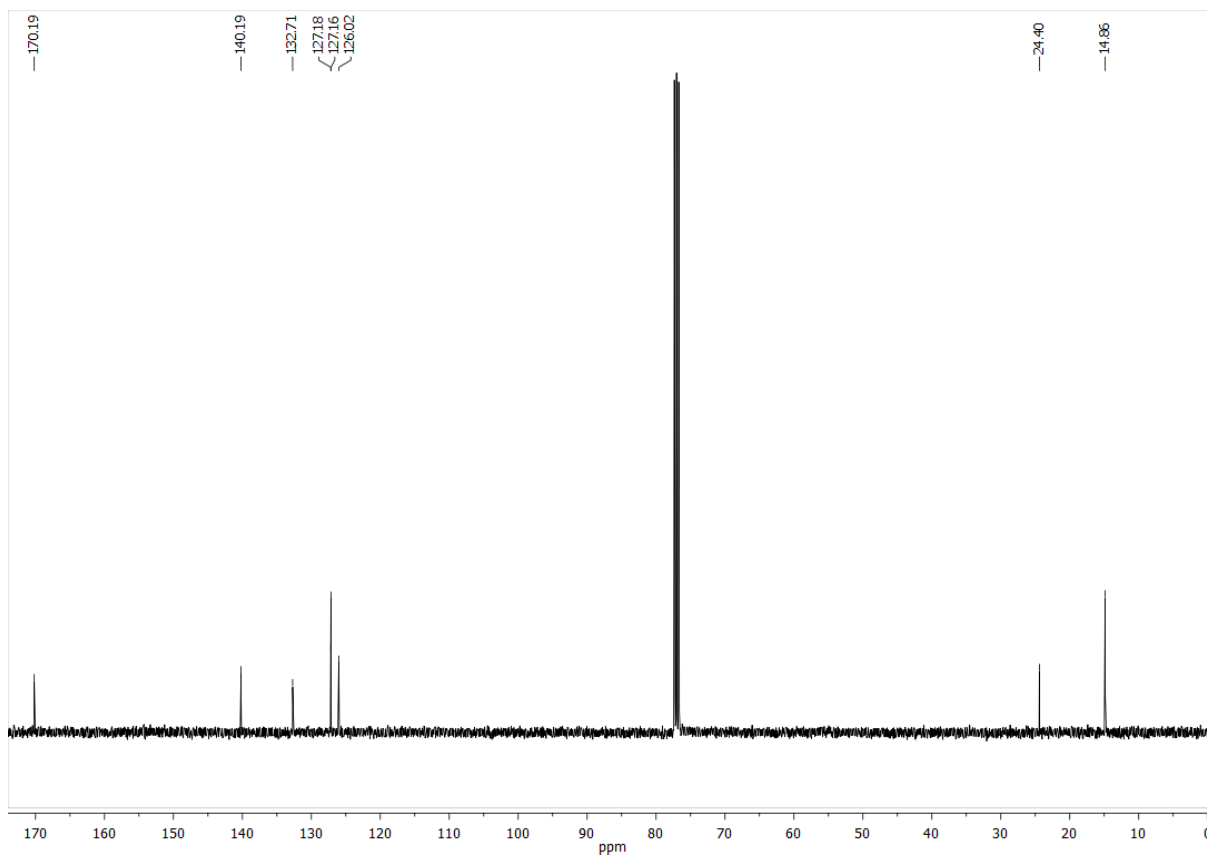
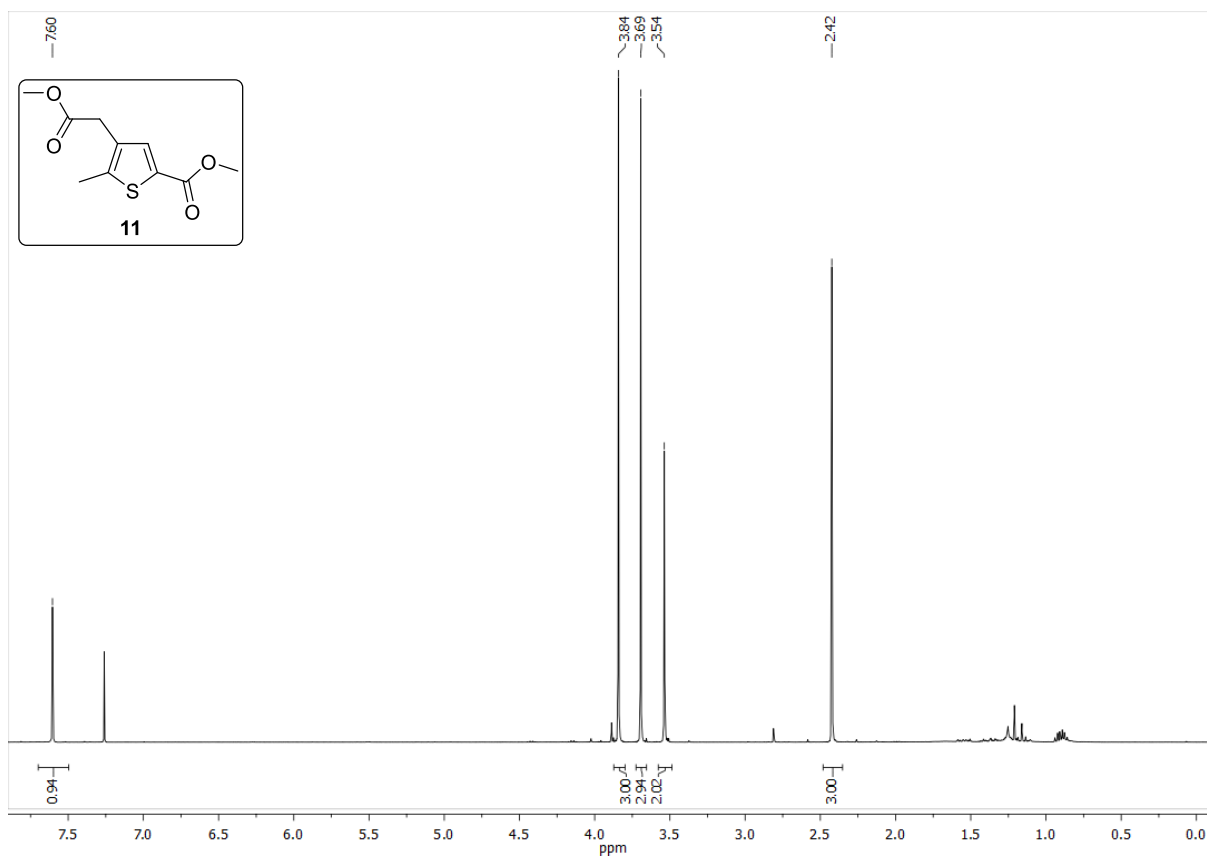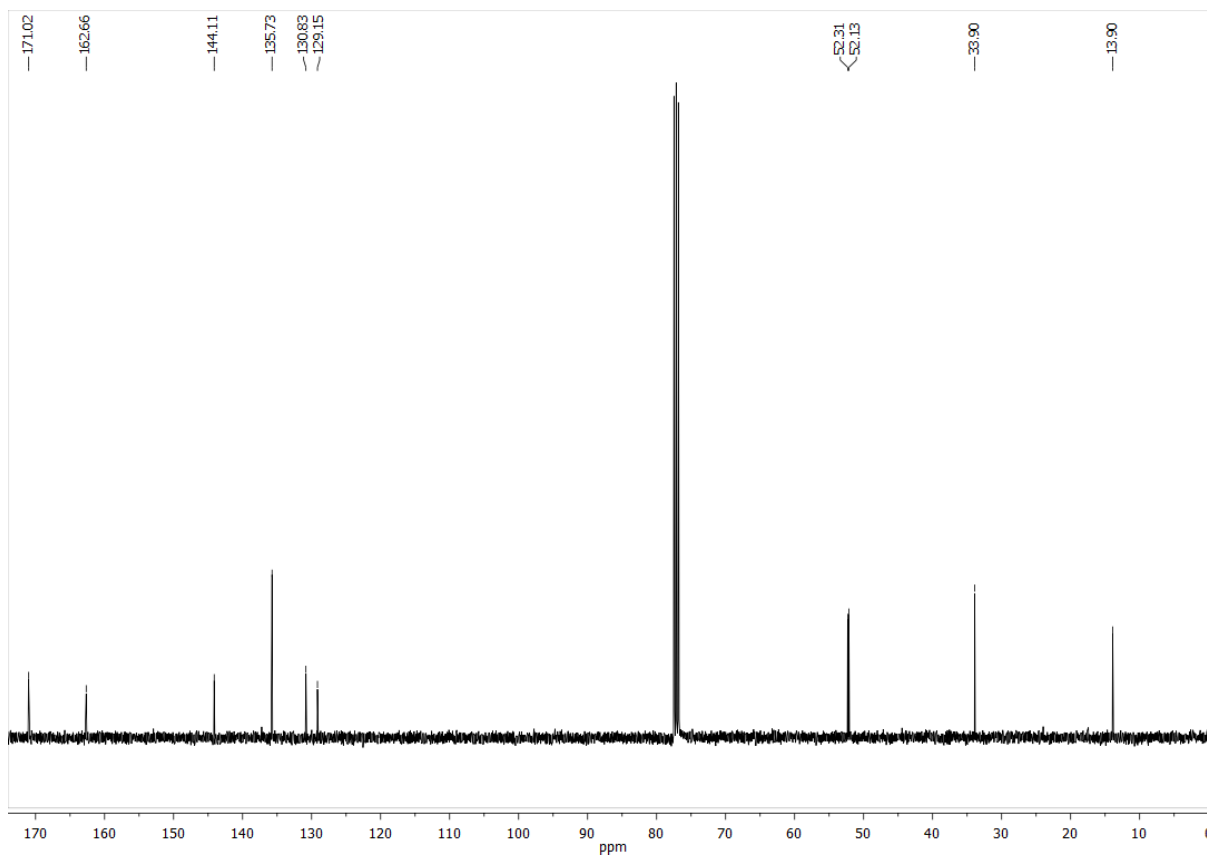^{1}H-NMR (400 MHz, CDCl$_3$) for compound **10**:

^{13}C-NMR (101 MHz, CDCl$_3$) for compound **10**:

^{1}H-NMR (400 MHz, CDCl$_3$) for compound **11**:

^{13}C-NMR (101 MHz, CDCl$_3$) for compound **11**:

^{1}H-NMR (400 MHz, CDCl$_3$) for compound **11S**:
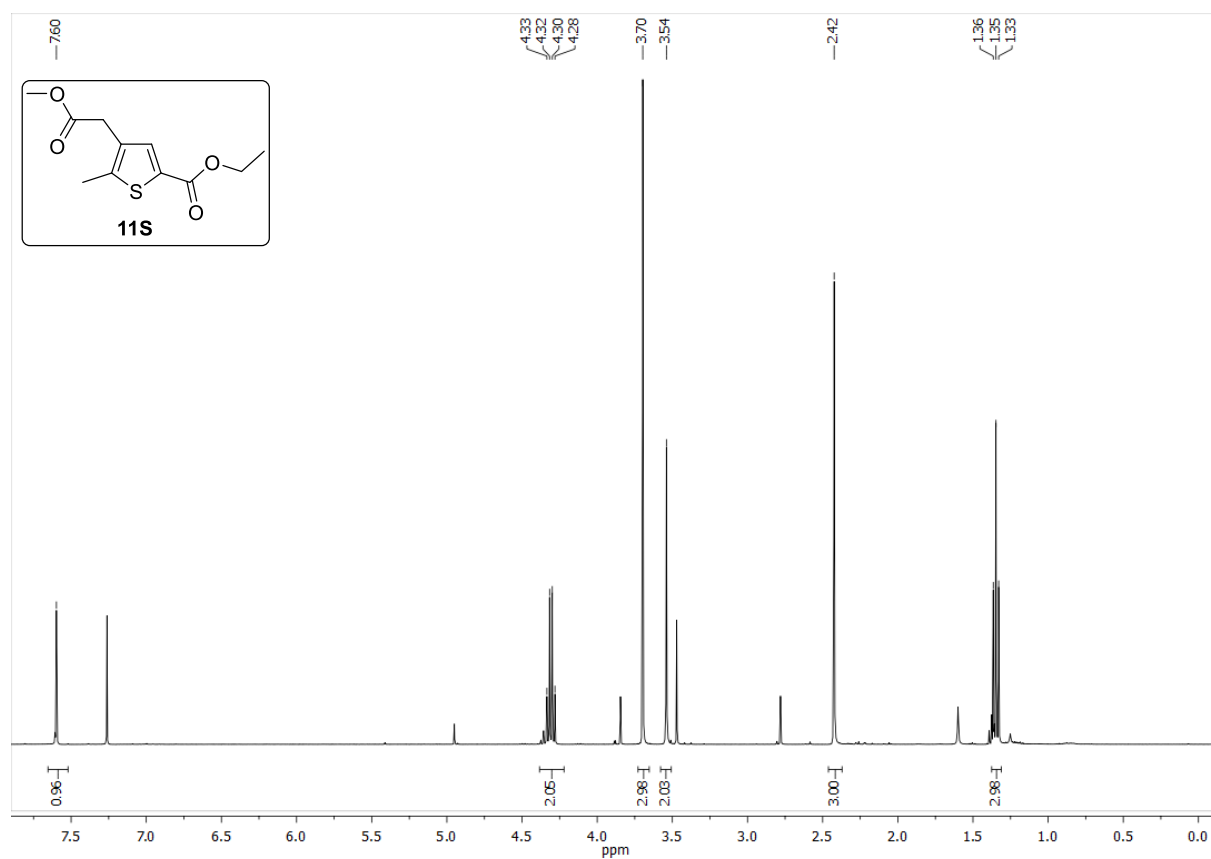
^{13}C-NMR (101 MHz, CDCl$_3$) for compound **11S**:
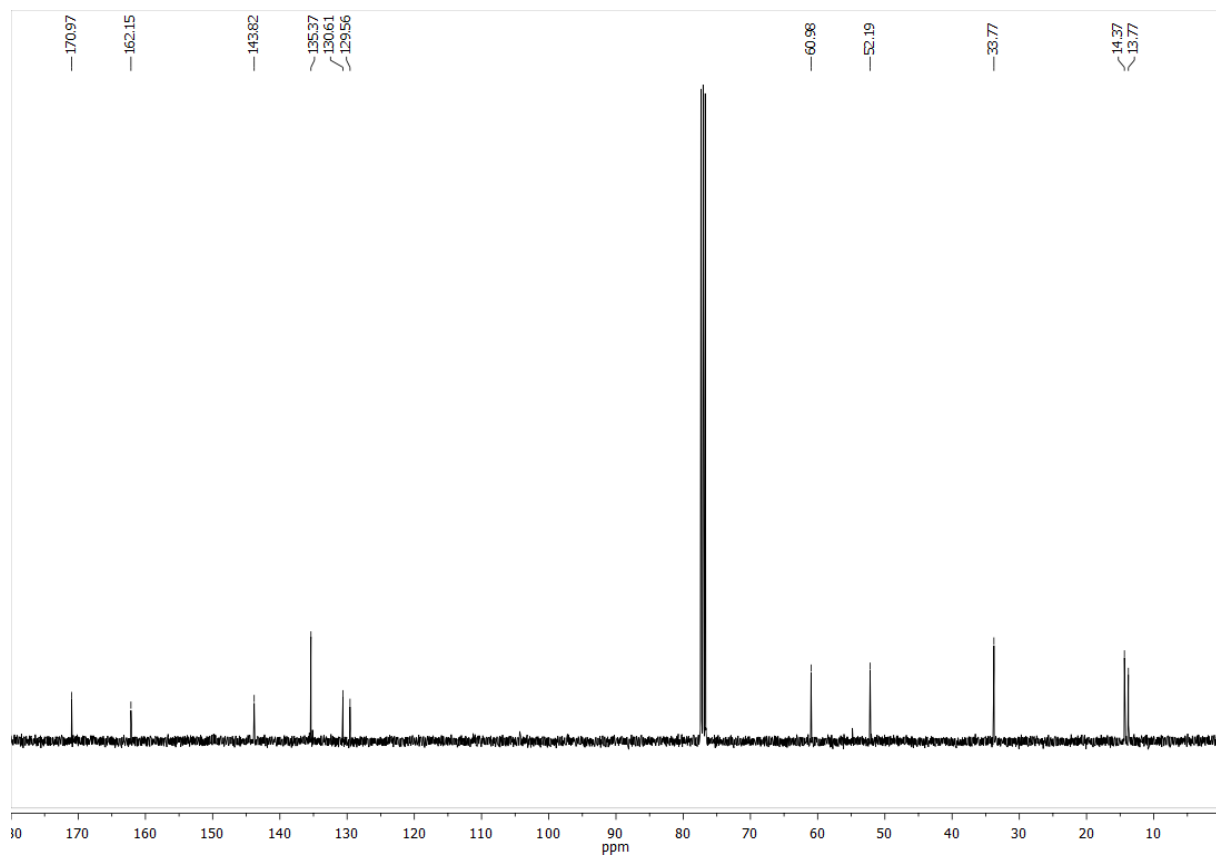
^{1}H-NMR (400 MHz, CDCl$_3$) for compound **12**:
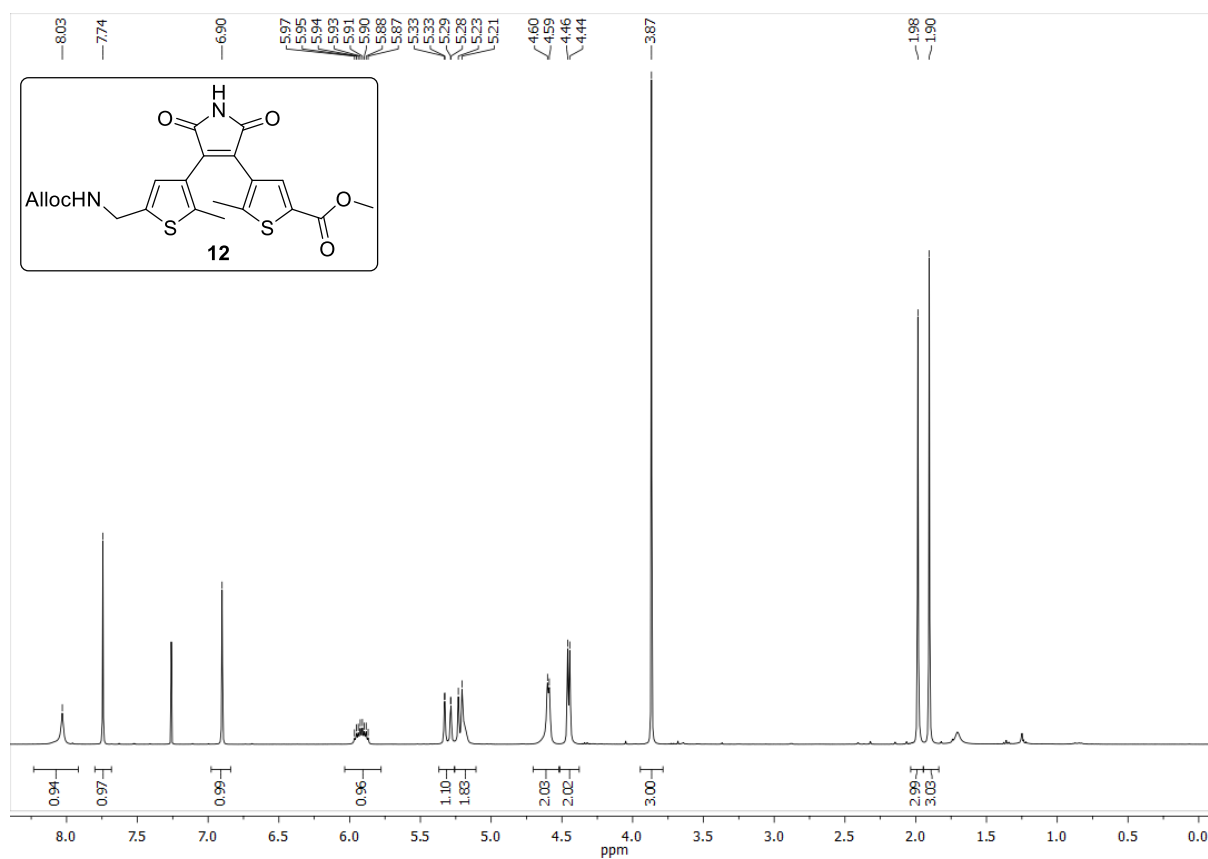
^{13}C-NMR (101 MHz, CDCl$_3$) for compound **12**:
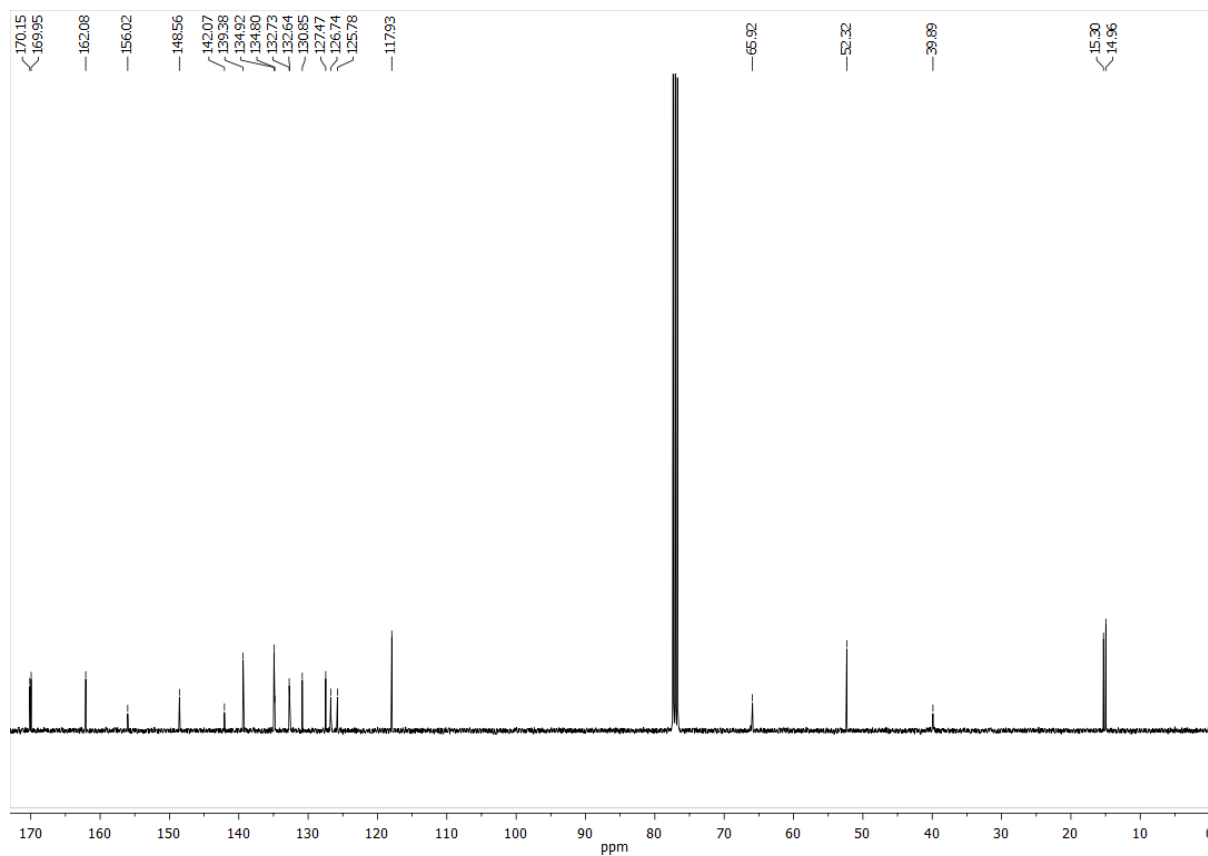
^{1}H-NMR (400 MHz, CDCl$_3$) for compound **12S**:
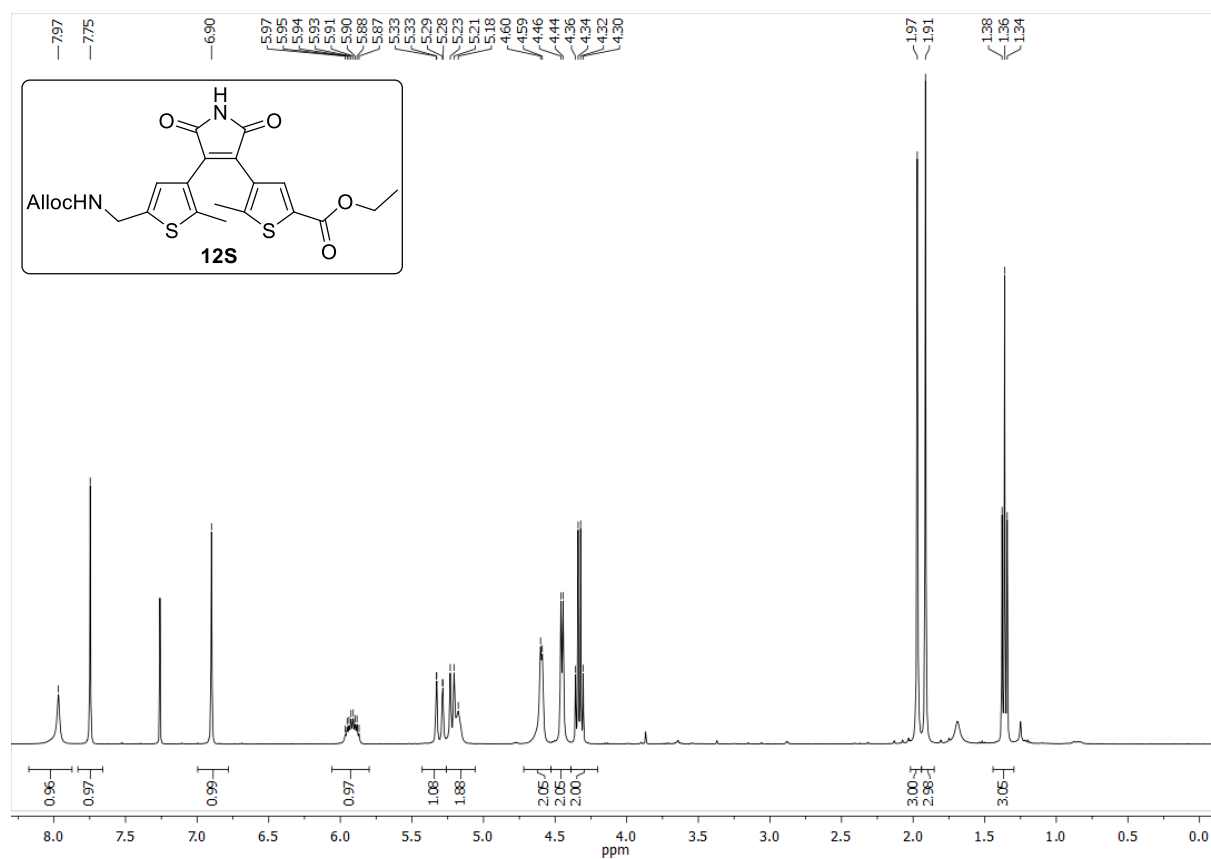
^{13}C-NMR (101 MHz, CDCl$_3$) for compound **12S**:
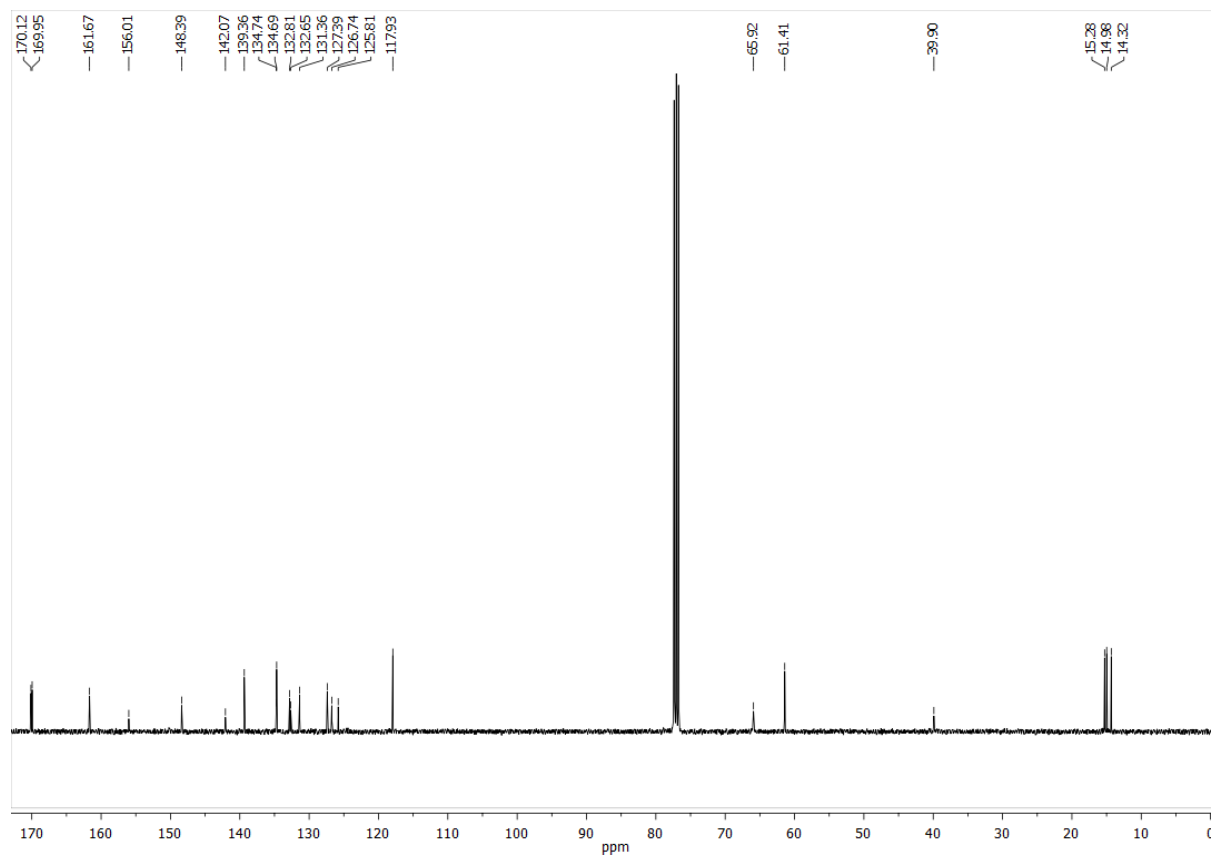
^{1}H-NMR (600 MHz, MeOD) for compound **13a**:
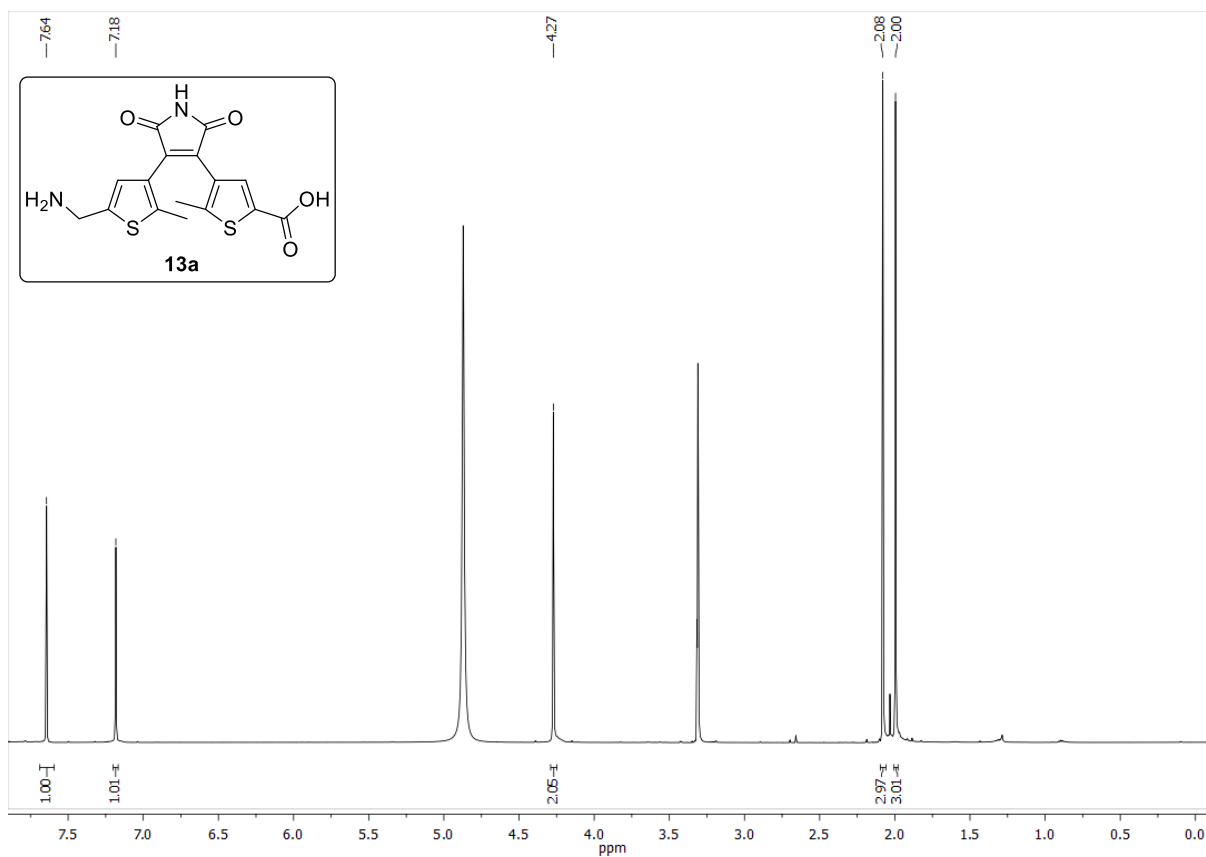
^{13}C-NMR (151 MHz, MeOD) for compound **13a**:
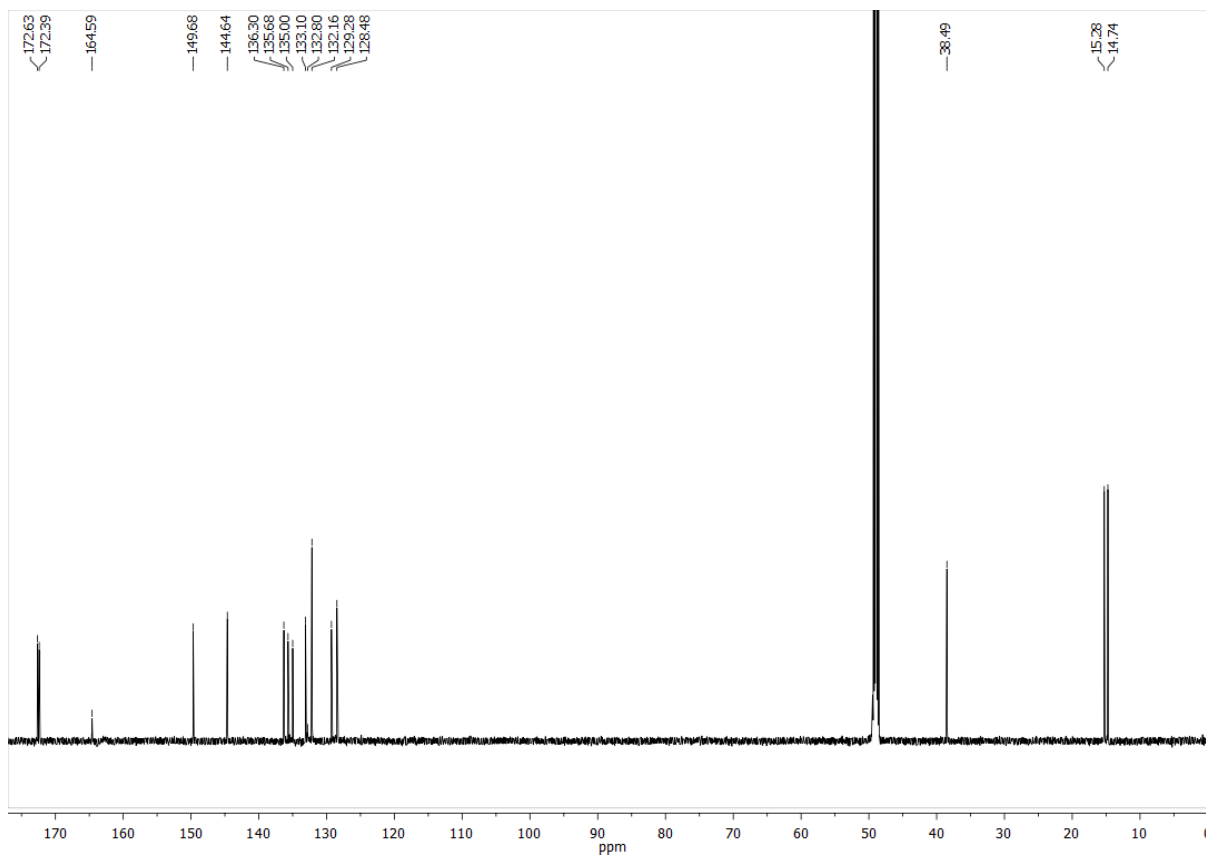
^{1}H-NMR (300 MHz, CD$_3$CN) for compound **13b**:

^{13}C-NMR (75 MHz, CD$_3$CN) for compound **13b**:

^{1}H-NMR (300 MHz, DMSO-d_6) for compound **13S**:
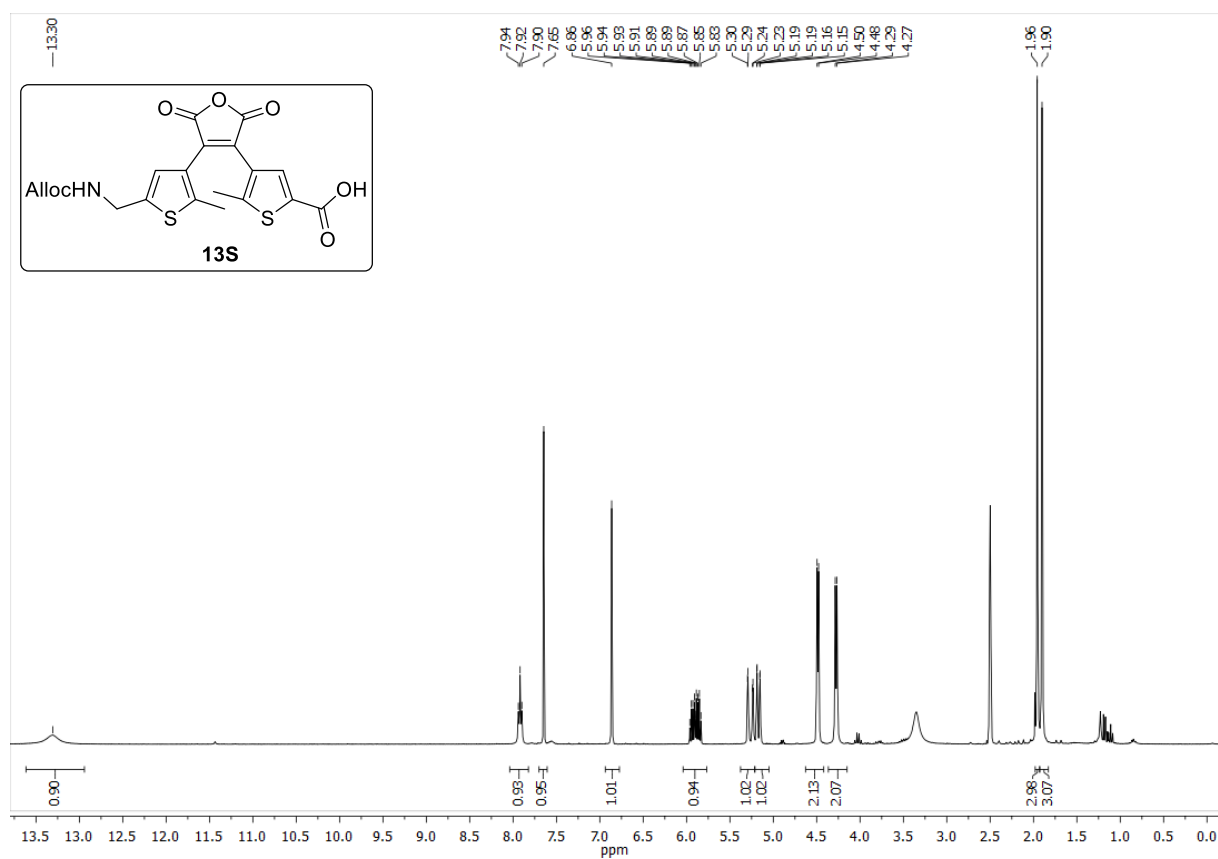
^{13}C-NMR (75 MHz, DMSO-d_6) for compound **13S**:
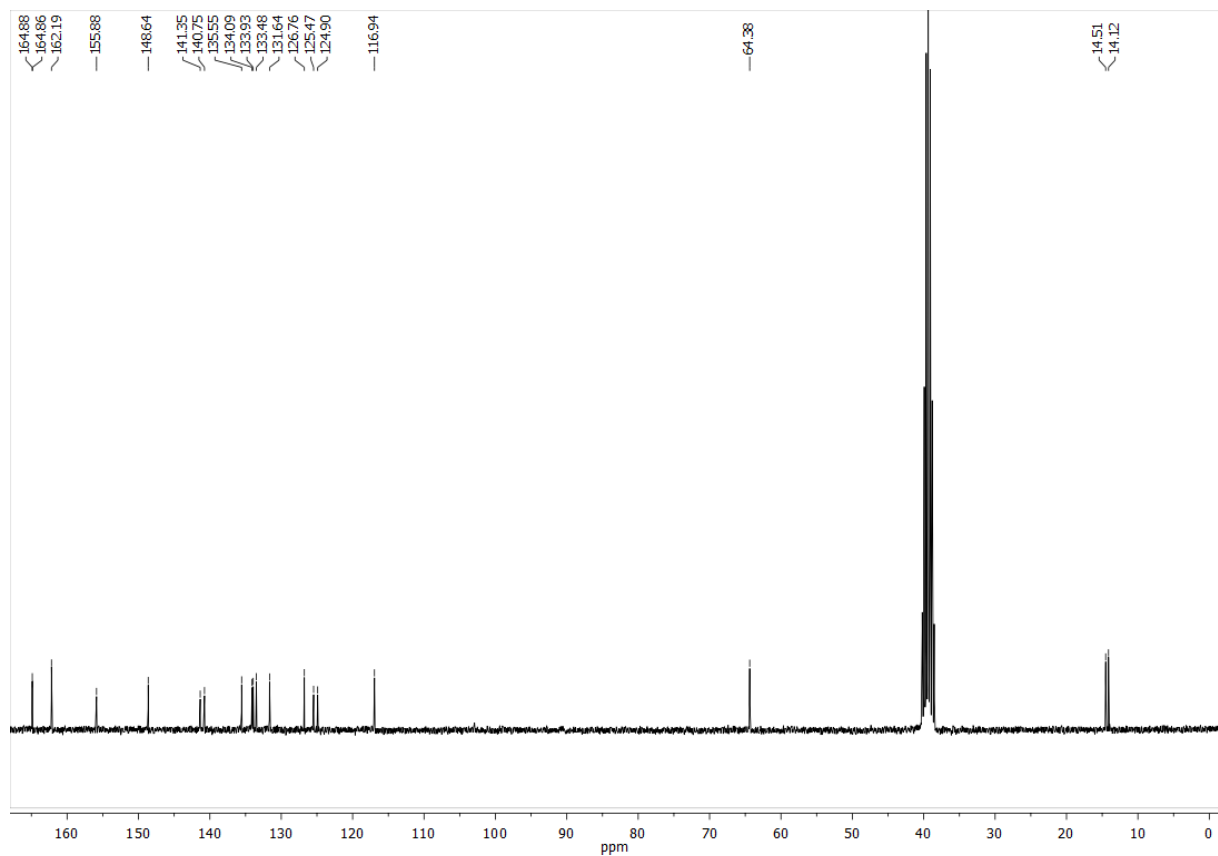
^{1}H-NMR (400 MHz, CDCl$_3$) for compound **17**:
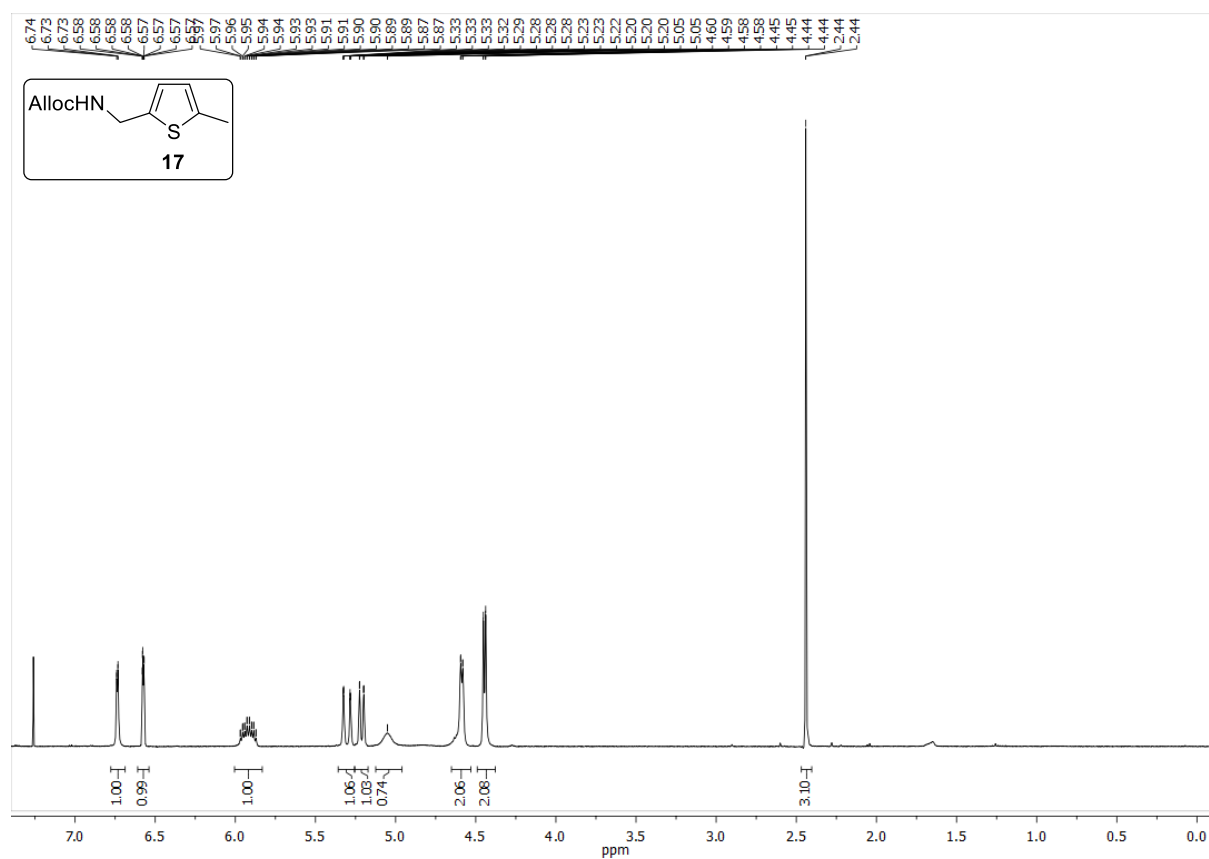
^{13}C-NMR (101 MHz, CDCl$_3$) for compound **17**:
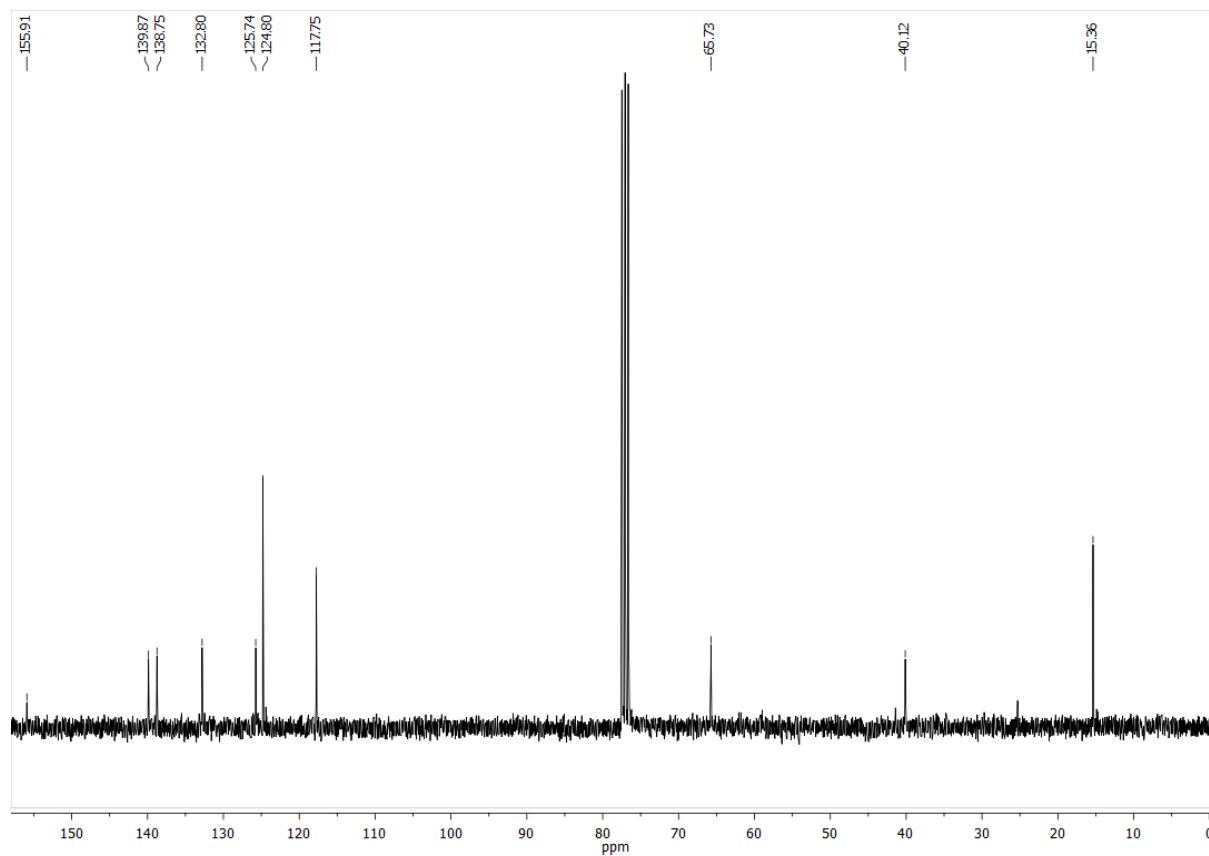
^{1}H-NMR (400 MHz, CDCl$_3$) for compound **18**:
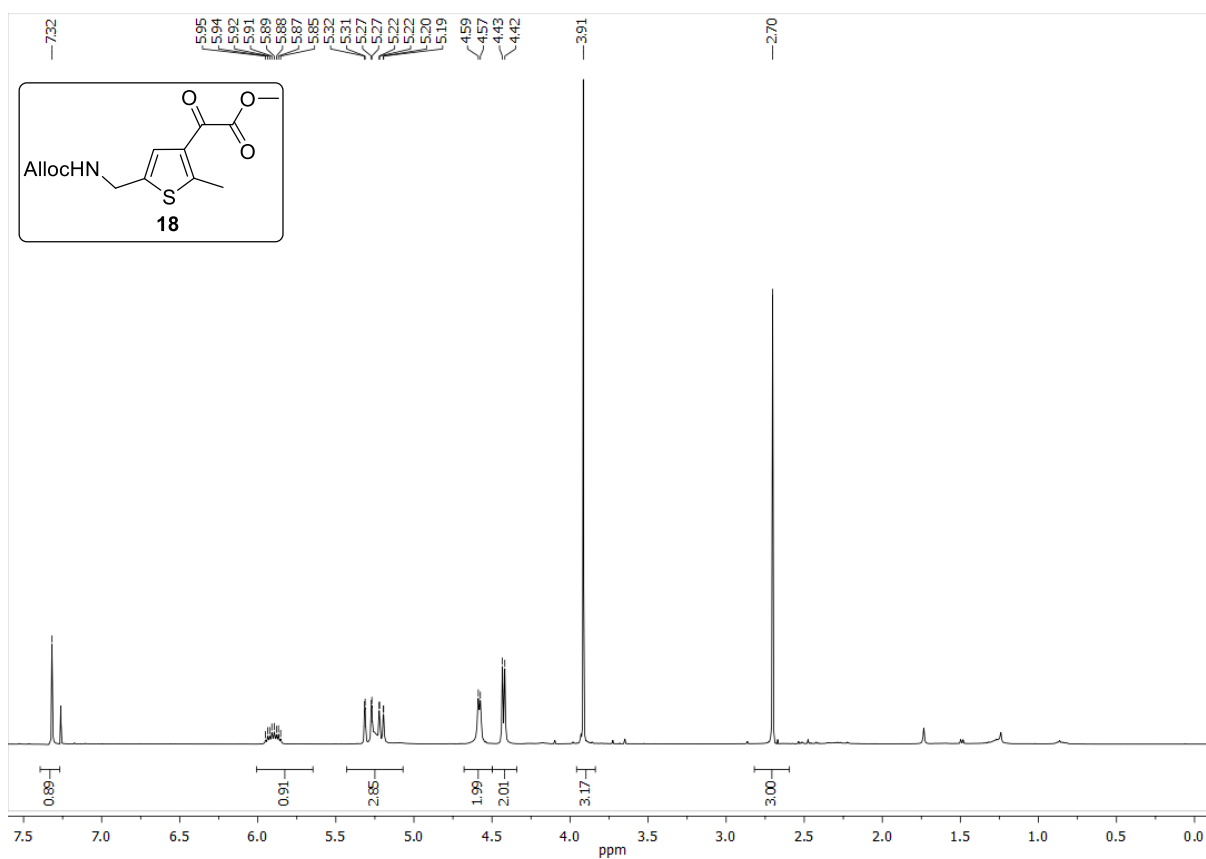
^{13}C-NMR (101 MHz, CDCl$_3$) for compound **18**:
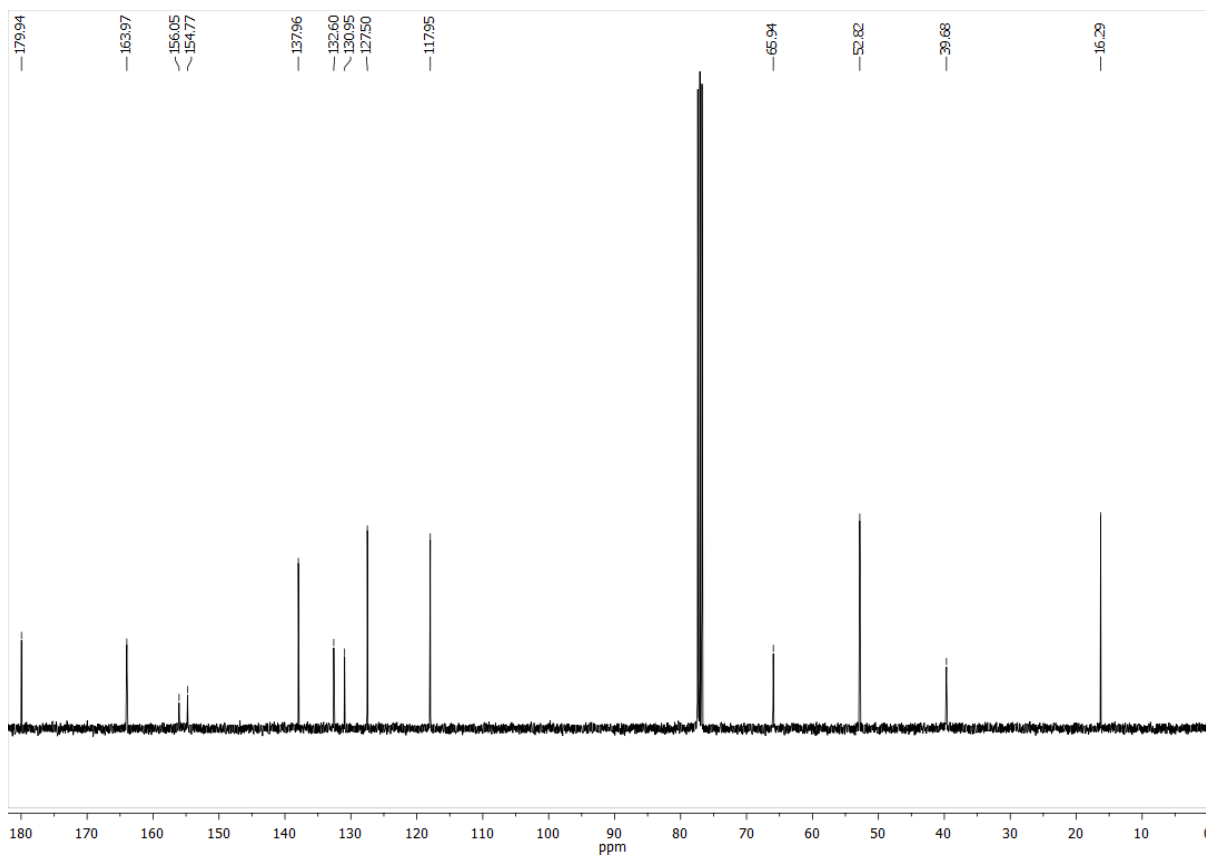
^{1}H-NMR (300 MHz, CDCl$_3$) for compound **21**:
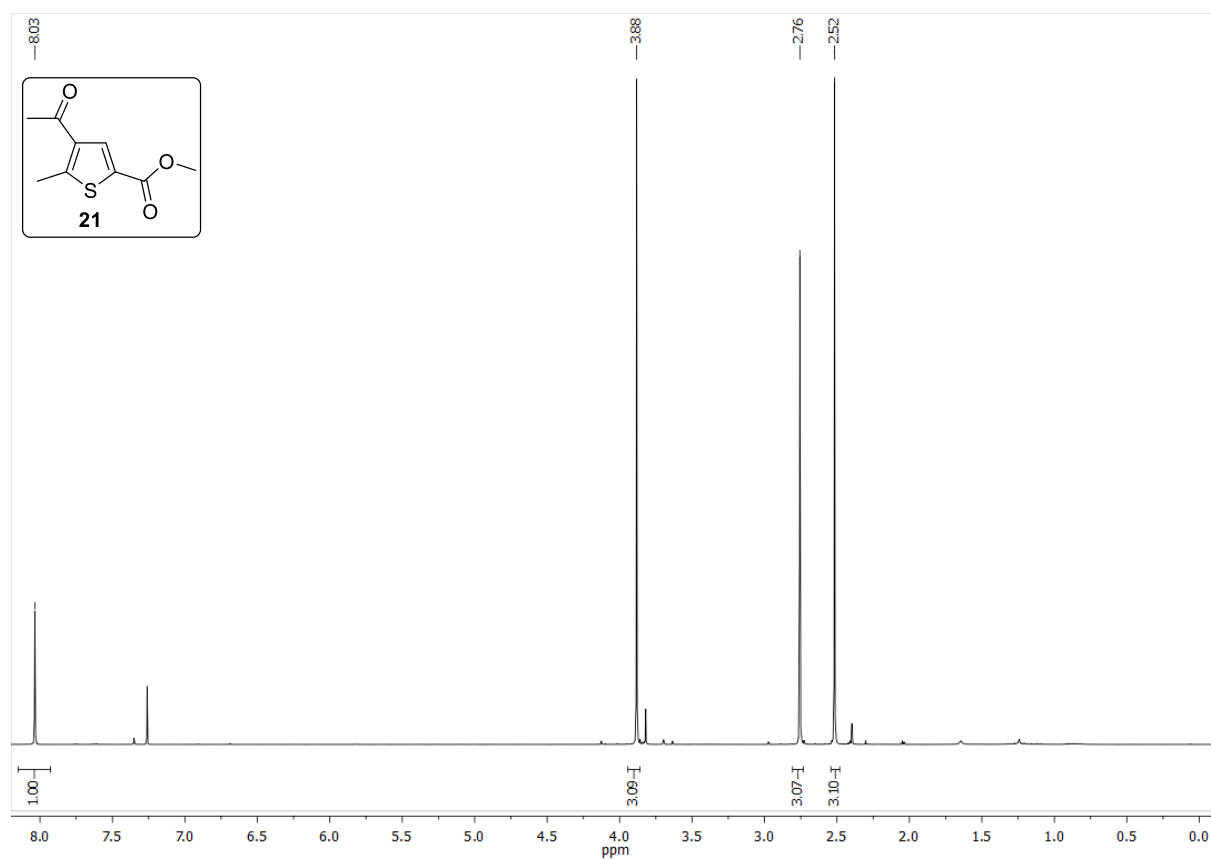
^{13}C-NMR (75 MHz, CDCl$_3$) for compound **21**:
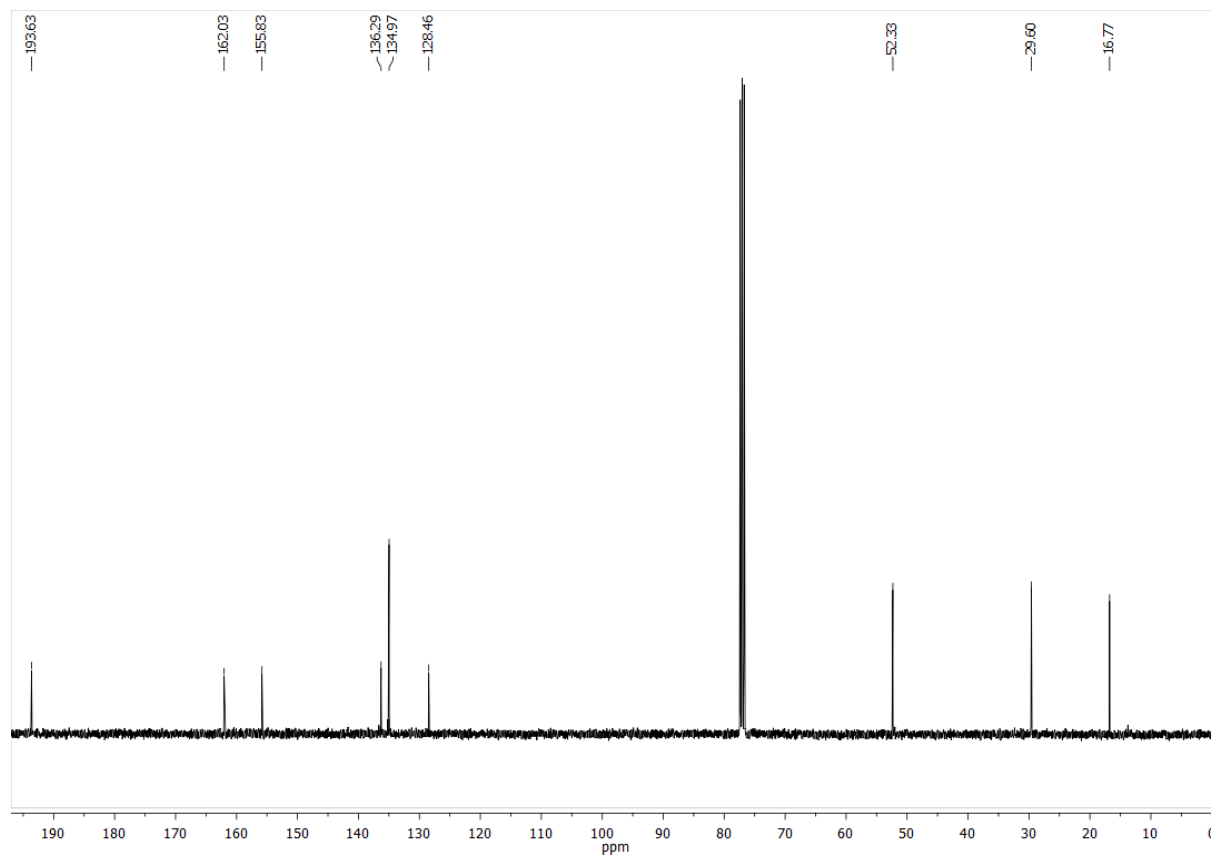
¹H-NMR (400 MHz, CDCl₃) for compound **21S**:
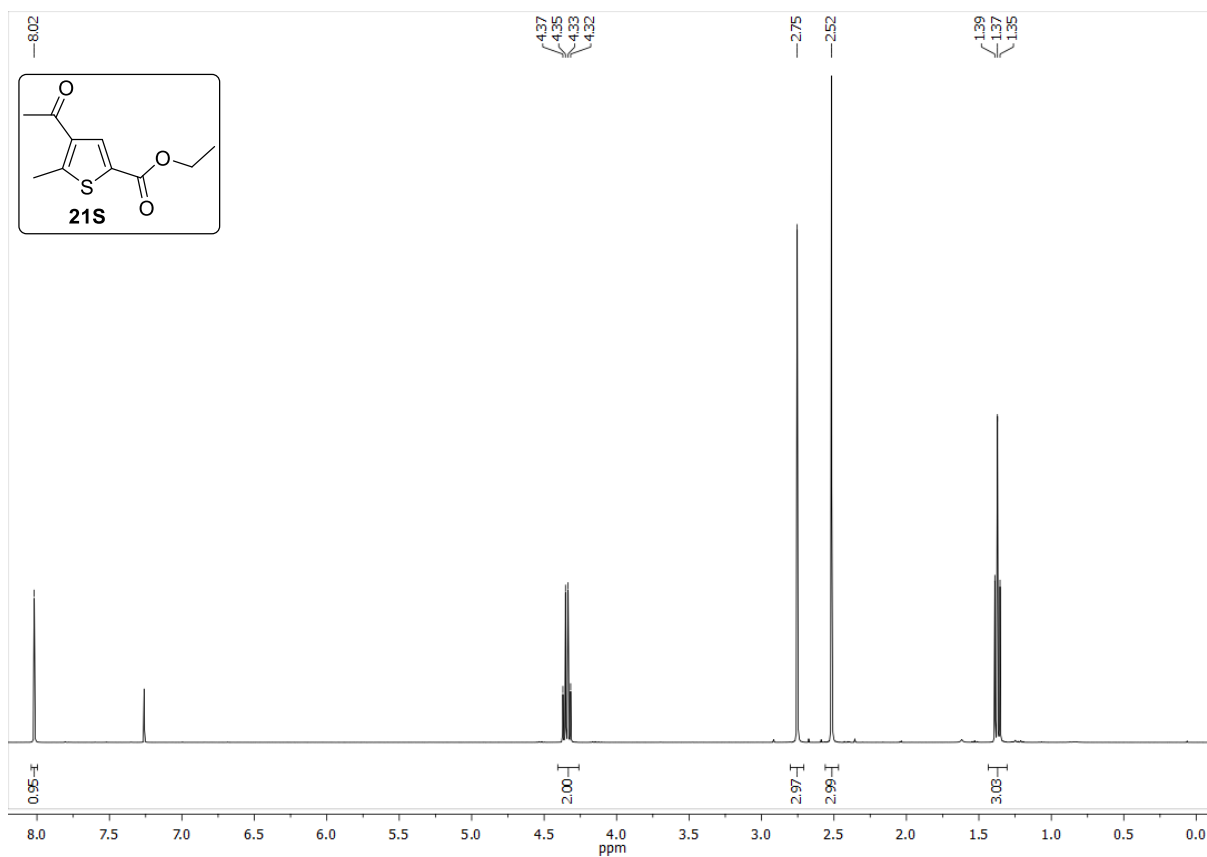
¹³C-NMR (101 MHz, CDCl₃) for compound **21S**:
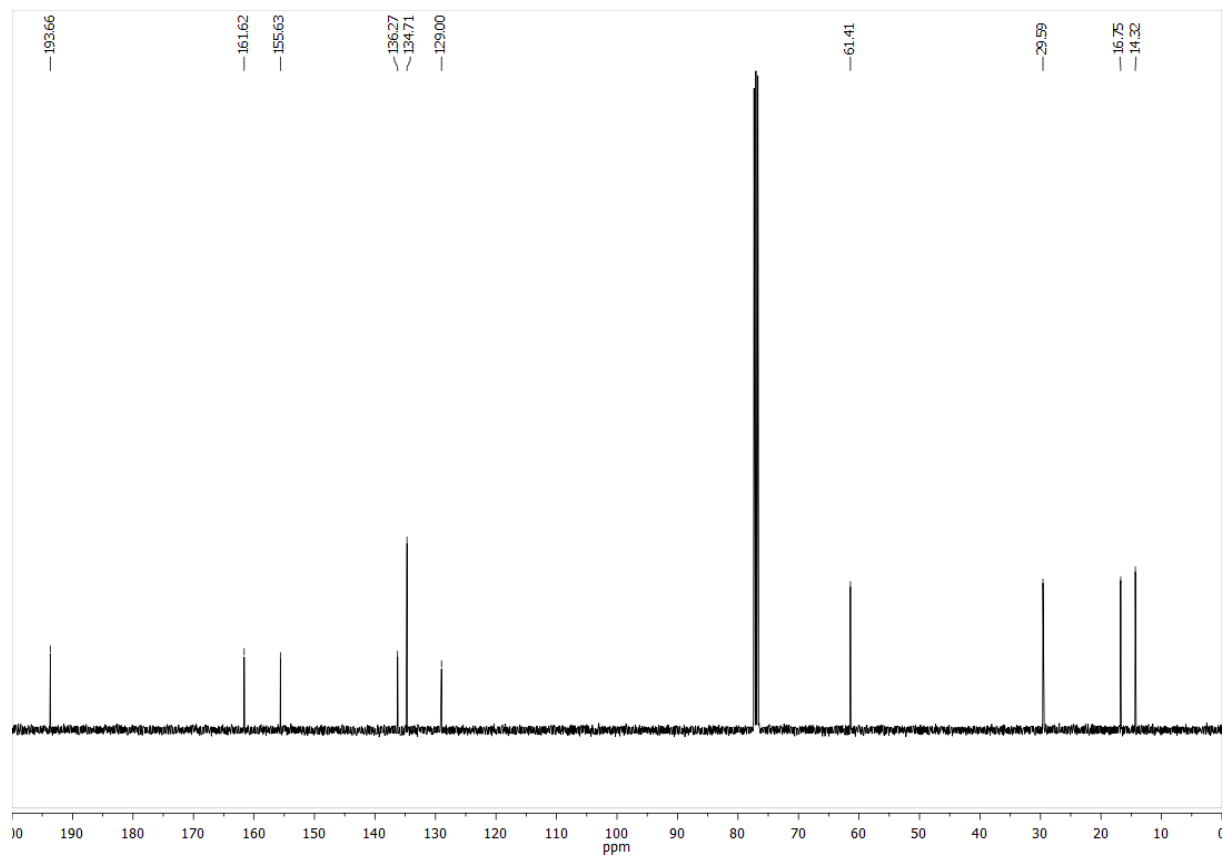
^{1}H-NMR (300 MHz, DMSO-d_6) for compound **23**:
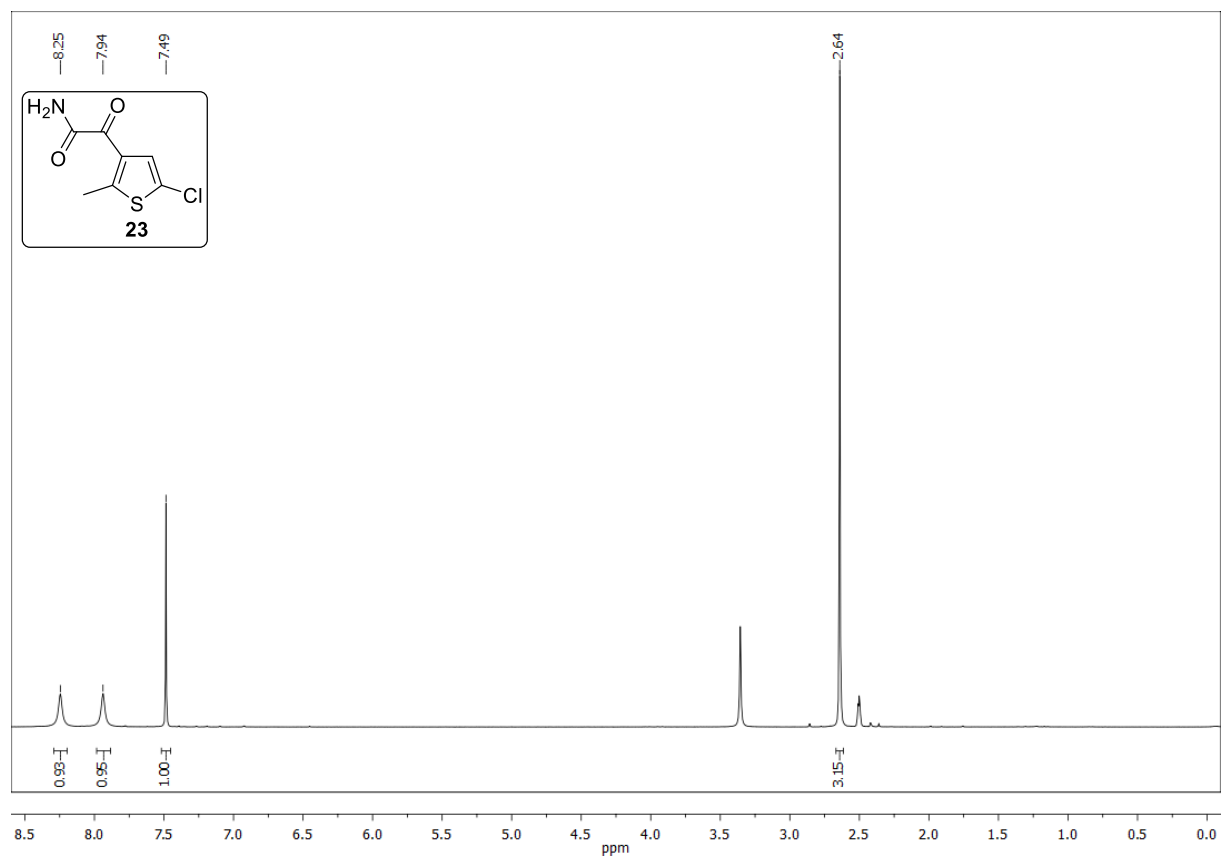
^{13}C-NMR (75 MHz, DMSO-d_6) for compound **23**:
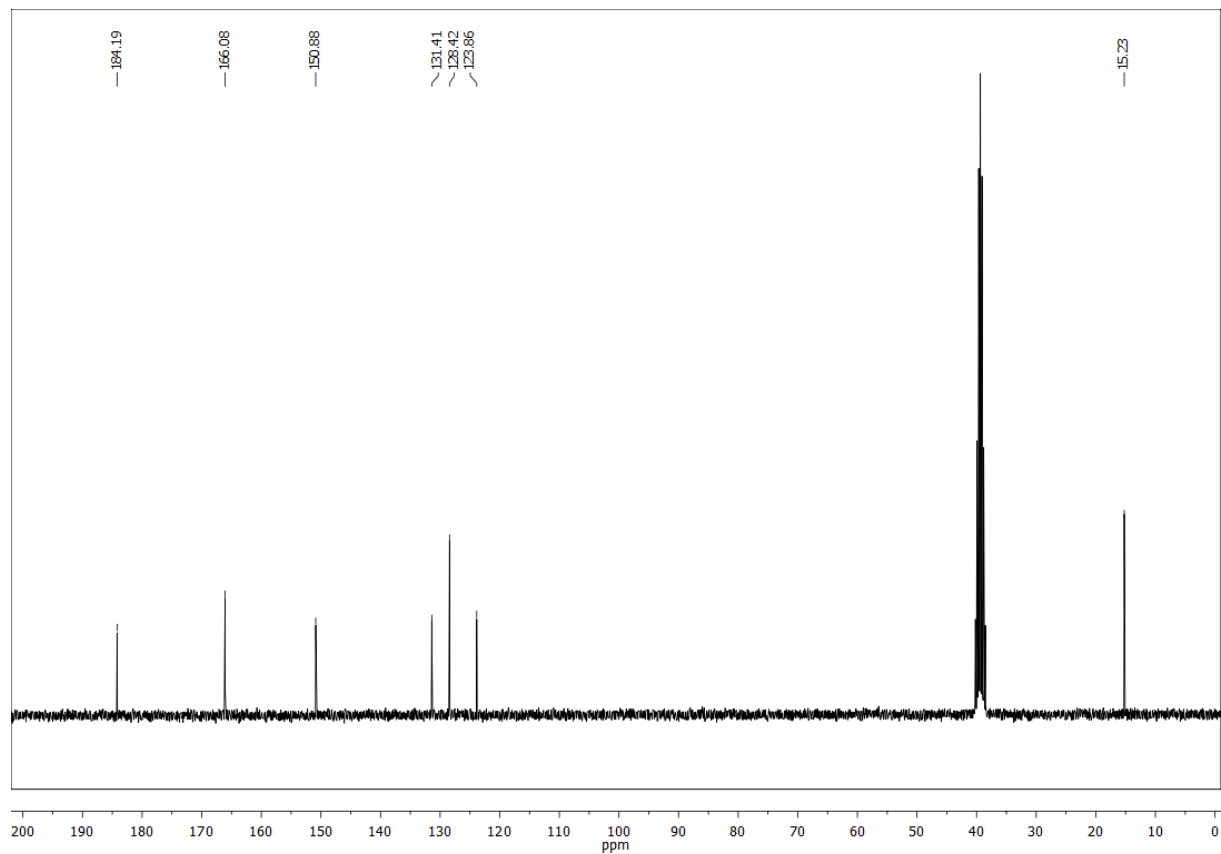
^{1}H-NMR (400 MHz, DMSO-d_6) for compound **24**:
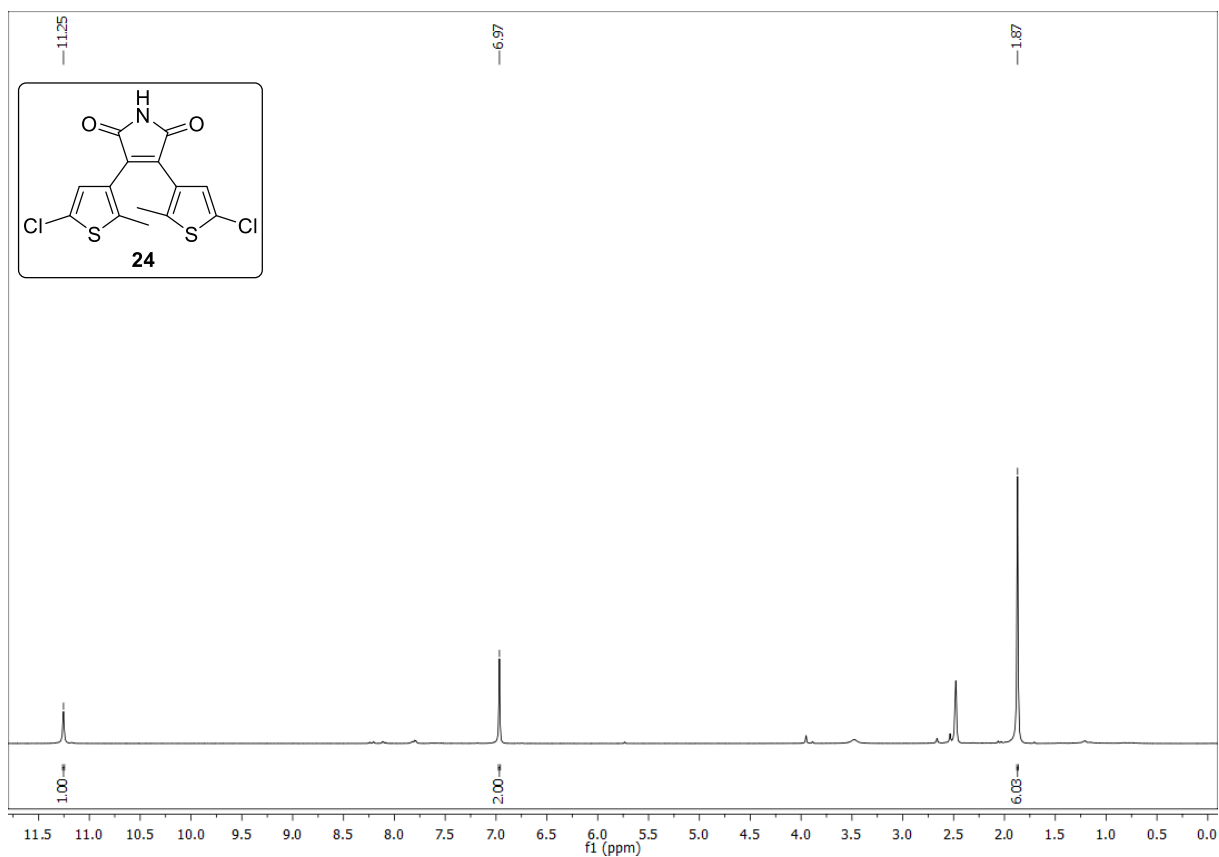
^{13}C-NMR (101 MHz, DMSO-d_6) for compound **24**:
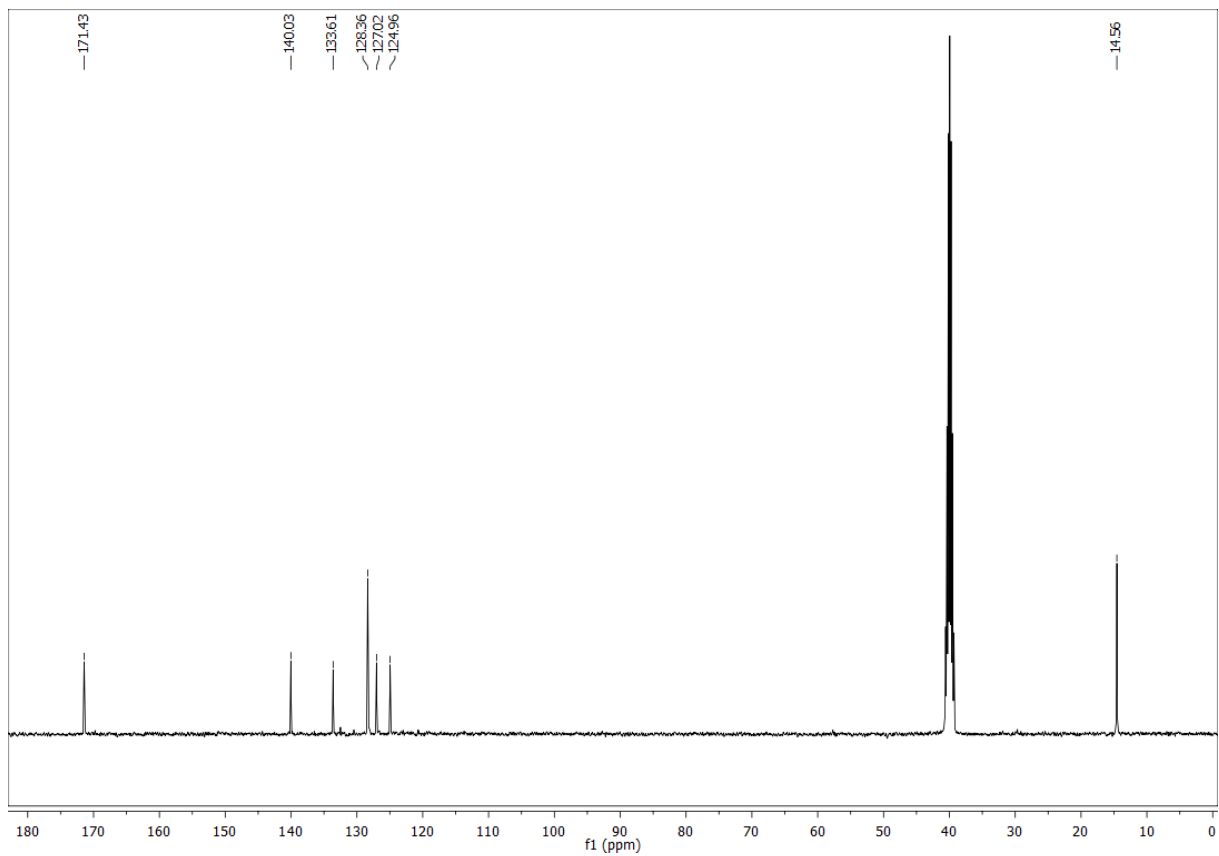
^{1}H-NMR (300 MHz, CDCl$_3$) for compound **26**:
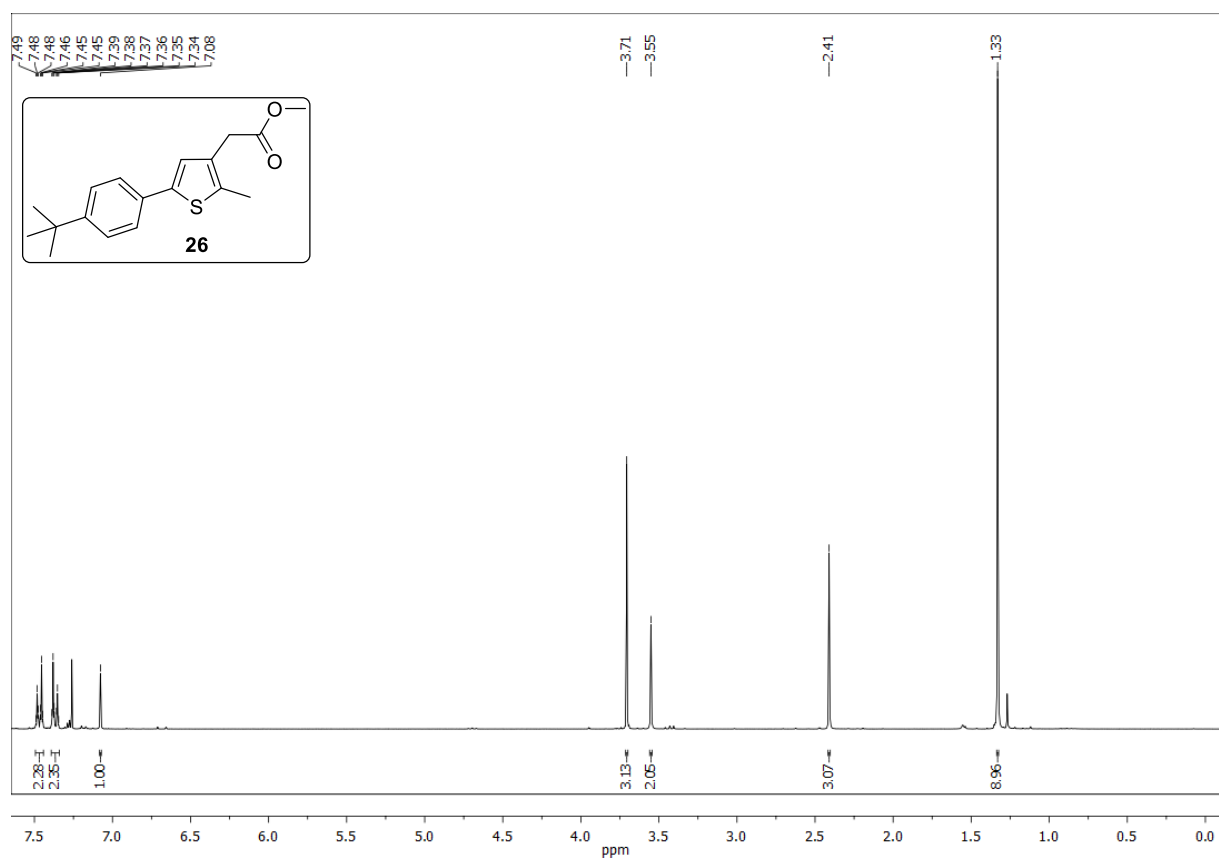
^{13}C-NMR (75 MHz, CDCl$_3$) for compound **26**:
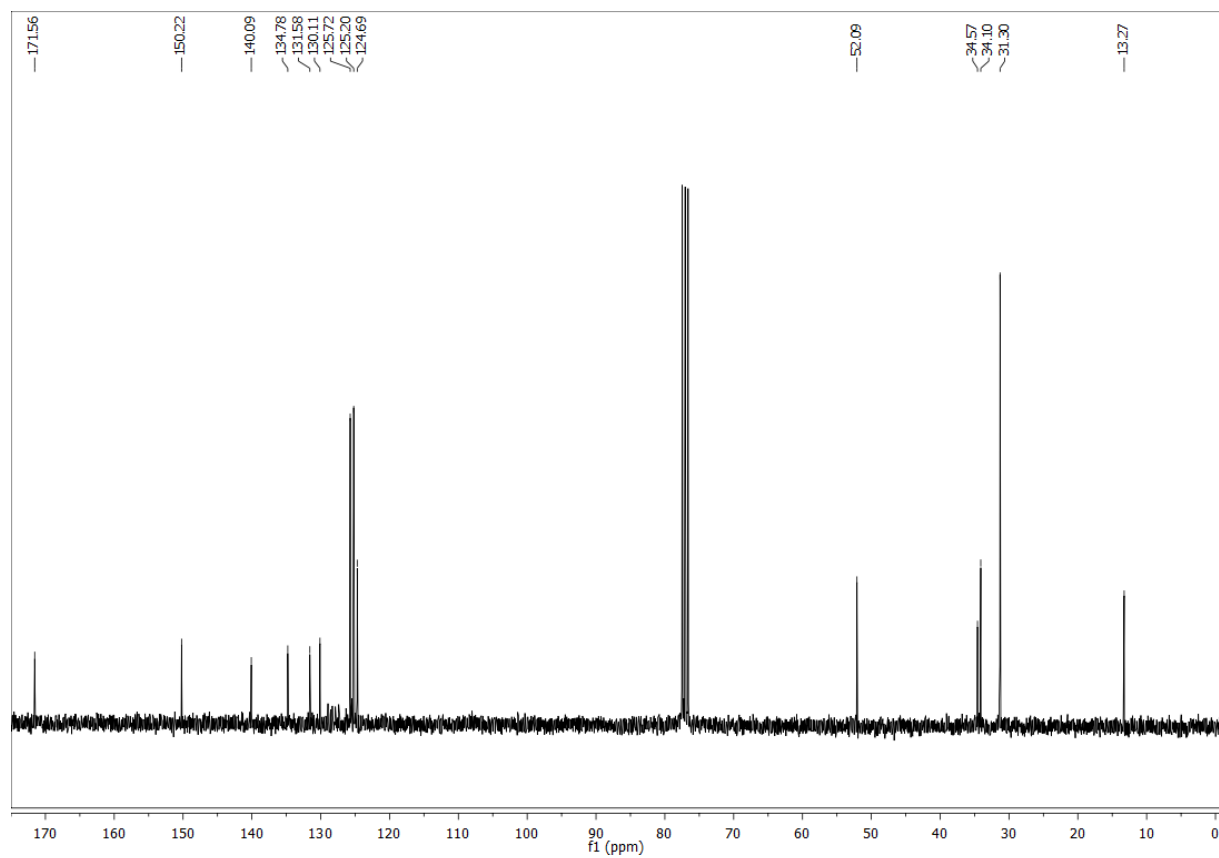
^{1}H-NMR (300 MHz, CDCl$_3$) for compound **27**:
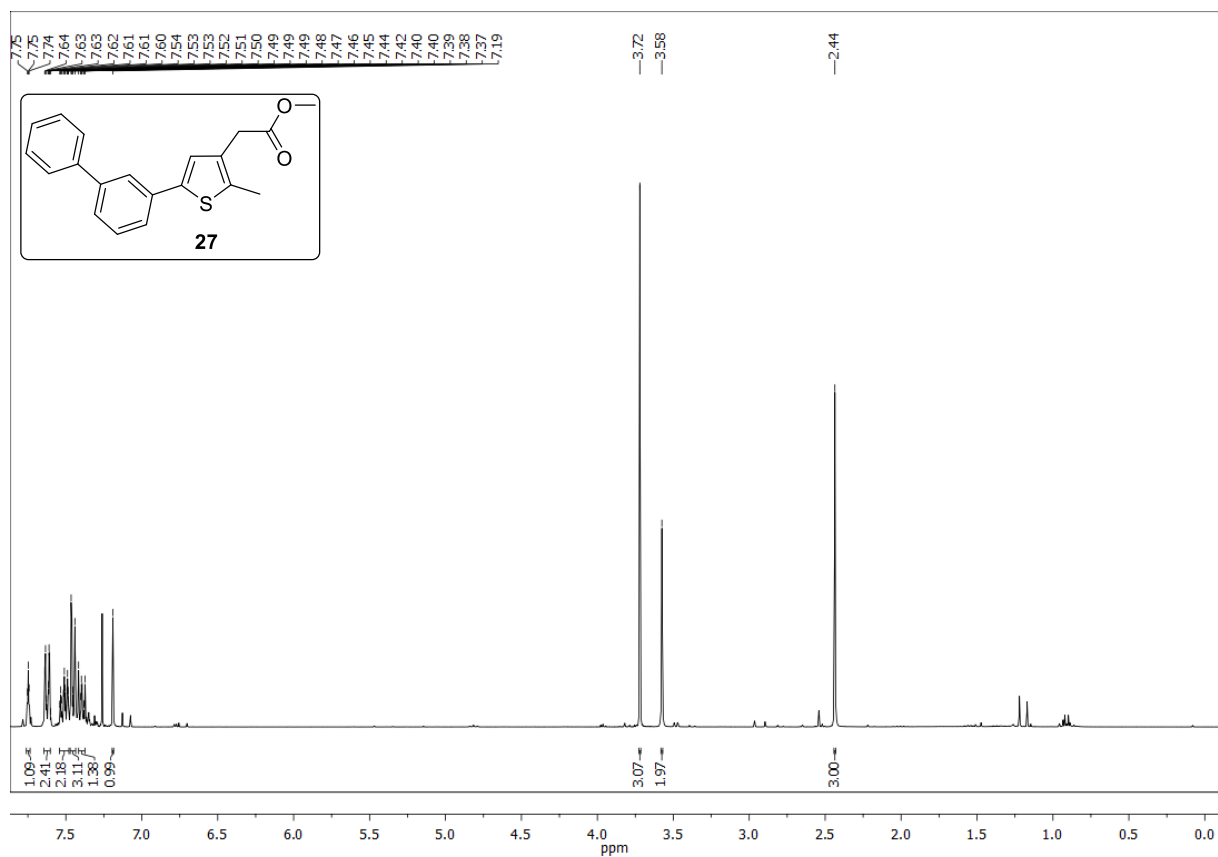
^{13}C-NMR (75 MHz, CDCl$_3$) for compound **27**:
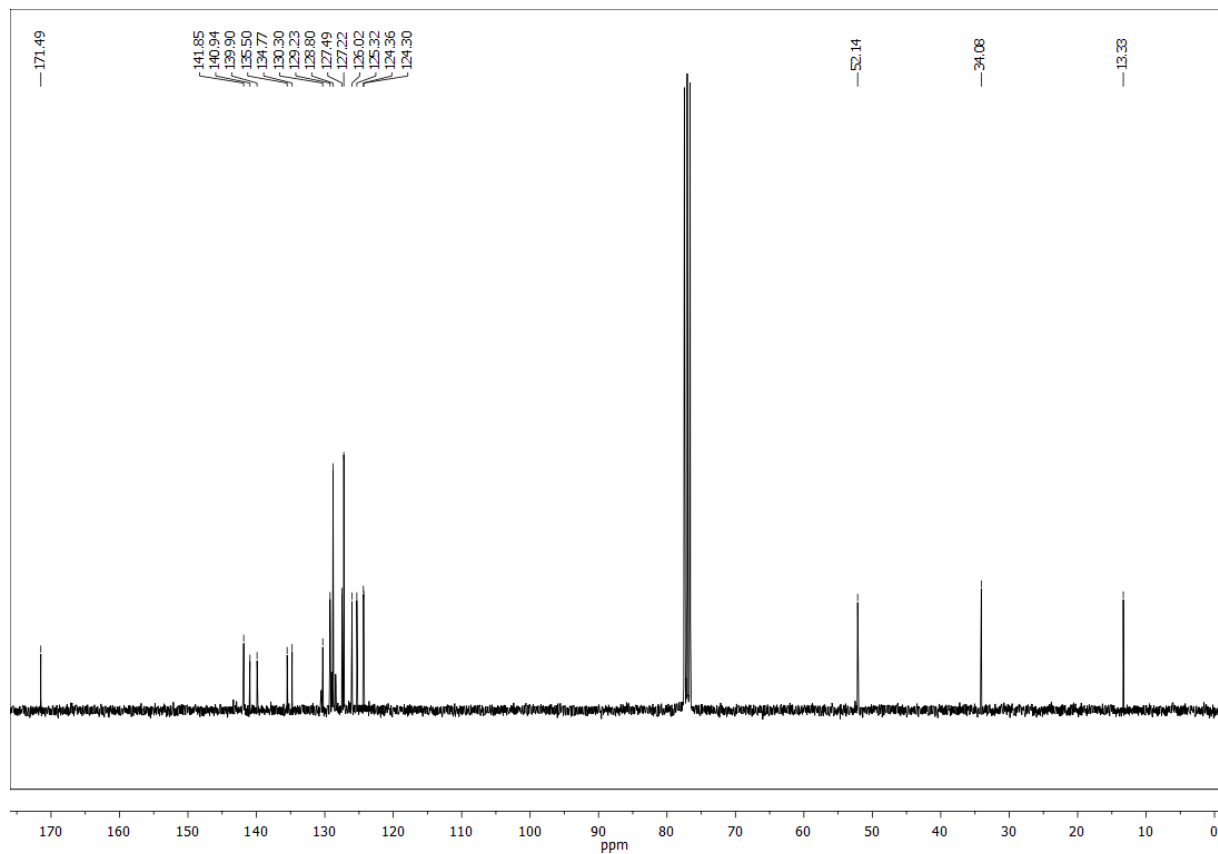
^{1}H-NMR (300 MHz, CDCl$_3$) for compound **30**:
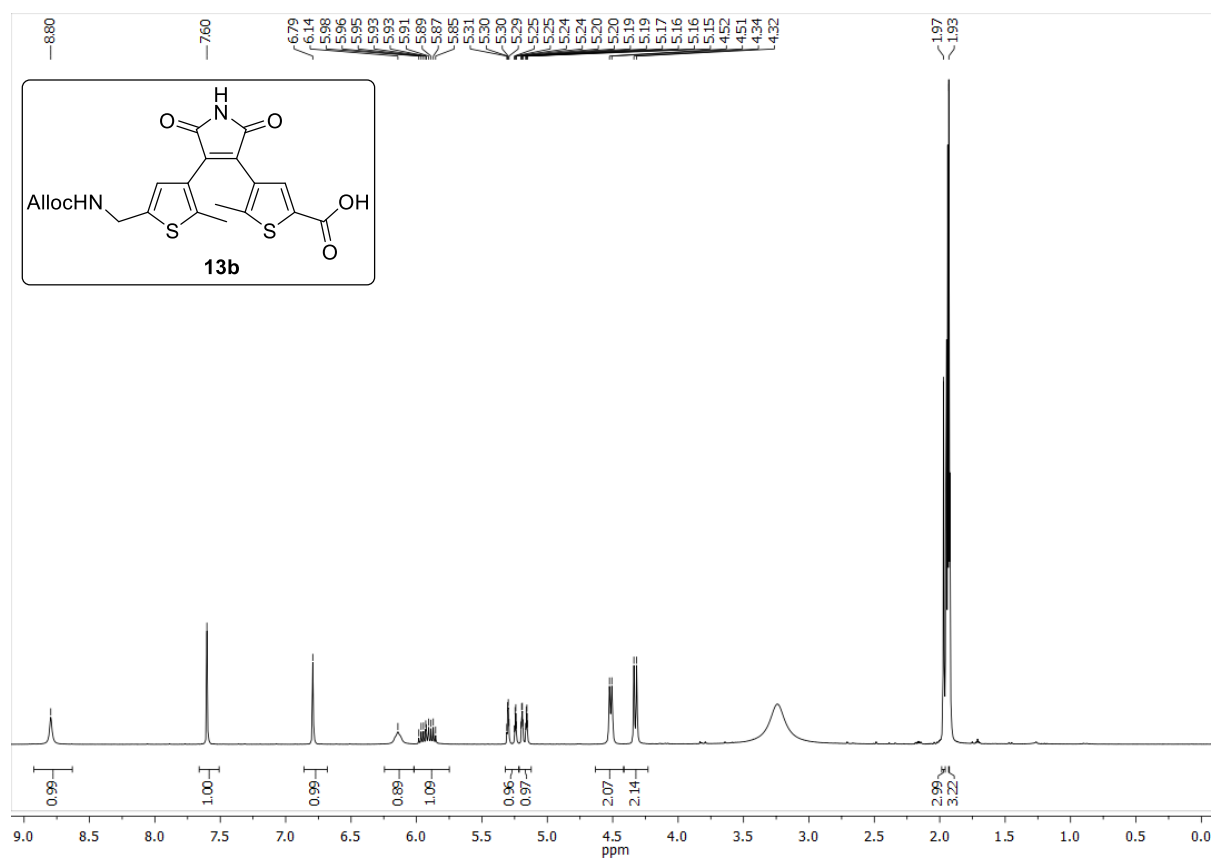

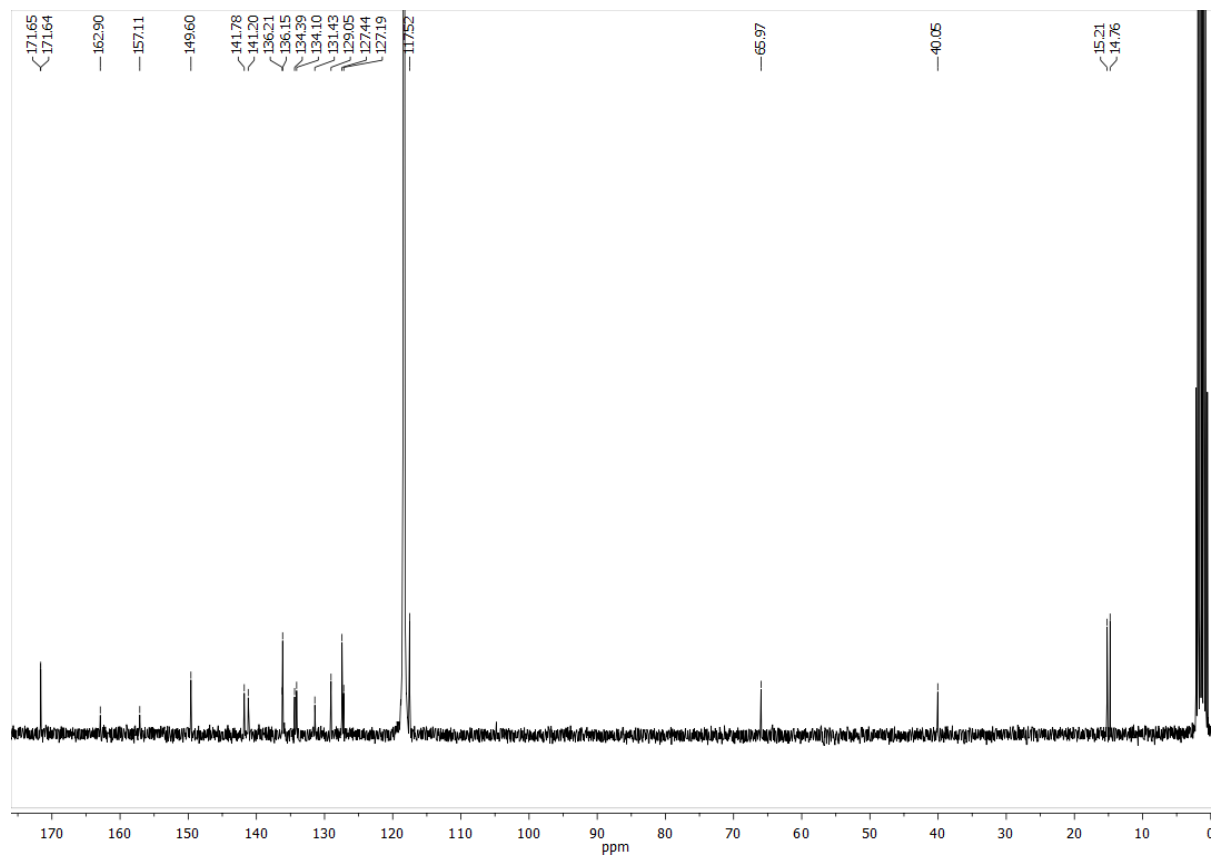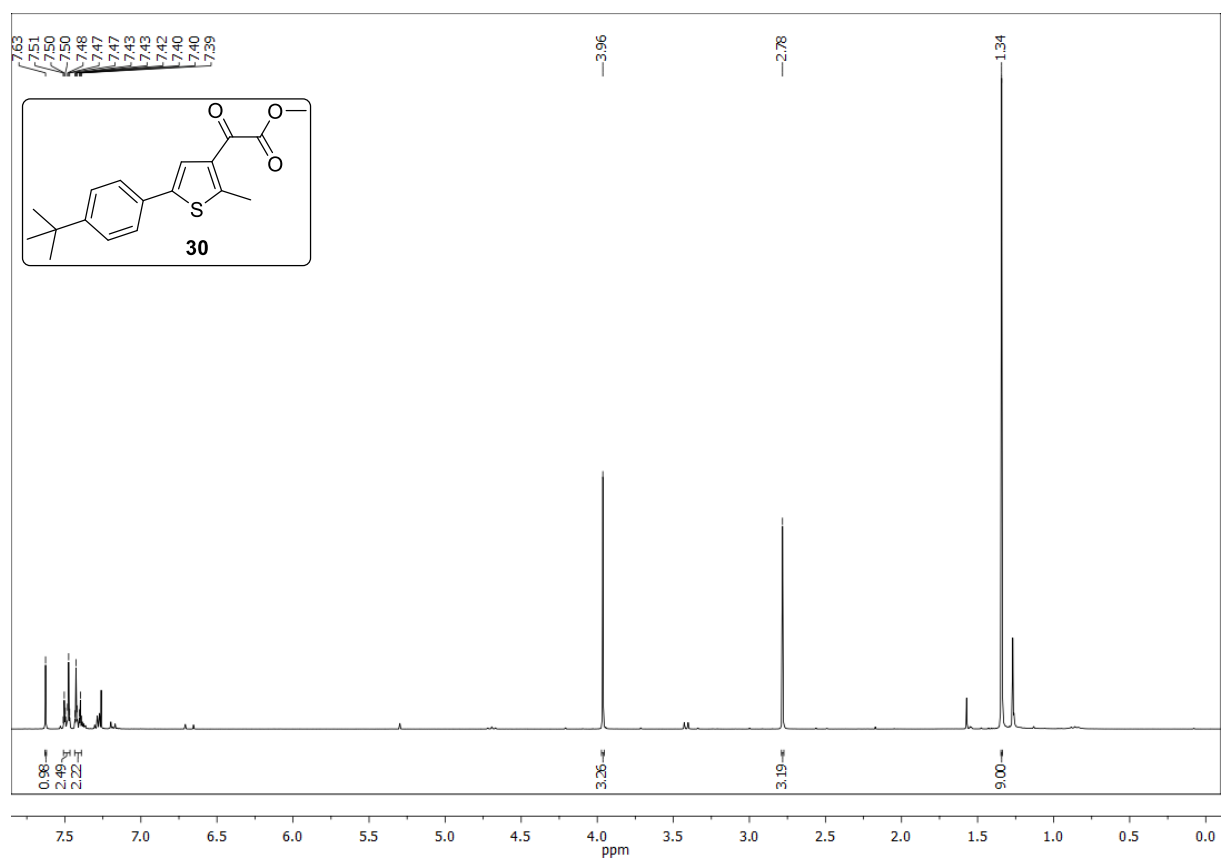^{13}C-NMR (75 MHz, CDCl$_3$) for compound **30**:

¹H-NMR (300 MHz, CDCl₃) for compound **31**:
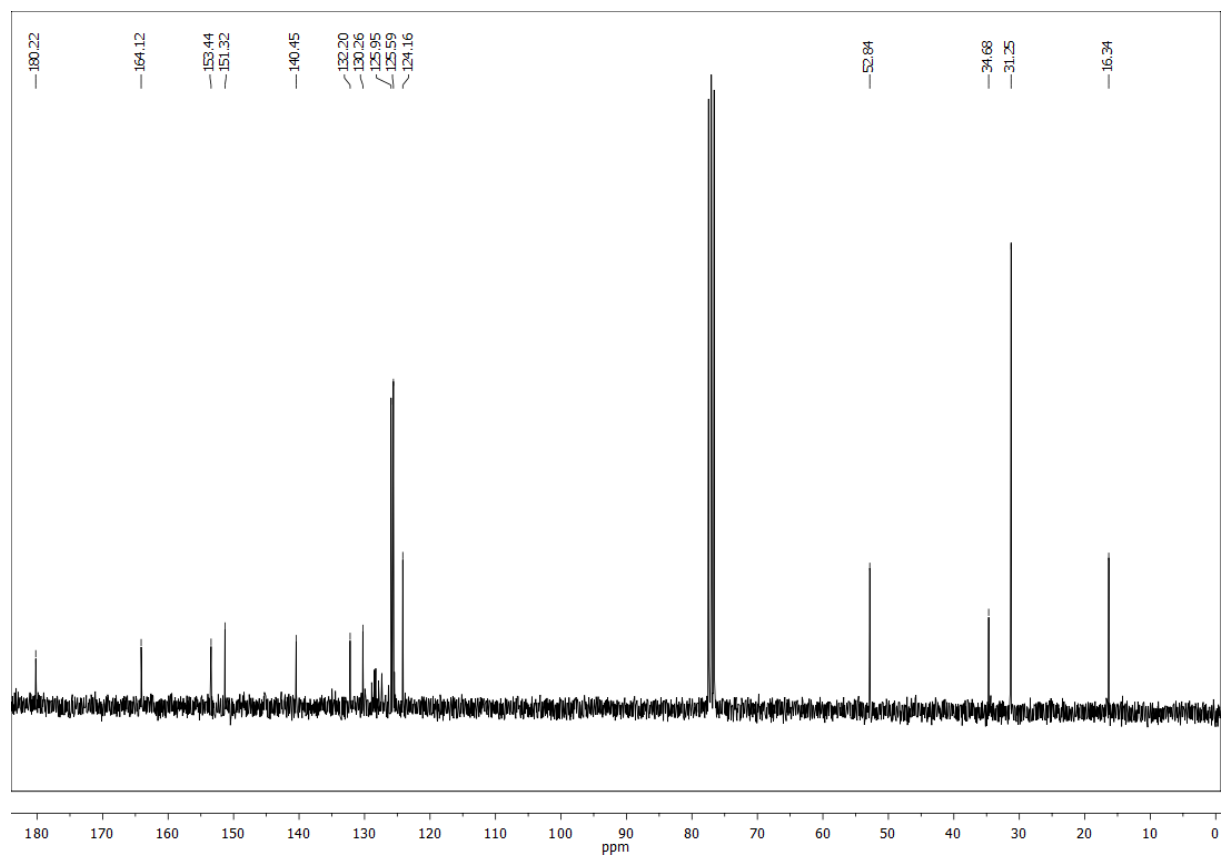
^{1}H-NMR (300 MHz, CDCl$_3$) for compound **31**:
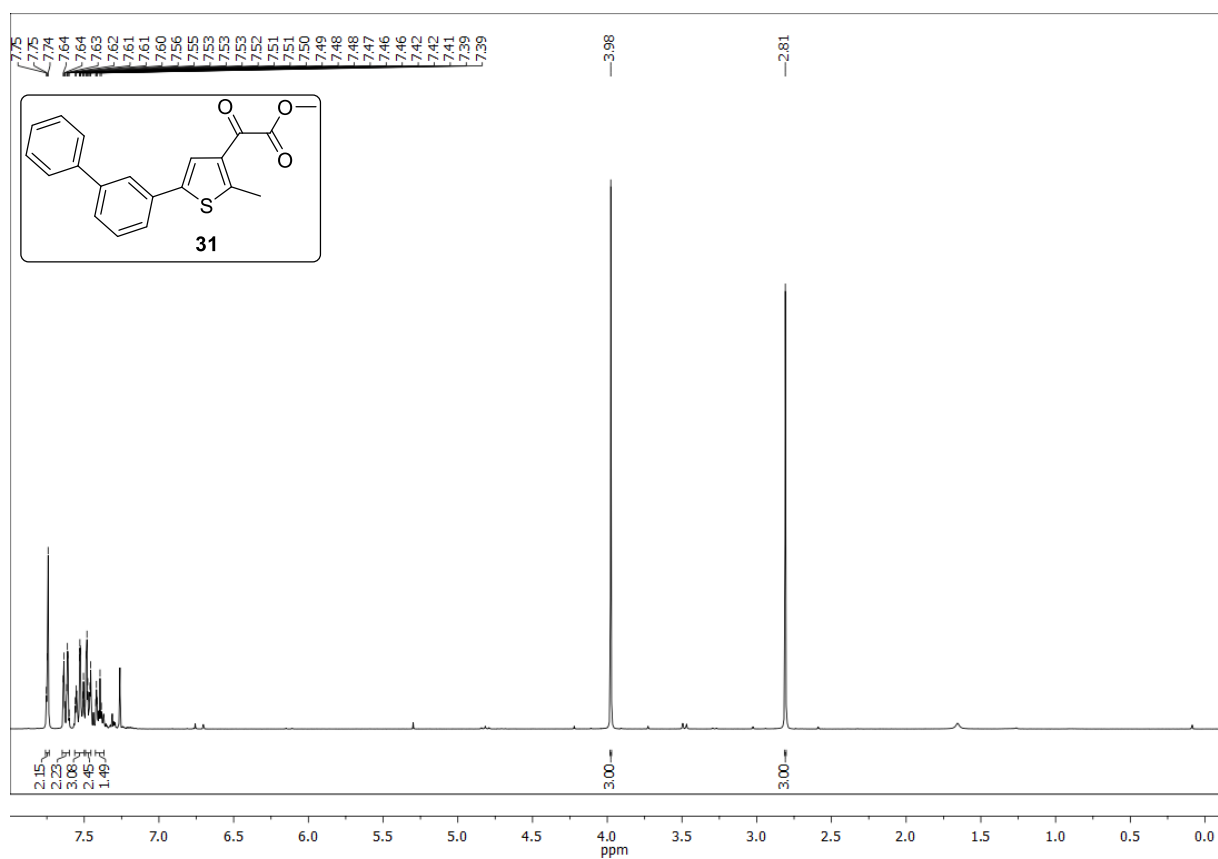
^{13}C-NMR (75 MHz, CDCl$_3$) for compound **31**:
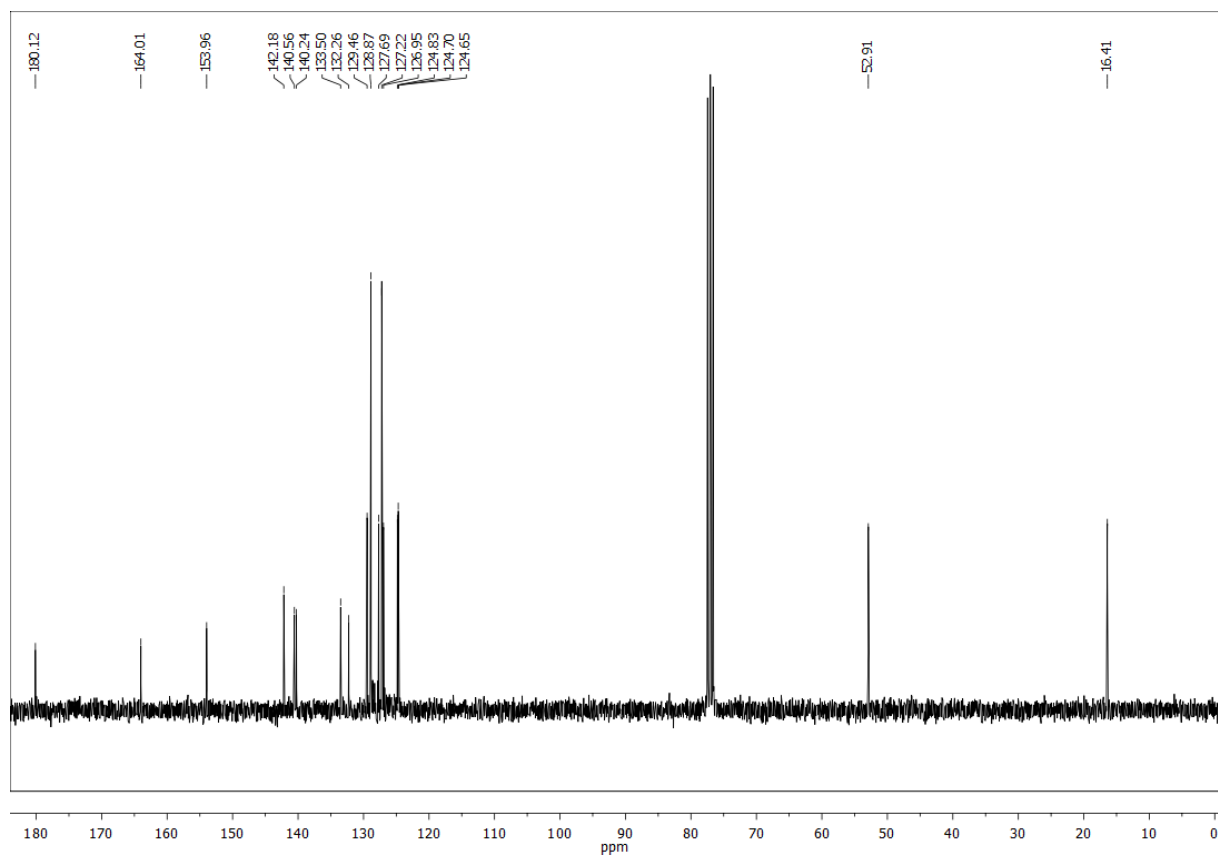
^{1}H-NMR (300 MHz, DMSO-d_6) for compound **33**:
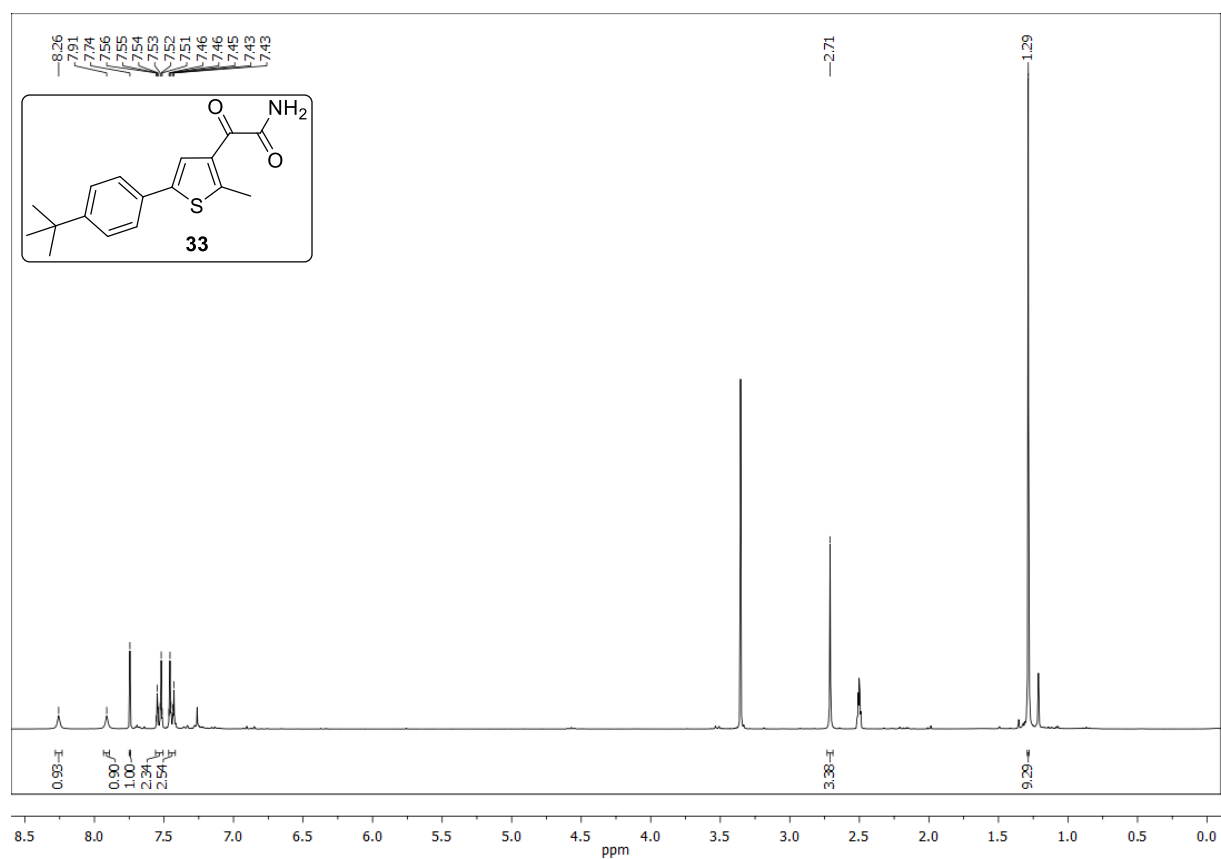
^{13}C-NMR (75 MHz, DMSO-d_6) for compound **33**:
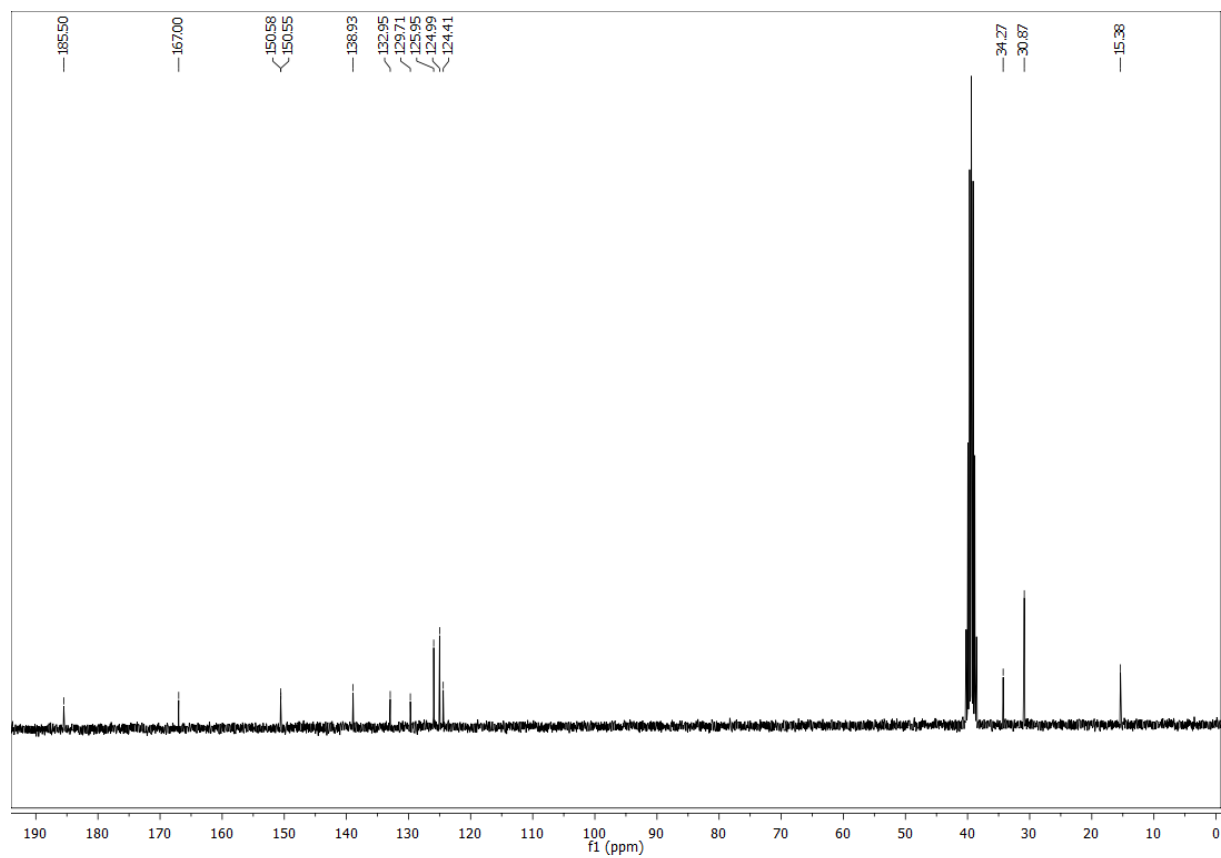
^{1}H-NMR (300 MHz, DMSO-d_6) for compound **34**:
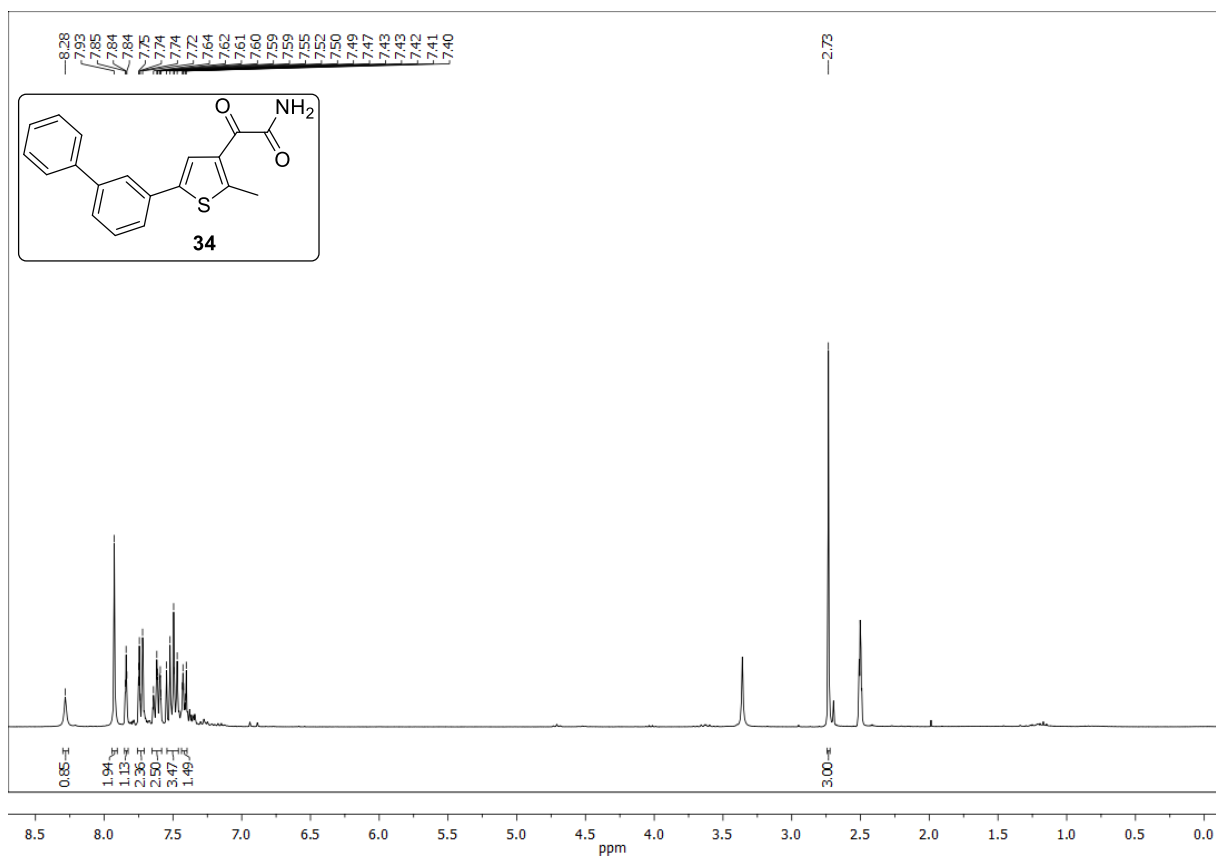
^{13}C-NMR (75 MHz, DMSO-d_6) for compound **34**:
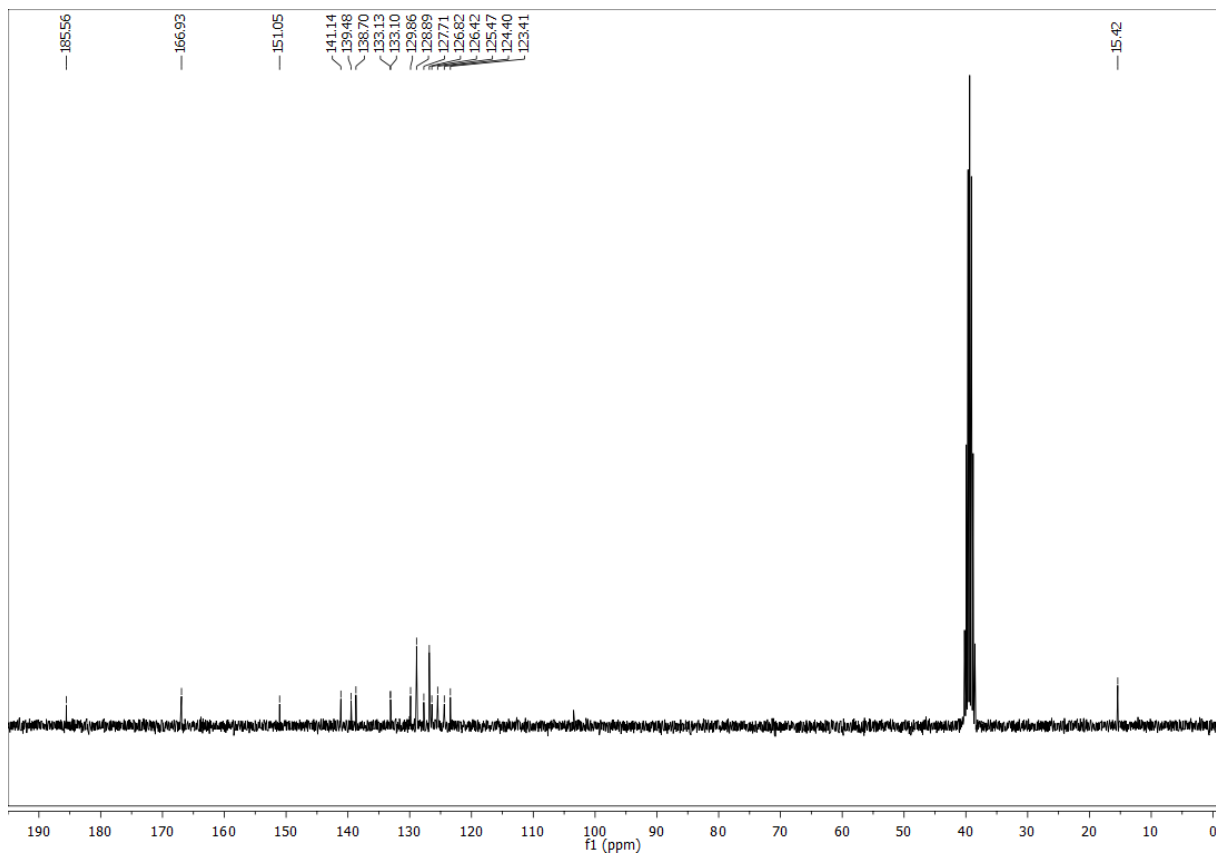
^{1}H-NMR (300 MHz, DMSO-d_6) for compound **35**:
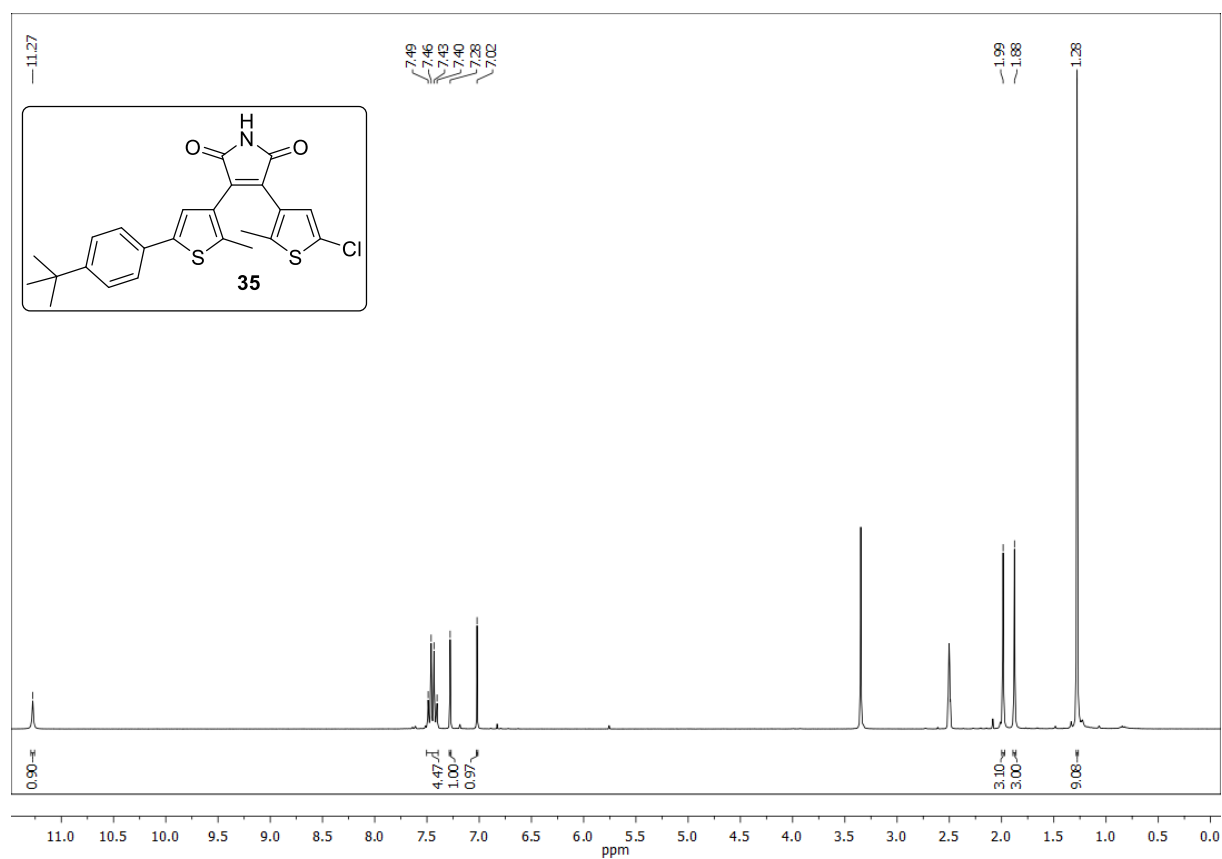
^{13}C-NMR (75 MHz, DMSO-d_6) for compound **35**:
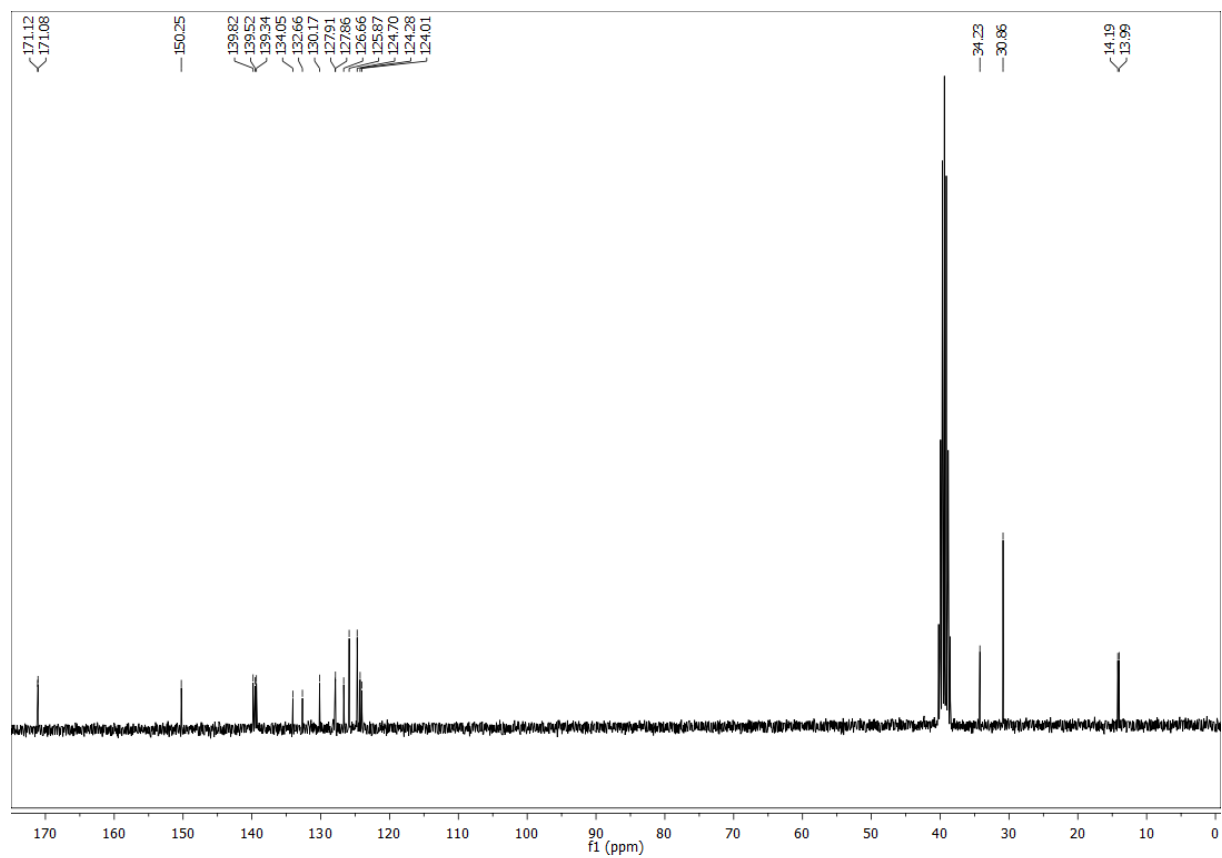
^{1}H-NMR (300 MHz, DMSO-d_6) for compound **36**:
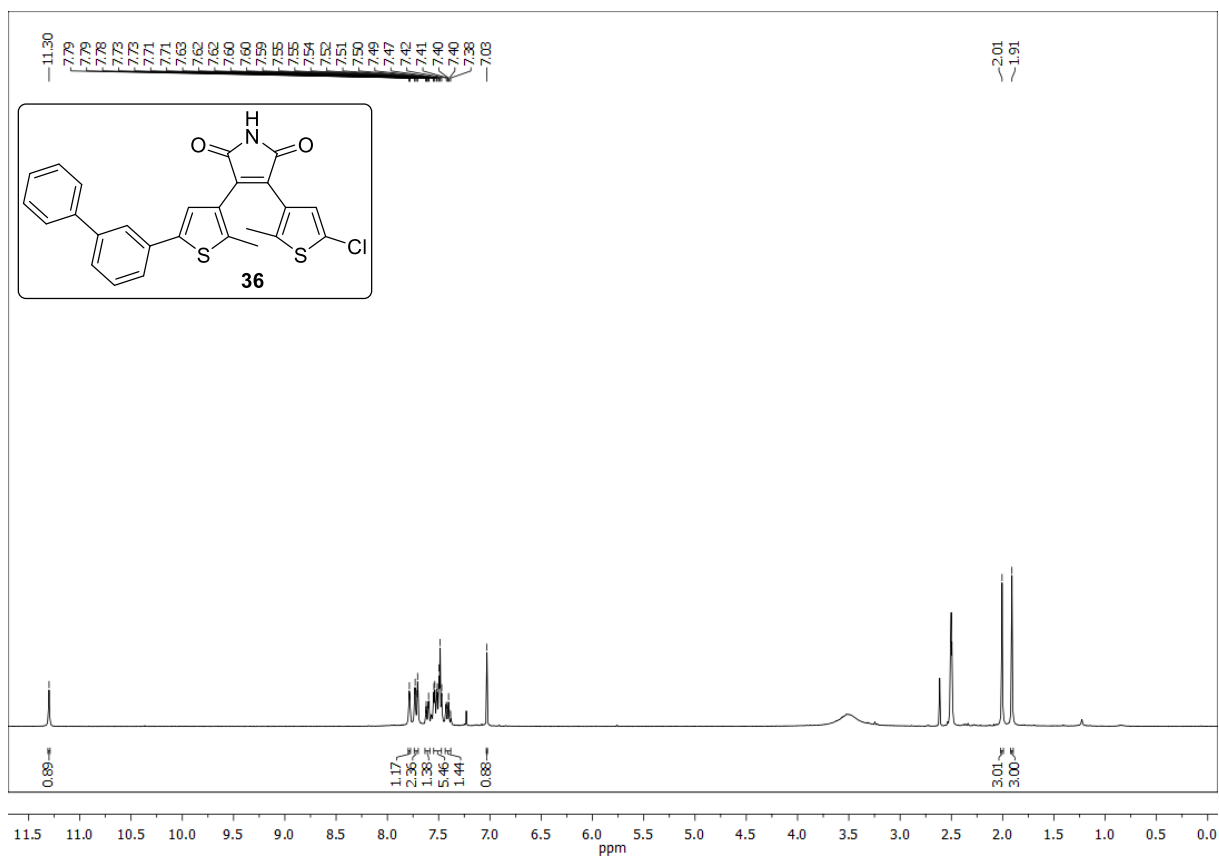
^{13}C-NMR (75 MHz, DMSO-d_6) for compound **36**:
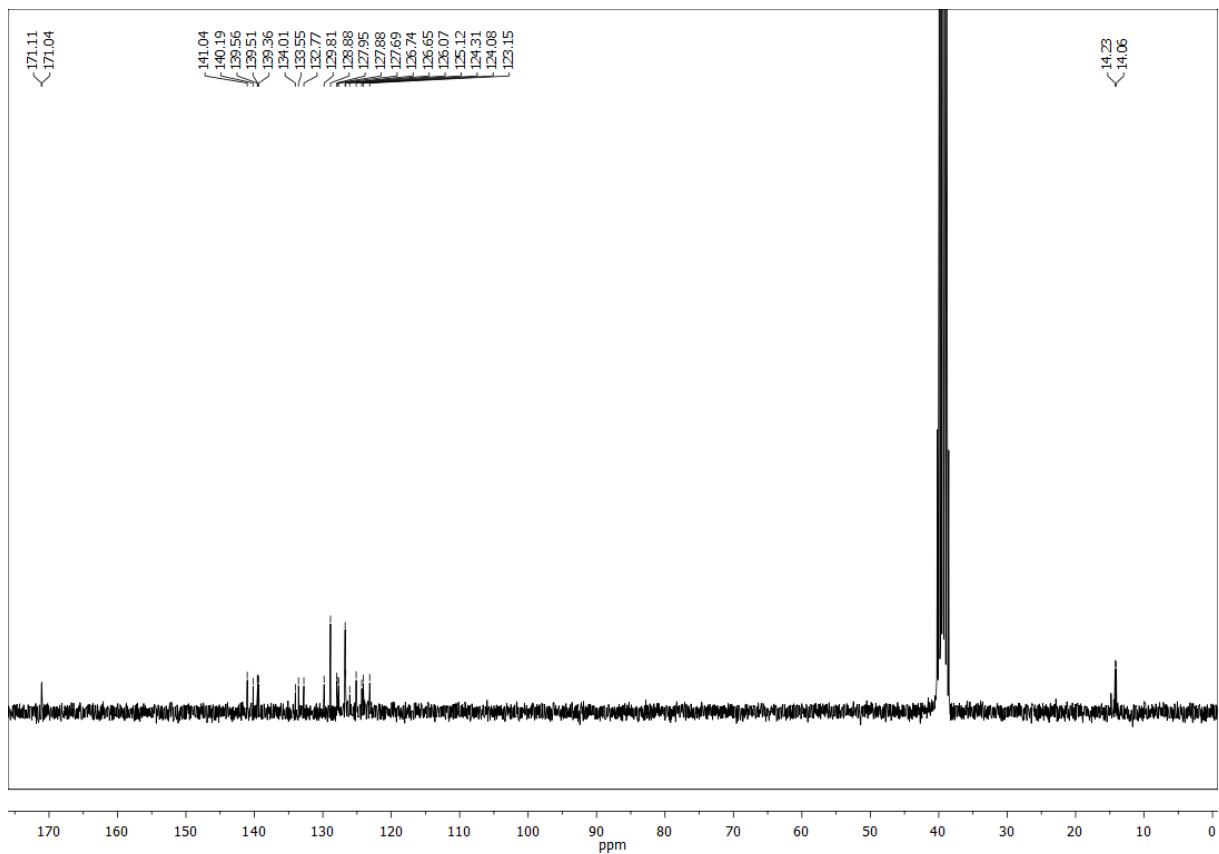
¹H-NMR (300 MHz, DMSO-d_6) for compound **37**:
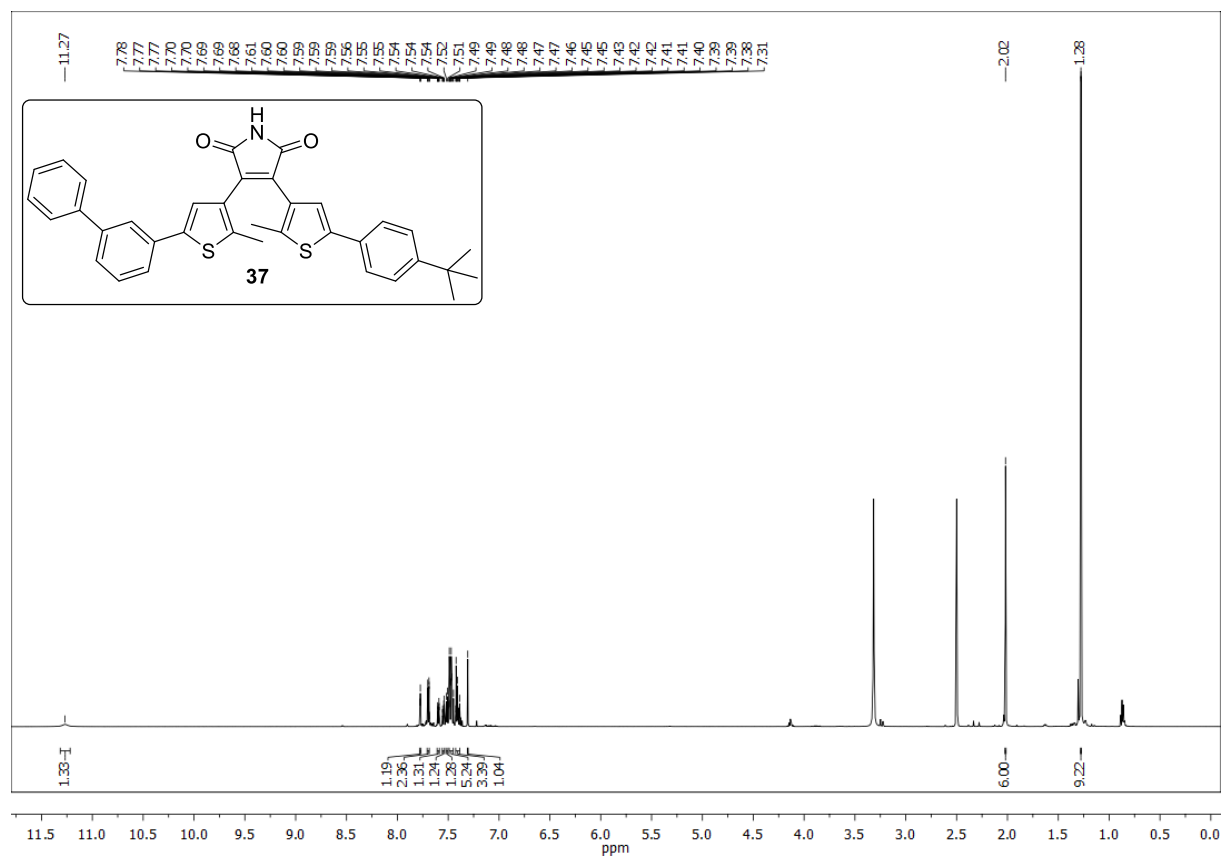
¹³C-NMR (75 MHz, DMSO-d_6) for compound **37**:
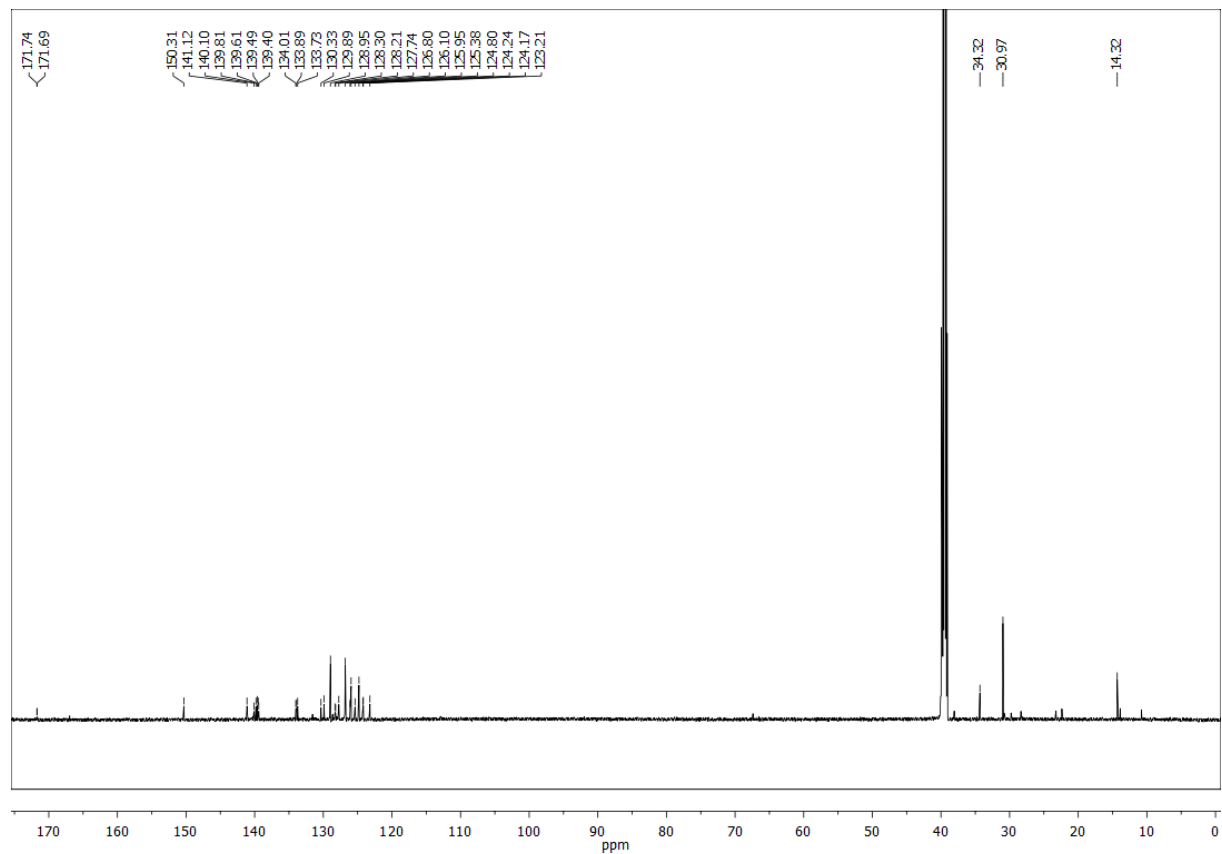
1.6 References

[1]   J. Zhang, Q. Zou, H. Tian, *Adv. Mater.* **2013**, *25*, 378-399.

[2]   W. Szymański, J. M. Beierle, H. A. V. Kistemaker, W. A. Velema, B. L. Feringa, *Chem. Rev.* **2013**, *113*, 6114-6178.

[3]   D. Gust, J. Andreasson, U. Pischel, T. A. Moore, A. L. Moore, *Chem. Commun.* **2012**, *48*, 1947-1957.

[4]   S. Kawata, Y. Kawata, *Chem. Rev.* **2000**, *100*, 1777-1788.

[5]   C. C. Corredor, Z. L. Huang, K. D. Belfield, *Adv. Mater.* **2006**, *18*, 2910-2914.

[6]   V. A. Barachevsky, M. M. Krayushkin, V. V. Kyiko, E. P. Grebennikov, *Phys. Status Solidi C* **2011**, *8*, 2841-2845.

[7]   D. Vomasta, C. Högner, N. R. Branda, B. König, *Angew. Chem. Int. Ed.* **2008**, *47*, 7644-7647.

[8]   D. Vomasta, A. Innocenti, B. König, C. T. Supuran, *Bioorg. Med. Chem. Lett.* **2009**, *19*, 1283-1286.

[9]   B. Reisinger, N. Kuzmanovic, P. Löffler, R. Merkl, B. König, R. Sterner, *Angew. Chem. Int. Ed.* **2014**, *53*, 595-598.

[10]   C. Falenczyk, M. Schiedel, B. Karaman, T. Rumpf, N. Kuzmanovic, M. Grötli, W. Sippl, M. Jung, B. König, *Chem. Sci.* **2014**, *5*, 4794-4799.

[11]   M. Singer, A. Jäschke, *J. Am. Chem. Soc.* **2010**, *132*, 8372-8377.

[12]   S. Barrois, H.-A. Wagenknecht, *Beilstein J. Org. Chem.* **2012**, *8*, 905-914.

[13]   H. Cahová, A. Jäschke, *Angew. Chem. Int. Ed.* **2013**, *52*, 3186-3190.

[14]   M. R. Banghart, A. Mourot, D. L. Fortin, J. Z. Yao, R. H. Kramer, D. Trauner, *Angew. Chem. Int. Ed.* **2009**, *48*, 9097-9101.

[15]   T. Fehrentz, M. Schönberger, D. Trauner, *Angew. Chem. Int. Ed.* **2011**, *50*, 12156-12182.

[16]   I. Tochitsky, M. R. Banghart, A. Mourot, J. Z. Yao, B. Gaub, R. H. Kramer, D. Trauner, *Nat. Chem.* **2012**, *4*, 105-111.

[17]   A. Mourot, T. Fehrentz, Y. Le Feuvre, C. M. Smith, C. Herold, D. Dalkara, F. Nagy, D. Trauner, R. H. Kramer, *Nat. Methods* **2012**, *9*, 396-402.

[18]   M. Schönberger, D. Trauner, *Angew. Chem. Int. Ed.* **2014**, *53*, 3264-3267.

[19]   M. Schönberger, M. Althaus, M. Fronius, W. Clauss, D. Trauner, *Nat. Chem.* **2014**, *6*, 712-719.

[20]   I. Tochitsky, A. Polosukhina, Vadim E. Degtyar, N. Gallerani, Caleb M. Smith, A. Friedman, Russell N. Van Gelder, D. Trauner, D. Kaufer, Richard H. Kramer, *Neuron* **2014**, *81*, 800-813.

[21]   W. A. Velema, J. P. van der Berg, M. J. Hansen, W. Szymanski, A. J. M. Driessen, B. L. Feringa, *Nat. Chem.* **2013**, *5*, 924-928.

[22]   O. Babii, S. Afonin, M. Berditsch, S. Reißer, P. K. Mykhailiuk, V. S. Kubyshkin, T. Steinbrecher, A. S. Ulrich, I. V. Komarov, *Angew. Chem. Int. Ed.* **2014**, *53*, 3392-3395.

[23]   U. Al-Atar, R. Fernandes, B. Johnsen, D. Baillie, N. R. Branda, *J. Am. Chem. Soc.* **2009**, *131*, 15966-15967.

[24]   W. A. Velema, W. Szymanski, B. L. Feringa, *J. Am. Chem. Soc.* **2014**, *136*, 2178-2191.

[25]   H. M. D. Bandara, S. C. Burdette, *Chem. Soc. Rev.* **2012**, *41*, 1809-1825.

[26]   G. Berkovic, V. Krongauz, V. Weiss, *Chem. Rev.* **2000**, *100*, 1741-1754.

[27]   Y. Yokoyama, *Chem. Rev.* **2000**, *100*, 1717-1740.

[28]   M. Irie, *Chem. Rev.* **2000**, *100*, 1685-1716.

[29]   H. Tian, S. Yang, *Chem. Soc. Rev.* **2004**, *33*, 85-97.

[30]   P. Raster, S. Weiss, G. Hilt, B. König, *Synthesis* **2011**, *2011*, 905-908.

[31]   M. Dubernet, V. Caubert, J. Guillard, M.-C. Viaud-Massuard, *Tetrahedron* **2005**, *61*, 4585-4593.

[32]   S. V. Shorunov, M. M. Krayushkin, F. M. Stoyanovich, M. Irie, *Russ. J. Org. Chem.* **2006**, *42*, 1490-1497.

[33]   A. El Yahyaoui, G. Félix, A. Heynderickx, C. Moustrou, A. Samat, *Tetrahedron* **2007**, *63*, 9482-9487.

[34]   M. M. Krayushkin, V. Z. Shirinyan, L. I. Belen'kii, A. A. Shimkin, A. Y. Martynkin, B. M. Uzhinov, *Russ. J. Org. Chem.* **2002**, *38*, 1335-1338.

[35]   M. Ohsumi, T. Fukaminato, M. Irie, *Chem. Commun.* **2005**, 3921-3923.

[36]   M. T. Indelli, S. Carli, M. Ghirotti, C. Chiorboli, M. Ravaglia, M. Garavelli, F. Scandola, *J. Am. Chem. Soc.* **2008**, *130*, 7286-7299.

[37]   M. M. Faul, L. L. Winneroski, C. A. Krumrich, *J. Org. Chem.* **1998**, *63*, 6053-6058.

[38]   M. M. Faul, L. L. Winneroski, C. A. Krumrich, *Tetrahedron Lett.* **1999**, *40*, 1109-1112.

[39]   W. Steglich, *Pure Appl. Chem.* **1989**, *61*, 281-288.

[40]   T. Tamaoki, H. Nakano, *Biotechnology (N Y)* **1990**, *8*, 732-735.

[41]   P. D. Davis, C. H. Hill, G. Lawton, J. S. Nixon, S. E. Wilkinson, S. A. Hurst, E. Keech, S. E. Turner, *J. Med. Chem.* **1992**, *35*, 177-184.

[42]   D. A. Cross, A. A. Culbert, K. A. Chalmers, L. Facci, S. D. Skaper, A. D. Reith, *J. Neurochem.* **2001**, *77*, 94-102.

[43]   L. Meijer, M. Flajolet, P. Greengard, *Trends Pharmacol. Sci.* **2004**, *25*, 471-480.

[44]   E. Khalifa, J. H. Bieri, M. Viscontini, *Helv. Chim. Acta* **1973**, *56*, 2911-2919.

[45]   J. T. van Herpt, M. C. A. Stuart, W. R. Browne, B. L. Feringa, *Chem. Eur. J.* **2014**, *20*, 3077-3083.

[46]   K. Fujimoto, T. Maruyama, Y. Okada, T. Itou, M. Inouye, *Tetrahedron* **2013**, *69*, 6170-6175.

[47]   K. Fuji, T. Kawabata, E. Fujita, *Chem. Pharm. Bull.* **1980**, *28*, 3662-3664.

[48]   J. W. Fisher, K. L. Trinkle, *Tetrahedron Lett.* **1994**, *35*, 2505-2508.

[49]   Y. Goldberg, H. Alper, *J. Org. Chem.* **1993**, *58*, 3072-3075.

[50]   O. E. Levy, E. L. Madison, J. E. Semple, A. P. Tamiz, M. Weinhouse, *US Pat.,* WO0214349 (A2), **2002**.

[51]   H. Chafiq, *US Pat.,* WO2013025424 (A1), **2013**.

[52]   A. McKillop, B. P. Swann, E. C. Taylor, *J. Am. Chem. Soc.* **1973**, *95*, 3340-3343.

[53]   T. Yamaguchi, M. Irie, *Chem. Lett.* **2004**, *33*, 1398-1399.

[54]   T. Yamaguchi, K. Uchida, M. Irie, *J. Am. Chem. Soc.* **1997**, *119*, 6066-6071.

[55]   M. Irie, K. Sayo, *J. Phys. Chem.* **1992**, *96*, 7671-7674.

2 Photochromic Histone Deacetylase Inhibitors based on Dithienylethenes and Fulgimides

2.1 Introduction

Photopharmacology has recently become a vibrant field of research providing tools for the investigation of cellular processes and pathogeneses in life sciences.[1-3] In contrast to optogenetics,[4] it aims at the artificial control of biological processes with synthetic photoswitches by light.[5] Light as an orthogonal control element towards most cellular processes can be applied in very high precision in regard to dose, energy, time and space.[6] By now various biological targets and functions could be triggered in a reversible manner with light, for instance enzyme activity,[7-19] bacterial growth,[20-22] neuronal activity,[23-29] the agility of living organisms,[30-33] oligonucleotides,[34-36] the restoration of vision[37, 38] and lipids.[39-41] Numerous photochromic scaffolds like azobenzenes,[42] spiropyrans as well as spirooxazines,[43] fulgides/fulgimides[44] and diarylethenes[45] have been developed. All these photoswitches can reversibly be interconverted between their photoisomers by light.

Cancer and other human diseases are linked to an abnormal expression and/or function of histone deacetylases.[46] Therefore, this family of enzymes became an interesting target in anticancer research as well as in the field of epigenetics due to their function as epigenetic regulators. These enzymes can be found in various organisms and catalyze among others the removal of acetyl groups from acetylated lysine residues of various protein substrates. The 18 HDACs identified in humans are subdivided in two families: the zinc dependent metalloproteins, composed of classes I (HDAC1-3 and 8), IIa (HDAC4, 5, 7 and 9), IIb (HDAC6 and 10) and IV; and the nicotinamide adenine dinucleotide (NAD$^+$) dependent class III (sirtuins).[47] Besides, HDAC inhibitors (HDACi) showed also antiproliferative and antiparasitic activities on major human parasitic diseases such as leishmaniasis, malaria, schistosomiasis, toxoplasmosis, and trypanosomiasis by addressing the HDACs of the parasites.[48] This new approach was further developed against schistosomiasis to overcome the reduced efficiency of praziquantel or even the resistance of first schistosome flatworm laboratory strains.[49] Praziquantel is still the only drug for mass treatment against schistosomiasis. In particular, the HDAC8 of *Schistosoma mansoni* (*sm*HDAC8), which is one of the main species of medical relevance, was successfully identified as potential therapeutic target due to its high abundance and expression at all life-cycle stages of the parasite.[50, 51] A dose dependent mortality of

schistosome larvae and adult worms could be evoked by treating them with generic HDAC inhibitors.[52] The HDAC inhibitors for eukaryotic zinc dependent HDACs are classified by their moiety interacting with the zinc cation at the polar bottom of the catalytic pocket: Hydroxamic acids, short-chain fatty acids, cyclic tetrapeptides and benzamides.[53, 54]

Different studies on azobenzene based photochromic HDAC inhibitors bearing aliphatic hydroxamic acids or benzamides, respectively, have been published recently.[9, 10, 55, 56] However, one major drawback of azobenzenes, which are widely used in biological applications, can be their thermal reversibility and possible incomplete photoconversion due to an substantial overlap of the absorption maxima of both photoisomers.[57] In contrast, DTEs as well as fulgides/fulgimides generally feature high photostationary states (PSS) with both photoisomers being thermally stable.[45, 58] Both photochromic scaffolds can be interconverted with light of specific wavelengths between their open and closed photoisomers, which differ in conformational flexibility and electronic conjugation (Scheme 1).
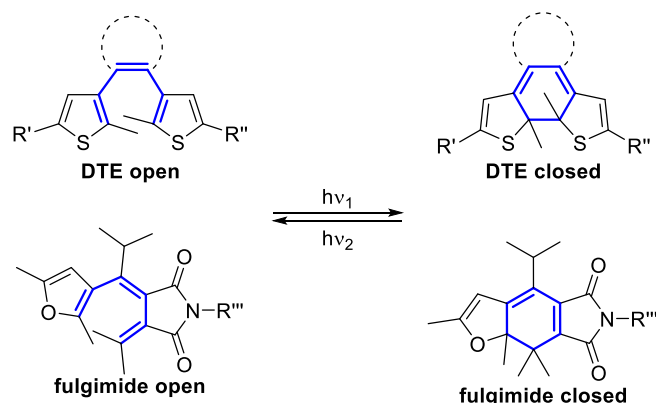
Scheme 1. Photochemical ring-closure and the reverse, ring-opening of a DTE and fulgimide scaffold. The required 1,3,5-hexatriene system is highlighted in blue.

We have chosen these two photoswitchable structures to functionalize them with aromatic hydroxamic acids which should allow light controllable inhibitory effects of zinc dependent HDACs. Aromatic hydroxamic acids have been selected to address the individual pockets observed in HDAC isoforms. Based on available X-ray structures of *h*HDAC6, *h*HDAC8 and *sm*HDAC8 in complex with aromatic hydroxamic acids it is known that this class of compounds can be substituted to get isoselective HDAC inhibitors.[59] These photochromic inhibitors could be used as a tool to further investigate the biological activity and molecular mechanism of HDACs. The comparison of the inhibitory effect of

the more flexible open photoisomer with the rigid and planar closed photoisomer should also allow to draw conclusions about the flexibility of the binding pocket of the particular HDAC in solution. Furthermore, fulgides and fulgimides are well known for applications in optical switching and data storage[60-63] but only few examples of their use in a biological context are known so far.[64, 65] Their outstanding photochromic properties in polar aqueous systems recommend them as a perfect chromophore for such applications.

2.2 Results and Discussion

2.2.1 Synthesis of DTE Derivatives
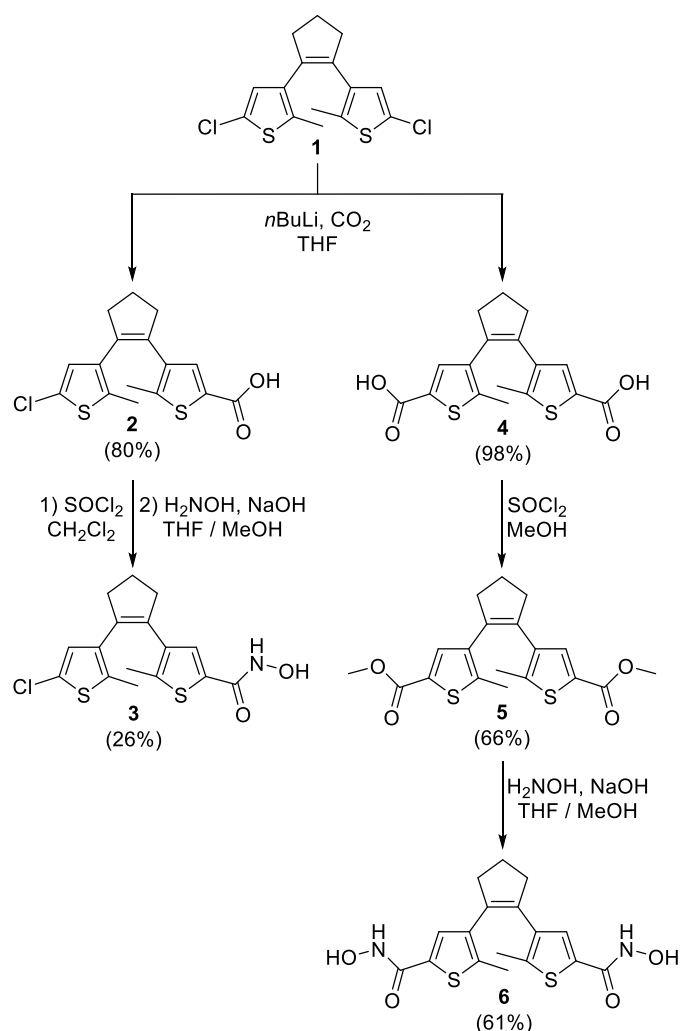
Scheme 2. Synthesis of photochromic mono- and bis-hydroxamic acid dithienylcyclopentenes **3** and **6**.

In a first and straightforward design the zinc chelating hydroxamic acid moiety was directly attached at the thiophene group of DTEs. Bis-chlorodithienylethene **1** was

synthesized according to the method described in literature.[66] Depending on the reaction conditions the chlorine/lithium exchange can be controlled to occur selectively on one or both thiophenes, respectively.[66, 67] The further reaction with gaseous carbon dioxide afforded the required carboxylic acid moieties in very good yields. The mono-acid **2** was further functionalized by activation with thionyl chloride and *in situ* reaction with aqueous hydroxylamine yielding target hydroxamic acid **3** in only 26%. A two-step synthesis improved this functionalization step for the symmetric bis-carboxylic acid **4**. After converting the carboxylic acids into methyl esters, they were reacted with aqueous hydroxylamine yielding photoswitch **6** in overall 40%. An overview of the synthesis is depicted in Scheme 2.
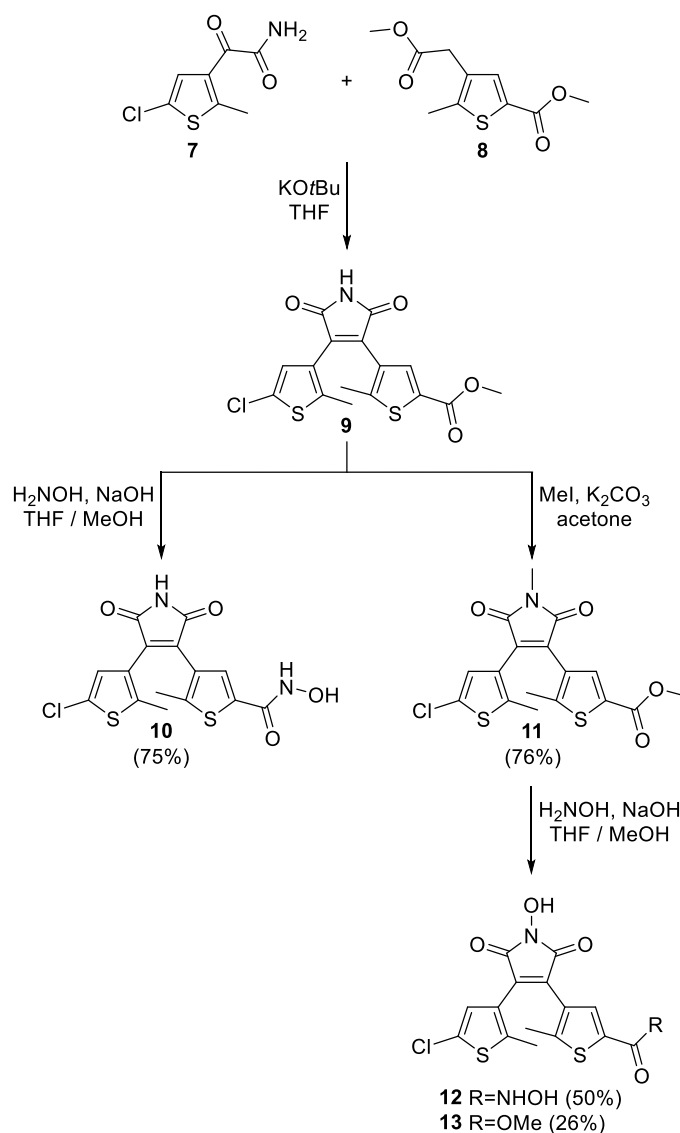
Scheme 3. Synthesis of dithienylmaleimides **10**, **12** and **13**.

In a second approach we attempted to utilize the higher water solubility of dithienylmaleimides compared to dithienylcyclopentenes. Therefore, DTE **9** was synthesized by a Perkin type condensation from known precursors **7** and **8** (Scheme 3).[68] A subsequent exchange of the ester moiety with the desired hydroxamic acid afforded dithienylmaleimide **10** in good yield. Unfortunately, all attempts to synthesize a symmetric dithienylmaleimide with a free NH group bearing a methyl ester on each thiophene were not successful. The maleimide of DTE **9** was subsequently methylated yielding a protected precursor **11** for further functionalization. However, all approaches to convert the chlorine of **11** into a carboxylic acid or methyl ester by various methods failed. In addition, the methyl ester of **11** could also not selectively be transformed into the corresponding hydroxamic acid without an undesired side reaction on the maleimide core. Depending on the reaction conditions we could isolate either **12** or **13** as main product indicating that the methylated maleimide shows a higher intrinsic reactivity with hydroxylamine than the methyl ester on the thiophene.

2.2.2 Photochromic Properties of the DTEs

The DTEs are a well-known class of photochromic scaffolds. In general, they are characterized by their excellent photochromic properties like almost quantitative photochemical conversion, high fatigue resistance and thermal stability of both photoisomers.[45] All these properties are beneficial for photochromic enzyme inhibitors. As dimethyl sulfoxide is a standard solvent for stock solutions in inhibitor screening it was used as solvent for the investigations of the photoisomerization of the prepared DTEs by UV-Vis absorption spectroscopy. Solutions (100 µM) of **3**, **6**, **10**, **12** and **13** were irradiated with UV light of 300 nm or 312 nm, respectively. In contrast to reports in literature that dithienylmaleimides cannot undergo photoisomerization in polar solvents like DMSO due to a twisted intramolecular charge transfer (TICT),[69-71] we could detect reversible photochromism of **10**. During irradiation ($\lambda = 300$ nm), a rapid color change from colorless to deep violet was observed. This resulted in new absorption bands at $\lambda_{max} = 369$ nm and 535 nm. The isosbestic points (Table 1) indicate a clean, two-component switching (see Supporting Information, Figure S1). Due to a substantial overlap of the absorption maxima of the open and closed isomers a maximum PSS of only 57% at UV-irradiation ($\lambda = 300$ nm)

could be reached. Repetitive cycle measurements of compound **10** showed good fatigue resistance (see Supporting Information, Figure S1b). However, compounds **12** and **13** did not show photochromic switching properties in DMSO at all. Compound **12** was also dissolved in a less polar toluene/THF mixture and irradiated (λ = 312 nm). Hardly any reversible photoisomerization was detected (see Supporting Information, Figure S2). Therefore, we suppose that a hydroxyl substitution of the maleimide nitrogen negatively affects the photophysical properties in general. In accordance with a recent report in literature[72] we also could not photocyclize dithienylmaleimide **10** by UV-exposure to the closed isomer in aqueous solution. In contrast, the closed photoisomer could be opened in aqueous solution by irradiation with visible light (λ = 530 nm). The solution was prepared by dissolving a DMSO stock solution of the closed photoisomer into aqueous PBS.

The photochromic properties of the synthesized dithienylcyclopentenes **3** and **6** differed from them of dithienylmaleimide **10**. Upon irradiation (λ = 312 nm) of **3** a quick color change from colorless to orange was observed because of an arising new maximum at λ_{max} = 488 nm. However, the lack of distinct isosbestic points in the spectral evolution as well as a fast degradation of **3** at repetitive switching cycle measurements indicate an irreversible side reaction (see Supporting Information, Figure S3). Further investigations by continuous UV-irradiation (λ = 312 nm) supposed the undesired, irreversible formation of a byproduct (Scheme 4).
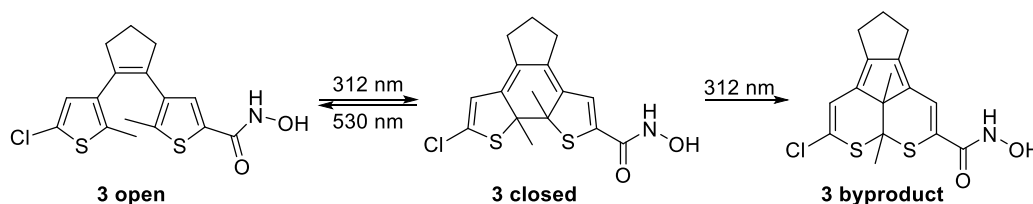
Scheme 4. Irreversible formation of the byproduct of **3** upon continuous UV-irradiation.

The phenomenon of this annulated isomer has been reported previously, but the mechanism of the byproduct formation which has to be related to the substitution pattern of the DTEs is not yet fully understood.[73-75] Following the photoisomerization by UV-Vis absorption spectroscopy upon continuous irradiation, a decrease of the evolving maximum at λ_{max} = 488 nm was observed. HPLC traces show that, upon reaching the PSS

after 45 s, at which the highest amount of the closed isomer (40%) is generated, 23% of the byproduct has already formed and the nearly quantitative formation of it is completed after 220 s of irradiation (see Supporting Information, Figure S4 and Figure S5). Nevertheless, the undesired byproduct was also used in the biological assays although its formation is irreversible and it cannot be reconverted to the open isomer. Dithienylcyclopentene **6** showed slightly different photochromic properties. Upon irradiation (λ = 312 nm) a quick color change from colorless to purple was observed. Compound **6** had a much higher fatigue resistance than compound **3** and upon reaching the PSS (80% closed isomer) after 60 seconds of irradiation only traces of the corresponding byproduct had been formed. However, the byproduct could be formed by further continuous irradiation with UV-light requiring a much longer irradiation time of 640 s compared to DTE **3** (see Supporting Information, Figure S6). The symmetric substitution of **3** and consequently a symmetric electron distribution in the DTE seems to prevent a quick formation of the byproduct. All photophysical properties of the DTEs **3**, **6**, and **10** are summarized in Table 1.

Table 1. Photochromic properties of DTEs **3**, **6**, and **10** (100 µM in DMSO).

Entry	Compound	λ_{max} **open** [nm]	λ_{max} **PSS** [nm]	Isosbestic points [nm]	PSS [%]*
1	**3**	-	488	-	40:37:23
2	**6**	-	348, 523	368, 426	80:17:3
3	**10**	367	369, 535	301, 394, 415	57:43:0

* determined by HPLC measurements (closed isomer:open isomer:byproduct).

2.2.3 Enzyme Inhibition

Next, the inhibitory effect of compounds **3** (open and byproduct), **6** (open and PSS), **10** (open and PSS), **12** and **13** against several HDACs was determined using two different assays. On the one hand, a homogenous histone deacetylase assay established by Jung *et al.* was used for *h*HDAC1 and *h*HDAC6. The enzymatic conversion was quantified by using (*S*)-[5-acetylamino-1-(4-methyl-2-oxo-2*H*-chromen-7-ylcarbamoyl)-pentyl]-carbamic acid benzyl ester also termed ZMAL[76] as fluorescent substrate for deacetylation followed by a tryptic digestion step.[77] On the other hand, the commercially available Fluor de Lys-HDAC8 Fluorometric Drug Discovery Assay Kit of EnzoLifeScience was used in a modified

way for *h*HDAC8 and *sm*HDAC8. Stock solutions (10 mM) of compounds **3**, **6** and **10** in DMSO were irradiated with UV-light to generate the corresponding closed isomer or byproduct prior to the biological assays, respectively. Table 2 summarizes an initial screening of inhibitory effects at two fixed inhibitor concentrations.

Table 2. Inhibitory effects of the respective isomers of compounds **3**, **6**, **10**, **12** and **13** against *h*HDAC1, *h*HDAC6, *h*HDAC8 and *sm*HDAC8.

Entry	Compound	Conc. [µM]	*h*HDAC1 [%]	*h*HDAC6 [%]	*h*HDAC8 [%]	*sm*HDAC8 [%]
1	**3 open**	50	69	97	92	75
2	**3 byprod.**	50	59	83	94	71
3	**3 open**	10	25	90	87	65
4	**3 byprod.**	10	14	63	89	61
5	**6 open**	50	86	100	98	73
6	**6 PSS**	50	84	99	98	82
7	**6 open**	10	53	99	97	73
8	**6 PSS**	10	60	97	99	89
9	**10 open**	50	81	97	100	95
10	**10 PSS**	50	90	97	100	96
11	**10 open**	10	50	92	89	84
12	**10 PSS**	10	59	87	99	89
13	**12**	50	64	84	99	91
14	**12**	10	19	59	95	75
15	**13**	50	n.i.	35	23	n.i.
16	**13**	10	n.i.	9	11	n.i.

n.i.: no inhibition

These preliminary results show strong inhibition for most compound species especially for *h*HDAC6 and *h*HDAC8. As expected, compound **13** exhibits only low or no inhibition effects on all tested zinc dependent HDACs due to the lack of the zinc chelating hydroxamic acid moiety. The hydroxylated maleimide does also not bind efficiently to the zinc cation because of the restricted size of the HDAC binding pocket. Subsequently, the

IC_{50} values of the most promising photochromic inhibitors **3** and **6** were determined (Table 3).

In general, very potent inhibition of *h*HDAC6 and *h*HDAC8 is observed for both isomers of compound **6** as well as a preference for the *human* over the *S. mansoni* isotype is registered. The activity on *h*HDAC1 is in the lower micromolar range which can be explained by the narrow binding pocket which does not allow a favorable coordination of the hydroxamic acid group to the zinc ion. Generally, the difference in the observed IC_{50} values of all compounds is too small to perform assays with direct irradiation.

Table 3. IC_{50} values of the respective isomers of DTEs **3** and **6** against different HDACs.

Entry	Compound	*h*HDAC1 [μM]	*h*HDAC6 [μM]	*h*HDAC8 [μM]	*sm*HDAC8 [μM]
1	**3 open**	15 ± 1.2	1.8 ± 0.2	1.6 ± 0.6	5.8 ± 1.1
2	**3 byprod.**	26 ± 2.5	3.9 ± 0.2	2.7 ± 0.9	22 ± 3.9
	ratio	< 2-fold	2-fold	< 2-fold	4-fold
3	**6 open**	4.2 ± 0.7	0.213 ± 0.018	0.248 ± 0.029	18 ± 2.1
4	**6 PSS**	5.1 ± 0.8	0.297 ± 0.041	0.262 ± 0.036	4.5 ± 0.8
	ratio	no difference	no difference	no difference	4-fold

2.2.4 Synthesis of the Fulgimide Derivatives

Due to the moderate photochromic properties and small difference in their biological inhibitory effects between the isomers of the prepared DTEs we changed the photochromic scaffold to fulgimides. They can be prepared by the reaction of the anhydride moiety of a fulgide with amines. The synthesis of our fulgimide based photochromic HDAC inhibitors is depicted in Scheme 5. Fulgide **16** was prepared by an optimized procedure[78] *via* Stobbe[79-81] condensation from precursors furan **14** and diethylsuccinate **15** in 20% yield. Further reaction with two different amines under basic conditions and CDI as coupling reagent to form the bisimide, which is the crucial step, afforded fulgimides **17** and **19**. Interestingly, the reaction with aniline worked best with potassium carbonate as base, the reaction of the primary amine with triethylamine. In a last step the hydroxamic acid moiety was introduced by treating esters **17** and **19** with

aqueous hydroxylamine solution, respectively. Due to the high nucleophilicity of hydroxylamine in basic media a lot of side reactions occurred in this step and the desired target compounds **18** and **20** could only be isolated in low yields.
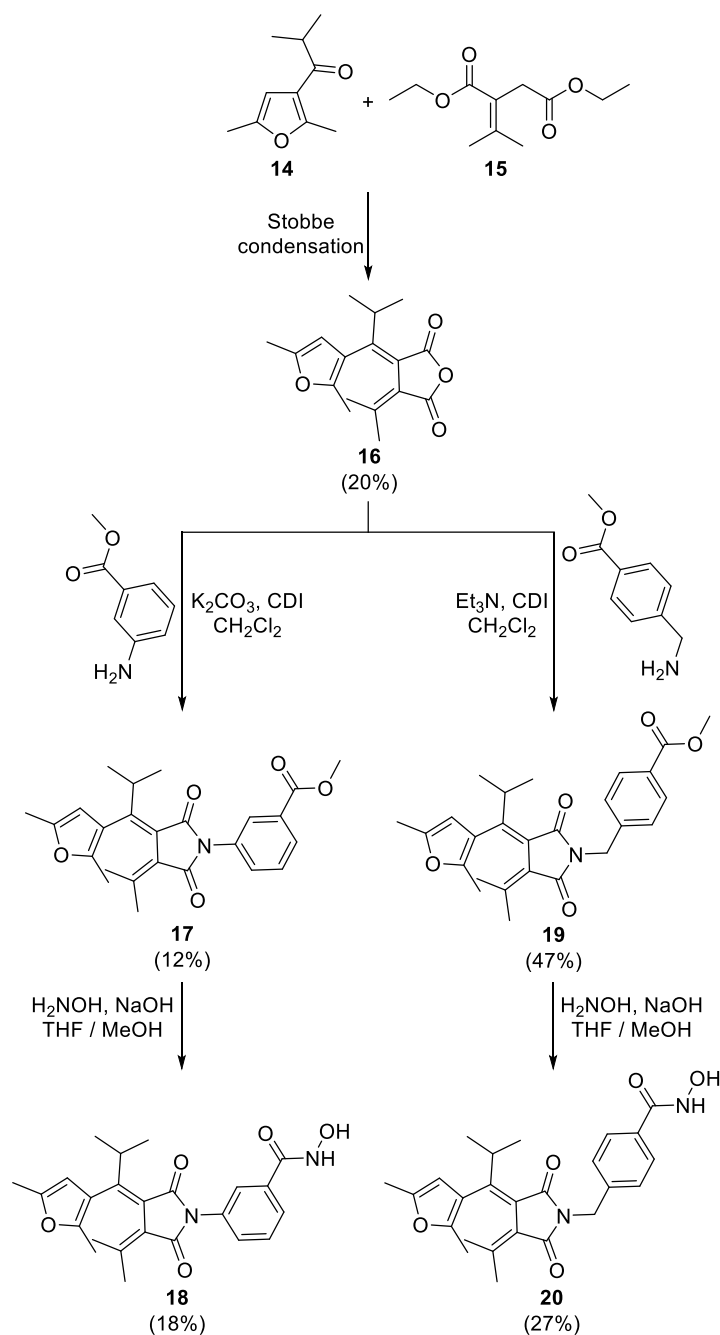
Scheme 5. Preparation of fulgimides **18** and **20**.

2.2.5 Photochromic Properties of the Fulgimides

The photochromism of fulgides and fulgimides has its origin in a concerted electrocyclization and occurs very fast. Therefore they are widely used in materials

science and optical data storage.[58] By introducing a bulky substituent on the 1,3,5 hexatriene system, like an isopropyl group in our case, the undesired UV-light induced *E/Z* isomerization from the open *E*-fulgimide isomer to the closed *Z*-isomer is suppressed (Scheme 6).[78]

Z-fulgimide open   **E-fulgimide open**   **fulgimide closed**
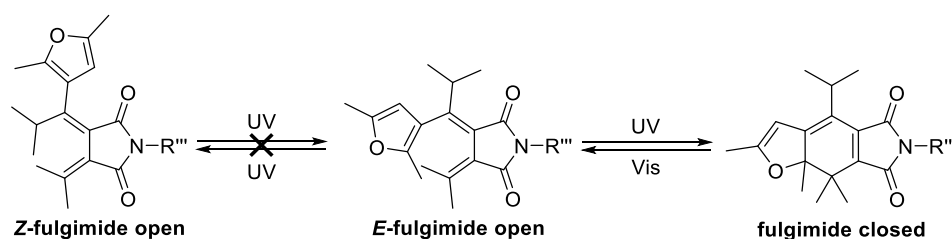
Scheme 6. Reversible photochemical isomerization of a fulgimide between the *E*-open and closed photoisomer by irradiation with light of different wavelength. The photochemical isomerization from the open *E*-isomer to the open *Z*-isomer is suppressed by the sterically demanding isopropyl group.

Only the open *E*-isomer can undergo a photocyclization to the closed isomer which is thermally stable. First, we investigated the photochromic properties of compounds **18** and **20** in DMSO (100 μM). Upon irradiation (λ = 365 nm) a quick color change from colorless to pink was observed, resulting in a new broad absorption band with a maximum around 520 nm for each compound. The photochromic properties of fulgimides **18** and **20** are summarized in Table 4. The PSS of both fulgimides exceeds 95% which is beneficial and advantageous for photochromic enzyme inhibitors as the interaction with the enzyme can be assigned to mainly one photoisomer.

Table 4. Photochromic properties of fulgimides **18** and **20** (100 μM in DMSO).

Entry	Compound	λ_{max} open [nm]	λ_{max} PSS [nm]	Isosbestic points [nm]	PSS [%]*
1	**18**	335 (shoulder)	519	280, 380	98
2	**20**	333 (shoulder)	518	293, 312, 388	96

* Determined by HPLC measurements.

By way of example, Figure 1a illustrates the spectral evolution (marked with arrows) of compound **20** upon irradiation (λ = 365 nm). The isosbestic points (Table 4) indicate a clear two-component switching. After 30 s of irradiation the PSS was reached and 96% of the open isomer were converted to the closed photoisomer. The repetitive cycle

performance with light of λ = 365 nm for closing and λ = 530 nm for opening shows a high fatigue resistance over seven cycles (Figure 1b).

In addition, the photochromic properties of fulgimides **18** and **20** were also investigated in aqueous PBS (pH = 7.4) with 1% of DMSO as solvent. Both compounds showed a similar reversible photochromic performance like in DMSO with slightly bathochromically shifted maxima. Only at the repetition of the photoisomerization a slightly reduced fatigue resistance was observed (see Supporting Information, Figure S8 and Figure S9). In summary, the outstanding photochromic properties of the prepared fulgimides in polar as well as aqueous systems make them perfect candidates for use in biological environment.
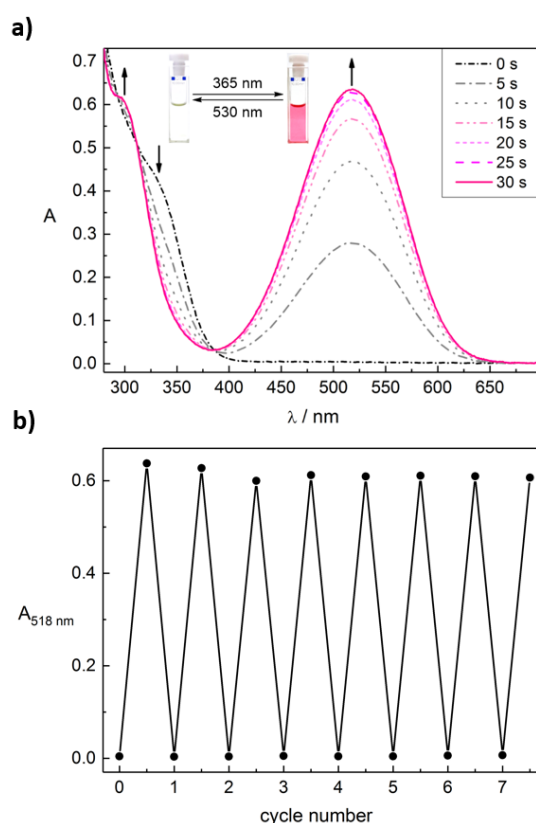
Figure 1. a) Changes in absorption spectra of fulgimide **20** (100 µM in DMSO) upon continuous irradiation for 0, 5, 10, 15, 20, 25, and 30 s with light of λ = 365 nm until the PSS is reached. The cuvettes show the color of the solution before and after irradiation. b) Cycle performance of the fulgimide **20** (100 µM in DMSO). Changes in absorption at 518 nm were measured during alternate irradiation with light of 365 nm for 30 s and 530 nm for 5 min.

2.2.6 Enzyme Inhibition

Analogous to the DTE inhibitors, the IC_{50} values of fulgimides **18** and **20** for hHDAC1, hHDAC6, hHDAC8 as well as smHDAC8 were quantified (Table 5).

For compound **18** low micromolar IC_{50} values are observed for hHDAC6, hHDAC8 and smHDAC8 and there is only little or no difference between the IC_{50} values of the two isomers. Compound **20** displays nanomolar affinity for hHDAC6 but again with a very small difference between the two different isomers. As above for the DTE derivatives, the difference of IC_{50} values did not provide a basis to perform assays under irradiation.

Table 5. IC_{50} values of the respective isomers of fulgimides **18** and **20** against different HDACs.

Entry	Comp.	hHDAC1 [µM]	hHDAC6 [µM]	hHDAC8 [µM]	smHDAC8 [µM]
1	**18 open**	28.5 ± 10.9	1.8 ± 0.5	1.1 ± 0.2	1.1 ± 0.2
2	**18 PSS**	87.7 ± 53.0	6.1 ± 1.7	0.88 ± 0.07	1.1 ± 0.1
	ratio	3-fold	3-fold	no difference	no difference
3	**20 open**	6.4 ± 1.0	0.047 ± 0.032	5.6 ± 1.3	8.9 ± 3.1
4	**20 PSS**	5.0 ± 1.0	0.075 ± 0.047	3.6 ± 1.0	5.7 ± 2.0
	ratio	no difference	< 2-fold	< 2-fold	< 2-fold

2.2.7 Molecular Docking

In order to rationalize the experimental biological data all the prepared compounds were docked to the different enzymes. The available crystal structures of hHDAC1, hHDAC6, hHDAC8 and smHDAC8 show the typical fold of zinc-dependent histone deacetylases.[51, 82] The catalytic zinc ion is bound by two aspartate and one histidine residue. The middle part of the acetyl-lysine binding pocket is formed by two conserved phenylalanine residues whereas the rim of the pocked is composed by flexible loops that are different in the various HDAC isoforms. As consequence the shape of the binding pocket of individual HDAC isoforms is rather different which enabled the development of isoform selective inhibitors.[83] HDACs have been cocrystallized with several hydroxamic acids that showed a bidental chelating of the zinc ion. In case of hHDAC6 the recently reported structures[84, 85] showed a slightly different binding mode of hydroxamic acids.

Here, a water molecule is bridging the interaction of the terminal hydroxy group to the zinc ion.

The *h*HDAC1 binding pocket is rather narrow and the docking of the bulky DTEs and fulgimides resulted generally in less favorable docking complexes. Due to the narrow pocket the distances between the hydroxamic acid carbonyl and hydroxy group are above 3 Å. In addition, the docking scores for all compounds are rather weak (see Supporting Information, Table S1). For compound **3 byproduct** no docking pose that showed a binding of the hydroxamic acid nearby the zinc ion was obtained.

Docking of the DTE inhibitors to *h*HDAC6 and *h*HDAC8 binding pockets showed that the hydroxamic acids are showing the favorable coordination to the zinc ion as observed for the cocrystallized inhibitors. The methylthiophene ring attached to the hydroxamic acid is embedded between two conserved phenylalanine residues of the HDAC binding pocket (F152 and F208 in *h*HDAC8, F620 and F680 in *h*HDAC6). In case of *h*HDAC6 and *h*HDAC8 the second hydroxamic acid groups of **6 open** and **6 closed** are making a hydrogen bond to S568 (*h*HDAC6) and D101 (*h*HDAC8) that are located on a flexible loop of the enzyme (Figure 2). S568 of *h*HDAC6 is interacting with the carbonyl group, whereas D101 of *h*HDAC8 is interacting with the NH group of the hydroxamic acid. These hydrogen bonds might explain the good inhibitory activity for both isoforms. The hydrogen bonds were observed for the open and the closed form. In case of **3 open** the lipophilic chlorothiophene is adopting a different conformation and is sticking out of the pocket (see Supporting Information, Figure S10). The less favorable interaction is also supported by the weaker docking scores compared to **6 open** and **6 closed** (see Supporting Information, Table S2 and Table S3). The bulky compound **3 byproduct** could not be docked into the *h*HDAC8 crystal structure used for the other inhibitors. However, docking into the *h*HDAC8 crystal structure complexed with an amino acid derivative (PDB ID 3SFF)[86] was resulting in a docking pose that showed coordination between the hydroxamic acid and the zinc ion. Due to the observed switch of Y306 in this *h*HDAC8 crystal structure the binding pocket becomes wider and accessible for the bulky **3 byproduct**. Enzyme *sm*HDC8 shows a different form of the binding pocket due to the flipping of one of the conserved phenylalanine residues (F151). Therefore, the favorable binding of the methylthiophene between two conserved phenylalanine (like in *h*HDAC6

and *h*HDAC8) is not possible resulting in lower inhibitory activities. In addition, D100 (which corresponds to D101 in *h*HDAC8) is not able to form a hydrogen bond to the NH of the second hydroxamic acid group of **6 open** and **6 closed** (see Supporting Information, Figure S11). The docking of the open form of **3** gave an unfavorable interaction of the hydroxamic acid with the zinc ion (distance CO-Zn 3.30 Å). Due to D100 the second thiophene-hydroxamic acid cannot adopt a similar conformation as observed for the docking pose at *h*HDAC8 (see Supporting Information, Figure S10b and Figure S11c). For compound **3 byproduct** no docking pose that showed a binding of the hydroxamic acid nearby the zinc ion was obtained (see Supporting Information, Table S4).
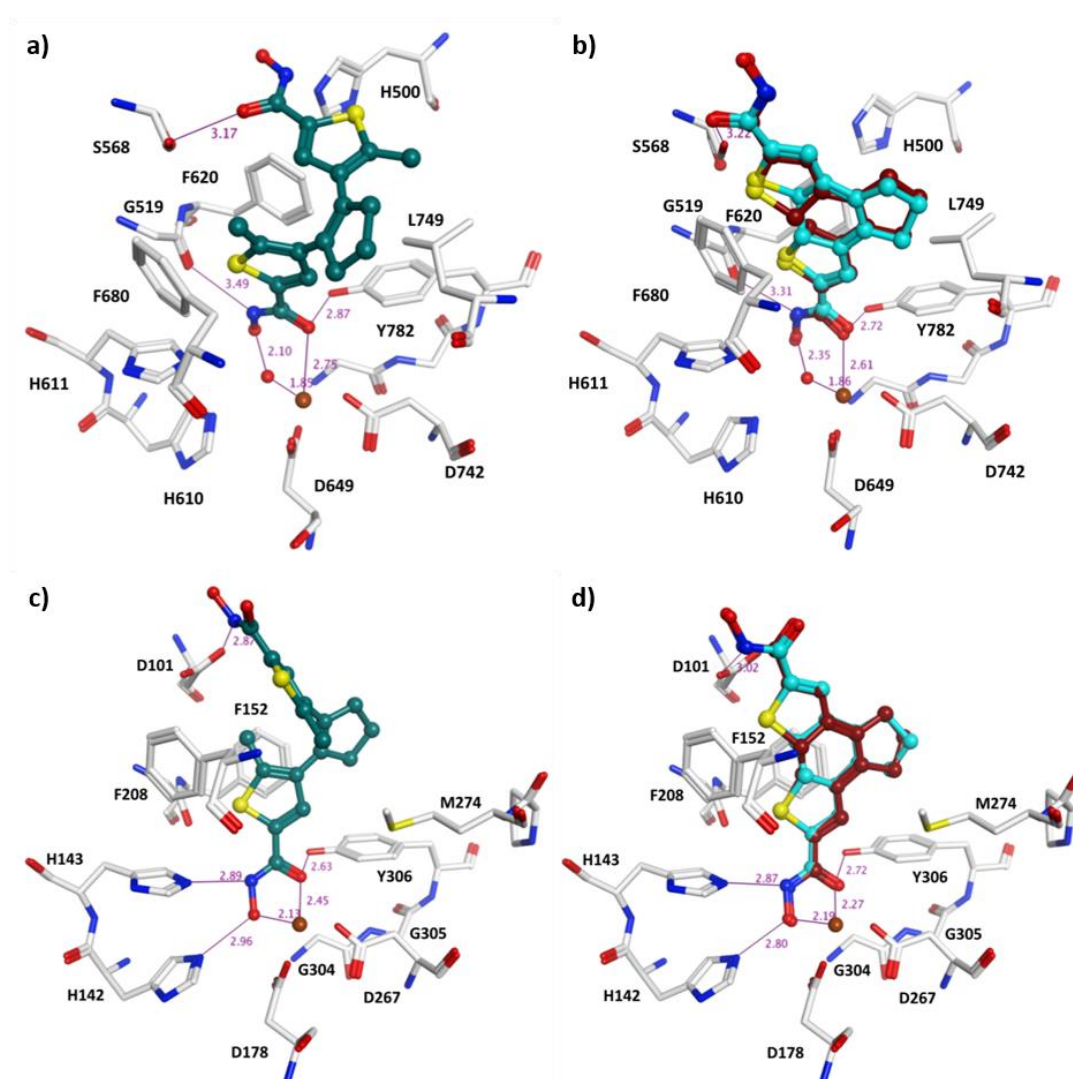
Figure 2. Docking poses of DTE **6** for *h*HDAC6 (**a**, **b**) and *h*HDAC8 (**c**, **d**) (**6 open** colored dark green, **6 closed** (*R,R*) colored cyan and **6 closed**, (*S,S*) colored brown). Only the interacting residues of the binding pockets are displayed. The zinc ion is shown as brown ball, the water molecule bridging the coordination to the zinc ion for hHDAC6 in **a** and **b** is shown as red ball. Distances of the metal coordination and hydrogen bonds are given in Å and are shown as lines colored in magenta.

Docking of the fulgimides to *h*HDAC1 showed that **18 open** and **18 closed** (results not shown) are not able to coordinate to the zinc ion whereas in case of **20 open** and **20 closed** (see Supporting Information, Figure S12) the additional methylene group and the movement of the bulky fulgimide group from meta to the para position of the benzohydroxamic acid is resulting in more favorable docking solutions (see Supporting Information, Table S1). The fulgimide part of **18 open** and **18 closed** is interacting with L271. Since the fulgimide part is located at the open part of the binding pocket it is obvious that both open and closed forms are tolerated by the enzyme.

In case of *h*HDAC6 the two compounds **20 open** and **20 closed** showed the best docking scores and the best shape complimentary (Figure 3a-d). The interaction of the highly active compounds is comparable to the reported and crystallized *h*HDAC6 inhibitor Nexturastat A[85] which has a reported IC$_{50}$ of 5 nM (Figure 3e). The fulgimide part is located in the so called side pocket and interacts with H500, F620 and L749 at the rim of the pocket. In addition, a hydrogen bond to S568 is observed for both forms of **20**. Also here, both forms show favorable interactions with the enzyme (see Supporting Information, Table S2). For the more rigid compounds **18 open** and **18 closed** the L749 side chain is hindering an optimal interaction of the compounds with the zinc ion (Figure 3f) resulting in less favorable docking scores and a significantly lower inhibitory activity.

Docking of the fulgimides to *h*HDAC8 showed a comparable binding mode as observed for *h*HDAC6 (see Supporting Information, Figure S13). However, due to the substitution of L749 (*h*HDAC6) to M274 (*h*HDAC8) the side pocket is larger and the fulgimide side chain of **18 open** and **18 closed** can be nicely accommodated (see Supporting Information, Figure S13d-f). In case of **20 open** and **20 closed** the sidechain of D100 is restricting the size of the pocket for the para-substituted benzohydroxamic acid (see Supporting Information, Figure S13a-c). Similar observations and docking poses were obtained for *sm*HDAC8 (results not shown).

In general, the docking poses derived for the individual HDAC isoforms show a good agreement with the biological data. For example the strong inhibition of *h*HDAC6 by both isomers of fulgimide **20** could be supported by the observed shape complimentary and the calculated docking scores.

Figure 3. Docking poses of the fulgimides (**20 open** colored green, **a** and **c**; **20 closed** (*S*) colored blue and **20 closed** (*R*) colored light grey, **b** and **d**; **18 open** colored yellow, **f**) for *h*HDAC6 in comparison to the cocrystallized inhibitor Nexturastat A (colored cyan, **e**). The zinc ion is shown as brown ball and the water molecule bridging the coordination to the zinc ion is shown as red ball. Distances of the metal coordination and hydrogen bonds are given in Å and are shown as lines colored Dithin magenta. The m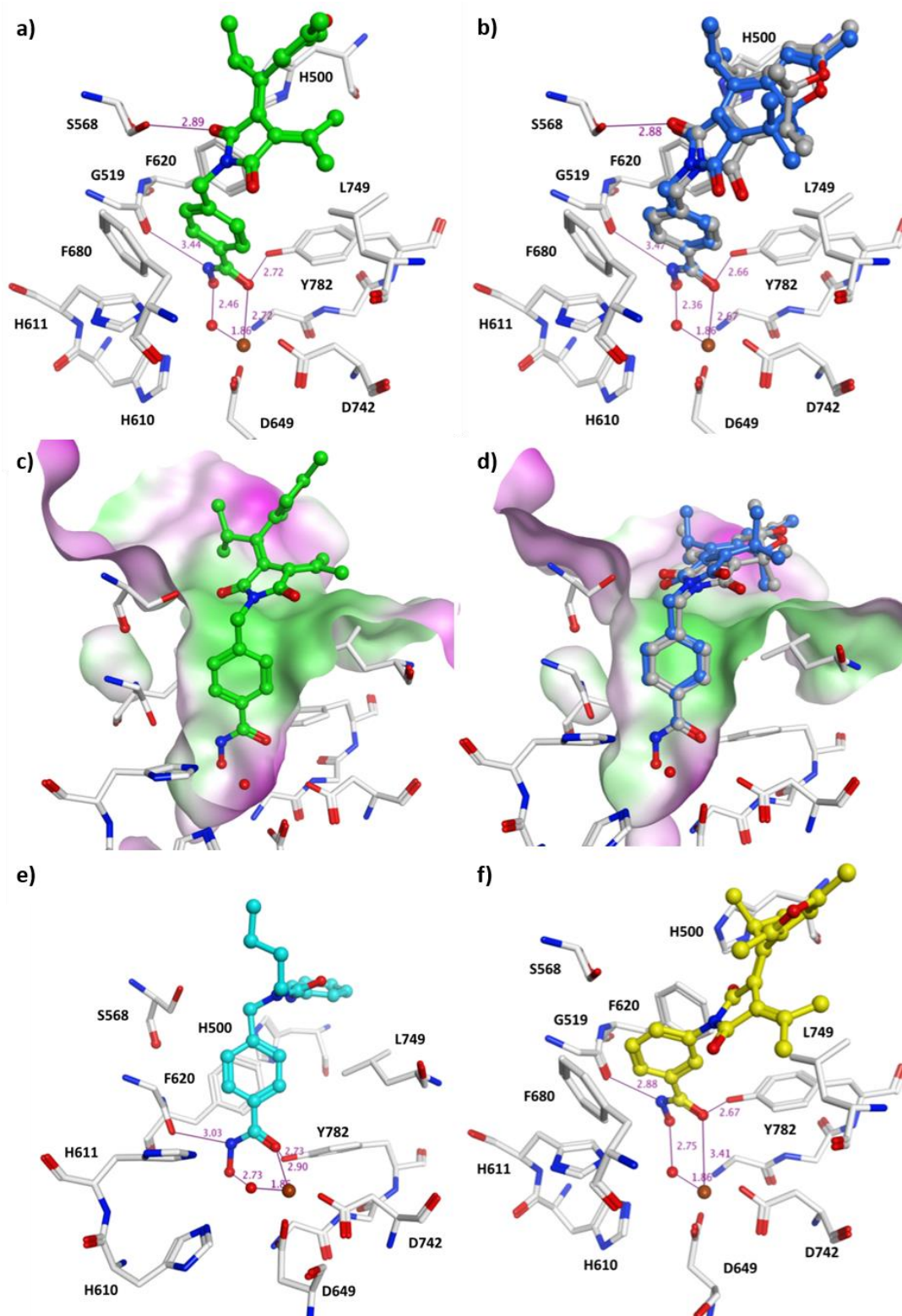olecular surface of the *h*HDAC6 binding pocket in **c** and **d** are colored according to the hydrophobicity (hydrophobic region are colored green, polar region are colored magenta).

2.3 Conclusion

In summary, we functionalized the two established photochromic scaffolds of DTEs and fulgimides with hydroxamic acid moieties to obtain photoswitchable inhibitors for zinc dependent HDACs. The two different classes of prepared DTEs, dithienylcyclopentenes and dithienylmaleimides, showed only moderate photochromic properties in DMSO and aqueous media. In contrast, the fulgimides provided excellent reversible photochromic performance in DMSO as well as aqueous PBS with very high photostationary states. These properties recommend them as perfect photochromic groups for biological applications. All target compounds showed an inhibitory effect of the tested hHDAC1, hHDAC6, hHDAC8 and smHDAC8 with IC$_{50}$ values in the range of 50 nM to 90 µM. We achieved a maximum four-fold difference in inhibitory ability between two corresponding photoisomers. This provides a good basis for the development of more efficient photochromic inhibitors with higher difference in activity triggered by light, which is necessary to beneficially utilize photopharmacology for HDACs. The in $vitro$ activities of our photochromic inhibitors were rationalized by molecular dockings showing that while potency could be explained well, the lack of selectivity between the open and closed forms was hard to predict. This might probably be due to the flexibility of HDACs that is documented by different crystal structures showing the plasticity of the binding pocket but is difficult to use in prospective analysis of photoswitchable HDAC inhibitors. Still, very potent HDAC inhibitors with new scaffolds especially for hHDAC6 could be realized.

2.4 Experimental

2.4.1 Chemistry

Compounds **1**,[66] **2**,[67] **4**,[66] **7**,[68] **8**,[68] **14**[78] and **15**[78] were prepared according to previously reported procedures. Commercial reagents and starting materials were purchased from Acros Organics, Alfa-Aesar, Fisher Scientific, Sigma Aldrich or VWR and used without any further purification. Solvents were used in p.a. quality and dried according to common procedures, if necessary. Dry nitrogen was used as inert gas atmosphere. Automated flash column chromatography was performed on a Biotage Isolera flash purification system with UV/Vis detector using Sigma Aldrich MN silica gel 60

M (40-63 µm, 230-400 mesh) for normal phase or pre-packed Biotage SNAP cartridges (KP C18 HS) for reversed phase chromatography. Reaction monitoring via TLC was performed on alumina plates coated with silica gel (Merck silica gel 60 F254, 0.2 mm). Melting points were determined using a Stanford Research Systems OptiMelt MPA 100 and are uncorrected. NMR spectra were measured on Bruker Avance 300 (^{1}H 300.13 MHz, ^{13}C 75.48 MHz), Bruker Avance 400 (^{1}H 400.13 MHz, ^{13}C 100.61 MHz), Bruker Avance III 600 (^{1}H 600.25 MHz, ^{13}C 150.95 MHz) and Bruker Avance 800 (^{1}H 800.20. MHz, ^{13}C 201.21 MHz) instruments. The spectra are referenced against the NMR-solvent (CDCl$_3$: δ_H = 7.26 ppm, δ_C = 77.16 ppm, DMSO-d_6: δ_H = 2.50 ppm, δ_C = 39.52 ppm) and chemical shifts δ are reported in ppm. Resonance multiplicity is abbreviated as: s (singlet), d (doublet), t (triplet), quint (quintet), sept (septet) and m (multiplet). Carbon NMR signals are reported using DEPT 135 and ^{1}H-^{13}C HSQC spectra with (+) for primary/tertiary, (−) for secondary and (q) for quaternary carbons. Mass spectra were recorded on an Agilent Q-TOF 6540 UHD (ESI-MS) instrument. UV/Vis absorption spectroscopy was performed using a Varian Cary BIO 50 UV/Vis spectrometer in 10 mm quartz cuvettes. IR-spectra were measured with an Agilent Cary 630 FT-IR spectrometer and the peak positions are reported in wavenumbers (cm^{-1}). Analytical HPLC measurements were performed on an Agilent 1290 series UHPLC-MS system (column: Phenomenex Luna C18(2), 3 µM, 100 Å, 150 x 2.00 mm; flow: 0.3 mL/min at 25 °C or 40 °C; solvent A: MilliQ water with 0.059 wt. % TFA; solvent B: MeCN) and an Agilent 1220 Infinity LC (column: Phenomenex Luna 3 µM C18(2) 100 Å, 150 x 2.00 mm; flow: 0.3 mL/min at 30 °C; solvent A: MilliQ water with 0.05 % vol. TFA; solvent B: MeCN). The ratios in the PSSs were determined at the isosbestic points. An Agilent 1260 system (column: Phenomenex Luna 10 µM C18(2) 100 Å, 250 x 21.2 mm; flow: 22.0 mL/min; solvent A: MilliQ water with 0.05 % vol. TFA; solvent B: MeCN) was used for preparative HPLC purification. Light sources for irradiation: λ = 300 nm (NIKKISO UV LED, 150 mA, 25 mW), λ = 312 nm (Herolab hand-held lamp UV-6 M, 6 W), λ = 365 nm (Herolab hand-held lamp UV-6 L, 6 W), λ = 470 nm (OSRAM Oslon SSL 80 LED, 700 mA, 1.12 W), λ = 530 nm (CREE-XP green LED, 700 mA, 3.7 W). The power of the light is given based on the specifications supplied by the company when the lamps were purchased. All tested final compounds possess a purity ≥95% determined by HPLC measurements with detection at 220 nm or 254 nm, respectively.

4-[2-(5-Chloro-2-methylthiophen-3-yl)-cyclopent-1-en-1-yl]-*N*-hydroxy-5-methylthio-phene-2-carboxamide (3)

To a stirred solution of **2** (100 mg, 0.28 mmol, 1.0 eq.) in CH_2Cl_2 (3 mL) $SOCl_2$ (64.2 µL, 0.85 mmol, 3.0 eq.) was added slowly at 0°C. After complete addition the solution was stirred at 40°C for 3 h. The mixture was cooled to room temperature and concentrated in *vacuo*. The residue was dissolved in THF/MeOH (1:1, 5 mL). Afterwards a solution of NaOH (90 mg, 2.24 mmol, 8.0 eq.) in an aqueous hydroxylamine solution (50 wt. %, 0.72 mL) was added dropwise to the mixture at 0°C. The resulting solution was stirred at room temperature overnight. The reaction was quenched with AcOH (1.50 mL) and concentrated in *vacuo*. Purification by automated flash column chromatography (CH_2Cl_2/MeOH, 5% - 10% MeOH) and subsequent preparative HPLC (60% - 98% MeCN in 10 min, t_R = 7.3 min) yielded **3** (28 mg, 26%) as colorless solid. R_f 0.29 (PE/EtOAc 1:1); m.p. 128 °C; ^{1}H-NMR (400 MHz, DMSO-d_6) δ = 11.05 (s, 1H), 9.01 (s, 1H), 7.35 (s, 1H), 6.83 (s, 1H), 2.73 (t, *J* = 7.5 Hz, 4H), 2.03 - 1.92 (m, 5H), 1.79 (s, 3H); ^{13}C-NMR (151 MHz, DMSO-d_6) δ = 159.4 (q), 138.6 (q), 135.9 (q), 134.9 (q), 134.4 (q), 133.9 (q), 133.0 (q, 2C) 128.4 (+), 127.3 (+), 123.6 (q), 38.0 (−), 37.8 (−), 22.2 (−), 14.1 (+), 13.7 (+); HRMS (ESI) calcd. for $C_{16}H_{15}ClNO_2S_2$ (M-H)$^-$ m/z = 352.0238; found: 352.0251.

Dimethyl-4,4'-(cyclopent-1-ene-1,2-diyl)bis(5-methylthiophene-2-carboxylate) (5)

$SOCl_2$ (0.52 mL, 7.20 mmol, 10.0 eq.) was added dropwise to a solution of **4** (250 mg, 0.72 mmol, 1.0 eq.) in anhydrous MeOH (15 mL) at 0°C under nitrogen atmosphere and stirred for 5 h at 65°C. The mixture was cooled to room temperature and concentrated in *vacuo*. The residue was suspended in EtOAc (15 mL) and washed with water (3 x 10 mL) and brine (10 mL). The organic layer was dried over Na_2SO_4, filtered and the solvent was removed under reduced pressure. Purification by automated flash column chromatography (PE/EtOAc, 5% - 30% EtOAc) yielded **5** (180 mg, 66%) as colorless solid. R_f 0.72 (PE/EtOAc 1:1); m.p. 163 °C; ^{1}H-NMR (400 MHz, $CDCl_3$) δ = 7.50 (s, 2H), 3.84 (s, 6H), 2.78 (t, *J* = 7.5 Hz, 4H), 2.06 (quint, *J* = 7.5 Hz, 2H) 1.90 (s, 6H); ^{13}C-NMR (101 MHz, $CDCl_3$) δ = 162.7 (q), 142.9 (q), 136.7 (q), 134.9 (q), 134.6 (+), 129.4 (q), 52.2 (+), 38.8 (−), 23.0 (−), 14.9 (+); HRMS (ESI) calcd. for $C_{19}H_{21}O_4S_2$ (M+H)$^+$ m/z = 377.0880; found: 377.0876.

_N_-Hydroxy-4-(2-[5-(hydroxycarbamoyl)-2-methylthiophen-3-yl]cyclopent-1-en-1-yl)-5-methylthiophene-2-carboxamide (6)

NaOH (135 mg, 3.38 mmol, 8.0 eq.) was dissolved in an aqueous hydroxylamine solution (50 wt. %, 1.1 mL). The solution was added dropwise to a solution of **5** (160 mg, 0.42 mmol, 1.0 eq.) in THF/MeOH (1:1, 7 mL) at 0°C. The resulting solution was stirred overnight at room temperature. The reaction was quenched with AcOH (1.5 mL) and concentrated _in vacuo_. Purification by automated reversed phase flash column chromatography (H_2O/MeOH, 5% - 100% MeOH) and subsequent preparative HPLC (20% - 98% MeCN in 12 min, t_R = 6.8 min) yielded **6** (100 mg, 61%) as colorless solid. R_f 0.05 (PE/EtOAc 1:1); m.p. 182 °C; ^{1}H-NMR (400 MHz, DMSO-d_6) δ = 11.04 (s, 2H), 9.01 (s, 2H), 7.35 (s, 2H), 2.74 (t, _J_ = 7.4 Hz, 4H), 2.00 (quint, _J_ = 7.4 Hz, 2H), 1.87 (s, 6H); ^{13}C-NMR (101 MHz, DMSO-d_6) δ = 159.4 (q), 138.5 (q), 135.9 (q), 134.2 (q), 132.9 (q), 128.4 (+), 38.0 (−), 22.3 (−), 14.1 (+); HRMS (ESI) calcd. for $C_{17}H_{19}N_2O_4S_2$ (M+H)$^+$ m/z = 379.0635; found:. 379.0640.

Methyl-4-[4-(5-chloro-2-methylthiophen-3-yl)-2,5-dioxo-2,5-dihydro-1_H_-pyrrol-3-yl]-5-methylthiophene-2-carboxylate (9)

KO_t_Bu (1 M in THF, 1.45 mL, 1.45 mmol, 1.2 eq.) was added to a solution of amide **7** (277 mg, 1.21 mmol, 1.0 eq.) in anhydrous THF (6 mL) at 0°C under nitrogen atmosphere. After stirring for 90 min ester **8** (296 mg, 1.45 mmol, 1.2 eq.) was added at 0°C and the mixture was stirred overnight at room temperature. The reaction was quenched with aqueous HCl solution (1 M, 15 mL) and diluted with EtOAc (15 mL). The organic phase was separated, washed with water (3 x 15 mL), brine (1 x 30 mL) and dried over $MgSO_4$. The solvent was removed under reduced pressure. Purification of the crude product was performed by automated flash column chromatography (PE/EtOAc, 5% - 30% EtOAc) yielding **9** (210 mg, 45%) as yellow solid. R_f 0.68 (PE/EtOAc 1:1); m.p. 183 °C; ^{1}H-NMR (400 MHz, DMSO-d_6) δ = 11.29 (s, 1H), 7.70 (s, 1H), 6.99 (s, 1H), 3.81 (s, 3H), 2.00 (s, 3H), 1.85 (s, 3H); ^{13}C-NMR (101 MHz, DMSO-d_6) δ = 171.0 (q), 171.0 (q), 161.3 (q), 148.0 (q), 139.6 (q), 135.2 (+), 133.4 (q), 133.1 (q), 129.3 (q), 128.0 (q), 127.9 (+), 126.6 (q), 124.6 (q), 52.3 (+), 14.6 (+), 14.1 (+); HRMS (ESI) calcd. for $C_{16}H_{13}ClNO_4S_2$ (M+H)$^+$ m/z = 381.9969; found: 381.9978.

4-[4-(5-Chloro-2-methylthiophen-3-yl)-2,5-dioxo-2,5-dihydro-1*H*-pyrrol-3-yl]-*N*-hydroxy-5-methylthiophene-2-carboxamide (10)

NaOH (75 mg, 1.88 mmol, 8.0 eq.) was dissolved in an aqueous hydroxylamine solution (50 wt. %, 0.60 mL). This solution was added dropwise to a solution of **9** (90 mg, 0.24 mmol, 1.0 eq.) in THF/MeOH (1:1, 5 mL) at - 20°C. The resulting solution was stirred for 20 min at - 20°C and was then warmed to - 3°C in 20 min. The reaction was quenched with AcOH (1.5 mL) and concentrated *in vacuo*. Purification by automated flash column chromatography (CH_2Cl_2/MeOH, 5% - 10% MeOH) and subsequent preparative HPLC (30% - 70% MeCN in 15 min, t_R = 9.4 min) yielded **10** (68 mg, 76%) as orange solid. R_f 0.25 (PE/EtOAc 1:1); m.p. 175 °C; ^{1}H-NMR (400 MHz, DMSO-d_6) δ = 11.27 (s, 2H), 9.09 (s, 1H), 7.51 (s, 1H), 6.99 (s, 1H), 2.00 (s, 3H), 1.84 (s, 3H); ^{13}C-NMR (101 MHz, DMSO-d_6) δ = 171.1 (q), 158.9 (q), 144.6 (q), 139.5 (q), 134.1 (q), 133.5 (q), 133.3 (q), 128.9 (q), 128.9 (+), 128.0 (+), 127.4 (q), 126.6 (q), 124.5 (q), 14.5 (+), 14.1 (+); HRMS (ESI) calcd. for $C_{15}H_{12}ClN_2O_4S_2$ (M+H)$^+$ m/z = 382.9922; found: 382.9925.

Methyl-4-[4-(5-chloro-2-methylthiophen-3-yl)-1-methyl-2,5-dioxo-2,5,-dihydro-1*H*-pyrrol-3-yl]-5-methylthiophene-2-carboxylate (11)

Methyl iodide (13 µL, 0.21 mmol, 2.0 eq.) was added dropwise to a solution of dithienylmaleimide **9** (40 mg, 0.11 mmol, 1.0 eq.) in anhydrous DMF (6 mL) at 0°C under nitrogen atmosphere. The solution was stirred overnight at room temperature and then diluted with water (5 mL) and EtOAc (5 mL). The aqueous phase was extracted with EtOAc (3 x 5 mL). The combined organic phases were dried over $MgSO_4$, filtered and the solvent was removed under reduced pressure. Dithienylmaleimde **11** was obtained as yellow solid (30 mg, 76%) and was used without further purification. R_f 0.78 (PE/EtOAc 1:1); m.p. 187 °C; ^{1}H-NMR (400 MHz, CDCl$_3$) δ = 7.75 (s, 1H), 6.88 (s, 1H), 3.88 (s, 3H), 3.14 (s, 3H), 2.04 (s, 3H), 1.88 (s, 3H); ^{13}C-NMR (201 MHz, CDCl$_3$) δ = 170.3 (q), 170.2 (q), 162.2 (q), 148.5 (q), 140.3 (q), 135.0 (+), 133.3 (q), 132.8 (q), 131.1 (q), 127.6 (q), 127.5 (q), 127.2 (+), 126.1 (q), 52.4 (+), 24.6 (+), 15.5 (+), 15.0 (+); HRMS (ESI) calcd. for $C_{17}H_{15}ClNO_4S_2$ (M+H)$^+$, m/z = 396.0126; found: 396.0131.

4-[4-(5-Chloro-2-methylthiophen3-yl)-1-hydroxy-2,5-dioxo-2,5-dihydro-1*H*-pyrrol-3-yl]-*N*-hydroxy-5-methylthiophene-2-carboxamide (12)

NaOH (32 mg, 0.81 mmol, 8.0 eq.) was dissolved in an aqueous hydroxylamine solution (50 wt. %, 0.26 mL). The solution was added dropwise to a solution of **11** (40 mg, 0.10 mmol, 1.0 eq.) in THF/MeOH (1:1, 5 mL) at 0°C. The resulting solution was stirred overnight at room temperature. The reaction was quenched with AcOH (1.5 mL) and concentrated *in vacuo*. Purification by automated reversed phase flash column chromatography (H_2O/MeOH, 5% - 100% MeOH) and subsequent preparative HPLC (25% - 80% MeCN in 15 min, t_R = 9.1 min) yielded **32** (21 mg, 50%) as yellow solid. R_f 0.05 (PE/EtOAc 1:1); m.p. 140 °C; ^{1}H-NMR (400 MHz, DMSO-d_6) δ = 11.29 (s, 1H), 10.69 (s, 1H), 9.11 (s, 1H), 7.52 (s, 1H), 7.01 (s, 1H), 2.00 (s, 3H), 1.85 (s, 3H); ^{13}C-NMR (101 MHz, DMSO-d_6) δ = 166.3 (q), 166.3 (q), 158.8 (q), 145.1 (q), 140.1 (q), 134.3 (q), 130.2 (q), 130.0 (q), 128.7 (+), 127.8 (+), 127.1 (q), 126.2 (q), 124.7 (q), 14.5 (+), 14.1 (+); HRMS (ESI) calcd. for $C_{15}H_{10}ClN_2O_5S_2$ (M-H)$^-$, m/z = 396.9725; found: 396.9732.

Methyl-4-[4-(5-chloro-2-methylthiophen-3-yl)-1-hydroxy-2,5-dioxo-2,5-dihydro-1*H*-pyrrol-3-yl]-5-methylthiophene-2-carboxylate (13)

NaOH (25.0 mg, 0.63 mmol, 8.0 eq.) was dissolved in an aqueous hydroxylamine solution (50 wt. %, 0.20 mL). The solution was added dropwise to a solution of **11** (30 mg, 0.08 mmol, 1.0 eq.) in THF/MeOH (1:1, 3 mL) at - 20°C. The resulting solution was stirred for 10 min at - 20°C and was warmed to - 8°C in 10 min afterwards. The reaction was quenched with AcOH (1.5 mL) and concentrated in *vacuo*. Purification by automated flash column chromatography (CH_2Cl_2/MeOH, 5% - 10% MeOH) and subsequent preparative HPLC (60% - 98% MeCN in 10 min, t_R = 6.5 min) yielded **13** (8 mg, 26%) as yellow solid. R_f 0.31 (PE/EtOAc 1:1); m.p. 193 °C; ^{1}H-NMR (600 MHz, DMSO-d_6) δ = 10.73 (s, 1H), 7.71 (s, 1H), 7.01 (s, 1H), 3.82 (s, 3H), 2.01 (s, 3 H), 1.86 (s, 3H); ^{13}C-NMR (151 MHz, DMSO-d_6) δ = 166.3 (q), 166.3 (q), 161.3 (q), 148.4 (q), 140.2 (q), 135.1 (+), 130.1 (q), 129.9 (q), 129.5 (q), 127.8 (+), 127.7 (q), 126.2 (q), 124.8 (q), 52.4 (+), 14.7 (+), 14.1 (+); HRMS (ESI) calcd. for $C_{16}H_{13}ClNO_5S_2$ (M+H)$^+$ m/z = 397.9918; found: 397.9929.

(*E*)-3-(1-(2,5-dimethylfuran-3-yl)-2-methylpropylidene)-4-(propan-2-ylidene) dihydro-furan-2,5-dione (16)

A solution of succinate **15** (2.55 g, 11.91 mmol, 1.0 eq.) in anhydrous THF (15 mL) was cooled to -105°C under N_2-atmosphere and a freshly prepared solution of LDA by adding a solution of *n*BuLi (1.6 M in hexane, 7.4 mL, 11.91 mmol, 1.0 eq.,) to a solution of diisopropylamine (1.7 mL, 11.91 mmol, 1.0 eq.) in anhydrous THF (6 mL) at -78°C under N_2-atmosphere was added dropwise at -105°C. After stirring for 30 min a precooled solution of furan **14** (1.98 g, 11.91 mmol, 1.0 eq.) in anhydrous THF (5 mL) was added dropwise. The reaction mixture was warmed to room temperature und stirred overnight. The solution was acidified with aqueous HCl (2 M) and the aqueous layer was extracted with EtOAc (3 x 50 mL). The combined organic layers were washed with brine (100 mL), dried over $MgSO_4$, and the solvent was evaporated under reduced pressure. The residue was dissolved in EtOH (60 mL) and a saturated aqueous solution of KOH (5 mL) was added. After stirring at 70°C for 24 h, the reaction mixture was poured onto ice and acidified with aqueous HCl (2 M). The aqueous layer was extracted with EtOAc (3 x 50 mL), and the combined organic layers were washed with brine (100 mL), dried over $MgSO_4$, and the solvent was removed *in vacuo*. The dark-brown residue was dissolved in acetyl chloride (20 mL) and the mixture was heated to 40°C overnight. The solvent was evaporated under reduced pressure and the crude product was purified by automated flash column chromatography (PE/EtOAc, 5% EtOAc) to obtain fulgide **16** (688 mg, 20%) as a pink solid. The analytical data were in accordance with data from literature.[78]

Methyl (*E*)-3-(3-(1-(2,5-dimethylfuran-3-yl)-2-methylpropylidene)-2,5-dioxo-4-(propan-2-ylidene)pyrrolidin-1-yl)benzoate (17)

A suspension of fulgide **16** (98 mg, 0.34 mmol, 1.0 eq.), methyl 3-aminobenzoate (154 mg, 1.02 mmol, 3.0 eq.) and K_2CO_3 (235 mg, 1.70 mmol, 5.0 eq.) in anhydrous CH_2Cl_2 (5 mL) was refluxed for 3 d. After filtration CDI (83 mg, 0.51 mmol, 1.5 eq.) was added and the mixture was stirred at room temperature for 1 d. The reaction mixture was acidified with aqueous HCl (1 M) and the aqueous layer was extracted with CH_2Cl_2 (3 x 10 mL). The combined organic layers were washed with brine (10 mL), dried over $MgSO_4$ and the solvent was evaporated under reduced pressure. Purification by automated flash column chromatography (PE/EtOAc, 3% - 15% EtOAc) afforded fulgimide **17** (17 mg, 12%) as

orange oil. R_f 0.30 (PE/EtOAc 9:1); ^{1}H-NMR (400 MHz, CDCl$_3$) δ = 8.08 (t, J = 1.9 Hz, 1H), 8.05 (dt, J = 7.6, 1.5 Hz, 1H), 7.61 (dt, J = 8.0, 1.6 Hz, 1H), 7.55 (t, J = 7.8 Hz, 1H), 5.96 (s, 1H), 4.48 (sept, J = 7.0 Hz, 1H), 3.92 (s, 3H), 2.29 (s, 3H), 2.27 (s, 3H), 1.95 (s, 3H), 1.41 (s, 3H), 1.33 (d, J = 7.1 Hz, 3H), 0.87 (d, J = 6.8 Hz, 3H); ^{13}C-NMR (101 MHz, CDCl$_3$) δ = 167.2 (q), 167.1 (q), 166.4 (q), 154.1 (q), 150.2 (q), 149.6 (q), 146.9 (q), 132.5 (q), 131.6 (+), 131.1 (q), 129.2 (+), 129.0 (+), 128.3 (+), 123.2 (q), 123.1 (q), 119.8 (q), 106.4 (+), 52.4 (+), 30.2 (+), 27.4 (+), 23.2 (+), 22.2 (+), 20.8 (+), 13.5 (+), 13.1 (+); IR (neat) ν = 3437, 2960, 1703, 1588, 1491, 1446, 1368, 1275, 1167, 1133, 958, 910, 850, 809, 753, 682 cm^{-1}; HRMS (ESI) calcd. for C$_{25}$H$_{38}$NO$_5$ (M+H)$^+$ m/z = 422.1962; found 422.1969.

(*E*)-3-(3-(1-(2,5-Dimethylfuran-3-yl)-2-methylpropylidene)-2,5-dioxo-4-(propan-2-ylidene)pyrrolidin-1-yl)-*N*-hydroxybenzamide (18)

A solution of NaOH (42 mg, 1.04 mmol, 8.0 eq.) in aqueous hydroxyl amine (50 wt. %, 335 µL) was added dropwise to a solution of fulgimide **17** (55 mg, 0.13 mmol, 1.0 eq.) in MeOH/THF (1:1, 2 mL) at − 15 °C. Then the mixture was stirred for 20 min at - 15 °C. The reaction was quenched with AcOH (744 µL) and concentrated *in vacuo*. Purification by preparative HPLC (50% - 98% MeCN in 20 min, t$_R$ = 15.0 min) yielded **18** (10 mg, 18%) as slightly pink solid. R_f 0.51 (CH$_2$Cl$_2$/MeOH 9:1); m.p. 93 °C; ^{1}H-NMR (400 MHz, DMSO-*d$_6$*) δ = 11.29 (s, 1H), 9.11 (s, 1H), 7.85 − 7.70 (m, 2H), 7.64 − 7.46 (m, 2H), 6.17 (s, 1H), 4.42 (sept, J = 7.0 Hz, 1H), 2.25 (s, 3H), 2.22 (s, 3H), 1.93 (s, 3H), 1.36 (s, 3H), 1.29 (d, J = 7.1 Hz, 3H), 0.82 (d, J = 6.9 Hz, 3H); ^{13}C-NMR (151 MHz, DMSO-*d$_6$*) δ = 166.4 (q), 166.4 (q), 163.3 (q), 152.1 (q), 149.8 (q), 148.1 (q), 146.5 (q), 133.3 (q), 132.3 (q), 130.4 (+), 128.8 (+), 126.3 (+), 126.3 (+), 122.9 (q), 122.8 (q), 119.2 (q), 106.3 (+), 29.2 (+), 26.7 (+), 22.8 (+), 21.4 (+), 20.5 (+), 13.0 (+), 12.5 (+); IR (neat) ν = 3258, 2926, 2855, 1752, 1700, 1584, 1525, 1484, 1439, 1368, 1282, 1170, 1129, 1088, 995, 801, 693 cm^{-1}; HRMS (ESI) calcd. for C$_{24}$H$_{27}$N$_2$O$_5$ (M+H)$^+$ m/z = 423.1914; found 423.1920.

Methyl (*E*)-4-((3-(1-(2,5-dimethylfuran-3-yl)-2-methylpropylidene)-2,5-dioxo-4-(propan-2-ylidene)pyrrolidin-1-yl)methyl)benzoate (19)

A solution of fulgide **16** (98 mg, 0.34 mmol, 1.0 eq.), methyl 4-(aminomethyl)benzoate hydrochloride (274 mg, 1.36 mmol, 4.0 eq.) and triethylamine (189 µL, 1.36 mmol,

4.0 eq.) in anhydrous CH_2Cl_2 (2 mL) was refluxed for 3 d. Then CDI (276 mg, 1.70 mmol, 5.0 eq.) was added and the mixture was refluxed for 1 d. The reaction mixture was acidified with aqueous HCl (1 M) and the aqueous layer was extracted with EtOAc (3 x 10 mL). The combined organic layers were washed with brine (20 mL), dried over $MgSO_4$ and the solvent was evaporated under reduced pressure. Purification by automated flash column chromatography (PE/EtOAc, 3% - 15% EtOAc) afforded fulgimide **19** (70 mg, 47%) as orange oil. R_f 0.31 (PE/EtOAc 9:1); ^{1}H-NMR (400 MHz, $CDCl_3$) δ = 7.98 (d, J = 8.3 Hz, 2H), 7.45 (d, J = 8.2 Hz, 2H), 5.92 (s, 1H), 4.79 (d, J = 8.5 Hz, 2H), 4.48 (sept, J = 7.0 Hz, 1H), 3.89 (s, 3H), 2.24 (s, 6H), 1.84 (s, 3H), 1.33 (s, 3H), 1.28 (d, J = 7.1 Hz, 3H), 0.83 (d, J = 6.8 Hz, 3H); ^{13}C-NMR (101 MHz, $CDCl_3$) δ = 168.1 (q), 168.0 (q), 167.0 (q), 153.1 (q), 150.1 (q), 148.7 (q), 146.9 (q), 142.0 (q), 130.1 (+), 129.6 (q), 128.5 (+), 123.5 (q), 123.4 (q), 119.7 (q), 106.5 (+), 52.2 (+), 41.1 (-), 30.0 (+), 27.2 (+), 23.1 (+), 22.1 (+), 20.8 (+), 13.5 (+), 12.9 (+); IR (neat) ν = 3422, 2960, 2874, 1692, 1633, 1435, 1387, 1342, 1275, 1219, 1178, 1100, 1021, 958, 924, 872, 835, 805, 757, 708 cm^{-1}; HRMS (ESI) calcd. for $C_{26}H_{30}NO_5$ $(M+H)^+$ m/z = 436.2118; found 436.2120.

(*E*)-4-((3-(1-(2,5-Dimethylfuran-3-yl)-2-methylpropylidene)-2,5-dioxo-4-(propan-2-ylidene)pyrrolidin-1-yl)methyl)-*N*-hydroxybenzamide (20)

A solution of NaOH (37 mg, 0.91 mmol, 8.0 eq.) in aqueous hydroxyl amine (50 wt. %, 309 µL) was added dropwise to a solution of fulgimide **19** (50 mg, 0.11 mmol, 1.0 eq.) in MeOH/THF (1:1, 2 mL) at 0 °C. Then the mixture was stirred for 25 min at 0 °C. The reaction was quenched with AcOH (652 µL) and concentrated *in vacuo*. Purification by preparative HPLC (50% - 97% MeCN in 25 min, t_R = 15.6 min) afforded **20** (13 mg, 27%) as slightly pink solid. R_f 0.59 (CH_2Cl_2/MeOH 9:1); m.p. 92 °C; ^{1}H-NMR (600 MHz, DMSO-d_6) δ = 11.16 (s, 1H), 9.01 (s, 1H), 7.70 (d, J = 8.3 Hz, 2H), 7.29 (d, J = 8.4 Hz, 2H), 6.14 (s, 1H), 4.71 (d, J = 2.5 Hz, 2H), 4.44 (sept, J = 7.1 Hz, 1H), 2.23 (s, 3H), 2.19 (s, 3H), 1.82 (s, 3H), 1.30 (s, 3H), 1.25 (d, J = 7.3 Hz, 3H), 0.77 (d, J = 6.9 Hz, 3H); ^{13}C-NMR (151 MHz, DMSO-d_6) δ = 167.2 (q), 167.2 (q), 163.9 (q, HMBC), 151.5 (q), 149.8 (q), 147.7 (q), 146.3 (q), 139.9 (q), 131.9 (q), 127.2 (+), 123.0 (q), 122.7 (q), 119.1 (q), 106.4 (+), 40.3 (−), 29.0 (+), 26.6 (+), 22.6 (+), 21.3 (+), 20.5 (+), 13.0 (+), 12.4 (+); IR (neat) ν = 3258, 2960, 2930, 2874, 1744,

1688, 1632, 1498, 1424, 1387, 1342, 1167, 1133, 1100, 962, 924, 902, 801 cm^{-1}; HRMS (ESI) calcd. for $C_{25}H_{29}N_2O_5$ (M+H)$^+$ m/z = 437.2071; found 437.2072.

2.4.2 Biological Investigations

Compounds **3** (λ = 312 nm, 36.5 min), **6** (λ = 312 nm, 11 min), **10** (λ = 365 nm, 7.5 min, resulting PSS: 30%), **18** (λ = 365 nm, 11 min) and **20** (λ = 365 nm, 11 min) were irradiated in a 10 mM stock solution in DMSO to form the closed or byproduct isomers prior to the biological assays, respectively. *In vitro* assays were performed as previously described.[51]

2.4.3 Molecular Docking

Crystal structures of *h*HDAC1 (PDB ID 5ICN),[87] *h*HDAC6 (PDB ID 5G0I),[84] *h*HDAC8 (PDB ID 2V5X)[88] and *sm*HDAC8 (PDB 5FUE)[50] were downloaded from the Protein Data Bank PDB.[89] Protein preparation was done using Schrödinger's Protein Preparation Wizard[90] by adding hydrogen atoms, assigning protonation states and minimizing the protein. Ligands were prepared in MOE[91] from smiles in neutral form. Multiple low energy starting conformations were generated with MOE within an energy window of 5 kcal/mol. Molecular docking was performed using the program Glide. The same protocol was applied successfully in previous studies.[92] Water molecules were removed from the protein structures beside one water molecule in HDAC6 that is bridging the interaction of the hydroxamate and the zinc ion in PDB 5G0I. Compounds **3 byproduct**, **6 closed**, **18 closed** and **20 closed** were generated in the possible stereoisomeric forms and were docked in the neutral form.

In our previous study we found that rescoring the docking poses by using a MM-GB/SA protocol resulted in a significant correlation between calculated interaction energies and *in vitro* inhibition data. Therefore, the same protocol was applied to the compounds under study. To calculate the binding free energy, we used the AMBER12EHT force field implemented in the MOE program together with the continuum solvation model GB/SA. The experimentally observed geometries of the zinc-hydroxamate complexes were best reproduced using this setup. Partial charges were fixed using the MOE Protonate3D tool according to the used force-field followed by a short minimization. To estimate the

binding free energy a minimizing of the protein-ligand complexes derived from the docking was carried out. During complex minimization the heavy atoms of the protein were tethered with a deviation of 0.5 Å (force constant $(3/2)$ kT / $(0.5)^2$). The complex showing the lowest binding free energy was chosen for each inhibitor and HDAC isoform. Using this docking and rescoring protocol the experimentally derived structures of the cocrystallized inhibitors of *h*HDAC6 (PDB ID 5G0I), *h*HDAC8 (PDB 2V5X) and *sm*HDAC8 (PDB ID 5FUE) could be reproduced with an RMSD value below 1.00 Å.

## 2.5 Supporting Information

Photochemical data
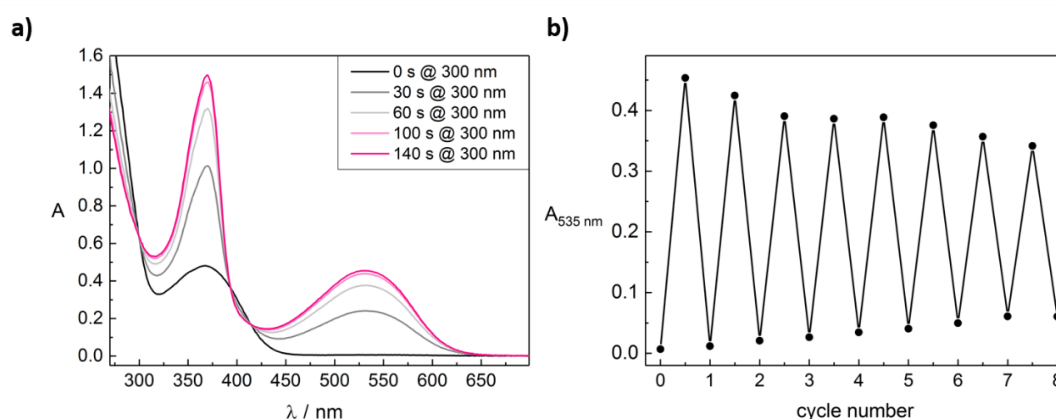
Figure S1. a) Changes in absorption spectra of DTE **10** (100 µM in DMSO) upon continuous irradiation for 0, 30, 60, 100 and 140 s with light of λ = 300 nm until the PSS is reached. **b)** Cycle performance of DTE **10** (100 µM in DMSO). Changes in absorption at 535 nm were measured during alternate irradiation with light of 300 nm for 140 s and 530 nm for 1 min.
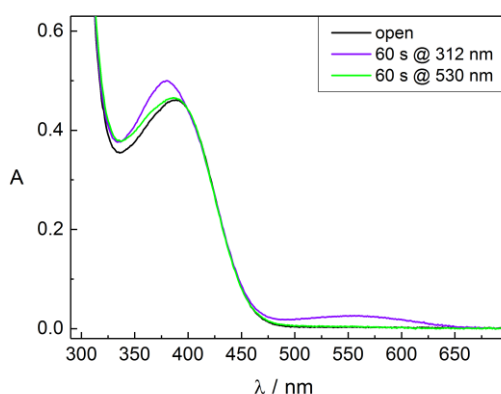

Figure S2. Absorption spectra of DTE **12** (100 µM in toluene/THF) open, after irradiation with λ = 312 nm for 60 s and subsequent irradiation with λ = 530 nm for 60 s.
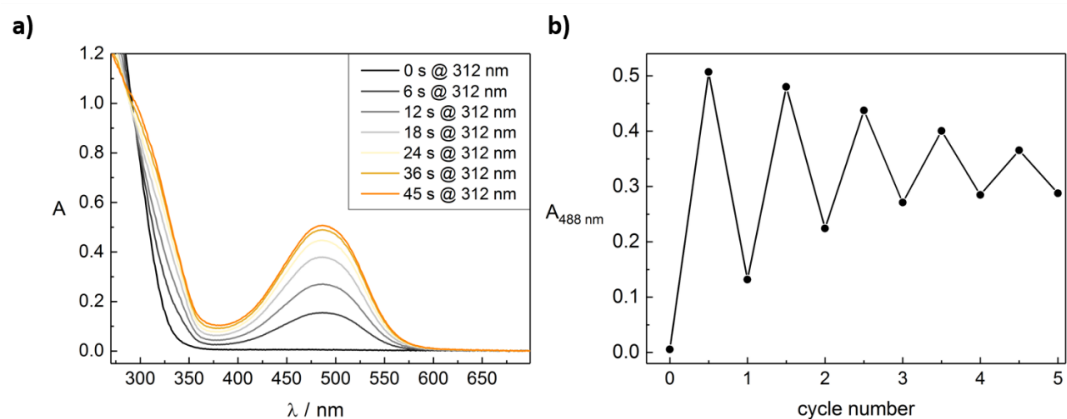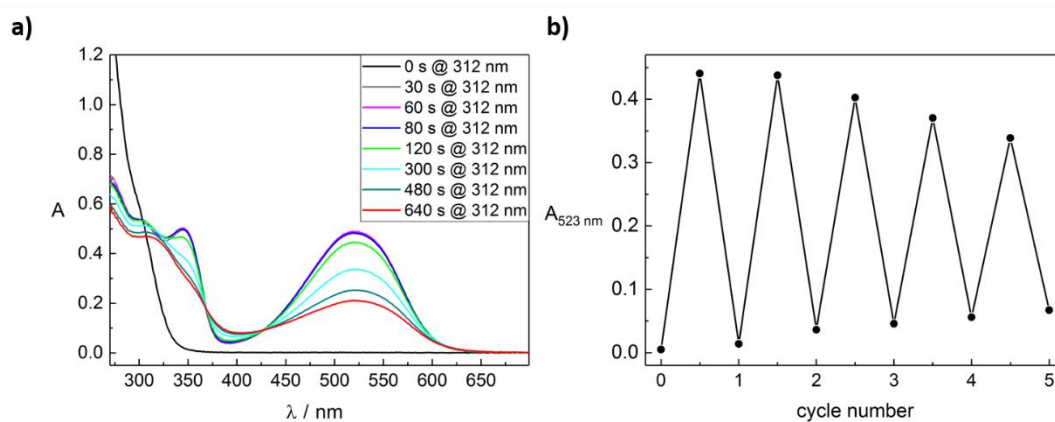
Figure S3. a) Changes in absorption spectra of DTE **3** (100 µM in DMSO) upon continuous irradiation for 0, 6, 12, 18, 24, 36 and 48 s with light of λ = 312 nm until the PSS is reached. **b)** Cycle performance of DTE **3** (100 µM in DMSO). Changes in absorption at 488 nm were measured during alternate irradiation with light of 312 nm for 48 s and 470 nm for 1 min.
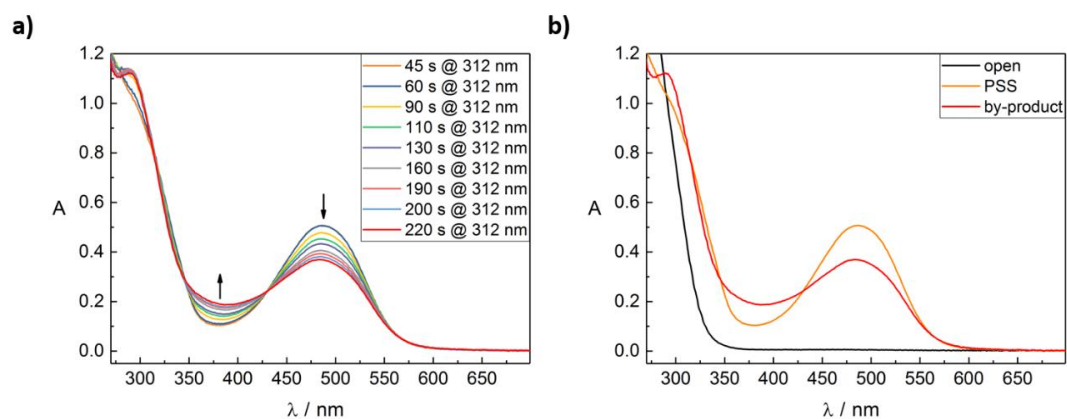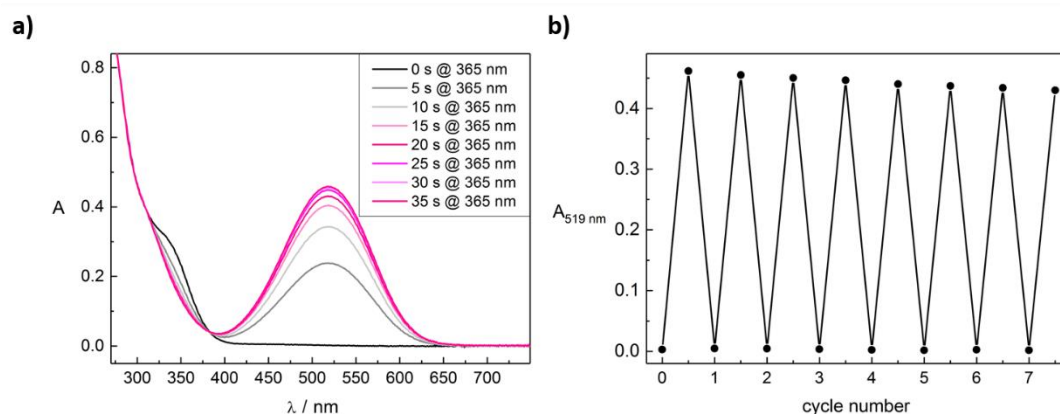

Figure S4. a) Changes in absorption spectra of DTE **3** (100 µM in DMSO) upon continuous irradiation for 48, 60, 92, 112, 132, 162, 192, 202 and 222 s with light of λ = 312 nm until the byproduct is completely formed. **b)** Comparison of the absorption spectra of the three occurring states/isomers of **3**: open (black), PSS (orange) and byproduct (red).
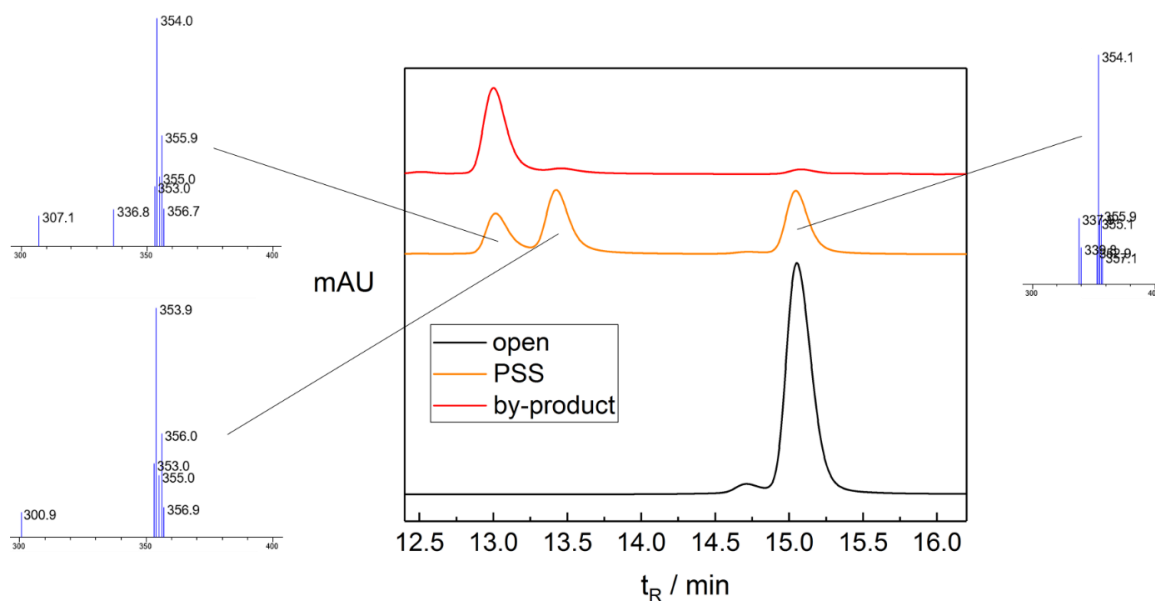
Figure S5. HPLC-MS traces recorded at 275 nm of the three different states/isomers of **3** (t_R open isomer: 15.05 min, m/z=354.1; t_R closed isomer: 13.42 min, m/z=353.9; t_R byproduct: 13.02 min, m/z=354.0; black: open isomer without irradiation; orange: PSS after 45 s of irradiation; red: byproduct after 220 s of irradiation). Upon reaching the PSS (orange) approximately 23% of the byproduct has already formed and its formation is completed after 220 s (red).
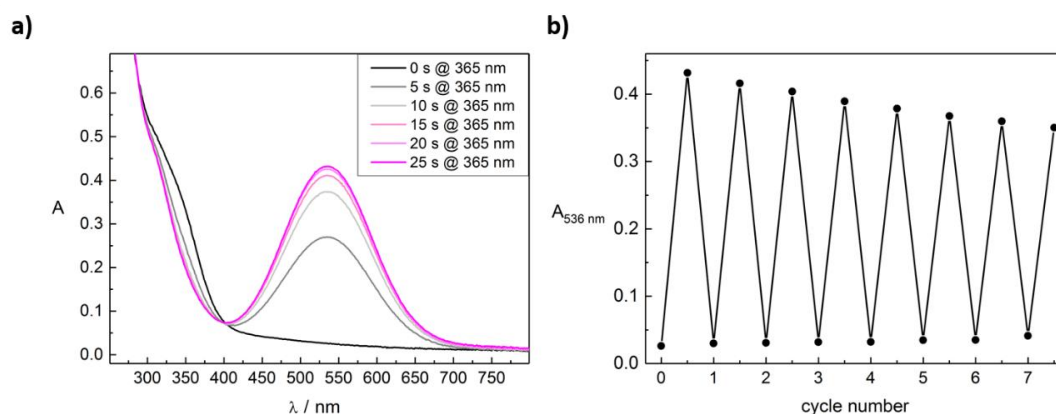

Figure S6. a) Changes in absorption spectra of DTE **6** (100 µM in DMSO) upon continuous irradiation for 0, 30, 60 (PSS), 80, 120, 300, 480 and 640 s (byproduct) with light of λ = 312 nm. b) Cycle performance of DTE **6** (100 µM in DMSO). Changes in absorption at 523 nm were measured during alternate irradiation with light of 312 nm for 60 s and 530 nm for 3 min.

a)

b)

Figure S7. a) Changes in absorption spectra of fulgimide **18** (100 µM in DMSO) upon continuous irradiation for 0, 5, 10, 15, 20, 25, 30 and 35 s with light of λ = 365 nm until the PSS is reached. **b)** Cycle performance of fulgimide **18** (100 µM in DMSO). Changes in absorption at 519 nm were measured during alternate irradiation with light of 365 nm for 35 s and 530 nm for 5 min.

a)

b)
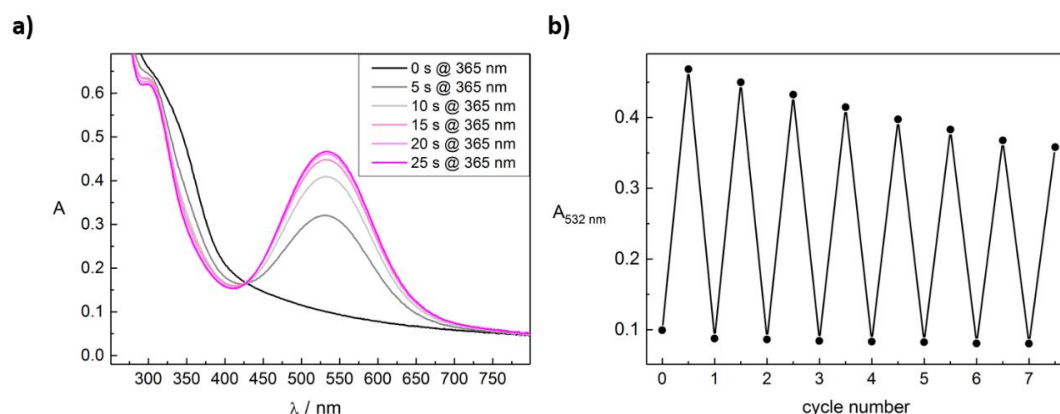
Figure S8. a) Changes in absorption spectra of fulgimide **20** (100 µM in PBS with 1% of DMSO, pH=7.4) upon continuous irradiation for 0, 5, 10, 15, 20 and 25 s with light of λ = 365 nm until the PSS is reached. **b)** Cycle performance of fulgimide **20** (100 µM in in PBS with 1% of DMSO, pH=7.4). Changes in absorption at 532 nm were measured during alternate irradiation with light of 365 nm for 25 s and 530 nm for 10 min.

a)

b)

Figure S9. a) Changes in absorption spectra of fulgimide **18** (100 µM in PBS with 1% of DMSO, pH=7.4) upon continuous irradiation for 0, 5, 10, 15, 20 and 25 s with light of λ = 365 nm until the PSS is reached. **b)** Cycle performance of fulgimide **18** (100 µM in in PBS with 1% of DMSO, pH=7.4). Changes in absorption at 536 nm were measured during alternate irradiation with light of 365 nm for 25 s and 530 nm for 10 min.

Docking results and additional docking poses

Table S1. Docking scores calculated for *h*HDAC1 (PDB ID 5ICN).

Entry	Compound	IC$_{50}$ *h*HDAC1 [µM]	pIC$_{50}$ *h*HDAC1	E GBSA [kcal/mol]
1	**3 open**	15 ± 1 .2	4.82	-38.54
2	**3 byproduct** (*R,R*)	26 ± 2.5	4.59	-
3	**3 byproduct** (*S,S*)	26 ± 2.5	4.59	-
4	**6 open**	4.2 ± 0.7	5.38	-35.05
5	**6 closed** (*R,R*)	5.1 ± 0.8	5.29	-37.25
6	**6 closed** (*S,S*)	5.1 ± 0.8	5.29	-37.05
7	**18 open**	28.5 ± 10.9	4.55	-37.48
8	**18 closed** (*R*)	87.5 ± 53.0	4.06	-29.52
9	**18 closed** (*S*)	87.5 ± 53.0	4.06	-31.83
10	**20 open**	6.4 ± 1.0	5.19	-41.57
11	**20 closed** (*R*)	5.0 ± 1.0	5.30	-42.80
12	**20 closed** (*S*)	5.0 ± 1.0	5.30	-44.16

Table S2. Docking scores calculated for *h*HDAC6 (PDB ID 5G0I).

Entry	Compound	IC$_{50}$ *h*HDAC6 [µM]	pIC$_{50}$ *h*HDAC6	E GBSA [kcal/mol]
1	**3 open**	1.8 ± 0.2	5.74	-41.90
2	**3 byproduct** (*R,R*)	3.9 ± 0.2	5.41	-30.82
3	**3 byproduct** (*S,S*)	3.9 ± 0.2	5.41	-30.12
4	**6 open**	0.213 ± 0.018	6.67	-45.20
5	**6 closed** (*R,R*)	0.297 ± 0.041	6.53	-47.75
6	**6 closed** (*S,S*)	0.297 ± 0.041	6.53	-47.86
7	**18 open**	1.8 ± 0.5	5.74	-40.08
8	**18 closed** (*R*)	6.1 ± 1.7	5.21	-40.48
9	**18 closed** (*S*)	6.1 ± 1.7	5.21	-41.77
10	**20 open**	0.047 ± 0.032	7.33	-73.55
11	**20 closed** (*R*)	0.075 ± 0.047	7.12	-72.90
12	**20 closed** (*S*)	0.075 ± 0.047	7.12	-71.91

Table S3. Docking scores calculated for *h*HDAC8 (PDB ID 2V5X).

Entry	Compound	IC$_{50}$ *h*HDAC8 [µM]	pIC$_{50}$ *h*HDAC8	E GBSA [kcal/mol]
1	**3 open**	1.6 ± 0.6	5.80	-60.59
2	**3 byproduct** (*R,R*)	2.7 ± 0.9	5.57	-
3	**3 byproduct** (*S,S*)	2.7 ± 0.9	5.57	-
4	**6 open**	0.248 ± 0.29	6.61	-67.62
5	**6 closed** (*R,R*)	0.262 ± 0.36	6.58	-65.18
6	**6 closed** (*S,S*)	0.262 ± 0.36	6.58	-65.47
7	**18 open**	1.1 ± 0.2	5.96	-63.56
8	**18 closed** (*R*)	0.88 ± 0.07	6.06	-63.49
9	**18 closed** (*S*)	0.88 ± 0.07	6.06	-63.13
10	**20 open**	5.6 ± 1.3	5.25	-58.40
11	**20 closed** (*R*)	3.6 ± 1.0	5.44	-60.62
12	**20 closed** (*S*)	3.6 ± 1.0	5.44	-60.26

Table S4. Docking scores calculated for *sm*HDAC8 (PDB ID 5FUE).

| Entry	Compound	IC$_{50}$ *sm*HDAC8 [µM]	pIC$_{50}$ *sm*HDAC8	E GBSA [kcal/mol]
1	**3 open**	1.6 ± 0.6	5.80	-60.59
2	**3 byproduct** (*R,R*)	2.7 ± 0.9	5.57	-
3	**3 byproduct** (*S,S*)	2.7 ± 0.9	5.57	-
4	**6 open**	0.248 ± 0.29	6.61	-67.62
5	**6 closed** (*R,R*)	0.262 ± 0.36	6.58	-65.18
6	**6 closed** (*S,S*)	0.262 ± 0.36	6.58	-65.47
7	**18 open**	1.1 ± 0.2	5.96	-63.56
8	**18 closed** (*R*)	0.88 ± 0.07	6.06	-63.49
9	**18 closed** (*S*)	0.88 ± 0.07	6.06	-63.13
10	**20 open**	5.6 ± 1.3	5.25	-58.40
11	**20 closed** (*R*)	3.6 ± 1.0	5.44	-60.62
12	**20 closed** (*S*)	3.6 ± 1.0	5.44	-60.26

Figure S10. Docking poses of DTE **3 open** for *h*HDAC6 (**a**) and *h*HDAC8 (**b**). Only the interacting residues of the binding pocket are displayed. The zinc ion is shown as brown ball. The water molecule bridging the coordination to the zinc ion in **a)** is shown as red ball. Distances of the metal coordination and hydrogen bonds are given in Å and are shown as lines colored in magenta.
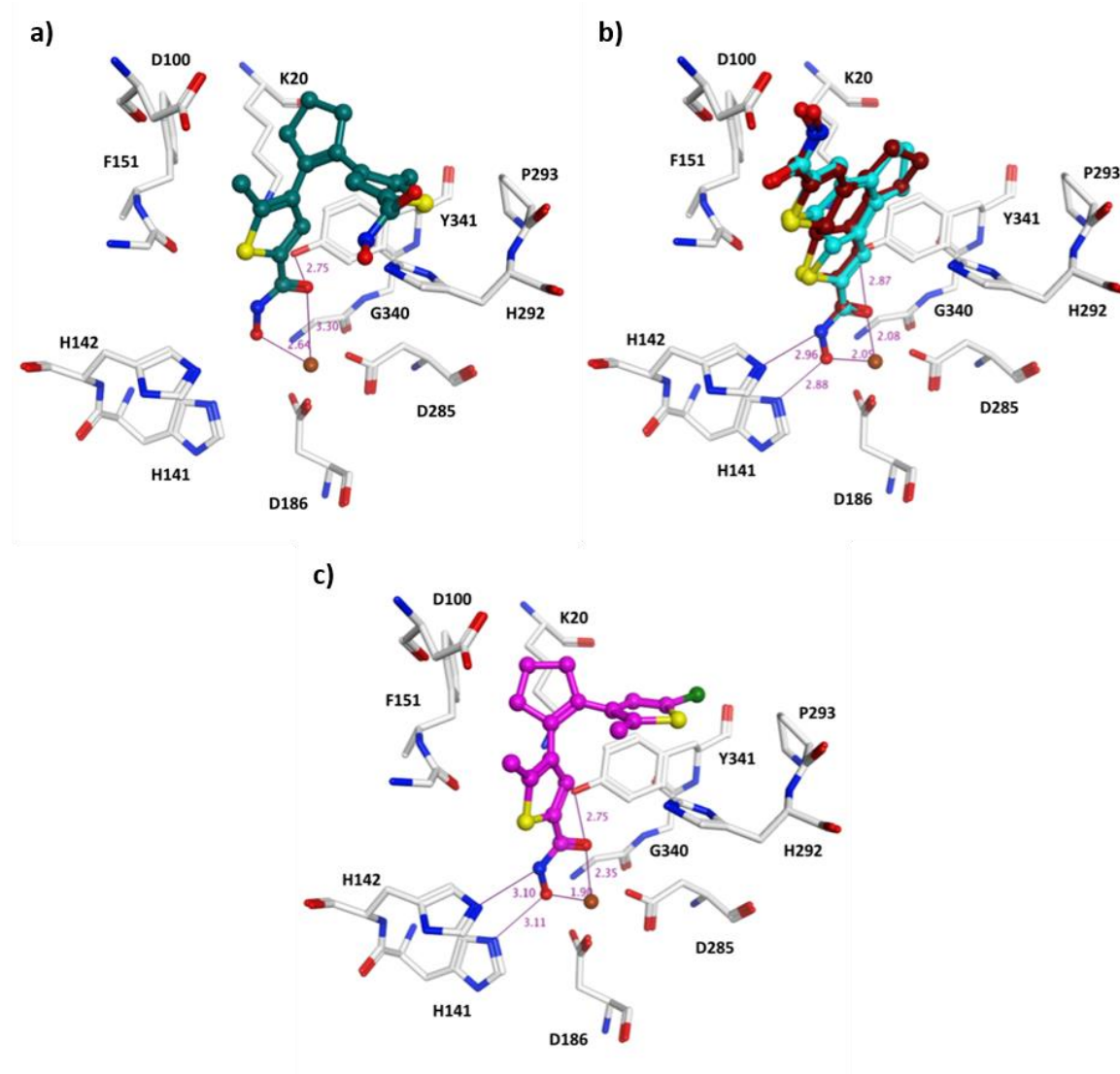
Figure S11. Docking poses of DTEs for *sm*HDAC8. **a) 6 open** colored dark green, **b) 6 closed** (*R,R*) colored cyan and **6 closed** (*S,S*) colored brown, **c) 3 open** colored magenta. Only the interacting residues of the binding pocket are displayed. The zinc ion is shown as brown ball. Distances of the metal coordination and hydrogen bonds are given in Å and are shown as lines colored in magenta.
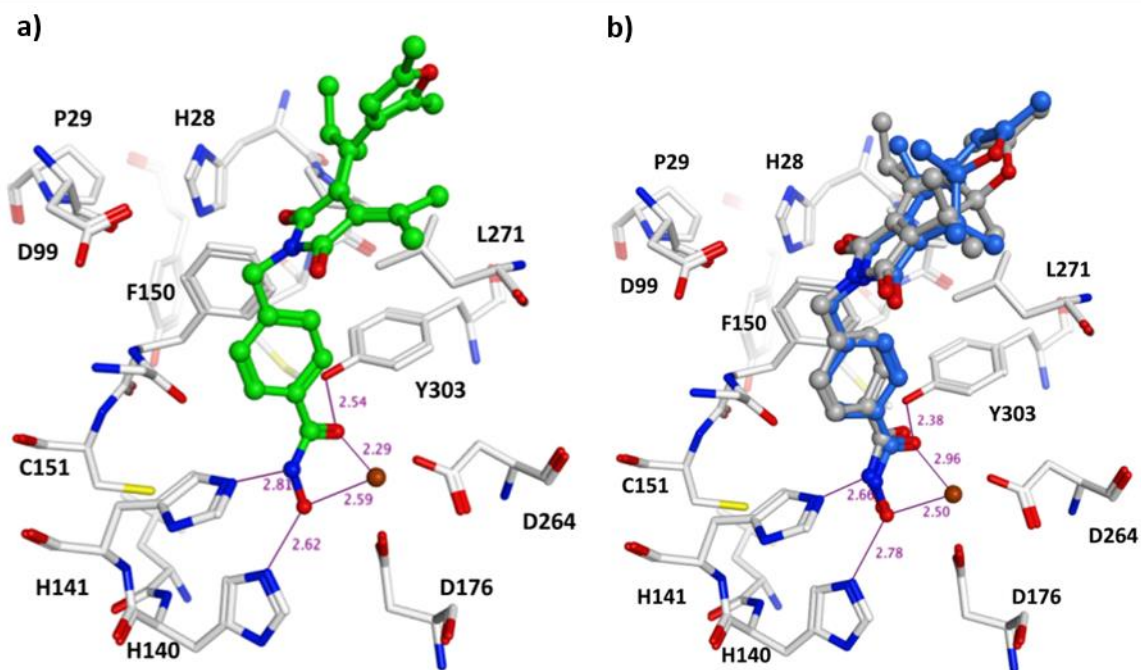
Figure S12. Docking poses of the fulgimide **20** for *h*HDAC1. **a) 20 open** colored green, **b) 20 closed** (*R*) colored blue and **20 closed** (*S*) colored light grey. The zinc ion is shown as brown ball. Distances of the metal coordination and hydrogen bonds are given in Å and are shown as lines colored in magenta.
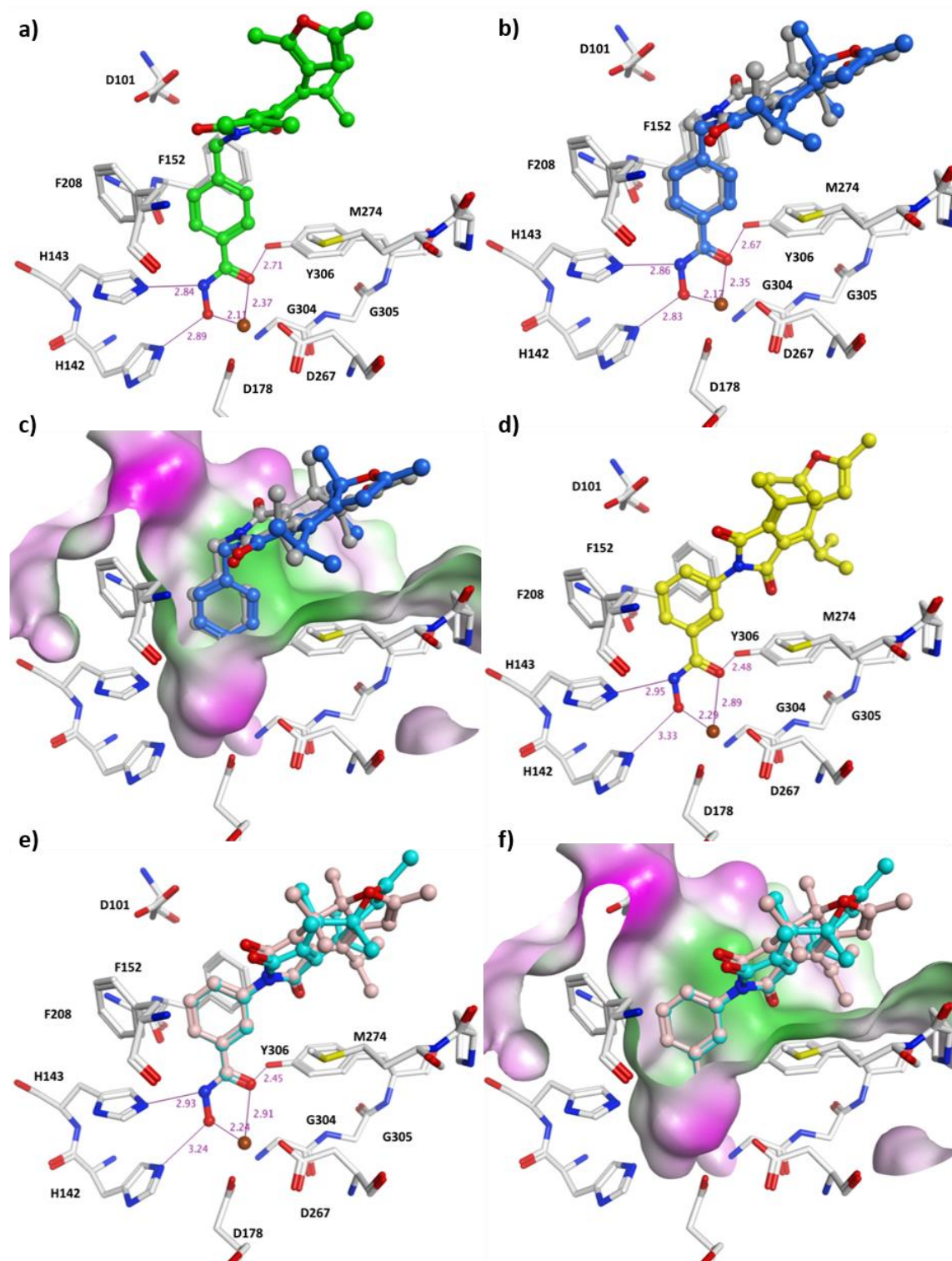
Figure S13. Docking poses of the fulgimides (**20 open** colored green, **20 closed** (*R*) colored blue, **20 closed** (*S*) colored light grey, **18 open** colored yellow, **18 closed** (*R*) colored cyan and **18 closed** (*S*) colored salmon) for *h*HDAC8. The zinc ion is shown as brown ball and the water molecule bridging the coordination to the zinc ion is shown as red ball. Distances of the metal coordination and hydrogen bon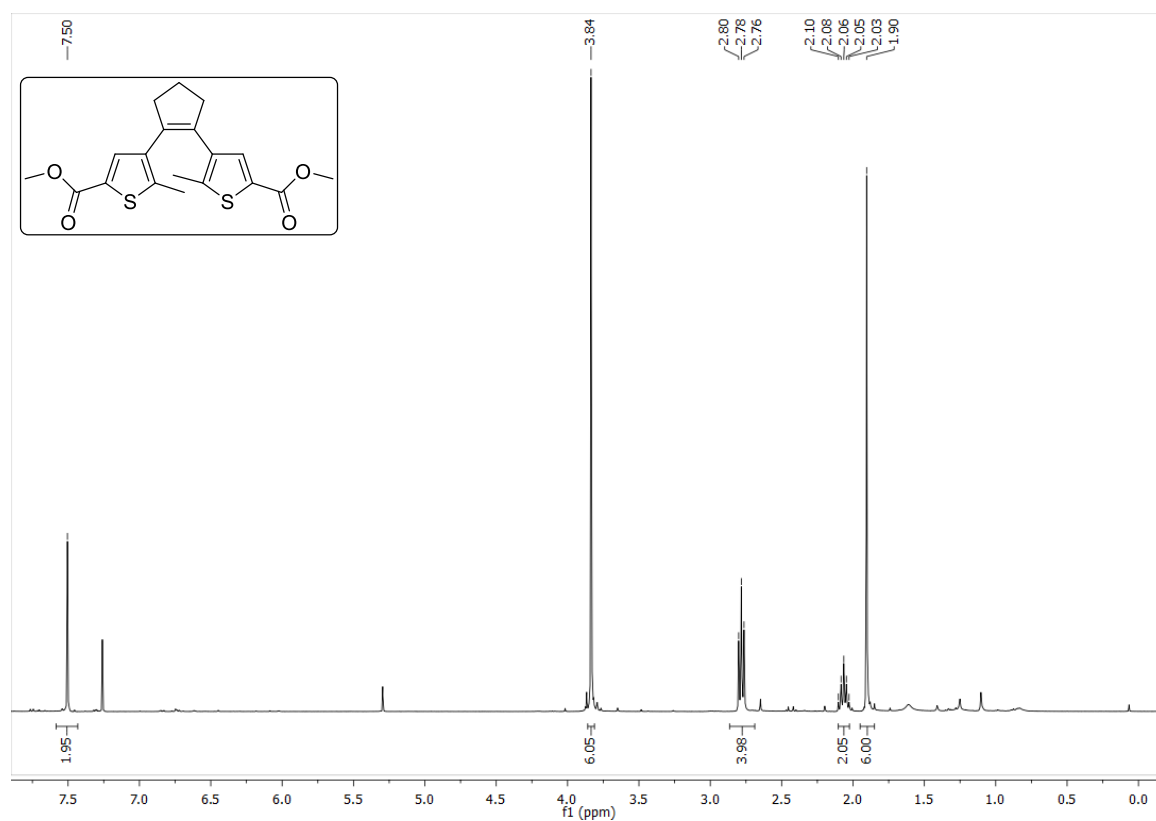ds are given in Å and are shown as lines colored in magenta. The molecular surface of the *h*HDAC8 binding pocket in **c)** and **f)** is colored according to the hydrophobicity (hydrophobic regions are colored green, polar regions are colored magenta).
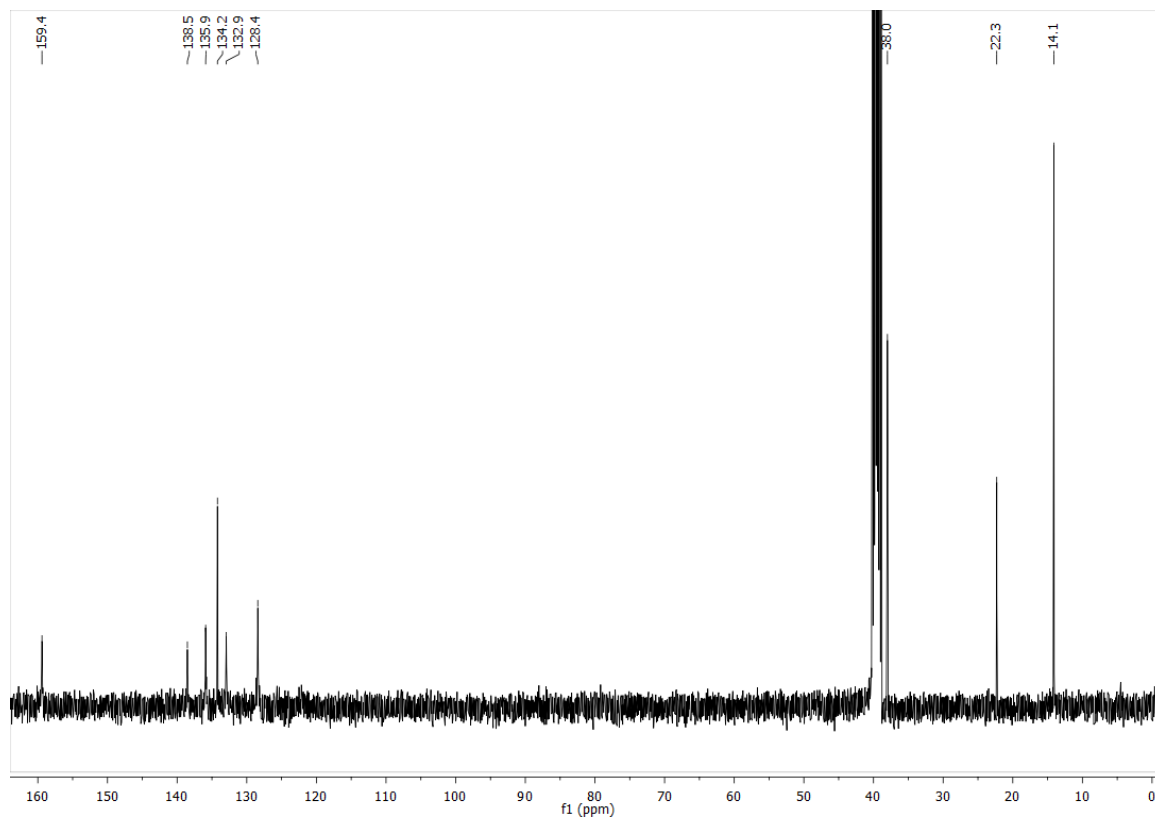
¹H- and ¹³C-NMR spectra

Compound **3**[A]
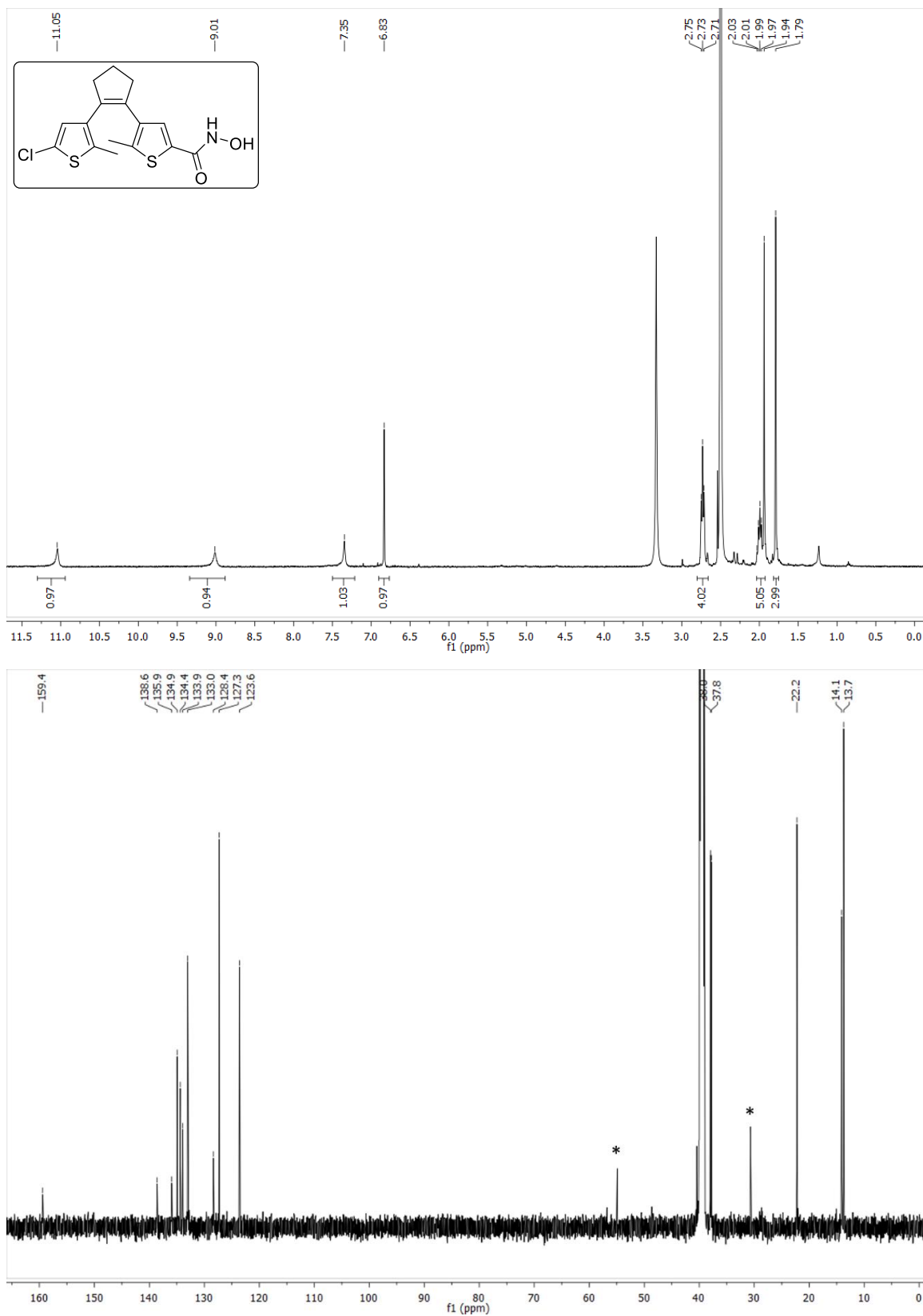
[A] ¹³C-NMR-spectrum contains traces of acetone and CH_2Cl_2; signals are marked with *

Compound **5**
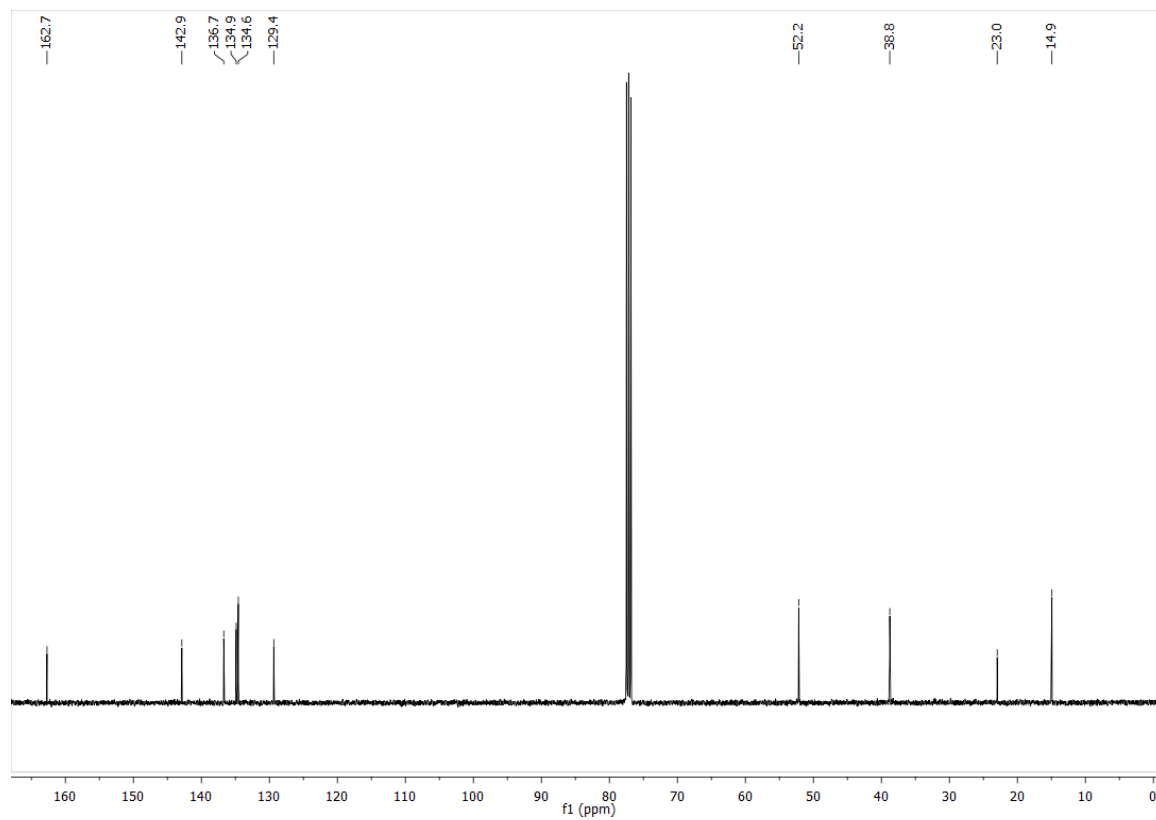
Compound **6**
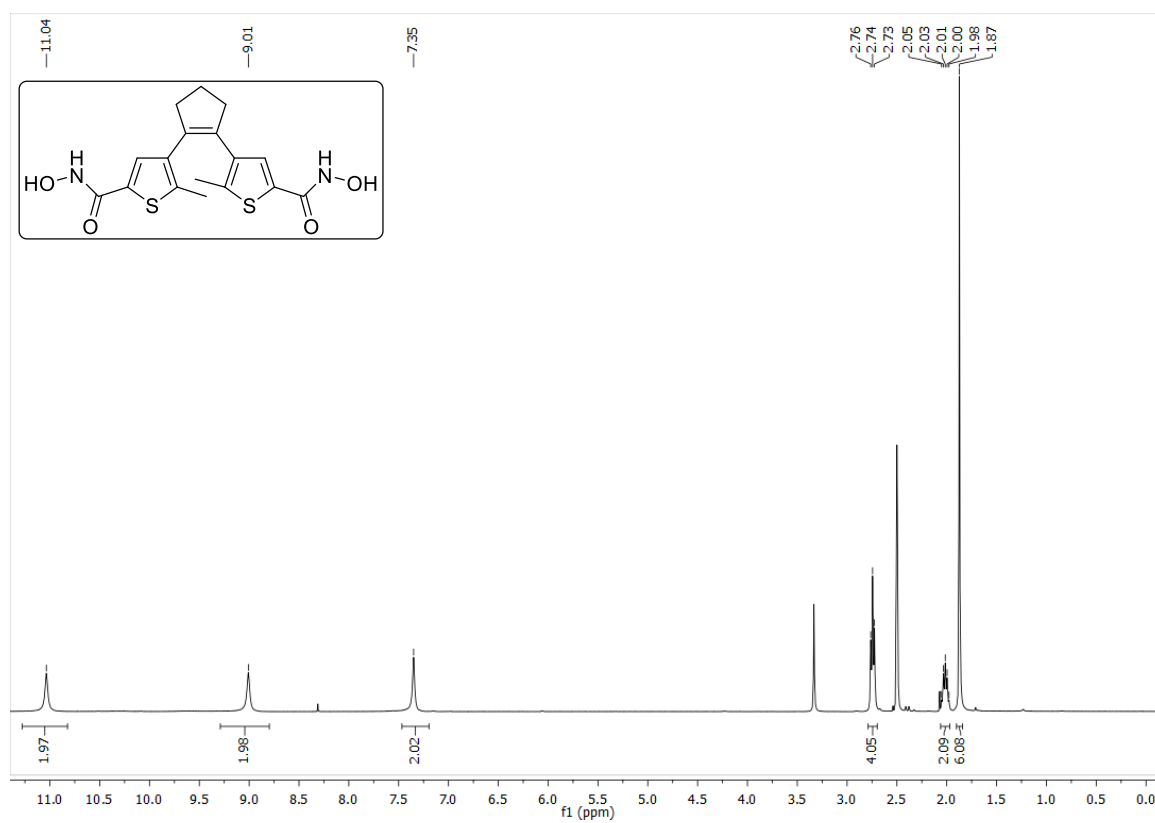
Compound **9**
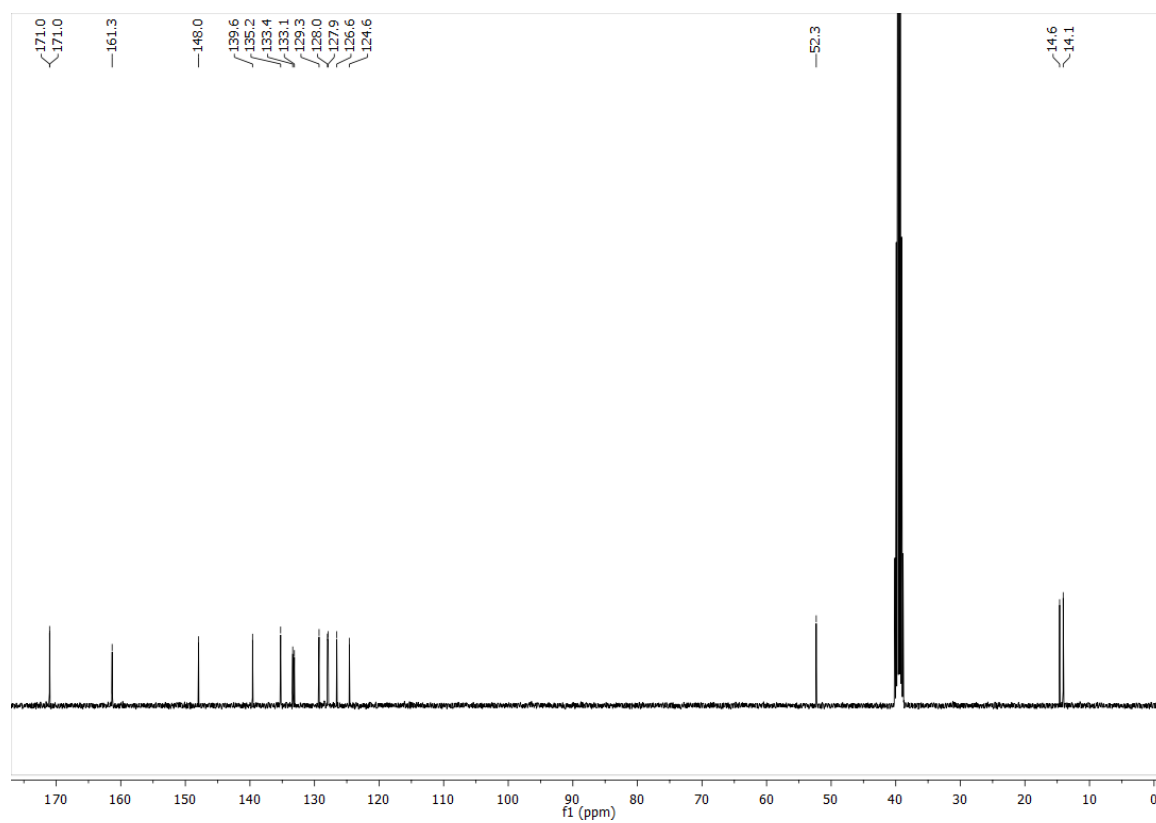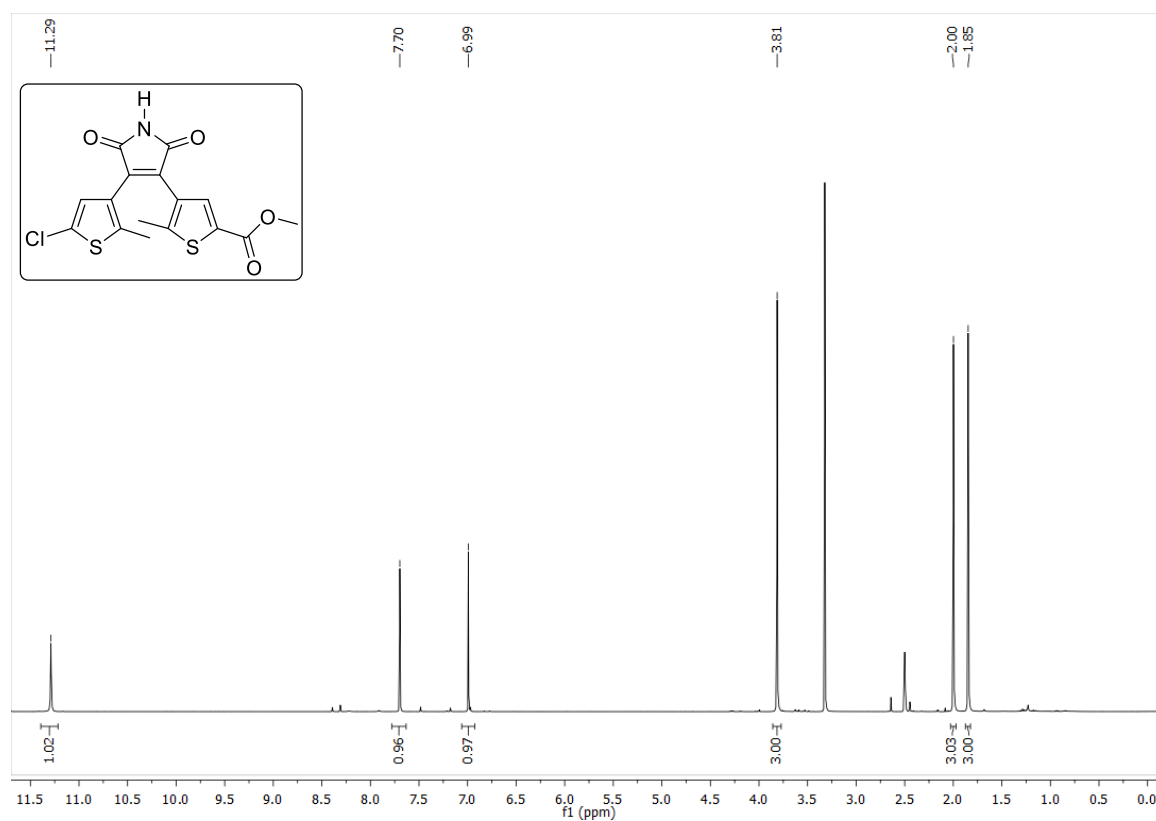
Compound **10**
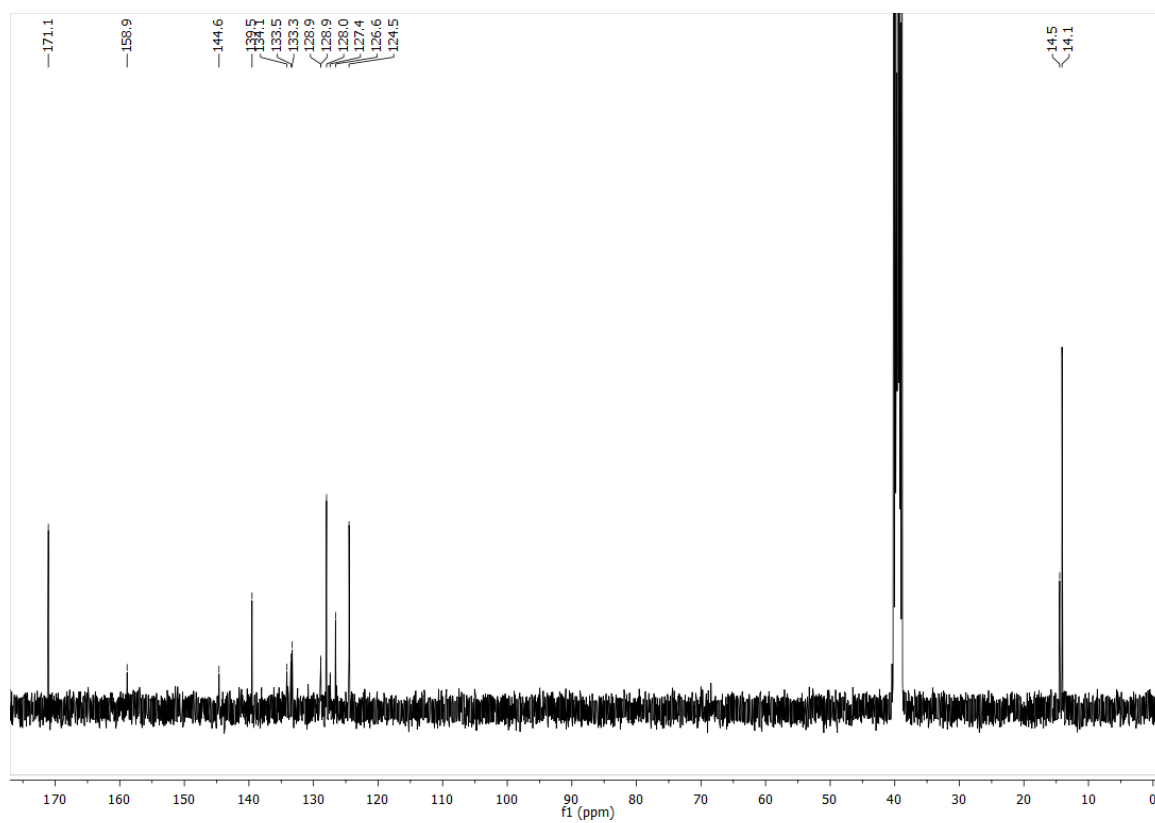
Compound 11
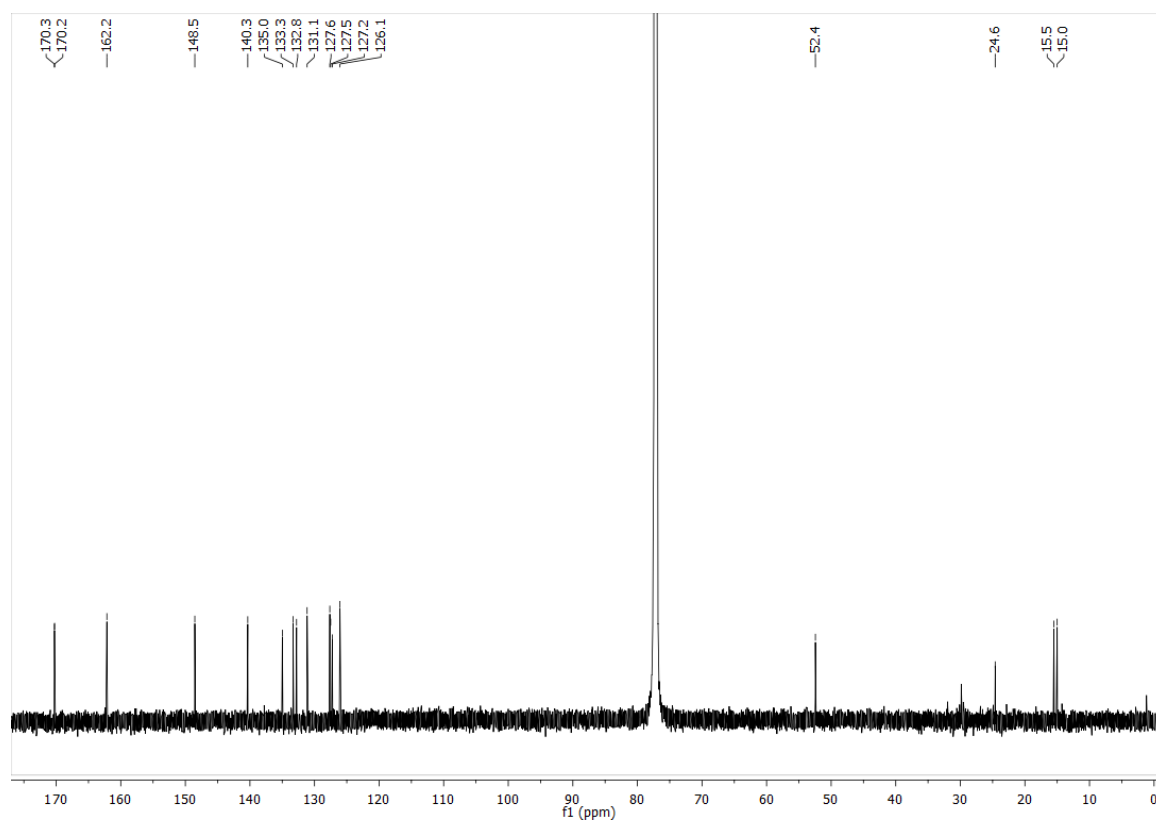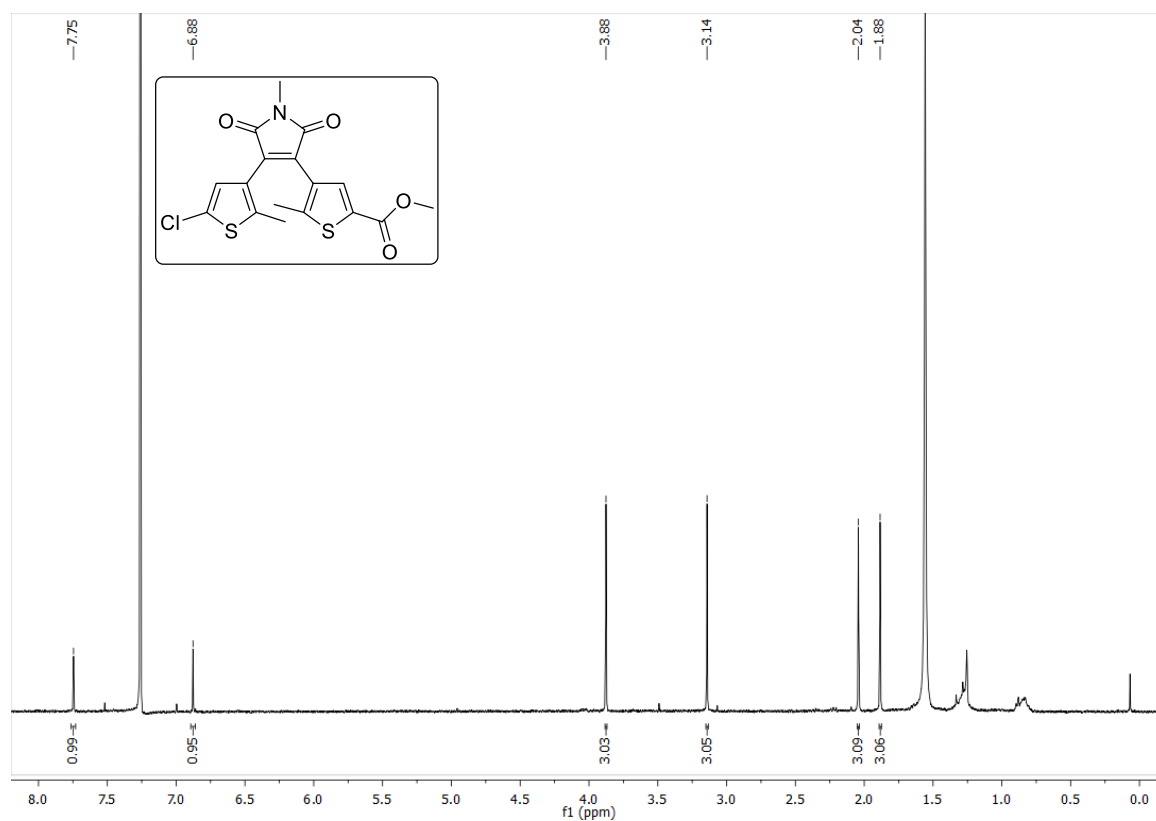
Compound **12**[B]

[B] NMR-spectra contain traces of CHCl$_3$ and CH$_2$Cl$_2$; signals are marked with *
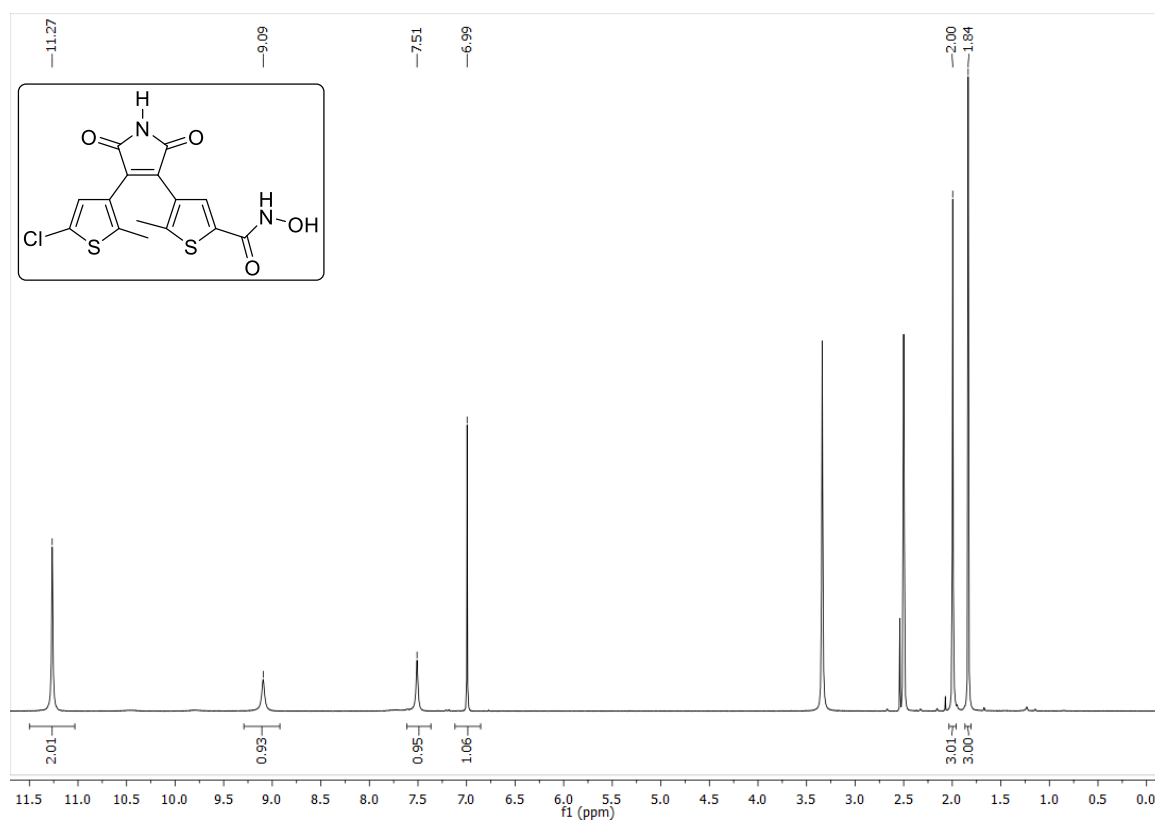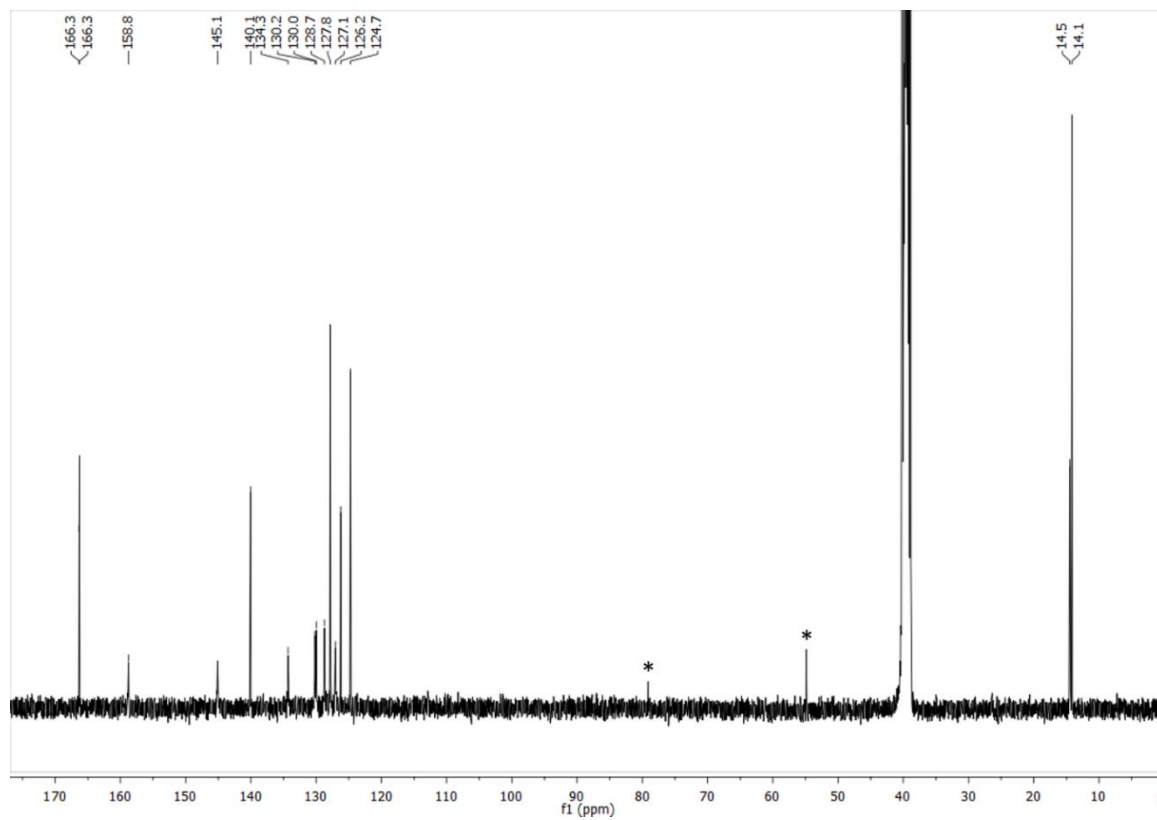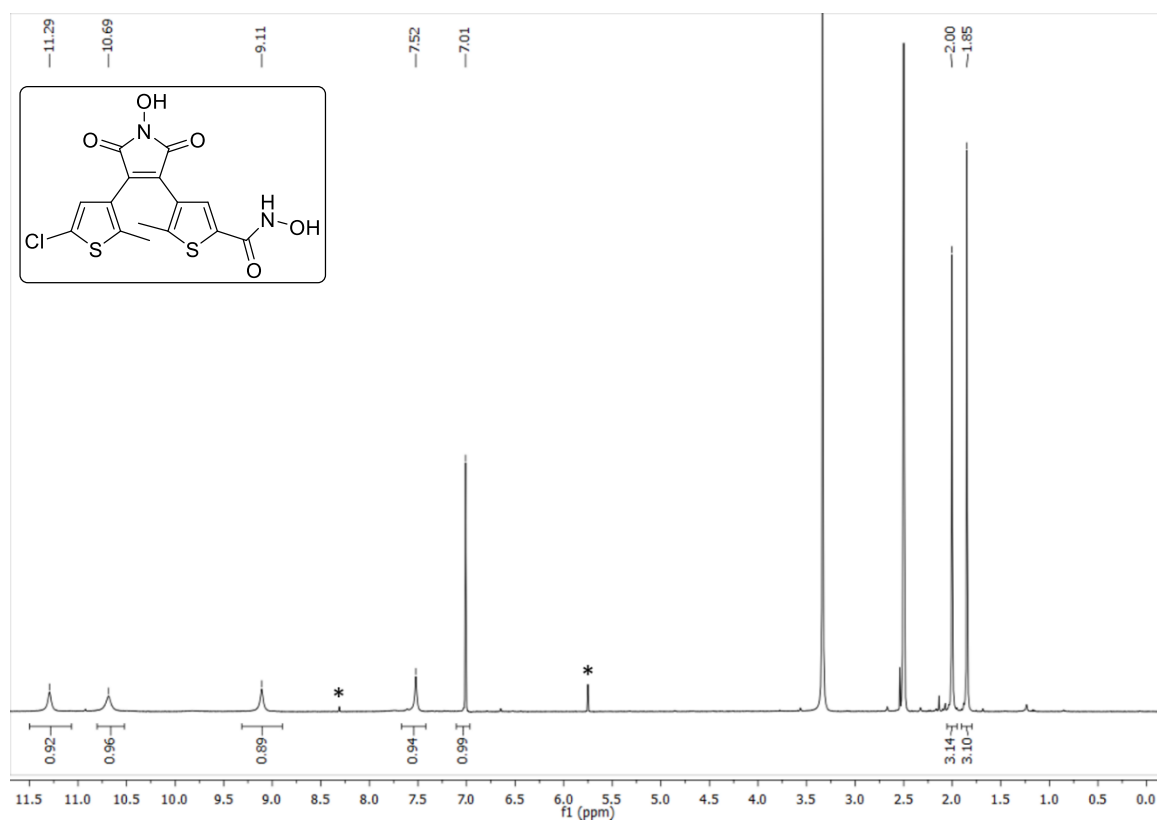
Compound 13
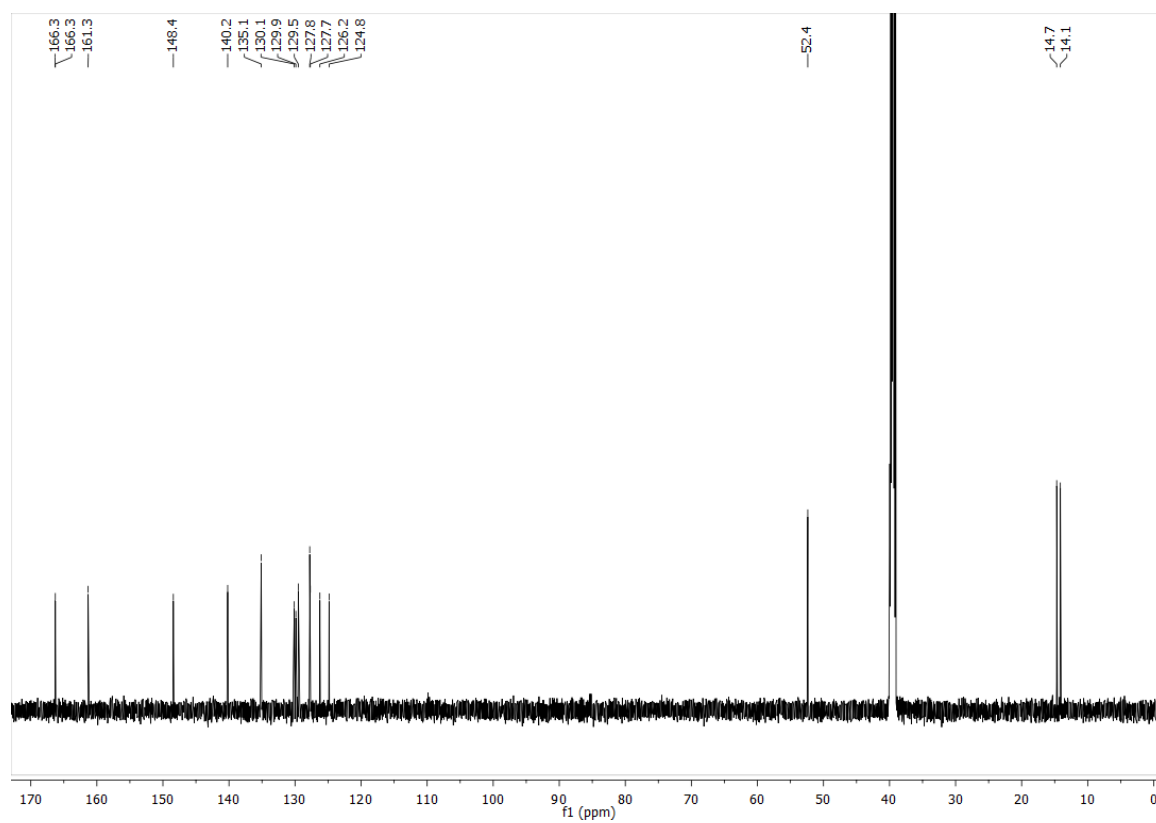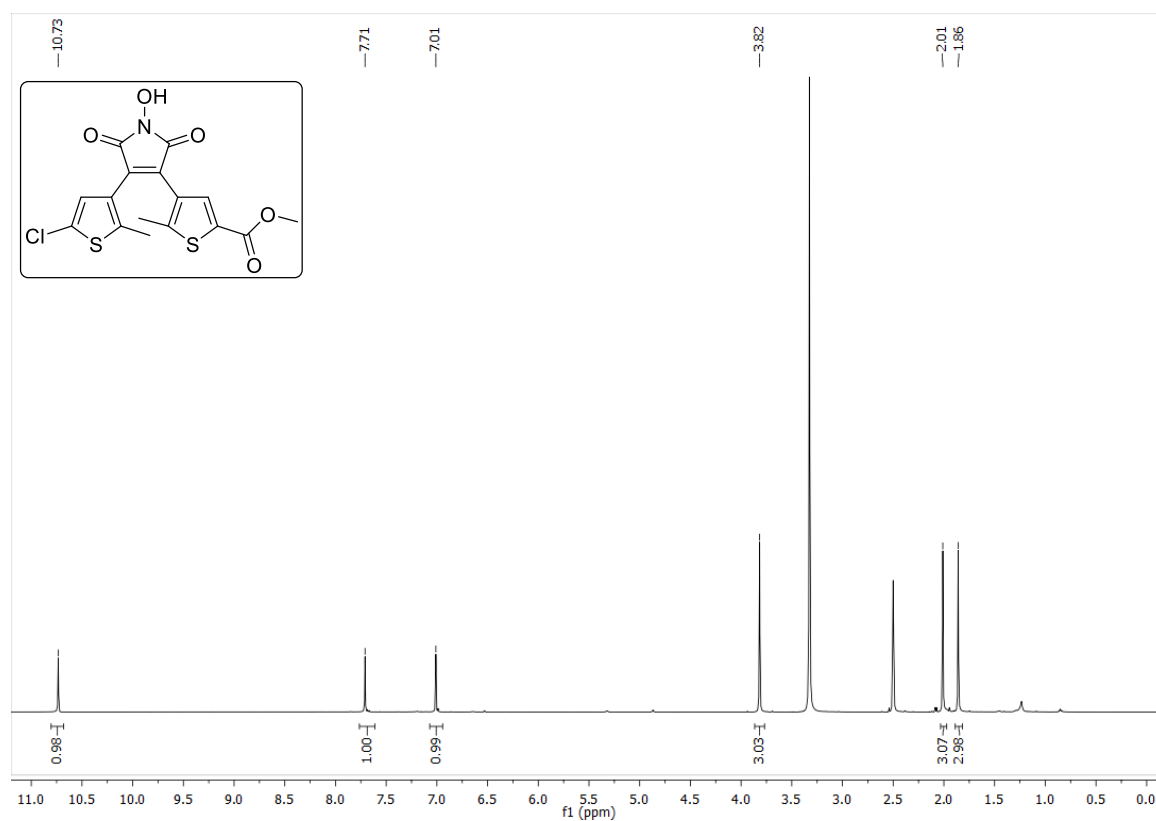
Compound **17**
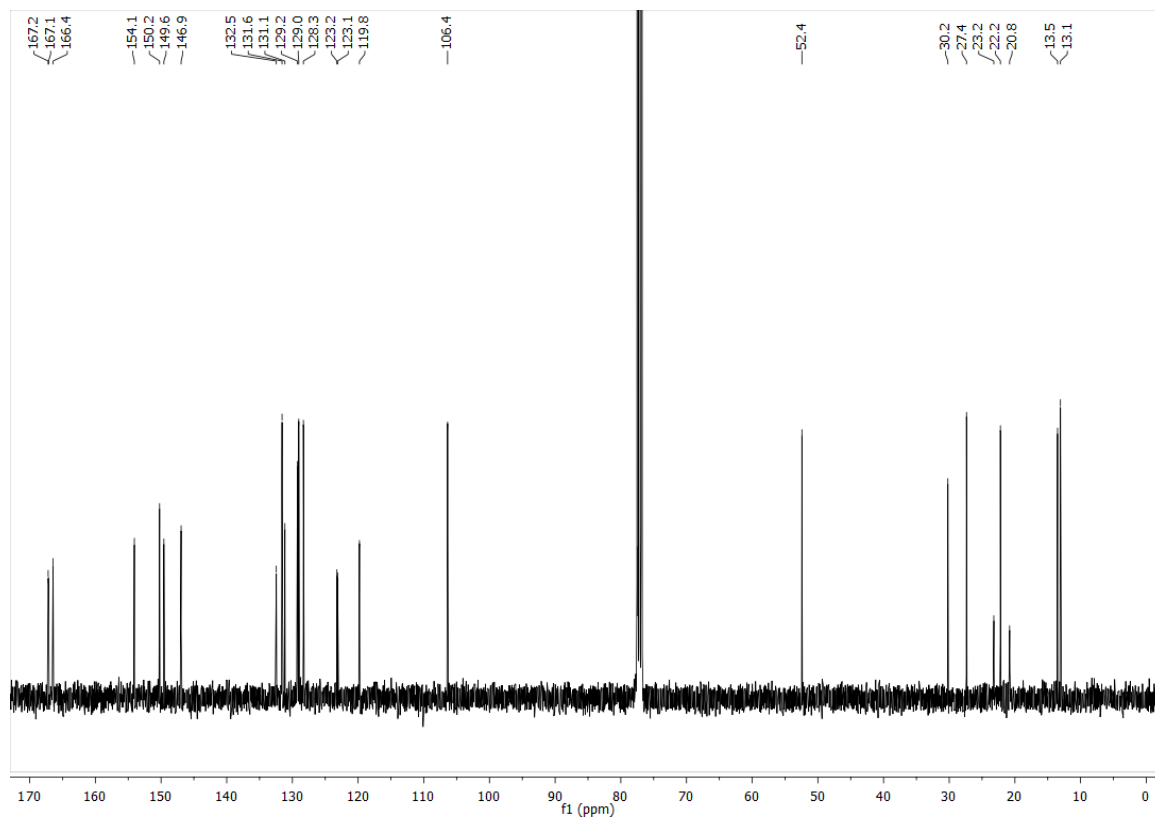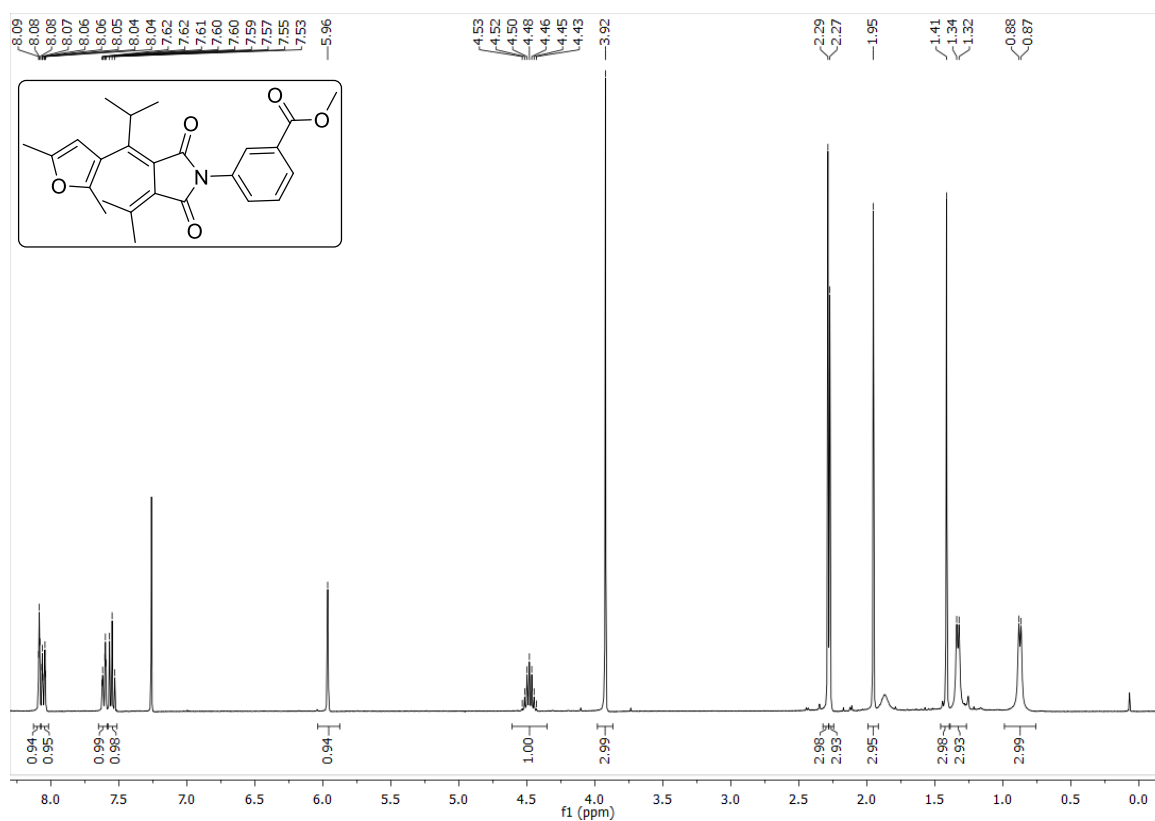
Compound **18**
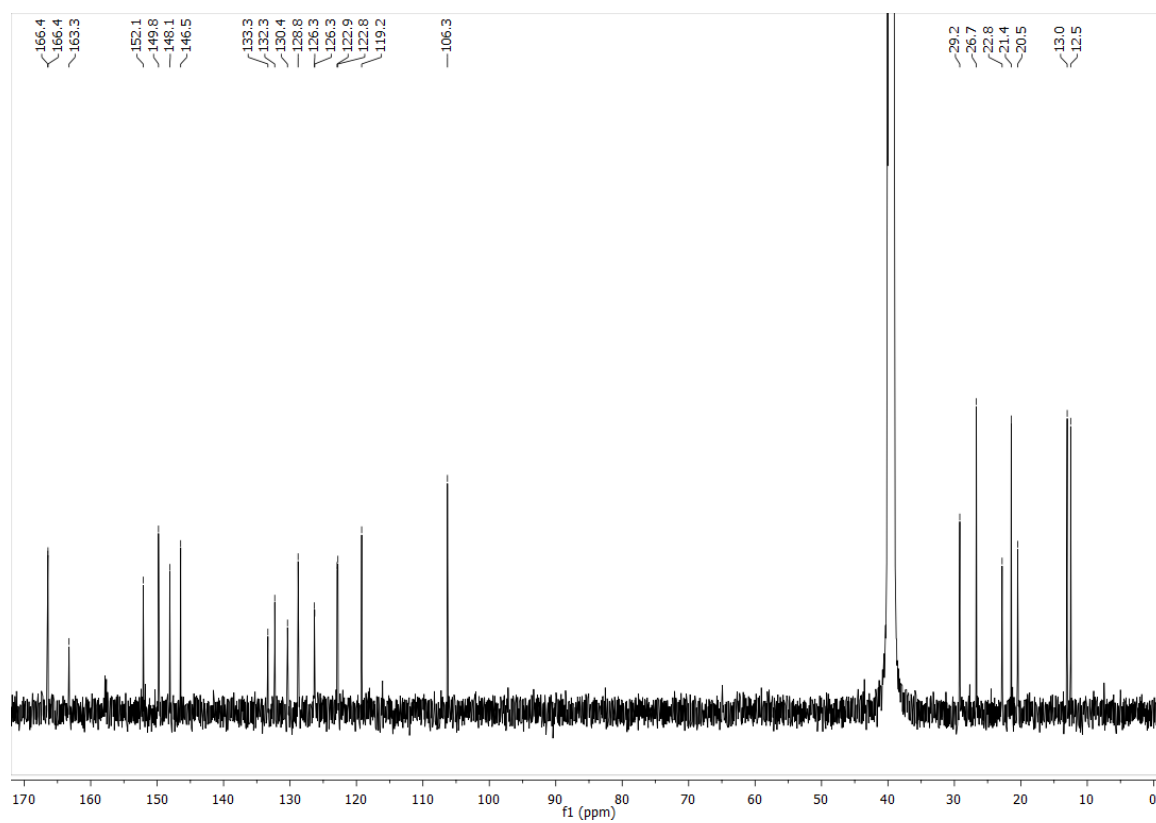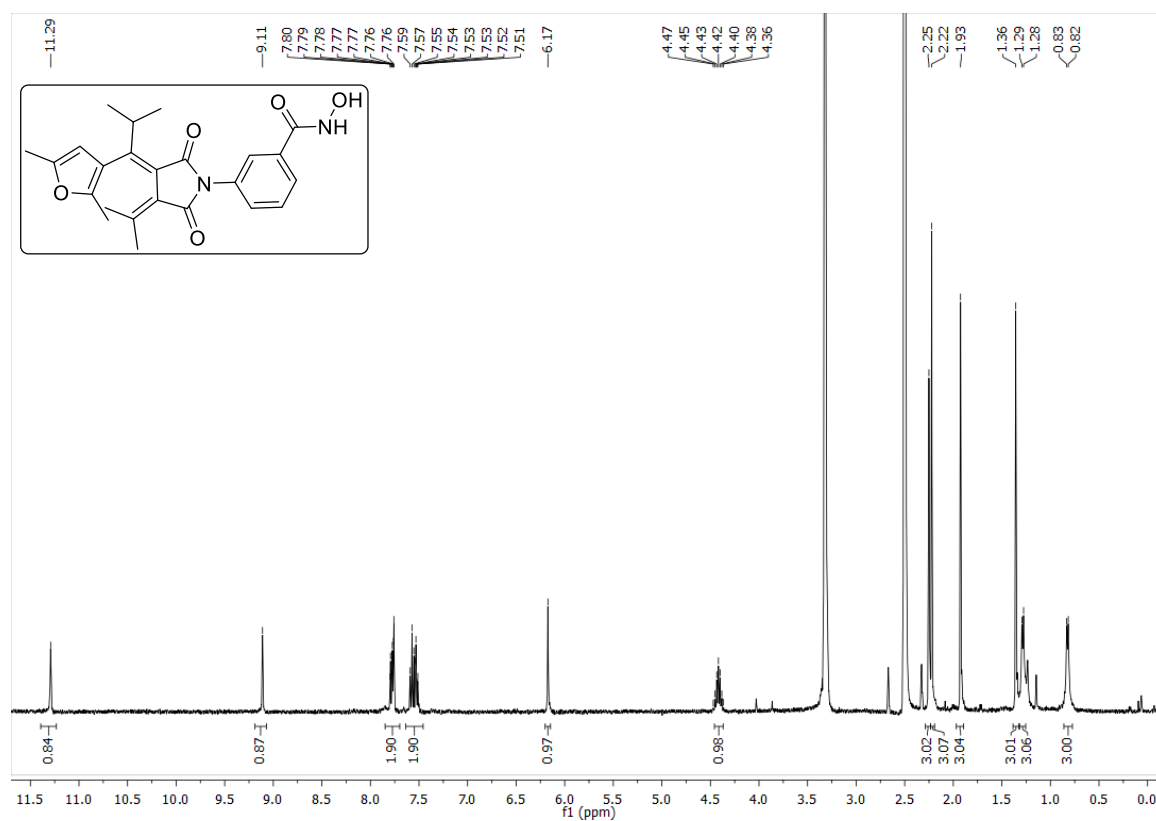
Compound **19**
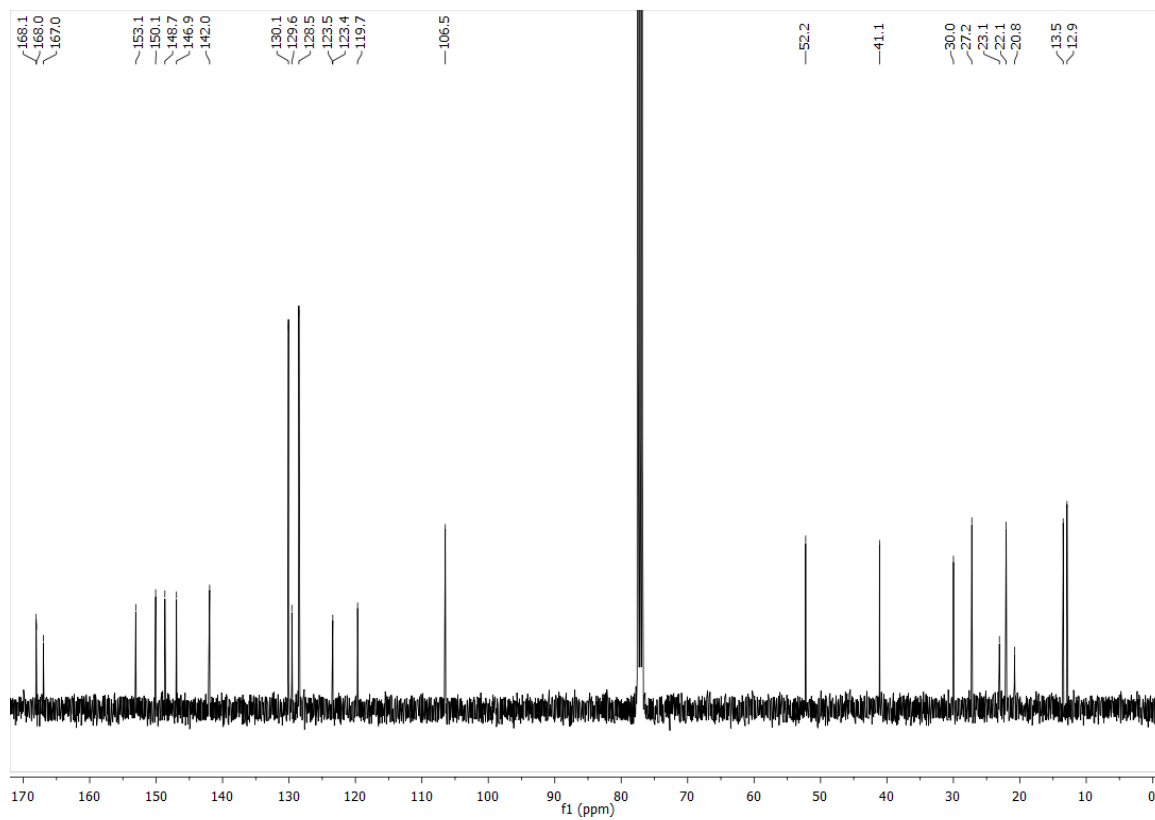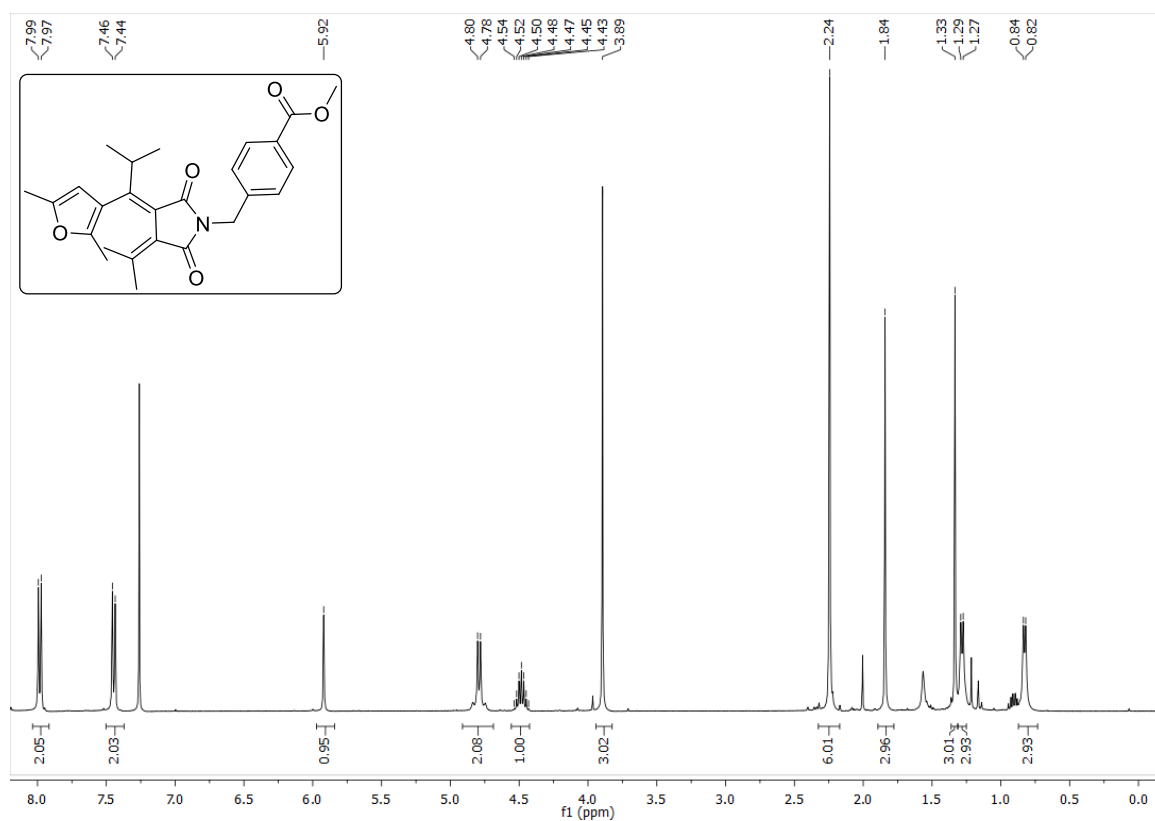
Compound **20**
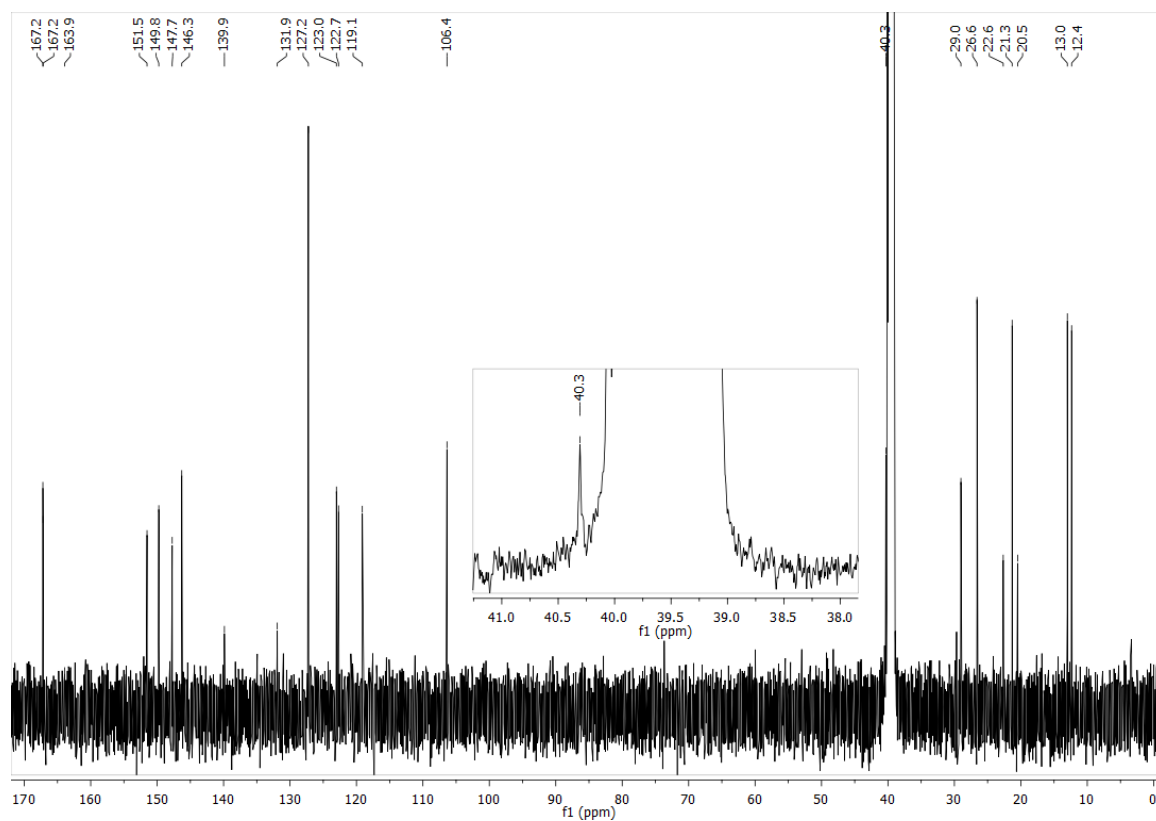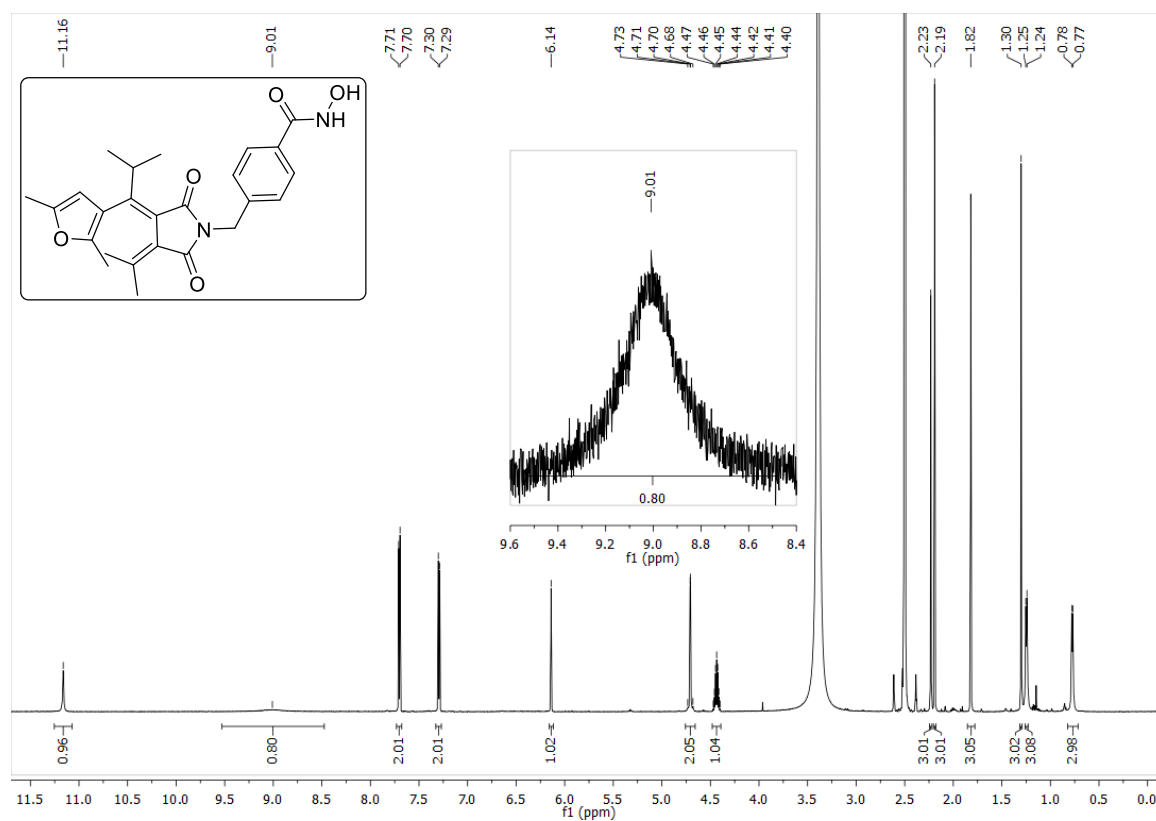
2.6 References

[1]   W. A. Velema, W. Szymanski, B. L. Feringa, *J. Am. Chem. Soc.* **2014**, *136*, 2178-2191.

[2]   W. Szymański, J. M. Beierle, H. A. V. Kistemaker, W. A. Velema, B. L. Feringa, *Chem. Rev.* **2013**, *113*, 6114-6178.

[3]   D. D. Young, A. Deiters, *Org. Bio. Chem.* **2007**, *5*, 999-1005.

[4]   K. Deisseroth, *Nat. Methods* **2011**, *8*, 26-29.

[5]   J. Broichhagen, J. A. Frank, D. Trauner, *Acc. Chem. Res.* **2015**, *48*, 1947-1960.

[6]   A. A. Beharry, G. A. Woolley, *Chem. Soc. Rev.* **2011**, *40*, 4422-4437.

[7]   D. Wilson, J. W. Li, N. R. Branda, *ChemMedChem* **2017**, *12*, 284-287.

[8]   R. J. Mart, R. K. Allemann, *Chem. Commun.* **2016**, *52*, 12262-12277.

[9]   C. E. Weston, A. Krämer, F. Colin, Ö. Yildiz, M. G. J. Baud, F.-J. Meyer-Almes, M. J. Fuchter, *ACS Infect. Dis.* **2017**, *3*, 152-161 .

[10]   W. Szymanski, M. E. Ourailidou, W. A. Velema, F. J. Dekker, B. L. Feringa, *Chem. Eur. J.* **2015**, *21*, 16517-16524.

[11]   R. Ferreira, J. R. Nilsson, C. Solano, J. Andréasson, M. Grøtli, *Scientific Reports* **2015**, *5*, 9769.

[12]   L. S. Runtsch, D. M. Barber, P. Mayer, M. Groll, D. Trauner, J. Broichhagen, *Beilstein J. Org. Chem.* **2015**, *11*, 1129-1135.

[13]   C. Falenczyk, M. Schiedel, B. Karaman, T. Rumpf, N. Kuzmanovic, M. Grøtli, W. Sippl, M. Jung, B. König, *Chem. Sci.* **2014**, *5*, 4794-4799.

[14]   M. J. Hansen, W. A. Velema, G. de Bruin, H. S. Overkleeft, W. Szymanski, B. L. Feringa, *ChemBioChem* **2014**, *15*, 2053-2057.

[15]   X. Chen, S. Wehle, N. Kuzmanovic, B. Merget, U. Holzgrabe, B. König, C. A. Sotriffer, M. Decker, *ACS Chem. Neurosci.* **2014**, *5*, 377-389.

[16]   J. Broichhagen, I. Jurastow, K. Iwan, W. Kummer, D. Trauner, *Angew. Chem. Int. Ed.* **2014**, *53*, 7657-7660.

[17]   B. Reisinger, N. Kuzmanovic, P. Löffler, R. Merkl, B. König, R. Sterner, *Angew. Chem. Int. Ed.* **2014**, *53*, 595-598.

[18]   D. Vomasta, C. Högner, N. R. Branda, B. König, *Angew. Chem. Int. Ed.* **2008**, *47*, 7644-7647.

[19]   D. Pearson, N. Alexander, A. D. Abell, *Chem. Eur. J.* **2008**, *14*, 7358-7365.

[20]   W. A. Velema, M. J. Hansen, M. M. Lerch, A. J. M. Driessen, W. Szymanski, B. L. Feringa, *Bioconjugate Chem.* **2015**, *26*, 2592-2597.

[21]   O. Babii, S. Afonin, M. Berditsch, S. Reiβer, P. K. Mykhailiuk, V. S. Kubyshkin, T. Steinbrecher, A. S. Ulrich, I. V. Komarov, *Angew. Chem. Int. Ed.* **2014**, *53*, 3392-3395.

[22]   W. A. Velema, J. P. van der Berg, M. J. Hansen, W. Szymanski, A. J. M. Driessen, B. L. Feringa, *Nat. Chem.* **2013**, *5*, 924-928.

[23]   J. B. Trads, J. Burgstaller, L. Laprell, D. B. Konrad, L. de la Osa de la Rosa, C. D. Weaver, H. Baier, D. Trauner, D. M. Barber, *Org. Bio. Chem.* **2017**, *15*, 76-81.

[24]   D. M. Barber, S.-A. Liu, K. Gottschling, M. Sumser, M. Hollmann, D. Trauner, *Chem. Sci.* **2017**, *8*, 611-615.

[25]   D. M. Barber, M. Schonberger, J. Burgstaller, J. Levitz, C. D. Weaver, E. Y. Isacoff, H. Baier, D. Trauner, *Chem. Sci.* **2016**, *7*, 2347-2352.

[26]   R. Huckvale, M. Mortensen, D. Pryde, T. G. Smart, J. R. Baker, *Org. Bio. Chem.* **2016**, *14*, 6676-6678.

[27]   M. Schönberger, M. Althaus, M. Fronius, W. Clauss, D. Trauner, *Nat. Chem.* **2014**, *6*, 712-719.

[28]   M. Schönberger, D. Trauner, *Angew. Chem. Int. Ed.* **2014**, *53*, 3264-3267.

[29]   M. Izquierdo-Serra, D. Trauner, A. Llobet, P. Gorostiza, *Front. Mol. Neurosci.* **2013**, *6*, article 3.

[30]   X. Gómez-Santacana, S. Pittolo, X. Rovira, M. Lopez, C. Zussy, J. A. R. Dalton, A. Faucherre, C. Jopling, J.-P. Pin, F. Ciruela, C. Goudet, J. Giraldo, P. Gorostiza, A. Llebaria, *ACS Cent. Sci.* **2017**, *3*, 81-91.

[31]   M. Stein, S. J. Middendorp, V. Carta, E. Pejo, D. E. Raines, S. A. Forman, E. Sigel, D. Trauner, *Angew. Chem. Int. Ed.* **2012**, *51*, 10500-10504.

[32]   U. Al-Atar, R. Fernandes, B. Johnsen, D. Baillie, N. R. Branda, *J. Am. Chem. Soc.* **2009**, *131*, 15966-15967.

[33]   S. Pittolo, X. Gómez-Santacana, K. Eckelt, X. Rovira, J. Dalton, C. Goudet, J.-P. Pin, A. Llobet, J. Giraldo, A. Llebaria, P. Gorostiza, *Nat. Chem. Biol.* **2014**, *10*, 813-815.

[34]   A. S. Lubbe, W. Szymanski, B. L. Feringa, *Chem. Soc. Rev.* **2017**, *46*, 1052-1079.

[35]   H. Cahová, A. Jäschke, *Angew. Chem. Int. Ed.* **2013**, *52*, 3186-3190.

[36]   S. Barrois, H.-A. Wagenknecht, *Beilstein J. Org. Chem.* **2012**, *8*, 905-914.

[37]   A. Polosukhina, J. Litt, I. Tochitsky, J. Nemargut, Y. Sychev, I. De Kouchkovsky, T. Huang, K. Borges, D. Trauner, Russell N. Van Gelder, Richard H. Kramer, *Neuron* **2012**, *75*, 271-282.

[38]   L. Laprell, K. Hüll, P. Stawski, C. Schön, S. Michalakis, M. Biel, M. P. Sumser, D. Trauner, *ACS Chem. Neurosci.* **2016**, *7*, 15-20.

[39]   J. A. Frank, H. G. Franquelim, P. Schwille, D. Trauner, *J. Am. Chem. Soc.* **2016**, *138*, 12981-12986.

[40]   J. A. Frank, M. Moroni, R. Moshourab, M. Sumser, G. R. Lewin, D. Trauner, *Nat. Commun.* **2015**, *6*, 7118.

[41]   J. A. Frank, D. A. Yushchenko, D. J. Hodson, N. Lipstein, J. Nagpal, G. A. Rutter, J.-S. Rhee, A. Gottschalk, N. Brose, C. Schultz, D. Trauner, *Nat. Chem. Biol.* **2016**, *12*, 755-762.

[42]   H. M. D. Bandara, S. C. Burdette, *Chem. Soc. Rev.* **2012**, *41*, 1809-1825.

[43]   V. I. Minkin, in *Molecular Switches*, Wiley-VCH Verlag GmbH & Co. KGaA, **2011**, pp. 37-80.

[44]   Y. Yokoyama, T. Gushiken, T. Ubukata, in *Molecular Switches*, Wiley-VCH Verlag GmbH & Co. KGaA, **2011**, pp. 81-95.

[45]   M. Irie, T. Fukaminato, K. Matsuda, S. Kobatake, *Chem. Rev.* **2014**, *114*, 12174-12277.

[46]   K. J. Falkenberg, R. W. Johnstone, *Nat. Rev. Drug Discov.* **2014**, *13*, 673-691.

[47]   K. V. Woan, E. Sahakian, E. M. Sotomayor, E. Seto, A. Villagra, *Immunol. Cell Biol.* **2012**, *90*, 55-65.

[48]   K. T. Andrews, A. Haque, M. K. Jones, *Immunol. Cell Biol.* **2012**, *90*, 66-77.

[49]   M. Marek, G. Oliveira, R. J. Pierce, M. Jung, W. Sippl, C. Romier, *Future Med. Chem.* **2015**, *7*, 783-800.

[50]   T. Heimburg, A. Chakrabarti, J. Lancelot, M. Marek, J. Melesina, A.-T. Hauser, T. B. Shaik, S. Duclaud, D. Robaa, F. Erdmann, M. Schmidt, C. Romier, R. J. Pierce, M. Jung, W. Sippl, *J. Med. Chem.* **2016**, *59*, 2423-2435.

[51]   M. Marek, S. Kannan, A.-T. Hauser, M. Moraes Mourão, S. Caby, V. Cura, D. A. Stolfa, K. Schmidtkunz, J. Lancelot, L. Andrade, J.-P. Renaud, G. Oliveira, W. Sippl, M. Jung, J. Cavarelli, R. J. Pierce, C. Romier, *PLOS Pathogens* **2013**, *9*, e1003645.

[52]   F. Dubois, S. Caby, F. Oger, C. Cosseau, M. Capron, C. Grunau, C. Dissous, R. J. Pierce, *Mol. Biochem. Parasitol.* **2009**, *168*, 7-15.

[53]   J. Tang, H. Yan, S. Zhuang, *Clin. Sci.* **2013**, *124*, 651-662.

[54]   J. E. Bolden, M. J. Peart, R. W. Johnstone, *Nat. Rev. Drug Discov.* **2006**, *5*, 769-784.

[55]   A. S. Madsen, C. A. Olsen, *Nat. Chem. Biol.* **2016**, *12*, 306-307.

[56]   R. Mazitschek, B. Ghosh, J. A. Hendricks, S. Reis, S. J. Haggarty, *US Pat.* WO2014160221 (A1), **2014**.

[57]   C. Brieke, F. Rohrbach, A. Gottschalk, G. Mayer, A. Heckel, *Angew. Chem. Int. Ed.* **2012**, *51*, 8446-8476.

[58]   Y. Yokoyama, *Chem. Rev.* **2000**, *100*, 1717-1740.

[59]   R. De Vreese and M. D'Hooghe, *Eur. J. Med. Chem.*, **2017**, *135*, 174-195.

[60]   Y. C. Liang, A. S. Dvornikov, P. M. Rentzepis, *PNAS* **2003**, *100*, 8109-8112.

[61]   S. Malkmus, F. O. Koller, S. Draxler, T. E. Schrader, W. J. Schreier, T. Brust, J. A. DiGirolamo, W. J. Lees, W. Zinth, M. Braun, *Adv. Funct. Mater.* **2007**, *17*, 3657-3662.

[62]   T. Kumpulainen, B. Lang, A. Rosspeintner, E. Vauthey, *Chem. Rev.* **2016**, DOI: 10.1021/acs.chemrev.6b00491.

[63]   M. Schulze, M. Utecht, A. Hebert, K. Rück-Braun, P. Saalfrank, P. Tegeder, *J. Phys. Chem. Lett.* **2015**, *6*, 505-509.

[64]   X. Chen, N. I. Islamova, S. P. Garcia, J. A. DiGirolamo, W. J. Lees, *J. Org. Chem.* **2009**, *74*, 6777-6783.

[65]   I. Willner, M. Lion-Dagan, S. Rubin, J. Wonner, F. Effenberger, P. Bäuerle, *Photochem. Photobiol.* **1994**, *59*, 491-496.

[66]   L. N. Lucas, J. J. D. d. Jong, J. H. v. Esch, R. M. Kellogg, B. L. Feringa, *Eur. J. Org. Chem.* **2003**, *2003*, 155-166.

[67]   A. J. Myles, Z. Zhang, G. Liu, N. R. Branda, *Org. Lett.* **2000**, *2*, 2749-2751.

[68]   D. Wutz, C. Falenczyk, N. Kuzmanovic, B. König, *RSC Adv.* **2015**, *5*, 18075-18086.

[69]   T. Yamaguchi, M. Irie, *Chem. Lett.* **2004**, *33*, 1398-1399.

[70]   T. Yamaguchi, K. Uchida, M. Irie, *J. Am. Chem. Soc.* **1997**, *119*, 6066-6071.

[71]   M. Irie, K. Sayo, *J. Phys. Chem.* **1992**, *96*, 7671-7674.

[72]   C. Fleming, P. Remón, S. Li, N. A. Simeth, B. König, M. Grøtli, J. Andréasson, *Dyes Pigment.* **2017**, *137*, 410-420.

[73]   M. Herder, B. M. Schmidt, L. Grubert, M. Pätzel, J. Schwarz, S. Hecht, *J. Am. Chem. Soc.* **2015**, *137*, 2738-2747.

[74]   J. R. Matis, J. B. Schonborn, P. Saalfrank, *PCCP* **2015**, *17*, 14088-14095.

[75]   M. Irie, T. Lifka, K. Uchida, S. Kobatake, Y. Shindo, *Chem. Commun.* **1999**, 747-750.

[76]   B. Heltweg, F. Dequiedt, E. Verdin, M. Jung, *Anal. Biochem.* **2003**, *319*, 42-48.

[77]   B. Heltweg, J. Trapp, M. Jung, *Methods* **2005**, *36*, 332-337.

[78]   F. Strübe, R. Siewertsen, F. D. Sönnichsen, F. Renth, F. Temps, J. Mattay, *Eur. J. Org. Chem.* **2011**, *2011*, 1947-1955.

[79]   H. Stobbe, *Chem. Ber.* **1905**, *38*, 3673-3682.

[80]   H. Stobbe, *Chem. Ber.* **1907**, *40*, 3372-3382.

[81]   H. Stobbe, *Liebigs Ann. Chem.* **1911**, *380*, 1-2.

[82]   P. M. Lombardi, K. E. Cole, D. P. Dowling, D. W. Christianson, *Current Opinion in Structural Biology* **2011**, *21*, 735-743.

[83]   C. Micelli, G. Rastelli, *Drug Discovery Today* **2015**, *20*, 718-735.

[84]   Y. Hai, D. W. Christianson, *Nat. Chem. Biol.* **2016**, *12*, 741-747.

[85]   Y. Miyake, J. J. Keusch, L. Wang, M. Saito, D. Hess, X. Wang, B. J. Melancon, P. Helquist, H. Gut, P. Matthias, *Nat. Chem. Biol.* **2016**, *12*, 748-754.

[86]   L. Whitehead, M. R. Dobler, B. Radetich, Y. Zhu, P. W. Atadja, T. Claiborne, J. E. Grob, A. McRiner, M. R. Pancost, A. Patnaik, W. Shao, M. Shultz, R. Tichkule, R. A. Tommasi, B. Vash, P. Wang, T. Stams, *Biorg. Med. Chem.* **2011**, *19*, 4626-4634.

[87]   P. J. Watson, C. J. Millard, A. M. Riley, N. S. Robertson, L. C. Wright, H. Y. Godage, S. M. Cowley, A. G. Jamieson, B. V. L. Potter, J. W. R. Schwabe, *Nat. Commun.* **2016**, *7*, 11262.

[88]   A. Vannini, C. Volpari, P. Gallinari, P. Jones, M. Mattu, A. Carfí, R. De Francesco, C. Steinkühler, S. Di Marco, *EMBO reports* **2007**, *8*, 879-884.

[89]   H. M. Berman, J. Westbrook, Z. Feng, G. Gilliland, T. N. Bhat, H. Weissig, I. N. Shindyalov, P. E. Bourne, *Nucleic Acids Res.* **2000**, *28*, 235-242.

[90]   Schrödinger Suite 2012 Protein Preparation Wizard; Epik Version 2.3, Schrödinger, LLC, New York, 2012; Impact Version 5.8, Schrödinger, LLC, New York, 2012; Prime Version 3.1, Schrödinger, LLC, New York, **2012**.

[91]   *Molecular Operating Environment (MOE)*, 2012.10; Chemical Computing Group Inc., 1010 Sherbooke St. West, Suite #910, Montreal, QC, Canada, H3A 2R7, **2012**.

[92]   J. Senger, J. Melesina, M. Marek, C. Romier, I. Oehme, O. Witt, W. Sippl, M. Jung, *J. Med. Chem.* **2016**, *59*, 1545-1555.

3 Photochromic Ligands for Modulation of GABA$_A$- and Glycine-Receptors by Light

3.1 Introduction

The two amino acids γ-aminobutyric acid (GABA) and glycine act as the major inhibitory neurotransmitters of the central nervous system by addressing their respective ionotropic chloride channel receptors to control the input-output relationship of excitatory drives impinging on neurons.[1] The ionotropic GABA receptors (GABA_A and GABA_C receptors) are mainly present in synapses in the brain while glycine-receptors (GlyRs) dominate in the spinal cord and brainstem.[2] Both of these receptors belong to the pentameric ligand-gated ion channel "Cys-loop" family.[3] The GABA_A-receptor (GABA_AR) is composed of five hetero-oligomeric subunits selected from different subunit classes forming a central ion conductive pore. The subunit composition determines the individual function and pharmacological properties.[4] Most GABA_ARs in the brain are composed of two alpha subunits subtype α_1, two beta subunits subtype β_2, and one gamma subunit subtype γ_2.[5] When two molecules of GABA bind to the receptor at the neighboring interfaces of the α and β subunits the channel opens and allows the influx of chloride ions into the cell which results in membrane hyperpolarization.[6] As their dysfunction is related to various neuronal diseases the GABA_ARs became an important drug target in pharmaceutical and clinical research. Benzodiazepines (BZDs), which are an important class of compounds among the variety of tranquilizers, bind at the extracellular interface of the α and γ subunit of GABA_ARs and act as positive allosteric modulators of these receptors.[7] They cause highly anxiolytic, sedative, hypnotic, anticonvulsant and muscle relaxant effects.[8] However, their long-term use is controversial due to undesired side effects, abuse and most importantly drug addiction.[9-11] Interestingly, BZDs can also interact with central nervous GlyRs.[12]

Also the GlyRs are assembled of five subunits arranged symmetrically around a central chloride selective pore. There are five different classes of subunits, four alpha and one beta. The alpha subunits can form homo- or heterogenic receptors in combination with the beta subunit.[13] The glycine binding sites are located at the interfaces of two alpha subunits or between an alpha and beta subunit. The binding properties of the beta-beta interface are unknown.[14] Like the ionotropic GABA receptors the GlyRs are chloride-permeable pores which open when an agonist like glycine is binding. This leads to a hyperpolarization of the membrane potential and inhibition of neuronal firing.[15]

Whereas strychnine is a very potent and famous antagonist of GlyRs, nicardipine, which belongs to the class of dihydropyridines, acts mainly as calcium channel blocker[16] but can also have a biphasic potentiating as well as an inhibitory effect on GlyRs.[17]

Light can be a powerful tool for the investigation of biological systems due to its high spatial and temporal controllability.[18] Different approaches of photocontrol have been developed and investigated: optogenetics,[19-20] the release of caged compounds by light,[18] photoswitchable tethered ligands (PTLs)[21-24] and photochromic ligands (PCLs).[25] The latter principle is most-common and the use of synthetic photoswitches to control biological activity with light has developed in a new vibrant field of research called photopharmacology.[26-28] Azobenzenes and dithienylethenes (DTEs) are the two main classes of photoswitches used in biological environment. Both scaffolds have a light-induced reversible conversion between two isomers in common. The isomers of the azobenzenes differ in geometry and dipole moment and for the DTEs in conformational flexibility and electronic properties.[28] Both classes of switches show high fatigue resistance. The open and closed form of DTEs are thermally stable[29] whereas the *cis* isomer of an ordinary azobenzene underlies a thermal relaxation with characteristic half-life, which can be advantageous depending on the particular application.[30] Another benefit of azobenzenes is their relatively easy synthesis by well-known methods like azo coupling or Mills reaction.[31] In the last years a lot of effort was made to successfully shift the wavelengths for the isomerization of azo compounds to the visible region, which is preferable for biological applications due to a higher tissue penetration of visible light.[32–33]

Among other ion channels[34-40] also the GABA$_A$-channel has been photocontrolled by PCLs based on propofol or gabazine.[41-43] We envisioned that merging azo switches with different known and highly biologically active pharmacophores as the benzodiazepine nitrazepam and the dihydropyridine nicardipine, (Figure 1) would lead to photochromic ligands for GABA$_A$Rs and GlyRs, respectively, which have not been targeted yet. For our target structure design the tertiary amine moiety of nicardipine had to be modified into an aniline for the functionalization with an azobenzene. The nitro group of nitrazepam was reduced and then used as reactive counterpart for Mills reactions with various aromatic nitroso compounds to generate the azo moiety. Herein, we report the synthesis,

photophysical characterization, initial biological evaluations and preliminary results of molecular docking studies for these photochromic ion channel ligands.
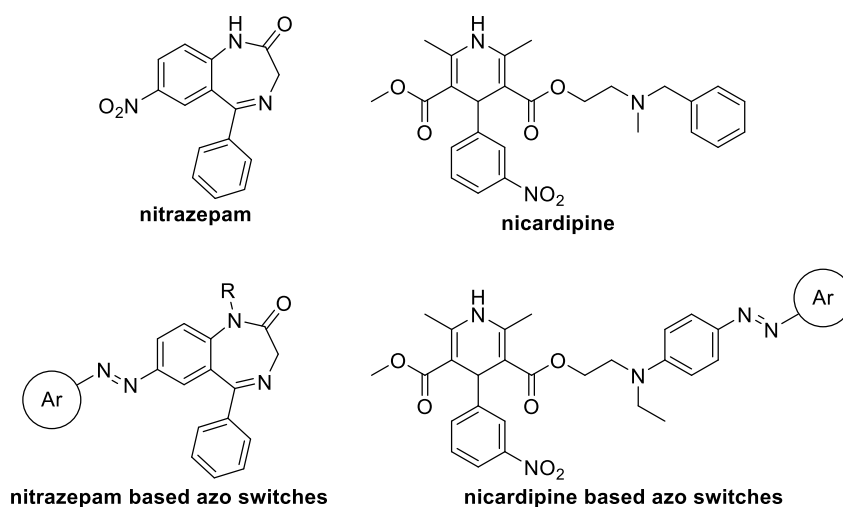
Figure 1. Molecular structures of the pharmacophores nitrazepam and nicardipine as well as general target structures of our photochromic azo ligands based on these pharmacophores.

3.2 Results and Discussion

3.2.1 Synthesis

Synthesis of the benzodiazepine core

First, a published synthesis[44] of nitrazepam starting from commercial benzophenone **1** was attempted but surprisingly afforded isomeric quinolone **4** as the main product (Scheme 1). Already the crude mixture of the reaction contained compounds **3** and **4** approximately in a 1:1 ratio. Trying to further purify compound **3** after column chromatography by recrystallization from toluene selectively transformed nitrazepam (**3**) into the undesired isomer **4**. This rearrangement of nitrazepam to quinolone **4** in highly boiling solvents is known,[45] but also seems to occur already during the reaction in refluxing ethanol efficiently.
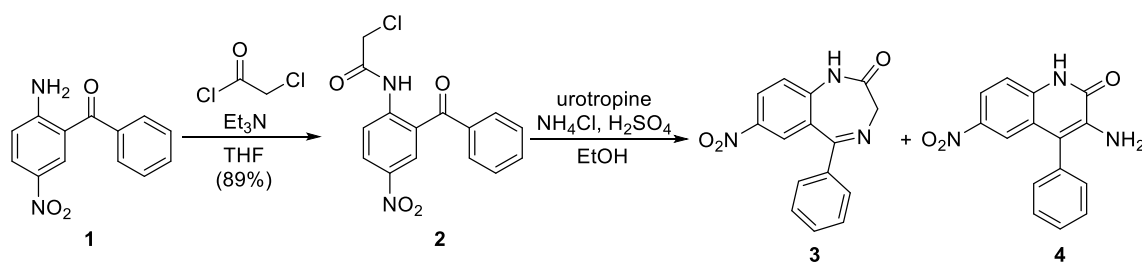
Scheme 1. Undesired synthesis of quinolone **4**.

Therefore, another published synthesis[46] for nitrazepam was accomplished and afforded the desired compound in two steps also starting from benzophenone **1**. The nitro group of **3** was subsequently reduced by hydrogenation with palladium on charcoal as catalyst providing aniline **6**[47] which can be used for further functionalization (Scheme 2). However, our analytical NMR data were in discrepancy with published ones,[48] but we could validate and prove our structure by X-ray crystallography.
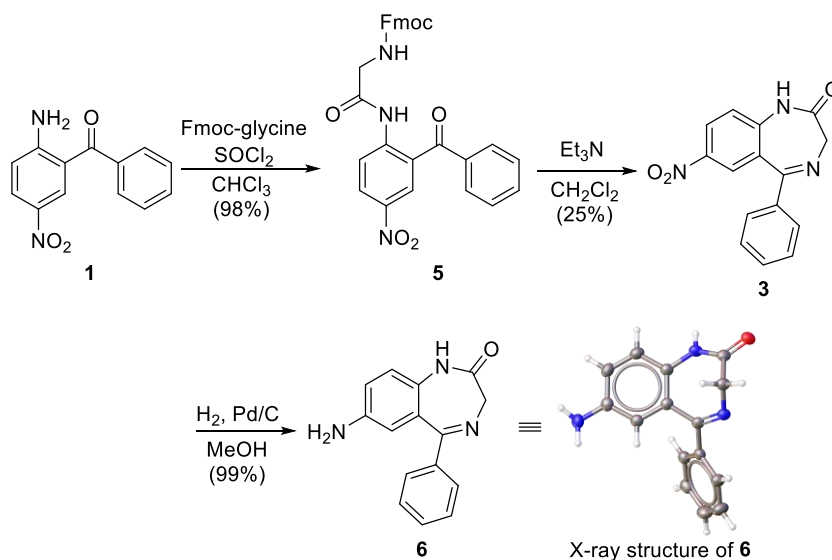
Scheme 2. Synthesis of nitrazepam (**3**) and subsequent reduction to 7-amino nitrazepam (**6**) with its corresponding X-ray structure.

Nitrazepam (**3**) was further functionalized with quaternary amine **7**[49] to increase its water solubility and introduce a positive charge (Scheme 3). For this purpose, it was alkylated on the amide group in an adapted heterogeneous microwave supported reaction[50] to compound **8** and then also hydrogenated to aniline **9** which was not isolated.
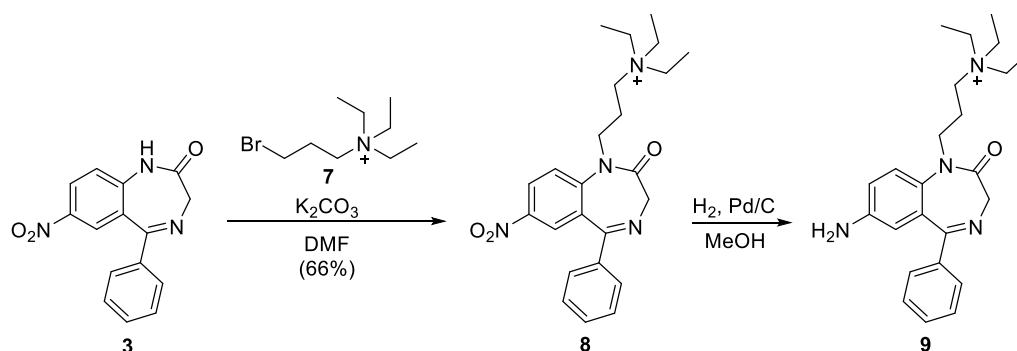
Scheme 3. Preparation of benzodiazepines **8** and **9**.

Synthesis of nitroso compounds

A variety of aromatic nitroso compounds bearing polar groups were synthesized according to known procedures (Scheme 4). Sulfanilic acid (**10**) was converted into its tetrabutylammonium salt **11** which is soluble in organic solvents to prevent it from overoxidation by oxone in a biphasic system in the next step (Scheme 4a).[51] Nevertheless, only a 1:1 mixture of nitroso compound **12** and its corresponding nitro compound **13** could be isolated. All attempts to purify this mixture and enrich compound **12** were not successful due to the instability and high reactivity of the nitroso group. Hence, this obtained mixture was used for further reactions. Two different nitrosobenzsulfonamides **15** and **18** were synthesized. Aniline **14** was reacted to its corresponding nitroso compound **15** by an oxone oxidation in a biphasic water/dichloromethane system in very low yield (Scheme 4b).[52]
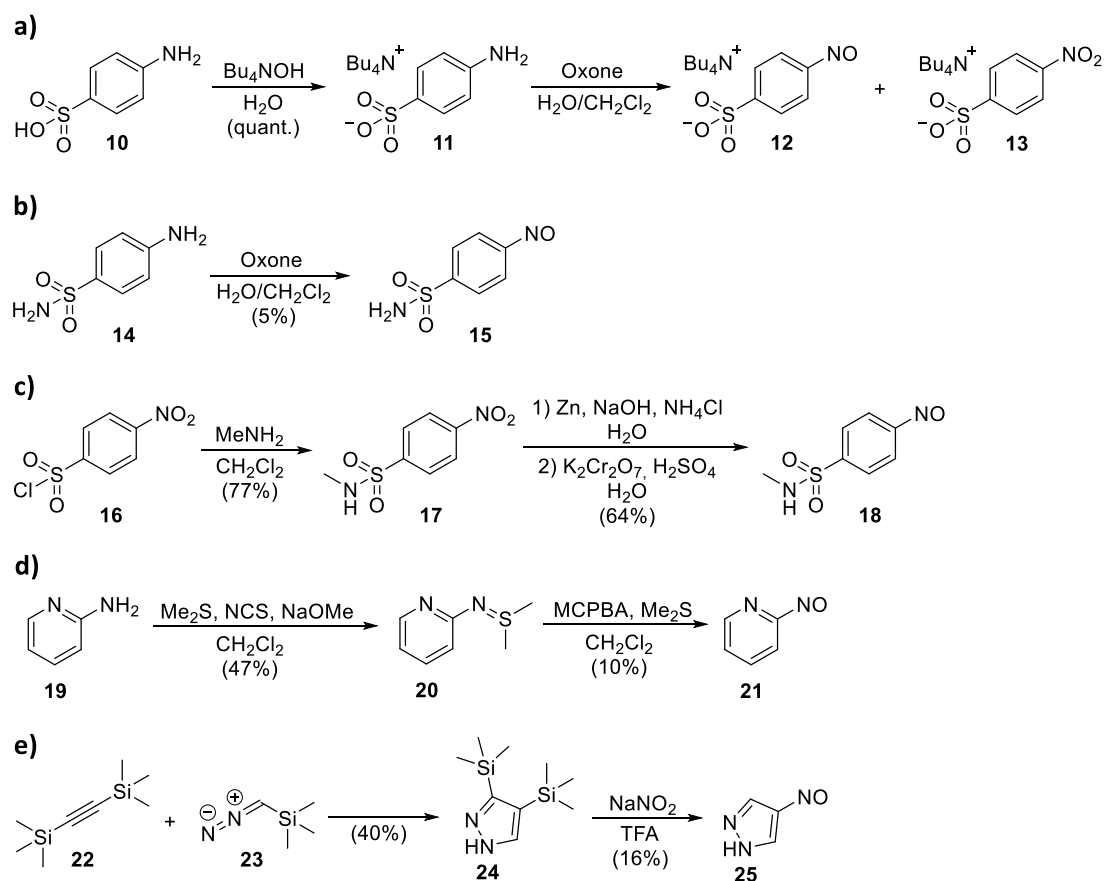
Scheme 4. Synthesis of nitroso compounds **12** (**a**), **15** (**b**), **18** (**c**), **21** (**d**) and **25** (**e**).

Sulfonyl chloride **16** was reacted with aqueous methylamine to gain sulfonamide **17**[53] which was further converted to nitrosobenzenesulfonamide **18** by a reduction with zinc

and subsequent oxidation with potassium dichromate (Scheme 4c).[54] Nitrosopyridine **21** was synthesized by an oxidation with *meta*-chloroperoxybenzoic acid of sulfilimine **20**, which was obtained starting from commercial aminopyridine **19** (Scheme 4d).[55] A microwave assisted 1,3-dipolar cycloaddition of acetylene **22** and diazo compound **23** yielded pyrazole **24**.[56] A further transformation with sodium nitrite in trifluoroacetic acid afforded nitrosopyrazole **25** in low yield (Scheme 4e).[57]

Synthesis of 7-azo benzodiazepines.

The Mills reaction was used as key step to form a photoisomerizable azo moiety between the prepared aromatic nitroso compounds **12**, **15**, **18**, **21** as well as **25** and the 7-amino benzodiazepines **6** and **9**. Therefore, each of the nitroso precursors was reacted with aniline **6** affording target structures **26** - **30** in a range of low (15%) up to good (73%) yields (Scheme 5).
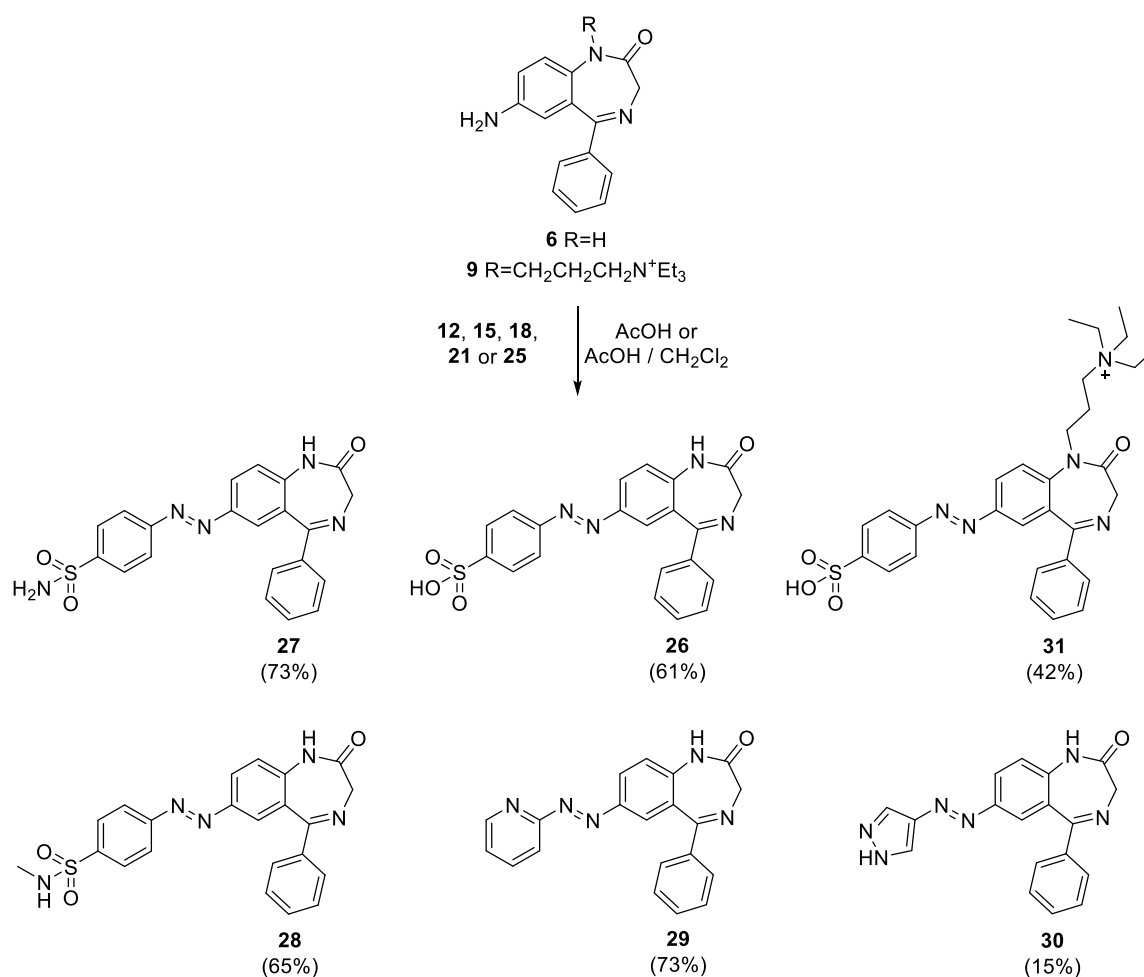
Scheme 5. Synthesis of target 7-azo benzodiazepines **26** - **31** by Mills reactions.

As solvent either pure acetic acid or a mixture of acetic acid and dichloromethane was used, which was beneficial for the solubility of the reagents. Under the biological testing conditions in aqueous buffer at pH-values around 7 sulfonic acid **26** is completely deprotonated bearing an overall negative charge (pK_a of benzenesulfonic acid = 0.7)[58]. To study the influence and potentially unfavorable interaction of the negative charge of compound **26** on chloride anion selective ion channels compound **31** which is also functionalized with a sulfonic acid moiety was synthesized by a Mills reaction being overall neutral under these conditions (Scheme 5).

Unfortunately, azo compound **28** showed very poor water solubility, which is essential for biological testing. Introducing a highly polar and charged group by post-functionalization solved this problem. Sulfonamide **28** was consequently alkylated with a tertiary amine. Because of the high reactivity and the use of two equivalents of the alkylating agent, it reacted also with its own tertiary amine group and accordingly azo benzodiazepine **32** was isolated as main product in 29% yield (Scheme 6).
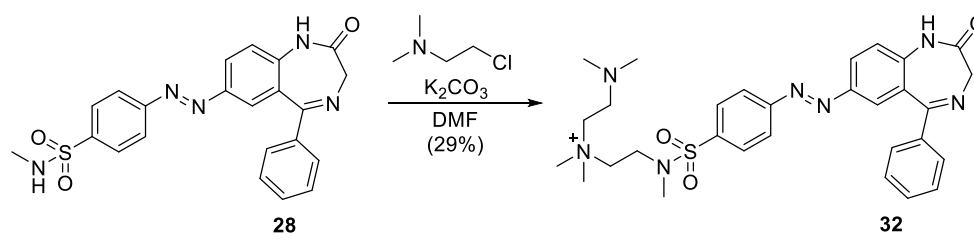
Scheme 6. Post-functionalization by alkylation of sulfonamide **28** to azo benzodiazepine **32**.

Attempt to synthesize fulgimide substituted benzodiazepines.

We also wanted to take advantage of the very good photochromic properties of fulgides/fulgimides and therefore attempted to attach them to benzodiazepine **9** (Scheme 7). In the first step fulgides **33** and **34** were reacted under basic conditions with benzodiazepine **9**. The aniline group of **9** efficiently attacked and opened the anhydride moieties of the fulgides which was investigated by LC-MS analysis. However, after adding CDI to the reaction with furan **33** and PyBOP to the reaction with benzothiophene **34** as coupling reagents to build the maleimide ring only traces of desired compounds **35** and **36** could be detected by LC-MS analysis besides a lot of other compounds. Additionally, we were also not able to recover any starting material and therefore suppose that the coupling reagents decompose the benzodiazepine scaffold. In a next attempt, the

coupling reagents have to be screened and carefully selected to avoid decomposition in order to succeed with the preparation of target compounds **35** and **36**.
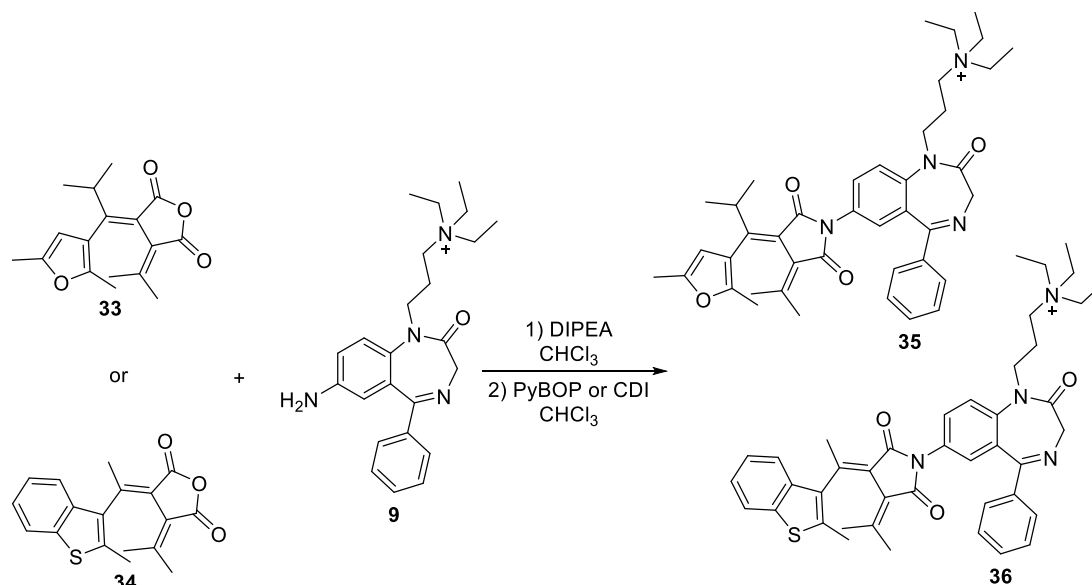
Scheme 7. Attempted synthesis of fulgimide substituted benzodiazepines **35** and **36**.

Synthesis of nicardipine based photoswitches.

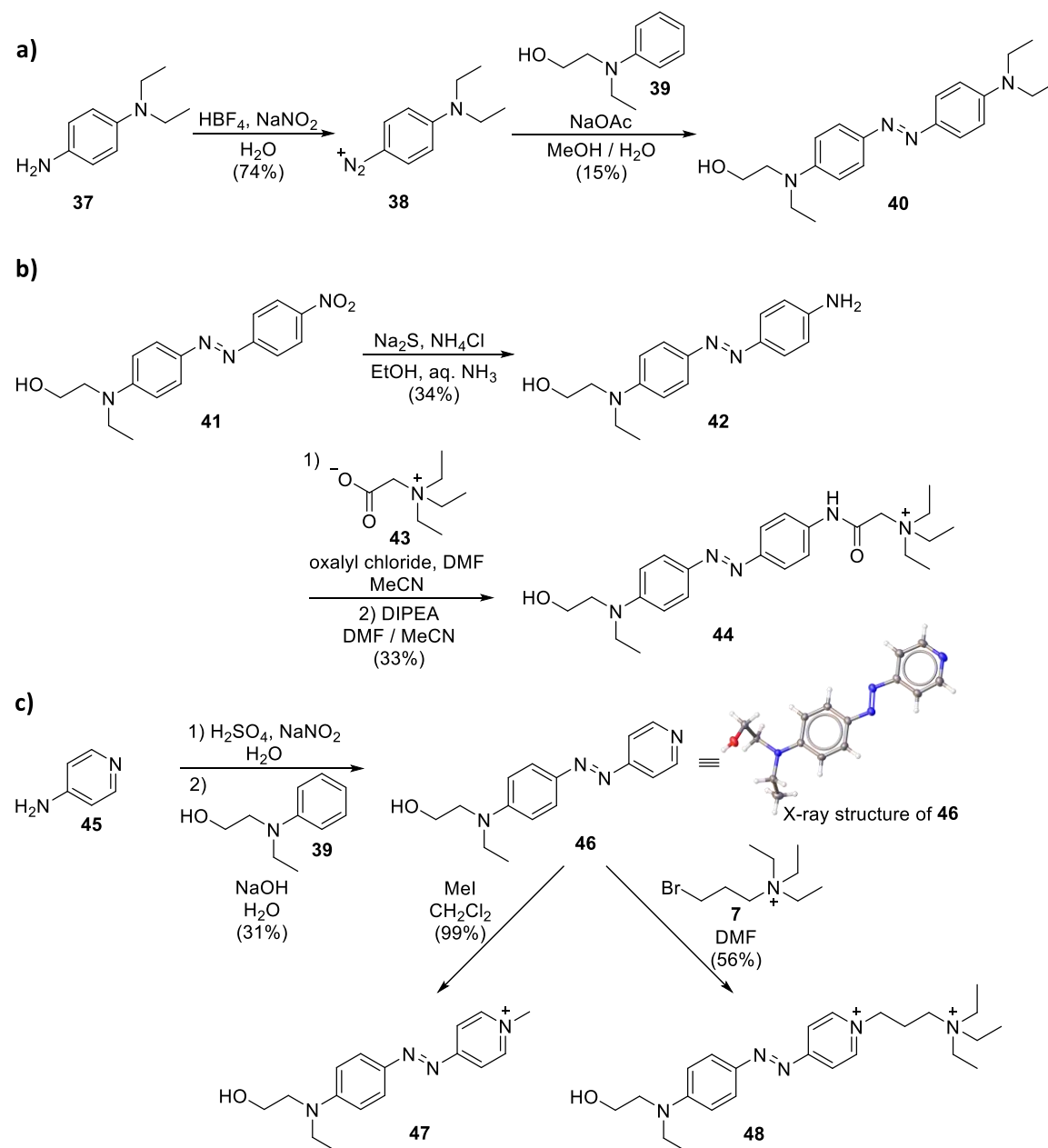For the preparation of a series of nicardipine based photochromic compounds different azobenzenes equipped with an aliphatic primary alcohol as linking group to the dihydropyridine pharmacophore were synthesized (Scheme 8). Azo compound **40** was generated by an adapted diazotization[59] of aniline **37** and subsequent coupling with aniline **39** yielded azo switch **40** in two steps with an overall yield of 11% (Scheme 8a). Commercially available azo dye **41** was reduced with sodium sulfide.[60] Betaine **43**[61] was activated by oxalyl chloride and then coupled with amine **42** under basic conditions obtaining compound **44** (Scheme 8b). Another diazotization reaction of pyridine **45** and subsequent azo coupling with aniline **39** yielded photoswitch **46**.[62] Further functionalization by alkylation with iodomethane and quaternary ammonium **7**[49] provided azo compounds **47** and **48** in quantitative and 56% yield, respectively (Scheme 8c). Interestingly, the proton NMR spectrum of compound **47** shows four sharp doublets each with an integral of two for the eight aromatic protons, but for one of the signals the corresponding cross-peak in the HSQC as well as the signal from the corresponding pair of carbons in the carbon NMR is missing. This unusual fact that a sharp proton signal does not give a cross-peak in the HSQC spectrum with a missing carbon

signal could be explained by the positive charge of the pyridinium ion which leads to a fast exchange in the aromatic system. The situation for pyridinium **48** is similar for the aromatic protons, but in this case two doublets in the proton NMR are sharp, one is broad and the last one very broad. Consequently, the corresponding carbon NMR signals for both pairs of carbons bound to the protons with the broad signals could not be detected.

Scheme 8. Synthesis of azo compounds **40** (**a**), **44** (**b**) and **46** - **48** (**c**) with the X-ray structure of **46**.

Finally, commercially available dihydropyridine **49** was activated with thionyl chloride and then esterified with azo switches **40**, **44** and **46** - **48** in low to moderate yields affording azo nicardipines **50** - **53** (Scheme 9). Modified nicardipine **54** was synthesized by the same

type of reaction and should serve as a reference and model compound for biological testing to investigate the effect of the structural change we made compared to the original nicardipine scaffold.
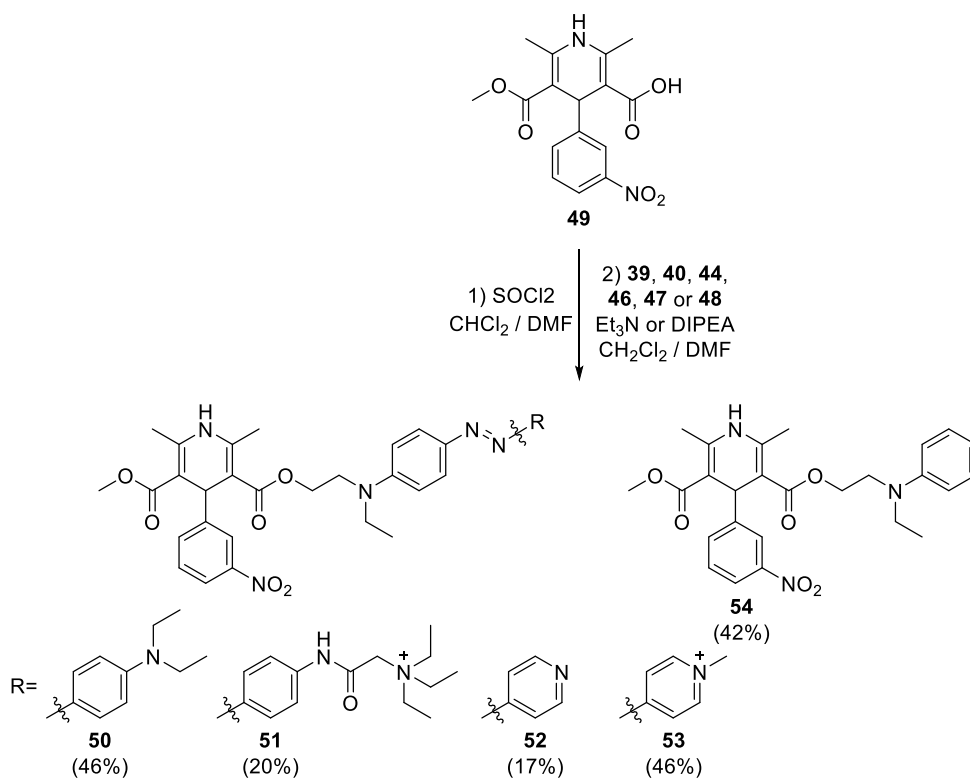
Scheme 9. Synthesis of modified nicardipine based compound **54** and azo derivatives **50** - **53**.

However, compound **54** as well as azo switches **50** and **52** unfortunately showed insufficient water solubility for biological testing. The desired product of the reaction of compound **49** with photoswitch **48** could be detected by LC-MS and NMR analysis but could not sufficiently be purified and isolated. Compound **53** shows the same phenomenon like already described for compound **47** of a missing cross-peak and a missing carbon signal in the NMR analysis despite sharp proton signals. In addition, determining the purity of compound **53** by analytical HPLC measurements revealed a specific impurity of about 10%. Further investigations by LC-MS analysis combined with the observation that also azo switch **52** showed an increasing decomposition tendency with decreasing pH value in aqueous solution suppose that compound **53** is also somehow decomposing. According to LC-MS measurements the impurity has to be uncharged with a molecular weight of 601 grams per mole and exhibits no absorption at 550 nm unlike azo dye **53**. Therefore, we suppose decomposition of **53** as depicted in Scheme 10.
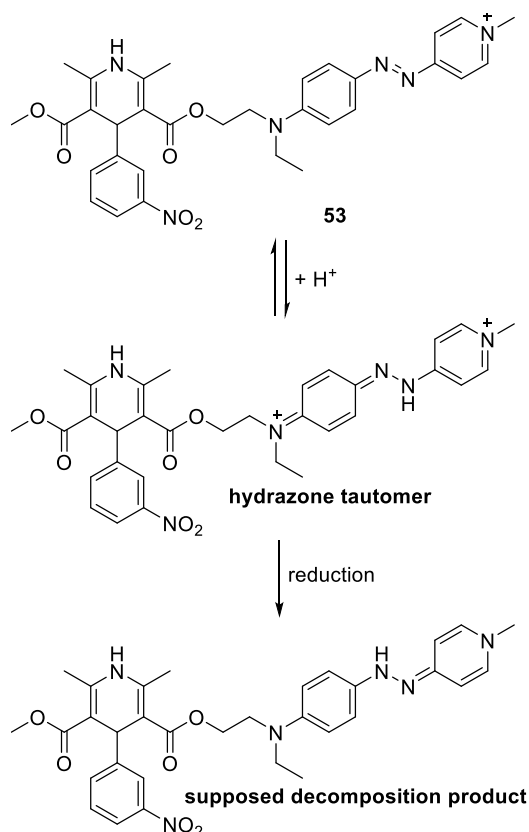
Scheme 10. Assumed formation of decomposition product of azo nicardipine **53**.

The first step is a protonation of compound **53** forming the hydrazine tautomer which is well known for such kind of azo systems.[63-64] A reduction of the hydrazine would then afford a compound which has no longer an absorption at 550 nm due to the interruption of the conjugated π-system and with the required molecular weight. However, we were not able to isolate, characterize or finally prove the structure of the impurity.

3.2.2 Photochromic Properties

The choice of the photochromic scaffold is crucial for the design of photoswitchable ligands. Beside their relatively easy preparation azobenzenes also exhibit efficient photoswitching, a low rate of photobleaching and outstanding fatigue resistance.[25,30] Upon irradiation with light of an appropriate wavelength the in general thermally more stable *trans* isomer of azobenzenes is converted to the corresponding *cis* isomer with a huge change in geometry and dipole moment. The *trans* isomer can be regenerated either by thermal back relaxation or by irradiation with light.[30] The photochromic properties of

our prepared photoswitchable ligands **26** - **32** and **50** - **53** dissolved in DMSO and aqueous PBS if sufficiently soluble are summarized in Table 1.

Table 1. Photochromic data of the synthesized ligands **26** - **32** and **50** - **53**.

Entry	Comp.	Conc. [μM]	Solvent	λ_{max} *trans* [nm]	λ_{max} *cis* [nm]	$t_{1/2}$ 25 °C	PSS *cis*[a] [%]*	PSS *tra.*[b] [%]*
1	**26**	50	DMSO	361	440	17.4 h	88	82
2	**26**	50	PBS + 0.1% DMSO	347	429	55.6 h	n.d.	n.d.
3	**27**	50	DMSO	365	442	21.1 h	88	82
4	**27**	30	PBS + 3% DMSO	348	427	30.4 h	n.d.	n.d.
5	**28**	50	DMSO	364	438	28.5 h	n.d.	n.d.
6	**29**	50	DMSO	357	435	7.8 h	80	84
7	**29**	50	PBS + 0.1% DMSO	348	425	82 min	n.d.	n.d.
8	**30**	50	DMSO	350	none	2.7 h	88	71
9	**30**	50	PBS + 0.1% DMSO	339	none	-[c]	n.d.	n.d.
10	**31**	50	DMSO	359	436	36.9 h	92	85
11	**31**	50	PBS + 1% DMSO	340	425	171 h	n.d.	n.d.
12	**32**	50	DMSO	352	451	34.3 h	82	89
13	**32**	50	PBS + 1% DMSO	342	437	78.1 h	n.d.	n.d.
14	**50**	10	DMSO	463	358	74 s	83[d]	n.d.
15	**51**	25	DMSO	434	376	0.3 s	-[e]	-[e]
16	**51**	25	PBS + 1% DMSO	422	none	<0.3 s[f]	-[e]	-[e]
17	**52**	25	DMSO	450	376	38 s	n.d.	n.d.
18	**53**	15	DMSO	552	-[g]	-[g]	-[g]	-[g]
19	**53**	15	PBS + 1% DMSO	566	-[g]	-[g]	-[g]	-[g]

n.d.: not determined; * determined by HPLC measurements with detection at isosbestic points; [a] PSS at photoconversion from the *trans* to the *cis* isomer; [b] PSS at photoconversion from the *cis* to the *trans* isomer; [c] could not be determined due to decomposition or precipitation after 5 h in PBS solution; [d] determined by direct irradiation in the NMR tube during proton NMR analysis (200 μM in DMSO-d_6); [e] was not determined due to very fast thermal back isomerization; [f] could only be estimated due to aggregation effects in aqueous solution and moreover a very fast thermal relaxation; [g] photoisomerization could not be detected at all due to very short thermal half-life beyond time resolution of UV-Vis spectroscopy.

All our photochromic ligands featured excellent photochromic properties with a high photostationary state (PSS) of ≥80% of the *cis* isomer at the *trans* to *cis* photoconversion. This fact is beneficial because a biological effect can then be assigned to mainly one photoisomer. All the benzodiazepine derivatives **26** - **32** show a similar photochromic behavior. They can be photoisomerized to the *cis* isomer by UV-light of 365 nm. The back isomerization to the *trans* isomer can most efficiently be triggered by blue light of 455 nm except for compound **30**. Due to the lack of a distinct absorption band for the *cis* isomer of **30** and an overlap of the UV-Vis spectra of both isomers light of a longer wavelength (530 nm) was used for back conversion to mostly avoid an absorption of the *trans* isomer. By way of example, Figure 2a illustrates the UV-Vis spectra of the *trans* isomer and the two PSSs of azo benzodiazepine **26** (50 μM in DMSO). Figure 2b shows the repetitive cycle performance with light of 365 nm and 455 nm at which no fatigue could be detected over ten measured cycles. Photochromic ligands **26** - **32** exhibit thermal half-lives in the range from 1.4 h to several days which can be advantageous due to the avoidance of continuous UV-irradiation for generating the *cis* isomer.
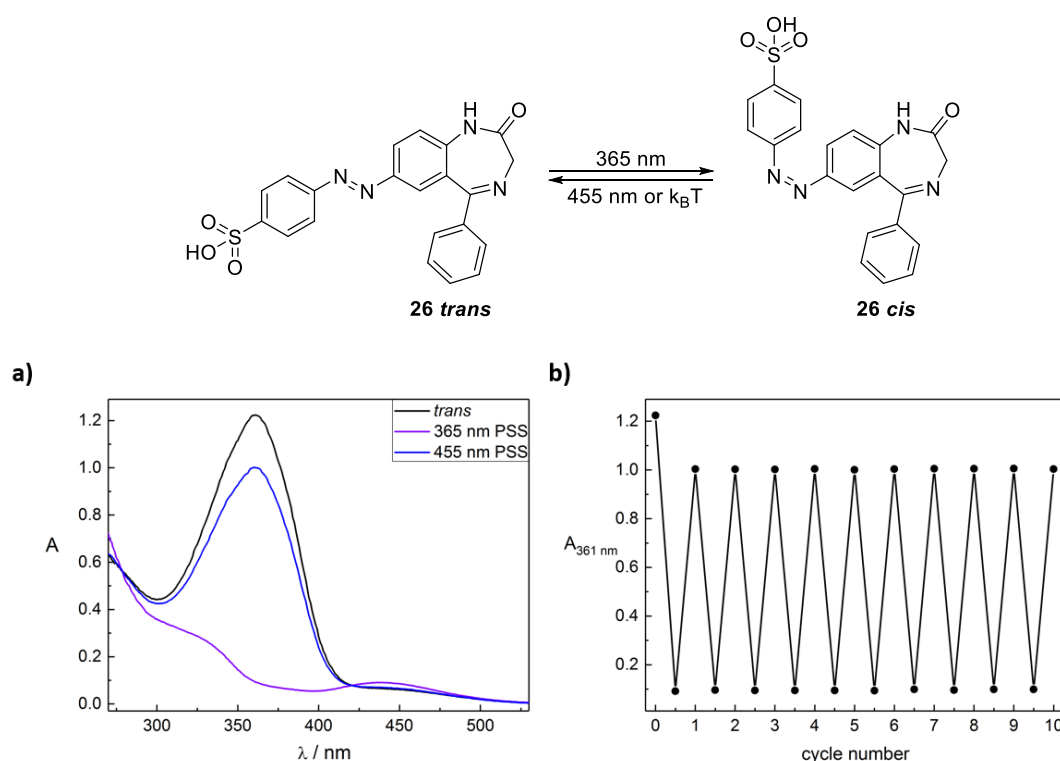
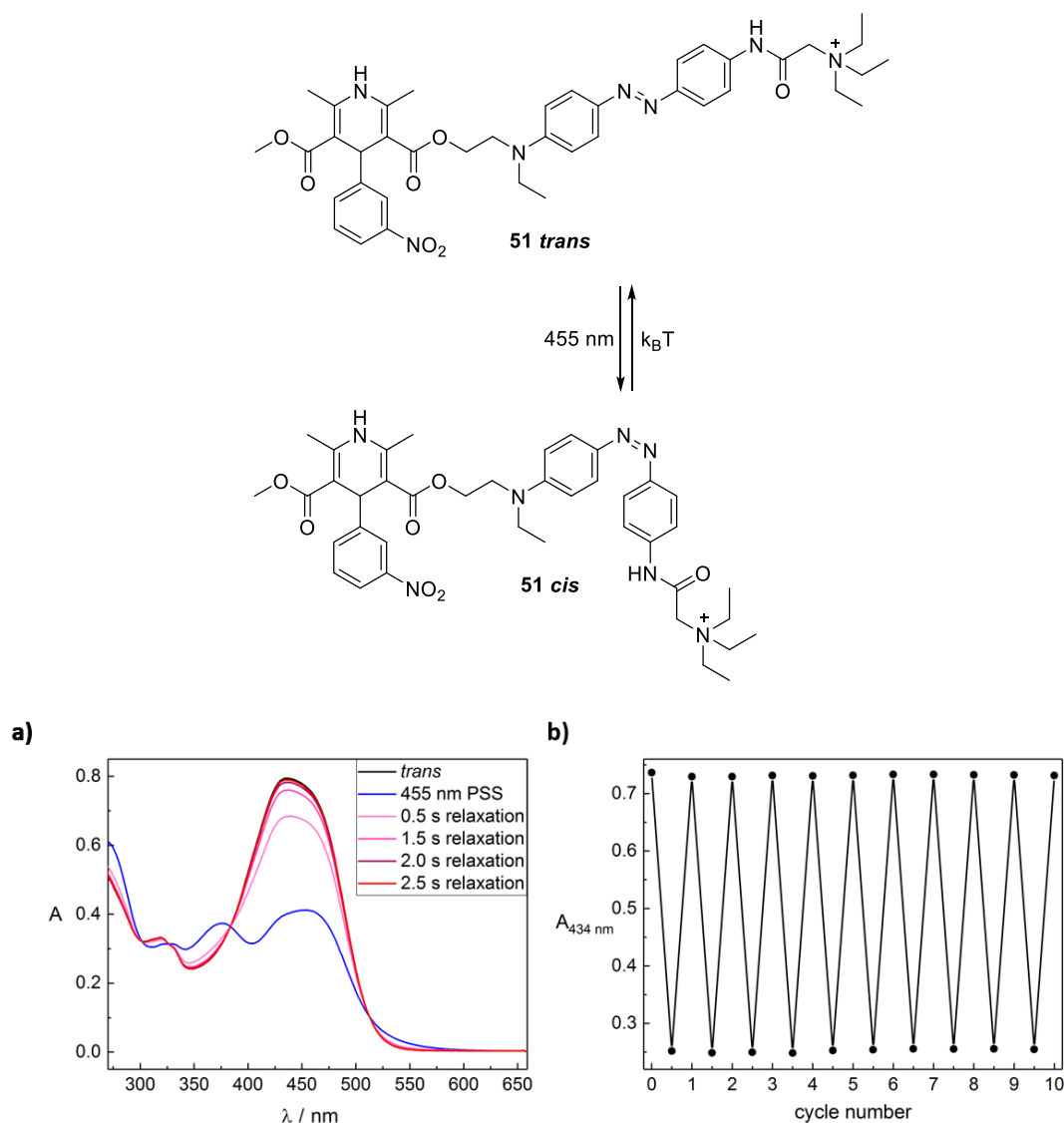**Figure 2. a)** UV-Vis spectra of azo benzodiazepine **26** (50 μM in DMSO) from the *trans* isomer, the PSS at irradiation with UV-light of 365 nm and the PSS at irradiation with blue light of 455 nm. **b)** Cycle performance of azo benzodiazepine **26** (50 μM in DMSO). Changes in absorption at 361 nm were measured during alternate irradiation with light of 365 nm for 15 s and 455 nm for three seconds.

Photochromic ligands **50** - **53** differ in photochromic properties compared to the azo benzodiazepines, because they all belong to the class of so called "push-pull" azobenzenes.[30] For compounds **51** - **53** it is quite obvious that the aniline acts as the donor part and the second aromatic moiety consisting of a pyridine, pyridinium or substituted with an electron withdrawing group as the acceptor part, respectively. Compound **50** can be transformed in such a system by simple protonation of one of the anilines.[40] These azobenzenes with a "push-pull" substitution generally show a red-shift in the absorption and shorter thermal half-lives.[30] We assume, but could not prove that the thermal relaxation of the *cis* isomer of **53** has to be really fast, because we were not able to detect any photoisomerization of azo switch **53** under continuous irradiation either in DMSO or aqueous phosphate buffer by standard UV-Vis spectroscopy. This is in accordance with a report of a related pyridinium switch.[40] The photoisomerization could be monitored by flash laser photolysis[65-66] or other readouts like biological effects. It has been shown that ion channels are able to recognize such a fast isomerization.[40]

The azo nicardipines **50** - **52** were isomerized to the corresponding *cis* isomers by irradiation with blue light of 455 nm. The back isomerization of compound **52** was achieved with light of 385 nm and for compound **50** with visible light of 590 nm. The thermal relaxation of the *cis* isomer of **51** is so fast that the use of irradiation for back isomerization is unnecessary. After stopping irradiation with 455 nm it just takes about three seconds to completely recover the *trans* isomer, which can be repeated without fatigue (Figure 3).

Due to this very short thermal half-life of about 0.3 s in DMSO it was also not possible to quantify the PSS under continuous irradiation in the NMR spectrometer, because it was beyond the time scale for NMR spectroscopy. Only by irradiating (λ = 455 nm) a sample of **51** dissolved in methanol at 200 K a second set of signals belonging to the *cis* isomer started to arise, which was detectable by NMR spectroscopy due to the longer half-life of the *cis* isomer at lower temperatures.

Figure 3. a) UV-Vis spectra of azo benzodiazepine **51** (25 µM in DMSO) from the *trans* isomer, the PSS at irradiation with blue light of 455 nm and the spectral evolution at thermal *cis* to *trans* relaxation which is completed after approximately three seconds. **b)** Cycle performance of azo benzodiazepine **51** (25 µM in DMSO). Changes in absorption at 434 nm were measured during alternating irradiation with light of 455 nm for three seconds and thermal relaxation for five seconds.

By investigating the photochromic properties of **51** in aqueous PBS (see Supporting Information, Figure S9) a much lower molar extinction coefficient at the maximum absorption of the *trans* isomer was observed. It dropped from $31.7 \cdot 10^3$ cm^{-1} M^{-1} in DMSO to $14.4 \cdot 10^3$ cm^{-1} M^{-1} in phosphate buffer with 1% of DMSO as solvent. This significant change could be explained by aggregation of **51** in aqueous solution, which is already known for other azobenzenes functionalized with a quaternary ammonium moiety due to their structure similarity with surfactants (so called azo surfactants).[67] In order to investigate the aggregation of compound **51** UV-Vis spectra in PBS as well as DMSO at

different concentrations were recorded and the concentration was plotted against the absorbance at the maximum absorption of the *trans* isomer in both solvents (Figure 4).
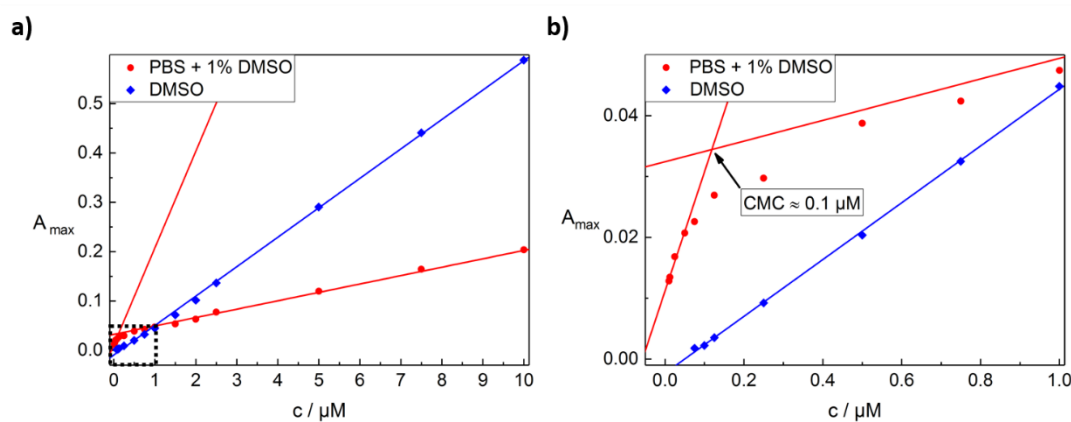

Figure 4. a) Absorbance versus concentration plot at the absorption maximum of compound **51** in DMSO (blue) and aqueous PBS + 1% of DMSO (red) with linear extrapolations. The marked area is shown magnified in b. **b)** CMC determination of azo nicardipine **51** in PBS + 1% of DMSO by intersection of the linear extrapolations.

As depicted in Figure 4a the absorbance at the maximum absorption of **51** in DMSO is increasing linearly with the concentration of **51** over the whole examined range of concentrations from 0.075 µM up to 10 µM. In contrast, the absorbance of **51** in the aqueous system is initially also increasing linearly from a concentration of 0.01 µM up to a concentration of almost 0.1 µM and then increasing further linearly with a flatter slope up to a 10 µM concentration (Figure 4a and 4b). The concentration at which the two extrapolated line segments are intersecting represents the onset of a micellization or aggregation process and is generally called critical micelle concentration (CMC).[68] The determined CMC value of around 0.1 µM for **51** is quite low compared to other related cationic azo surfactants which have critical micelle concentrations in the range from 0.1 to 10 mM.[67] Therefore, we assume that the large organic and nonpolar nicardipine based part of compound **51** is further facilitating an aggregation in aqueous solution already at very low concentrations.

3.2.3 Biological Investigations and Molecular Docking

Electrophysiology[A]

The activity of the synthesized photochromic ligands **26**, **29** and **30** was investigated by patch-clamp recordings with transfected CHO-cells expressing the respective ion channel. First, the effect of azo benzodiazepine **26** on heteromeric $\alpha_1\beta_2\gamma_2$ GABA$_A$Rs was studied. The sensitivity of the expressed GABA$_A$-receptors to GABA was analyzed and a mean EC$_{50}$ of 8 ± 3 μM (data from 6 cells) was determined as depicted in Figure5a.
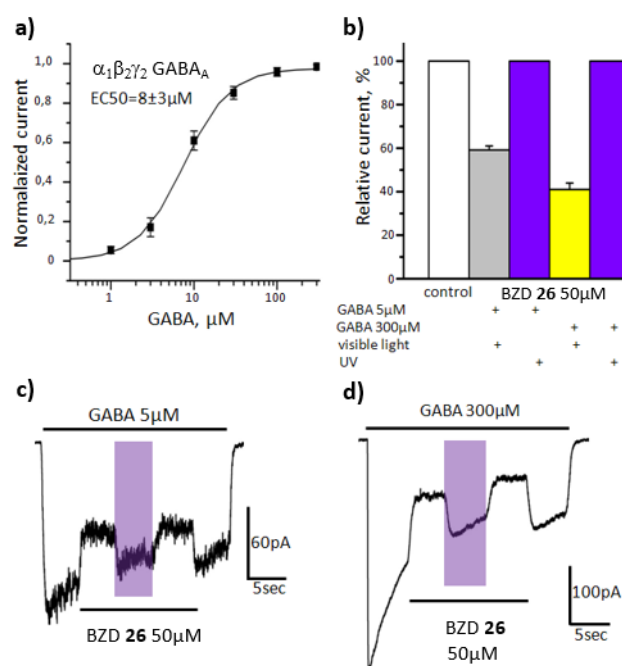
**Figure 5. a)** Dose-response curve for GABA$_A$. Mean EC$_{50}$ for GABA comprised 8 ± 3 μM (n = 6 cells). **b)** Relative amplitudes of GABA$_A$-mediated currents in control (white column), during application of 50 μM of photochromic benzodiazepine **26** (GABA 5 μM – gray column, GABA 300 μM – yellow column) and upon UV illumination (violet columns). **c)** Representative trace of the current induced by 5 μM of GABA, application of a mixture of GABA 5 μM + compound **26** 50 μM started at the 5th second of registration and finished at the 20th second. Duration of UV illumination from the 10th until the 15th second of registration is indicated by the violet rectangle. **d)** Representative trace of the current induced by 300 μM of GABA, application of mixture GABA 300 μM + compound **26** 50 μM started at the 5th second of registration and finished at the 20th. Duration of UV illumination from the 10th until the 15th second of registration is indicated by the violet rectangle.

Therefore, GABA concentrations of 5 μM (below EC$_{50}$) and 300 μM (saturating concentration) were used to activate the GABA$_A$-receptors in the next experiments. The application of **26** (50 μM) induced an inhibition of GABA$_A$-mediated currents to $59 \pm 2\%$

(n = 6 cells; Figure 5b and c) when the channels were activated by 5 µM concentration of GABA and to 41 ± 3% (n = 8 cells; Figure 5b and d) when the channels were activated by 300 µM of GABA. This inhibitory effect is contrary to the general mode of action of benzodiazepines as positive allosteric modulators of $GABA_A$Rs. Upon UV illumination in both cases the inhibitory action of azo benzodiazepine **26** was abolished.

The effect of azo benzodiazepine **26** on GlyRs was studied on α_1 zebrafish, α_1 human, α_2 zebrafish, α_2 mouse, α_3 human and α_1 human G254A mutant homomeric receptors. Initially, we determined the sensitivity of α_1 zebrafish GlyRs to glycine and found a mean EC_{50} of 35 ± 10 µM (n = 6 cells) as depicted in Figure 6a.
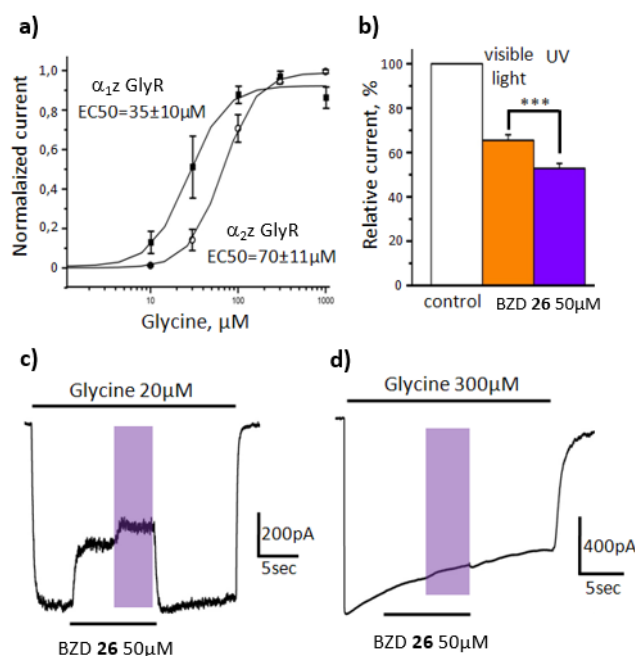

Figure 6. a) Averaged dose-response curves for α_1 and α_2 zebrafish GlyRs. **b)** Relative amplitudes of currents mediated by α_1 zebrafish GlyRs in control (glycine 20 µM), during application of 50 µM of photochromic benzodiazepine **26** in visible light (orange column) and in UV light (violet column). **c)** Representative trace of the current induced by 20 µM of glycine, application of a mixture of glycine 20 µM + compound **26** 50 µM started at the 5th second of registration and finished at the 15th second. Duration of UV illumination from the 10th until the 15th second of registration is indicated by the violet rectangle. **d)** Representative trace of the current induced by 300 µM of glycine, application of a mixture of glycine 300 µM + compound **26** 50 µM started at the 5th second of registration and finished at the 15th second. Duration of UV illumination from the 10th until the 15th second of registration is indicated by the violet rectangle.

The application of azo benzodiazepine **26** (50 µM) caused an inhibition of currents evoked by 20 µM of glycine to 66 ± 2% (n = 6). UV illumination provoked an additional decrease of the current amplitude to 53 ± 2% (n = 6) (Figure 6b and c). However, the effect of **26**

was not observed during the activation of α_1 zebrafish GlyRs with a saturating concentration of glycine (300 µM) shown in Figure 6d.

As depicted in Figure 6a the mean glycine EC$_{50}$ for α_2 zebrafish Gly-receptors comprised 70 ± 11 µM (n = 6). Under visible light benzodiazepine **26** inhibited α_2 mediated currents. The amplitude of currents evoked by 50 µM of glycine decreased to 9 ± 5% (n = 3, Figure 7a and c). The current evoked by 300 µM of glycine decreased to 24 ± 9% (n = 3, Figure 7b and c). Upon UV illumination the inhibitory effect of compound **26** was completely abolished.
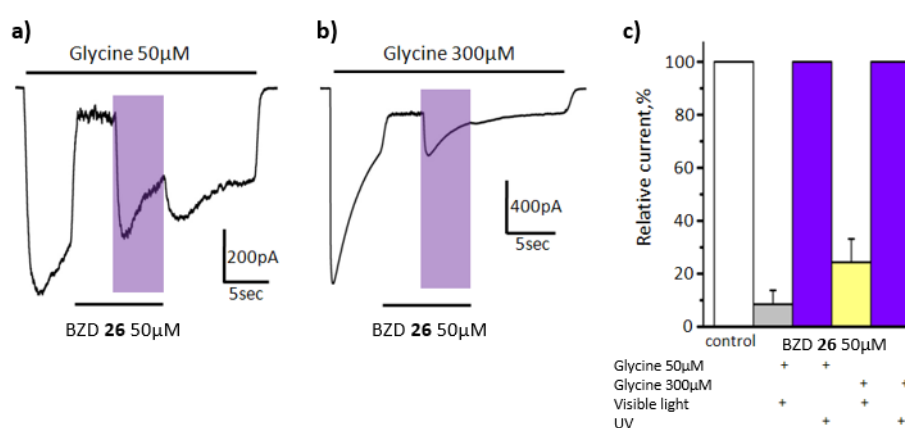
Figure 7. a) Representative trace of the current induced by 50 µM of glycine at α_2 zebrafish GlyRs, application of a mixture of glycine 50 µM + compound **26** 50 µM started at the 5th second of registration and finished at the 15th second. Duration of UV illumination from the 10th until the 15th second of registration is indicated by the violet rectangle. **b)** Representative trace of the current induced by 300 µM of glycine, application of a mixture of glycine 300 µM + compound **26** 50 µM started at the 5th second of registration and finished at the 15th second. Duration of UV illumination from the 10th until the 15th second of registration is indicated by the violet rectangle. **d)** Relative amplitudes of glycine-mediated currents in control (white column), during application of 50 µM of photochromic benzodiazepine **26** (50 µM of glycine – gray column, 300 µM of glycine – yellow column) and upon UV illumination (violet columns).

The action of benzodiazepine **26** on α_2 mouse GlyRs was similar to its action on α_2 zebrafish GlyRs. Currents induced by 30 µM of glycine were inhibited to 34 ± 3% (n = 9) by application of 50 µM of compound **26**. Upon UV illumination the inhibitory effect of **26** was abolished. Also the effect of **26** on α_3 human Gly-receptors was similar to its action on α_2 zebrafish and α_2 mouse GlyRs. The currents which were induced by 30 µM of glycine were inhibited to 38 ± 3% (n = 7) by application of **26** (50 µM). The inhibitory action was also abolished upon UV illumination.

Photochromic ligand **26** showed also similar effects on α_1 human GlyRs like described for α_1 zebrafish GlyRs. The currents evoked by 30 µM of glycine were inhibited to 85 ± 4% under visible light and to 72 ± 2% upon UV illumination (n = 4, Figure 8a and c).
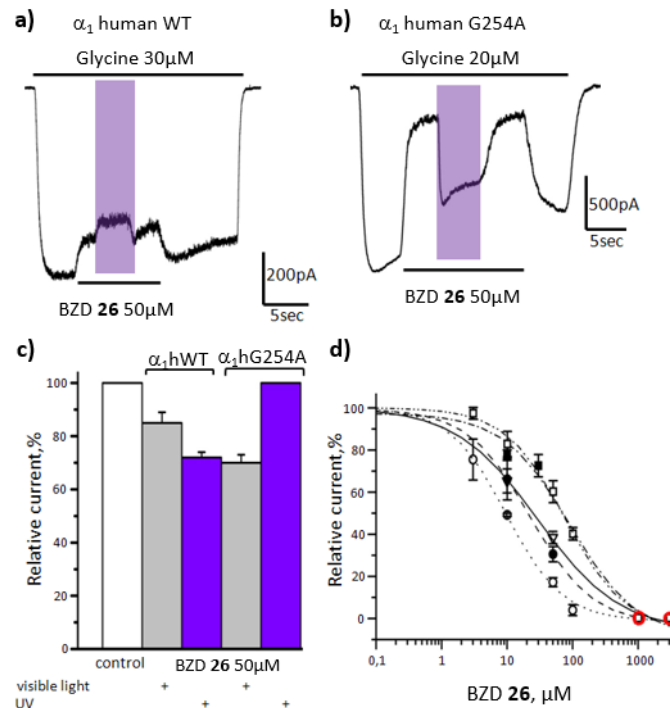
Figure 8. a) Representative trace of the current mediated by wild type α_1 human GlyRs. The current was evoked by application of 30 µM of glycine, application of a mixture of glycine 30 µM + compound **26** 50 µM started at 5th second of the registration and finished at the 15th second. Duration of UV illumination from the 8th until the 10th second of registration is indicated by the violet rectangle. **b)** Representative trace of the current mediated by mutant G254A α_1 human GlyRs. The current was evoked by application of 20 µM of glycine, application of a mixture of glycine 20 µM + compound **26** 50 µM started at the 5th second of registration and finished at the 20th second. Duration of UV illumination from the 10th until the 15th second of registration is indicated by the violet rectangle. **c)** Relative amplitudes of the currents mediated by WT and mutant α_1 GlyRs in control (white column), during application of BZD **26** 50 µM (gray columns) and upon UV illumination (violet columns). **d)** IC$_{50}$ values of azo benzodiazepine **26** for α_1 human (91 µM, filled rectangle, dashed/dotted line); α_1 zebrafish (76 µM, empty rectangle, dashed/dotted/dotted line); α_2 mouse (22 µM, empty circle, dashed line); α_2 zebrafish (10 µM, filled circle, dotted line) and α_3 human (29 µM, triangle, solid line) GlyRs.

Interestingly, compound **26** exhibited opposite effects on α_1 and α_2 GlyRs upon UV illumination. Moreover, it was active at α_2 receptors activated by a saturating concentration of the agonist glycine whereas it was not active at α_1 receptors activated by a saturating concentration of the agonist. This fact suggests that azo benzodiazepine **26** acts as a pore blocker of α_2 GlyRs and as a competitive antagonist of α_1 human receptors. To further prove this hypothesis the effect of compound **26** on α_1 human

mutant G254A GlyRs was investigated. The mutation is located in the TM2 domain of the receptor which forms the pore of the ion channel and the mutation transforms the ion pore of α_1 receptors to the ion pore of the α_2 receptors.

The receptors formed by the mutant G254A α_1 GlyRs responded to the application of compound **26** and UV illumination similarly to α_2 GlyRs (Figure 8b) and in a different way compared to α_1 wild type GlyRs (Figure 8c). As depicted, the currents mediated by α_1 wild type GlyRs were inhibited to 85 ± 4% under visible light and to 72 ± 2% upon UV illumination (n = 4) whereas the currents mediated by mutant α_1 G254A GlyRs were inhibited by photochromic benzodiazepine **26** (50 µM) in visible light to 70 ± 3% (n = 7) and this effect was completely abolished upon UV illumination. The dose response curves to determine the IC$_{50}$ values of azo benzodiazepine **26** for α_1 human (91 µM), α_1 zebrafish (76 µM), α_2 mouse (22 µM), α_2 zebrafish (10 µM) and α_3 human (29 µM) Gly-receptors are shown in Figure 8d.

In summary, photochromic ligand **26** inhibits the pore of GABA$_A$ as well as α_2 zebrafish, α_2 mouse, α_2 human and α_3 human Gly-receptors in *trans* configuration. In *cis* configuration compound **26** loses this ability and its inhibitory effect. Apart from that compound **26** acts as a competitive antagonist on α_1 zebrafish as well as α_1 human GlyRs and its inhibitory activity increases upon UV illumination.

Azo benzodiazepine **29** showed similar effects on all subunits of the tested Gly-receptors (α_1 human, α_2 mouse and α_3 human). In *trans* configuration it inhibited the glycine induced currents. For α_1 GlyRs it was reduced by 9 ± 4% (n = 3), for α_2 by 38 ± 7% (n = 4) and for α_3 by 22 ± 7% (n = 2). Upon UV illumination the strength of the inhibition increased and comprised. The currents were reduced by 33 ± 6% for α_1 GlyRs, by 73 ± 6% for α_2 and by 41 ± 9% for α_3 compared to the control (Figure 9). With increasing glycine concentration the inhibitory effect of compound **29** decreased, suggesting a competitive mechanism of the antagonistic action.
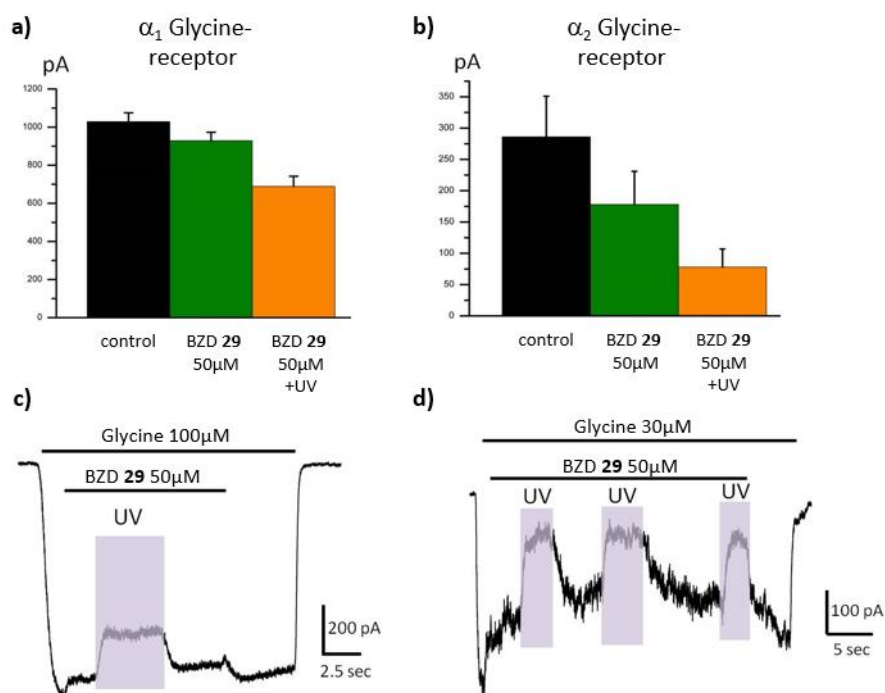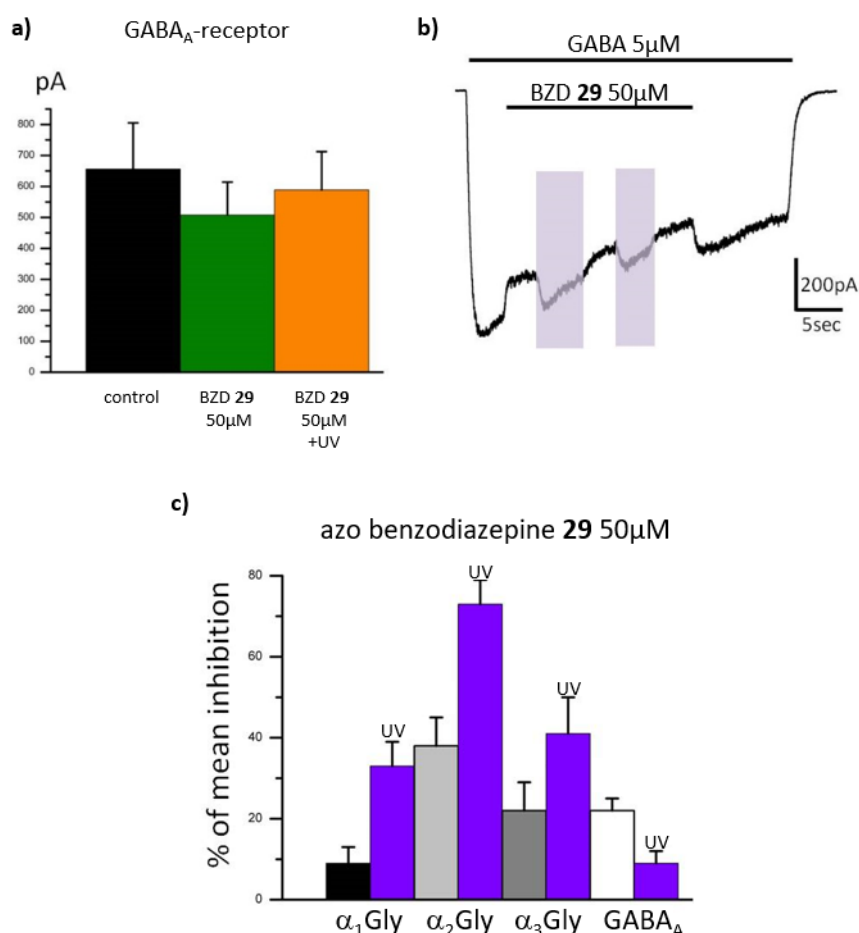
Figure 9. a) Mean amplitudes of glycine (100 µM) induced currents mediated by α_1 GlyRs in control (black), upon application of 50 µM azo benzodiazepine **29** (green) and during UV illumination (orange, n = 3). **b)** Mean amplitudes of glycine (30 µM) induced currents mediated by α_1 GlyRs in control (black), upon application of 50 µM azo benzodiazepine **29** (green) and during UV illumination (orange, n = 4). **c)** Representative trace of the current mediated by α_1 GlyRs. The durations of glycine (100 µM) and compound **29** (50 µM) applications are indicated by bars above the trace. The UV illumination is indicated by the violet rectangle. **d)** Representative trace of the current mediated by α_2 GlyRs. The durations of glycine (30 µM) and compound **29** (50 µM) applications are indicated by bars above the trace. The UV illumination is indicated by the violet rectangles.

Compound **29** showed also an inhibitory effect on the currents evoked by GABA in $\alpha_1\beta_2\gamma_2$ GABA$_A$-receptors. However, irradiation with UV light led to a decreased inhibition in contrast to all the GlyRs (Figure 10a and b). Figure 10c summarizes the mean inhibition values of azo benzodiazepine **29** for all investigated receptors both with and without UV illumination. Further electrophysiological investigations with compound **29** are still ongoing.

Azo benzodiazepine **30** had a minor inhibitory effect on GABA$_A$Rs and showed almost no UV-dependent activity (Figure 11). It was not active at α_1 human GlyRs but further investigations are accomplished.

Figure 10. a) Mean amplitudes of GABA (5 µM) induced currents mediated by $\alpha_1\beta_2\gamma_2$ GABA$_A$-receptors in control (black), upon application of 50 µM azo benzodiazepine **29** (green) and during UV illumination (orange, n = 3). **b)** Representative trace of the current mediated by $\alpha_1\beta_2\gamma_2$ GABA$_A$-receptors**.** The durations of GABA (5 µM) and compound **29** (50 µM) applications are indicated by bars above the trace. The UV illumination is indicated by the violet rectangles. **c)** Comparison of the mean inhibition (percentage) of α_1 Gly (black column), α_2 Gly (light gray), α_3 Gly (gray) and GABA$_A$ (white) receptors mediated currents by azo benzodiazepine **29** in *trans* configuration and upon UV irradiation (violet columns).
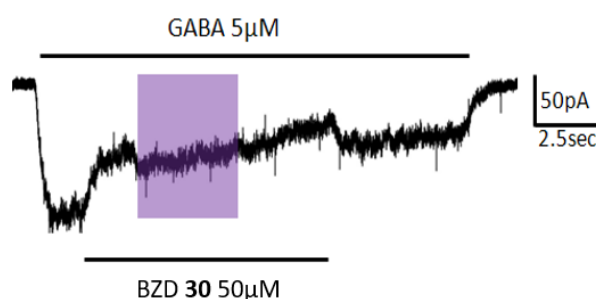
Figure 11. Representative trace of the current mediated by $\alpha_1\beta_2\gamma_2$ GABA$_A$-receptors**.** The durations of GABA (5 µM) and compound **30** (50 µM) applications are indicated by the bars above and below the trace. The UV illumination is indicated by the violet rectangle.

Preliminary investigations with benzodiazepine **27** resulted in a much lower detected activity on all tested ion channels. Therefore, it is supposed that the sulfonic acid group of compound **26** plays a crucial role for the interaction with the pores, but further experiments with compound **27** are necessary to confirm the obtained results. The electrophysiological effects of photochromic ligands **31**, **32**, **51**, and **53** are also currently investigated.

In vivo characterization[B]

Next, the photochromic ligands were tested in living animals to evaluate light-dependent responses in their behavior. First, we chose zebrafish larvae (*Danio rerio*, Tupfel long strain) as model animal and a behavioral assay to monitor the zebrafish activity was developed. The activity was measured as swum distance in millimeters during large activity periods in which the animal speed is higher than six millimeters per second. The distances or activity in all data and graphs are given as cumulative intense activity periods within one minute. Zebrafish larvae have naturally cyclic periods of low and high speed movements when they are unstressed. After applying the respective treatment with the photochromic ligands (100 µM diluted stock solutions of the *trans* isomers in DMSO) to the animals they were kept in the dark for 20 minutes without light changes or external mechanic stimuli (relaxation period). Then they were exposed to UV and blue light cycles for in total twelve minutes with alternating continuous illumination with 365 nm and 455 nm for two minutes, respectively. The corresponding tracking of the activity over time is depicted in Figure 12.


[B] All *in vivo* experiments were carried out in the group of Prof. Dr. Pau Gorostiza by Alexandre Gomila and Dr. Núria Camarero at the Institute of Bioengineering of Catalonia, Barcelona, Spain.
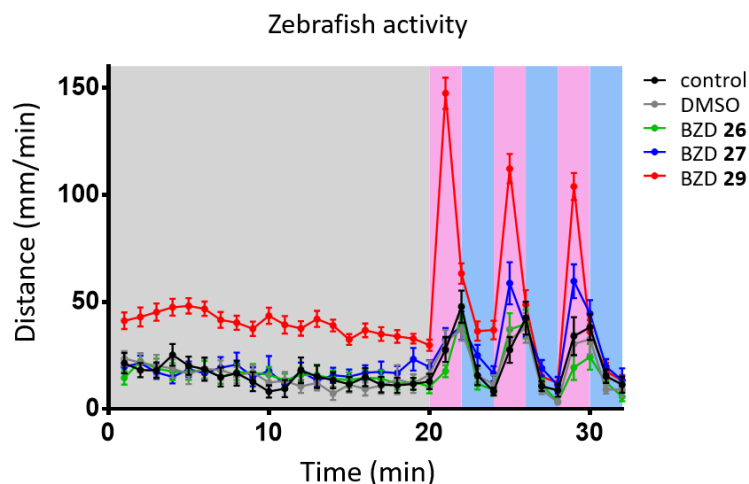
Figure 12. Experimental zebrafish activity over time for control (without any treatment, black), DMSO (1%, gray) and treatments with azo benzodiazepines **26** (100 µM, green), **27** (100 µM, blue) and **29** (100 µM, red). Dark conditions are drawn with gray background, UV illumination with violet and blue light illumination with blue background.

Among the three tested photochromic ligands **26**, **27** and **29** only compound **29** shows a clear excitatory effect onto zebrafish behavior. During the initial relaxation period under dark conditions the animals do not return to their natural activity levels and remain in an excitatory state (Figure 13a). Therefore, we assume that the *trans* isomer of azo compound **29** has an overall antagonistic effect to the inhibitory pathways in zebrafish. Under UV illumination (365 nm) an overreaction with permanent high speed movements during the first minute of irradiation is observed in every cycle due to the blockade of the inhibitory pathways by the *trans* isomer of compound **29**. This excitatory state decreased during the second minute of UV illumination because most of the *trans* isomer is converted to the *cis* isomer (PSS of 80% at 365 nm see Table 1, entry 6) which seems to be inactive *in vivo*. This behavior in the second minute under UV illumination is reversed to the activity observed for the control animals as they get continuously more active in the two minutes of UV illumination. Under each cycle of blue light irradiation all animals return to levels of their basal activity while compound **29** isomerizes back from its *cis* to the active *trans* isomer (PSS of 84% at 455 nm see Table 1, entry 6). Therefore, the animals under treatment of **29** again overreact in the next cycle of UV illumination. However, the overall activity from the second UV cycle is always reduced compared to the first one until a plateau (approximately in the third UV cycle) is reached because the back isomerization with visible light to the *trans* isomer is always incomplete. Nevertheless, the maintaining

levels of overreaction in the following UV cycles are significantly higher than the control levels. Combining the higher inhibitory effect of the *trans* isomer *in vivo* with the results from electrophysiological measurements supposes that the *in vivo* activity of compound **29** results mainly from acting on the zebrafish glycine-receptors. Interestingly, by reducing the concentration of compound **29** to 50 µM (not shown in Figure 12) its excitatory effect completely vanished and activity levels were similar to them of treatments with 100 µM of **26** or **27**. The total activities under UV as well as blue light illumination of all investigated treatments are depicted in Figure 13b and c indicating with Figure 13a that compounds **26** and **27** do not have an *in vivo* activity as their activity levels are always in the range of the activity of the control animals.
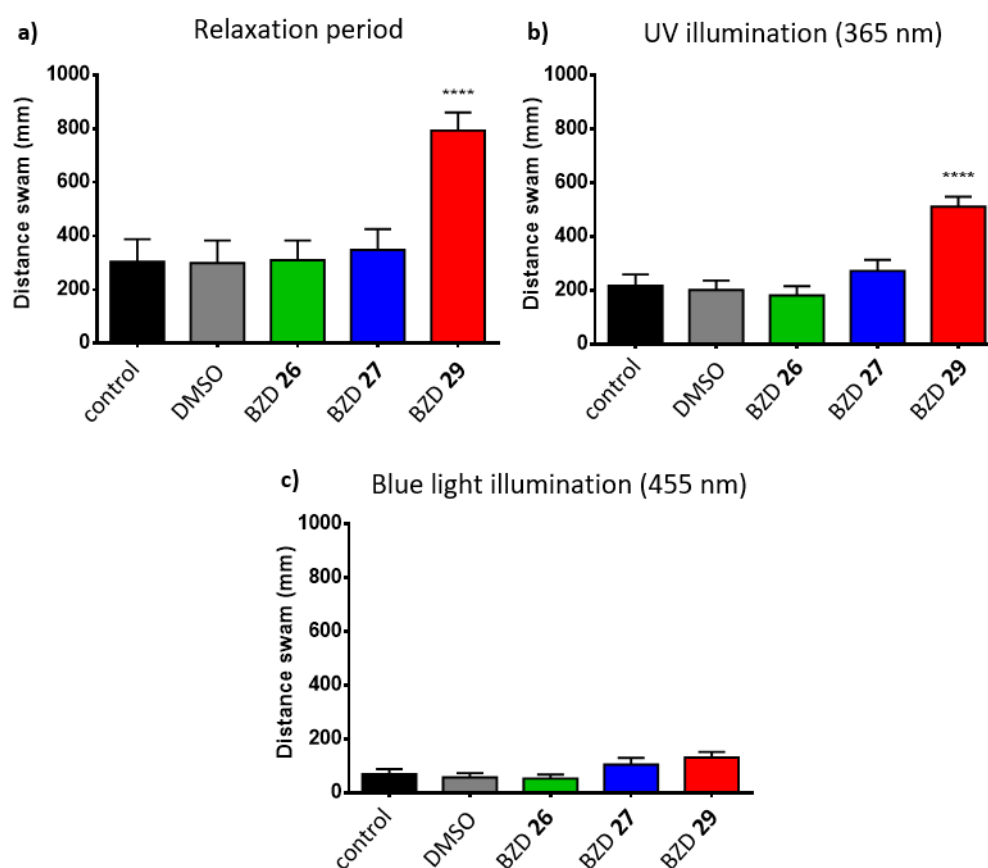
Figure 13. Total activity during the 20 minutes of relaxation period (**a**), six minutes of UV illumination (three cycles of two minutes illumination with 365 nm, **b**) and six minutes of blue light illumination (three cycles of two minutes illumination with 455 nm, **c**) for control (without any treatment, black), DMSO (1%, gray) and treatments with azo benzodiazepines **26** (100 µM, green), **27** (100 µM, blue) and **29** (100 µM, red).

The *in vivo* inactivity of azo benzodiazepine **26** which is in contradiction to its determined electrophysiological effects *in vitro* could be explained by its opposite effects under UV light to the main inhibitory ligand-gated receptors GABA$_A$ and α_1 Gly. Further experiments are performed to investigate this discrepancy. Due to the moderate effects of compound **30** in electrophysiology and a similar inactivity in zebrafish larvae like compound **26** in preliminary assays it was neglected for further experiments. The light-dependent effect of photochromic ligands **31**, **32**, **51** and **53** will also be investigated in zebrafish larvae after their electrophysiological evaluation is completed. In addition, further and more complex zebrafish assays for the investigation of other changes in behavior than the swum distance by treatment with our photochromic ligands will be developed.

In a second approach the photochromic ligands **26**, **29** and **30** were also investigated in tadpoles from *Xenopus tropicalis* in the same manner like described for zebrafish larvae. However, all treatments caused no significant effect in the behavior and activity of the tadpoles.

Molecular docking[C]

In order to rationalize the observed *in vitro* activities docking of benzodiazepine **26** in two different conformations[69] of the seven membered ring each in *trans* and *cis* configuration of the azo group to GABA$_A$R and the different subtypes of GlyRs was carried out.

First, the *trans* isomer of compound **26** was docked in the classical benzodiazepine binding site between the α and γ subunits of a GABA$_A$R homology model[70] to compare its binding with diazepam. As depicted in Figure 14 the binding of **26** on this site is very unfavored and therefore the docking also suggests another mode of action as pore blocker like already assumed from the electrophysiological data.

[C] All molecular docking experiments were performed in the group of Prof. Dr. Carme Rovira by Alba Nin-Hill and Dr. Mercedes Alfonso-Prieto at the University of Barcelona, Spain.
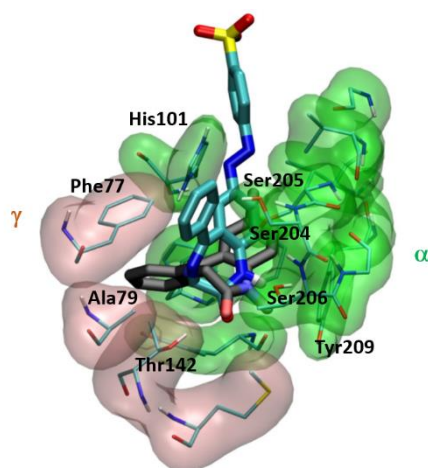
Figure 14. Comparison of the binding mode of the *trans* isomer of azo benzodiazepine **26** (cyan) and diazepam (black) in the classical benzodiazepine binding site between the α and γ subunits of the GABA$_A$-receptor.

Azo benzodiazepine **26** was then docked to the human α_1 and α_3 GlyRs whose crystal structures were recently solved and published.[15, 71] The dockings on the closed α_1 and α_3 human GlyRs revealed that both photoisomers of benzodiazepine **26** are able to bind to the pores and block them, occupying the $T^{6'}$, $G^{2'}$ or $A^{2'}$ and $P^{-2'}$ region of the receptor, respectively. However, the binding of the *cis* isomer of azo benzodiazepine **26** is less favored because the negatively charged sulfonic acid moieties are located in the nonpolar $G^{2'}$ and $A^{2'}$ position, respectively. In contrast, the *trans* isomer is able to form hydrogen bonds in the $T^{6'}$ position and the charge of the sulfonic acid group points to the solvent (Figure 15). On the one hand these results for the α_1 subtype are in accordance with the experimental *in vitro* data that both *trans* and *cis* isomer of azo benzodiazepine show inhibitory effects on this receptor. On the other hand they cannot explain the loss of inhibition on the α_3 subtype of the *cis* isomer of compound **26**. We can only hypothesize that the extra methyl group being present in α_3-Ala2' compared to α_1-Gly2' makes this position more apolar and thus the binding of the sulfonic acid moiety of azo benzodiazepine **26** less favored which could unblock the closed pore.

A docking of the two photoisomers of compound **26** to the open human α_1 and α_3 GlyRs showed that at least two molecules of **26** are needed to block the pore. For the α_1 subtype all possible poses with two *cis* isomers of **26** block the pore whereas only some possible poses for the *trans* isomers. These findings are in good agreement with the experimental results. For the human α_3 subtype the preliminary results are not so clear because there

are possible poses for two molecules of both isomers which block as well as do not block the pore. Further simulations for the open receptors are ongoing.
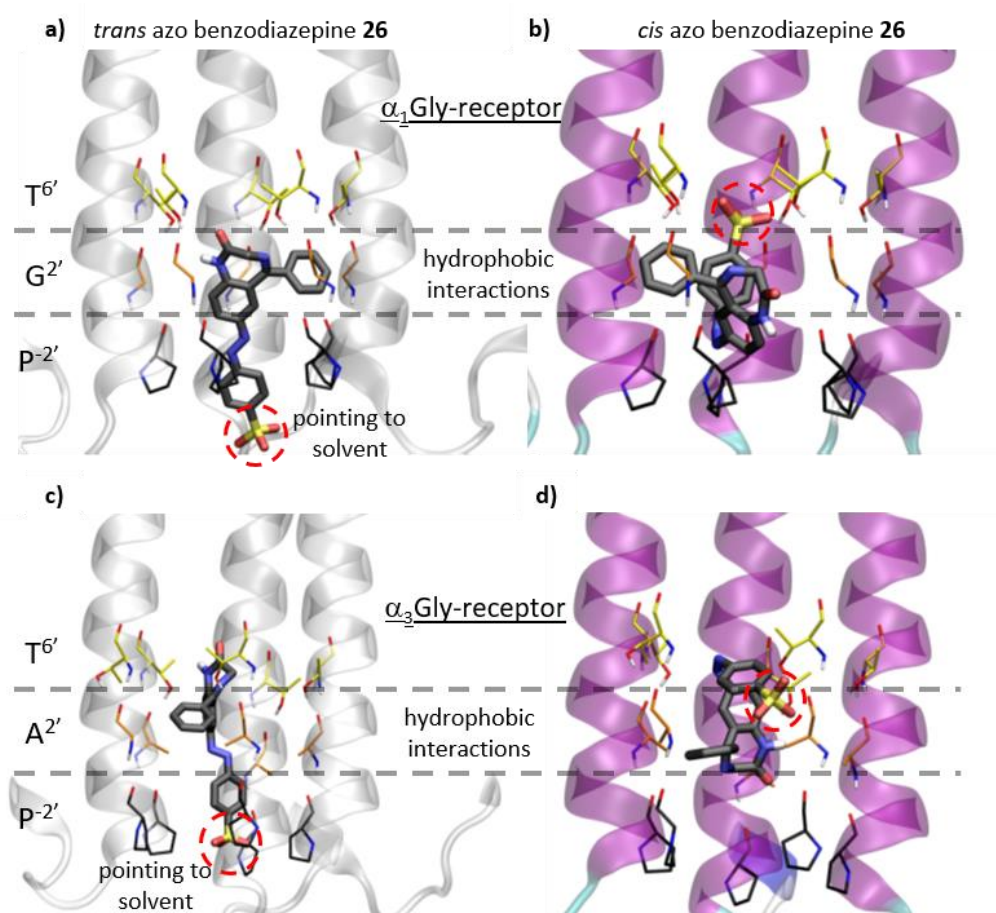
Figure 15. Dockings of azo benzodiazepine **26** to the α_1 human glycine-receptor (**a**: *trans* isomer; **b**: *cis* isomer) as well as to the α_3 human glycine-receptor (**c**: *trans* isomer; **d**: *cis* isomer).

Finally, a docking in which azo benzodiazepine **26** was allowed to explore all the α_3 GlyR (both the extracellular and the transmembrane domains) was performed. Thereby some poses of *trans* as well as *cis* azo benzodiazepine **26** are located in the novel pocket recently found by Huang *et al*. (Figure 16).[72] However, their calculated docking scores are much worse compared to reference compound AM3607 and therefore we suppose that the most favorable binding mode is in the T$^{6'}$, A$^{2'}$ and P$^{-2'}$ region of the α_3 receptor.
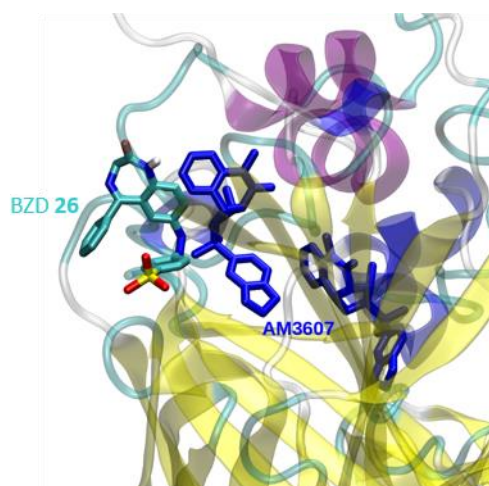
Figure 16. Comparison of the binding of azo benzodiazepine **26** and reference compound **AM3607** at the recently discovered novel binding site of the α_3 GlyR.[72]

3.3 Conclusion

In summary, we merged structural elements of nitrazepam and nicardipine, which are well-known pharmacophores, with photoswitchable azobenzenes to yield photochromic ligands for modulation of $GABA_A$ and glycine-receptors by light. A small series of azo benzodiazepines was synthesized by using Mills reactions of 7-amino nitrazepam with different nitroso precursors as the synthetic key step. The low water solubility of one of the obtained target compounds could successfully be increased by post-functionalization. The azo nicardipines were synthesized by esterification of the basic dihydropyridine core with different hydroxyl substituted azo switches. The photochromic properties of all prepared ligands were excellent with very good fatigue resistance and high photostationary states in DMSO as well as aqueous phosphate buffer. The electrophysiological investigations of the first benzodiazepine derivatives identified one very promising compound. It acts as an UV sensitive blocker of $GABA_A$-receptors which loses its inhibitory effect upon irradiation. Simultaneously, it shows subtype specific effects on glycine-receptors. On the one hand it lost also its ability to block the channels under illumination on all tested α_2 and α_3 glycine-receptors from different species. On the other hand the inhibitory effect on subtype α_1 glycine-receptors was even increased under irradiation. A further molecule showed weaker, but similar effects in electrophysiology, but no subtype specific effects on the different glycine-receptors. However, only the latter compound exhibited significant influence on the activity of

zebrafish larvae *in vivo*. Preliminary assays indicate that the *trans* isomer operates as an excitatory drug with an overall antagonistic effect on the inhibition pathways of zebrafish. Therefore, the fishes overreact to external stimuli which can be measured by their higher activity and faster movements. This overreaction is lost by photoisomerizing the compound to the *cis* isomer. Molecular dockings could partly rationalize the *in vitro* activity of the most active compound, but more detailed calculations have to be carried out to get a better insight into the mode of action on the particular receptors.

3.4 Experimental

3.4.1 Chemistry

Compounds **2**,[47] **3**,[46] **5**,[59] **6**,[47] **11**,[51] **12**,[51] **15**,[52] **17**,[53] **18**,[54] **20**,[55] **21**,[55] **24**,[56] **25**,[57] **38**,[59] **42**[60] and **46**[62] were synthesized according to reported or adapted procedures. Commercial reagents and starting materials were purchased from Acros Organics, Alfa-Aesar, Fisher Scientific, Sigma Aldrich or VWR and used without any further purification. Solvents were used in p.a. quality and dried according to common procedures, if necessary. Commercially PBS (pH = 7.4) was used for investigations of the photochromic properties. Dry nitrogen was used as inert gas atmosphere. Microwave-assisted reactions were performed in an Anton Paal Monowave 400 microwave. A Biotage Isolera flash purification system with UV/Vis detector using Sigma Aldrich MN silica gel 60 M (40-63 µm, 230-400 mesh) for normal phase or pre-packed Biotage SNAP cartridges (KP C18 HS) for reversed phase chromatography was used for automated flash column chromatography. Reaction monitoring via TLC and determination of R$_f$ values was accomplished on alumina plates coated with silica gel (Merck silica gel 60 F254, 0.2 mm). Melting points were measured with a Stanford Research Systems OptiMelt MPA 100 device and are uncorrected. NMR spectra were measured on Bruker Avance 300 (^{1}H 300.13 MHz, ^{13}C 75.48 MHz), Bruker Avance 400 (^{1}H 400.13 MHz, ^{13}C 100.61 MHz) and Bruker Avance III 600 (^{1}H 600.25 MHz, ^{13}C 150.95 MHz) instruments. The spectra are referenced against the NMR-solvent (DMSO-d_6: δ_H = 2.50 ppm, δ_C = 39.52 ppm, MeOH-d_4: δ_H = 4.87 ppm, δ_C = 49.00 ppm, D$_2$O: δ_H = 4.79 ppm) and chemical shifts δ are reported in ppm. Resonance multiplicity is abbreviated as: s (singlet), d (doublet), t (triplet), q

(quartet), m (multiplet) and b (broad). Carbon NMR signals are reported using DEPT 135 and ^{1}H-^{13}C HSQC spectra with (+) for primary/tertiary, (−) for secondary and (q) for quaternary carbons. An Agilent Q-TOF 6540 UHD (ESI-MS) instrument was used for recording mass spectra. UV/Vis absorption spectroscopy was accomplished using a Varian Cary BIO 50 UV/Vis spectrometer in 10 mm quartz cuvettes. IR-spectra were recorded on an Agilent Cary 630 FT-IR spectrometer and the peak positions are reported in wavenumbers (cm^{-1}). Analytical HPLC measurements were performed on an Agilent 1220 Infinity LC (column: Phenomenex Luna 3 μM C18(2) 100 Å, 150 x 2.00 mm; flow: 0.3 mL/min at 30 °C; solvent A: MilliQ water with 0.05 % vol. TFA; solvent B: MeCN). The ratios in the PSSs were determined by HPLC measurements with a detection wavelength at the isosbestic points or by ^{1}H-NMR-spectroscopy with direct irradiation inside the NMR tube during the measurements. For determination of the thermal half-lives the solutions were irradiated until the photostationary state was reached. Then the solutions were left at 25 °C and the recovery of the absorbance of the *trans* isomer at λ_{max} was measured. Consequently, the thermal half-life was calculated by fitting the data with a single exponential function. An Agilent 1260 system (column: Phenomenex Luna 10 μM C18(2) 100 Å, 250 x 21.2 mm; flow: 22.0 mL/min at room temperature; solvent A: MilliQ water with 0.05 % vol. TFA; solvent B: MeCN) was used for preparative HPLC purification. Light sources for irradiation: λ = 365 nm (Herolab hand-held lamp UV-6 L, 6 W), λ = 385 nm (NICHIA NCSU034B, 500 mA, 21 mW) λ = 455 nm (OSRAM Oslon SSL 80 LED, 700 mA, 1.12 W), λ = 530 nm (CREE-XP green LED, 700 mA, 3.7 W), λ = 590 nm (OSRAM Oslon SSL 80 LED, 700 mA, 1.12 W). The power of the light is given based on the specifications supplied by the company when the lamps were purchased. If not otherwise stated, final compounds for biological testing possess a purity ≥95% determined by HPLC measurements with detection at 220 nm and 254 nm.

7-Amino-5-phenyl-1,3-dihydro-2*H*-benzo[*e*][1,4]diazepin-2-one (6)

Nitrazepam (**3**) (149 mg, 0.53 mmol) was dissolved in MeOH (15 mL) and hydrogenated using Pd/C (9 mg, 10 wt. % Pd) in an autoclave (2 bar of H$_2$) at room temperature for 45 min. The mixture was centrifuged, filtered over celite and the solvent was removed *in vacuo*. The residue was purified by automated reversed phase flash column

chromatography (PE/CH$_2$Cl$_2$ with 1% Et$_3$N, 70% - 100% CH$_2$Cl$_2$ with 1% Et$_3$N) yielding **6** (130 mg, 99%) as yellow solid. An analytical sample was crystallized from Et$_2$O with a minimal amount of MeOH. Samples for biological testing were further purified by preparative HPLC (2% - 30% MeCN in 15 min, t$_R$ = 9.1 min) affording the corresponding trifluoroacetate salt. ^{1}H-NMR (300 MHz, DMSO-d_6) δ = 10.03 (s, 1H), 7.56 − 7.36 (m, 5H), 6.93 (d, J = 8.6 Hz, 1H), 6.77 (dd, J = 8.6, 2.5 Hz, 1H), 6.39 (d, J = 2.4 Hz, 1H), 5.16 (s, 2H), 4.05 (bs, 2H); ^{13}C-NMR (75 MHz, DMSO-d_6) δ = 170.0 (q), 169.6 (q), 144.0 (q), 139.4 (q), 129.9 (+), 129.2 (+), 128.1 (+), 127.2 (+), 122.0 (+), 118.0 (+), 113.5 (+), 57.0 (−); HRMS (ESI) calcd. for C$_{15}$H$_{14}$N$_3$O (M+H)$^+$ m/z = 252.1131; found 252.1134.

N,N,N-Triethyl-3-(7-nitro-2-oxo-5-phenyl-2,3-dihydro-1*H*-benzo[*e*][1,4]diazepin-1-yl) propan-1-aminium (8)

Nitrazepam (101 mg, 0.36 mmol, 1.0 eq.), **49** (164 mg, 0.54 mmol, 1.5 eq.) and K$_2$CO$_3$ (159 mg, 1.15 mmol, 3.2 eq.) were suspended in DMF (3.3 mL) and heated to 80 °C for 7.5 min in a microwave reactor. After removing K$_2$CO$_3$ by filtration the solvent was evaporated *in vacuo*. The residue was purified by automated flash column chromatography (CH$_2$Cl$_2$/MeOH, 3% - 30% MeOH) and subsequent preparative HPLC (70% - 98% MeCN in 9 min, 98% MeCN for further 6 min, t$_R$ = 10.3 min) yielding compound **8** bromide (119 mg, 66%) as yellow solid. R$_f$ 0.07 (CH$_2$Cl$_2$/MeOH 9:1); m.p. 144 °C; ^{1}H-NMR (300 MHz, MeOH-d_4) δ = 8.52 (dd, J = 9.1, 2.7 Hz, 1H), 8.17 (d, J = 2.7 Hz, 1H), 7.86 (d, J = 9.1 Hz, 1H), 7.73 − 7.66 (m, 2H), 7.65 − 7.57 (m, 1H), 7.57 − 7.46 (m, 2H), 4.73 (d, J = 11.0 Hz, 1H), 4.34 (dt, J = 13.7, 6.6 Hz, 1H), 4.08 − 3.87 (m, 2H), 3.27 − 2.96 (m, 8H), 2.15 (dtt, J = 6.2 Hz, 1H), 1.96 (dtt, J = 6.1 Hz, 1H), 1.12 (t, J = 7.2 Hz, 9H); ^{13}C-NMR (75 MHz, MeOH-d_4) δ = 171.3 (q), 171.2 (q), 148.9 (q), 145.1 (q), 138.6 (q), 132.9 (+), 131.0 (q), 130.8 (+), 130.0 (+), 127.8 (+), 127.1 (+), 125.1 (+), 57.7 (−), 55.6 (−), 54.0 (−), 46.2 (−), 21.9 (−), 7.5 (+); IR (neat) ν = 3086, 2997, 1774, 1737, 1681, 1610, 1525, 1484, 1450, 1420, 1346, 1185, 1133, 1003, 913, 842, 783, 701 cm^{-1}; HRMS (ESI) calcd. for C$_{24}$H$_{31}$N$_4$O$_3$ M$^+$ m/z = 423.2391; found 423.2401.

(*E*)-4-((2-Oxo-5-phenyl-2,3-dihydro-1*H*-benzo[*e*][1,4]diazepin-7-yl)diazenyl)benzene-sulfonic acid (26)

A 1:1 mixture of tetrabutylammonium 4-nitrosobenzenesulfonate and its corresponding nitro derivative (236 mg, 0.54 mmol, 1.0 eq. of nitroso compound) was added to a solution of benzodiazepine **6** (68 mg, 0.27 mmol, 1.0 eq.) in acetic acid (2 mL) and CH_2Cl_2 (1 mL). After stirring the mixture for 24 h at room temperature the solvent was removed *in vacuo*. Purification by automated flash column chromatography (CH_2Cl_2/MeOH, 3% - 25% MeOH) and subsequent preparative HPLC (2% - 65% MeCN in 10 min, t_R = 7.2 min) yielded **26** (69 mg, 61%) as yellow solid. R_f 0.03 (CH_2Cl_2/MeOH 9:1); m.p. 280 °C (decomposition); ^{1}H-NMR (600 MHz, DMSO-d_6) δ = 11.32 (s, 1H), 8.23 (dd, *J* = 8.8, 2.4 Hz, 1H), 7.81 − 7.78 (m, 2H), 7.77 − 7.73 (m, 3H), 7.68 (t, J = 7.4 Hz, 1H), 7.64 (dd, J = 8.3, 1.3 Hz, 2H), 7.57 (t, J = 7.7 Hz, 2H), 7.52 (d, J = 8.9 Hz, 1H), 4.34 (s, 2H); ^{13}C-NMR (151 MHz, DMSO-d_6) δ = 172.5 (q), 168.9 (q), 151.4 (q), 151.1 (q), 146.5 (q), 143.0 (q), 135.8 (q),132.5 (+), 130.7 (+), 128.8 (+), 128.6 (+), 126.8 (+), 126.2 (+), 124.4 (q), 122.9 (+), 122.2 (+), 54.6 (−); IR (neat) ν = 3489, 3135, 2930, 1715, 1614, 1484, 1435, 1387, 1342, 1230, 1163, 1115, 1029, 1006, 846, 742, 697 cm^{-1}; HRMS (ESI) calcd. for $C_{22}H_{16}N_4O_4S$ (M+H)$^+$ m/z = 421.0965; found 421.0964.

(*E*)-4-((2-Oxo-5-phenyl-2,3-dihydro-1*H*-benzo[*e*][1,4]diazepin-7-yl)diazenyl)benzene-sulfonamide (27)

Freshly prepared 4-nitrosobenzenesulfonamide (238 mg, 1.38 mmol, 3.0 eq.) was added to a solution of benzodiazepine **6** trifluoroacetate salt (168 mg, 0.46 mmol, 1.0 eq.) in CH_2Cl_2 (6 mL) and acetic acid (2 mL). After stirring the mixture for 24 h at 40 °C the solvent was removed *in vacuo*. The residue was purified by automated flash column chromatography (CH_2Cl_2/MeOH, 3% - 10% MeOH) yielding compound **27** (140 mg, 73%) as orange solid. Material for analytical characterization as well as for biological testing was further purified by preparative HPLC (10% - 75% MeCN in 18 min, t_R = 11.1 min). R_f 0.14 (CH_2Cl_2/MeOH 97:3); m.p. 207 °C; ^{1}H-NMR (400 MHz, DMSO-d_6) δ = 11.08 (s, 1H), 8.16 (dd, *J* = 8.8, 2.3 Hz, 1H), 7.98 (s, 4H), 7.79 (d, *J* = 2.3 Hz, 1H), 7.58 − 7.46 (m, 8H), 4.27 (s, 2H); ^{13}C-NMR (101 MHz, DMSO-d_6) δ = 170.1 (q), 169.8 (q), 153.2 (q), 146.2 (q), 146.0 (q) 143.0 (q), 138.0 (q), 131.1 (q), 129.7 (+), 128.5 (+), 127.8 (+), 127.1 (+), 126.1 (q), 124.9 (+),

123.0 (+), 122.6 (+), 56.5 (−); IR (neat) ν = 3243, 3071, 1700, 1674, 1610, 1484, 1390, 1334, 1200, 1163, 1014, 902, 842, 798, 746, 697 cm^{-1}; HRMS (ESI) calcd. for C$_{21}$H$_{18}$N$_5$O$_3$S (M+H)$^+$ m/z = 420.1133; found 420.1125.

(_E_)-_N_-Methyl-4-((2-oxo-5-phenyl-2,3-dihydro-1_H_-benzo[_e_][1,4]diazepin-7-yl)diazenyl) benzenesulfonamide (28)

_N_-Methyl-4-nitrosobenzenesulfonamide (120 mg, 0.60 mmol, 2.0 eq.) was added to a solution of benzodiazepine **6** trifluoroacetate salt (110 mg, 0.30 mmol, 1.0 eq.) in CH$_2$Cl$_2$ (3 mL) and acetic acid (1 mL). After stirring the mixture for 24 h at room temperature the solvent was removed _in vacuo_. The residue was purified by automated flash column chromatography (CH$_2$Cl$_2$/MeOH, 3% - 10% MeOH) and subsequent preparative HPLC (10% - 98% MeCN in 15 min, t$_R$ = 9.4 min) affording compound **28** (85 mg, 65%) as orange solid. R$_f$ 0.24 (CH$_2$Cl$_2$/MeOH 97:3); m.p. 252 °C; ^{1}H-NMR (300 MHz, DMSO-d_6) δ = 11.08 (s, 1H), 8.17 (dd, _J_ = 8.8, 2.3 Hz, 1H), 8.05 − 7.89 (m, 4H), 7.79 (d, _J_ = 2.3 Hz, 1H), 7.64 (q, _J_ = 4.9 Hz, 1H), 7.59 − 7.54 (m, 3H), 7.53 − 7.44 (m, 3H), 4.27 (s, 2H), 2.44 (d, _J_ = 4.9 Hz, 3H); ^{13}C-NMR (101 MHz, DMSO-d_6) δ = 170.1 (q), 169.7 (q), 153.5 (q), 146.2 (q), 143.1 (q), 141.2 (q), 138.0 (q), 131.0 (q), 129.7 (+), 128.5 (+), 128.1 (+), 127.8 (+), 126.1 (q), 124.9 (+), 123.2 (+), 122.5 (+), 56.5 (−), 28.6 (+); IR (neat) ν = 3094, 2937, 1674, 1610, 1484, 1390, 1331, 1234, 1200, 1163, 1092, 1014, 842, 783, 742, 697 cm^{-1}; HRMS (ESI) calcd. for C$_{22}$H$_{20}$N$_5$O$_3$S (M+H)$^+$ m/z = 434.1288; found 434.1281.

(_E_)-5-Phenyl-7-(pyridin-2-yldiazenyl)-1,3-dihydro-2_H_-benzo[_e_][1,4]diazepin-2-one (29)

2-Nitrosopyridine (108 mg, 1.00 mmol, 2.0 eq.) was added to a solution of benzodiazepine **6** (126 mg, 0.50 mmol, 1.0 eq.) in CH$_2$Cl$_2$ (3 mL) and acetic acid (1 mL). After stirring the mixture for 24 h at room temperature the solvent was removed _in vacuo_. The residue was purified by automated reversed phase flash column chromatography (MeCN/H$_2$O with 0.05% TFA, 5% - 100% MeCN) and subsequent preparative HPLC (10% - 60% MeCN in 20 min, t$_R$ = 13.4 min) yielding compound **29** (125 mg, 73%) as yellow solid. R$_f$ 0.63 (CH$_2$Cl$_2$ + 1% Et$_3$N/MeOH 9:1); m.p. 222 °C; ^{1}H-NMR (600 MHz, DMSO-d_6) δ = 10.98 (s, 1H), 8.67 (ddd, _J_ = 4.7, 1.8, 0.8 Hz, 1H), 8.17 (dd, _J_ = 8.7, 2.3 Hz, 1H), 8.00 (ddd, _J_ = 8.1, 7.4, 1.8 Hz, 1H), 7.79 (d, _J_ = 2.2 Hz, 1H), 7.68 (dt, _J_ = 8.0, 1.0 Hz, 1H), 7.56 − 7.51 (m, 4H), 7.48 −

7.44 (m, 3H), 4.25 (s, 2H); ^{13}C-NMR (151 MHz, DMSO-d_6) δ = 170.1 (q), 169.3 (q), 162.6 (q), 149.4 (+), 146.1 (q), 143.0 (q), 138.9 (+), 138.8 (q), 130.5 (+), 129.3 (+), 128.4 (+), 126.8 (+), 126.7 (q), 125.8 (+), 125.1 (+), 122.4 (+), 113.3 (+), 57.2 (−); IR (neat) ν = 3105, 3058, 2930, 2881, 1707, 1610, 1487, 1424, 1327, 1245, 1174, 1111, 936, 846, 790, 753, 701 cm^{-1}; HRMS (ESI) calcd. for C$_{20}$H$_{16}$N$_5$O (M+H)$^+$ m/z = 342.1349; found 342.1358.

(*E*)-7-((1*H*-Pyrazol-4-yl)diazenyl)-5-phenyl-1,3-dihydro-2*H*-benzo[*e*][1,4]diazepin-2-one (30)

4-Nitroso-1*H*-pyrazole (71 mg, 0.73 mmol, 1.2 eq.) was added to a solution of benzodiazepine **6** (153 mg, 0.61 mmol, 1.0 eq.) in glacial acetic acid (8 mL). Then the mixture was stirred 3 d at room temperature, quenched by adding a saturated aqueous solution of NaHCO$_3$ (30 mL) and diluted with EtOAc (30 mL). After separation of the layers, the aqueous layer was extracted with EtOAc (3 x 20 mL). The combined organic layers were dried over Na$_2$SO$_4$, filtered and the solvent was removed under reduced pressure. Purification by preparative HPLC (15% - 45% MeCN in 25 min, t_R = 18.8 min) afforded **30** (30 mg, 15%) as yellow solid. R$_f$ 0.55 (CH$_2$Cl$_2$/MeOH 9:1); m.p. 133 °C; ^{1}H-NMR (600 MHz, DMSO-d_6) δ = 13.21 (bs, 1H), 10.86 (s, 1H), 8.22 (bs, 2H), 7.98 (dd, *J* = 8.7, 2.3 Hz, 1H), 7.56 (d, *J* = 2.3 Hz, 1H), 7.55 − 7.51 (m, 3H), 7.48 − 7.43 (m, 2H), 7.39 (d, *J* = 8.8 Hz, 1H), 4.21 (s, 2H); ^{13}C-NMR (151 MHz, DMSO-d_6) δ = 170.0 (q), 169.7 (q), 158.1 (+), 157.9 (+), 146.7 (q), 141.2 (q), 140.8 (q), 138.6 (q), 130.6 (+), 129.4 (+), 128.4 (+), 126.4 (q), 125.0 (+), 124.4 (+), 122.2 (+), 56.9 (−); IR (neat) ν = 3138, 2866, 1707, 1674, 1614, 1487, 1439, 1394, 1346, 1200, 1133, 995, 839, 798, 723 cm^{-1}; HRMS (ESI) calcd. for C$_{18}$H$_{15}$N$_6$O (M+H)$^+$ m/z = 331.1302; found 331.1303.

(*E*)-*N*,*N*,*N*-Triethyl-3-(2-oxo-5-phenyl-7-((4-sulfophenyl)diazenyl)-2,3-dihydro-1*H*-benzo[*e*][1,4]diazepin-1-yl)propan-1-aminium (31)

Compound **8** bromide (111 mg, 0.22 mmol) was dissolved in MeOH (5 mL) and hydrogenated to the corresponding amino derivative using Pd/C (8 mg, 10 wt. % Pd) in an autoclave (2 bar of H$_2$) at room temperature for 45 min. The mixture was centrifuged, filtered over celite and the solvent was removed *in vacuo*. The amino derivative bromide (103 mg) was used without further purification.

A 1:1 mixture of tetrabutylammonium 4-nitrosobenzenesulfonate and its corresponding nitro derivative (192 mg, 0.44 mmol, 1.0 eq. of nitroso compound) was added to a solution of freshly prepared amino derivative of **8** (103 mg, 0.22 mmol, 1.0 eq.) in acetic acid (2 mL) and CH$_2$Cl$_2$ (1 mL). After stirring the mixture for 24 h at room temperature the solvent was removed *in vacuo*. Purification by preparative HPLC (3% - 55% MeCN in 15 min, t$_R$ = 10.6 min) had to be performed twice to afford **31** trifluoroacetate salt (62 mg, 42%) as yellow solid. R$_f$ 0.02 (CH$_2$Cl$_2$/MeOH 9:1); m.p. 210 °C; ^{1}H-NMR (400 MHz, DMSO-d_6) δ = 8.14 (dd, J = 8.9, 2.4 Hz, 1H), 7.87 (d, J = 9.0 Hz, 1H), 7.83 − 7.79 (m, 2H), 7.78 − 7.74 (m, 3H), 7.74 − 7.67 (m, 2H), 7.59 − 7.54 (m, 1H), 7.53 − 7.46 (m, 2H), 4.63 (d, J = 10.7 Hz, 1H), 4.25 (dt, J = 13.7, 6.7 Hz, 1H), 3.95 − 3.85 (m, 2H), 3.17 − 2.99 (m, 7H), 2.94 (dt, J = 13.0, 4.6 Hz, 1H), 1.96 (dtt, J = 6.3 Hz, 1H), 1.84 (dtt, J = 6.3 z, 1H), 0.99 (t, J = 7.1 Hz, 9H); ^{13}C-NMR (101 MHz, DMSO-d_6) δ = 169.2 (q), 169.0 (q), 158.3 (q, quartet), 151.4 (q), 151.2 (q), 147.4 (q), 144.5 (q), 131.1 (+), 129.5 (q), 129.4 (+), 128.6 (+), 126.8 (+), 125.1 (+), 124.7 (+), 123.9 (+), 122.3 (+), 115.3 (q, quartet), 56.7 (−), 53.8 (−), 52.2 (−), 43.9 (−), 20.3 (−), 6.9 (+); IR (neat) ν = 3440, 2989, 1677, 1607, 1484, 1454, 1398, 1334, 1189, 1118, 1029, 846, 783, 701 cm^{-1}; HRMS (ESI) calcd. for C$_{30}$H$_{36}$N$_5$O$_4$S M$^+$ m/z = 562.2483; found 562.2490.

(*E*)-*N*^{1},*N*^{1},*N*^{2},*N*^{2}-Tetramethyl-*N*^{1}-(2-((N-methyl-4-((2-oxo-5-phenyl-2,3-dihydro-1*H*-benzo[*e*][1,4]diazepin-7-yl)diazenyl)phenyl)sulfonamido)ethyl)ethane-1,2-diaminium (32)

A suspension of benzodiazepine **28** (27 mg, 0.06 mmol, 1.0 eq.), 2-chloro-*N,N*-dimethylethylamine hydrochloride (18 mg, 0.13 mmol, 2.0 eq.) and K$_2$CO$_3$ (87 mg, 0.63 mmol, 10.0 eq.) in DMF (1 mL) was stirred overnight at room temperature. Then a saturated aqueous solution of NaHCO$_3$ (10 mL) was added and the mixture extracted with EtOAc (3 x 5 mL) and CH$_2$Cl$_2$ (3 x 5 mL). The combined organic layers were dried over Na$_2$SO$_4$, filtered and the solvent was removed under reduced pressure. The residue was purified by preparative HPLC (3% - 70% MeCN in 15 min, t$_R$ = 8.9 min) affording **32** bis-trifluoroacetate salt (14 mg, 29%) as orange solid. R$_f$ 0.02 (CH$_2$Cl$_2$/MeOH 9:1); m.p. 90 °C; ^{1}H-NMR (400 MHz, DMSO-d_6) δ = 10.08 (bs, 1H), 9.75 (bs, 1H), 8.22 (dd, J = 8.9, 2.4 Hz, 1H), 8.11 − 8.05 (m, 2H), 8.05 − 7.99 (m, 2H), 7.93 (d, J = 9.0 Hz, 1H), 7.78 (d, J = 2.4 Hz,

1H), 7.71 – 7.64 (m, 2H), 7.59 – 7.52 (m, 1H), 7.51 – 7.47 (m, 2H), 4.68 (d, J = 10.8 Hz, 1H), 4.50 (dt, J = 14.6, 7.3 Hz, 1H), 4.23 (dt, J = 14.1, 6.8 Hz, 1H), 3.92 (d, J = 10.8 Hz, 1H), 3.33 (s, 6H), 2.86 (s, 6H), 2.76 (s, 6H), 2.74 (s, 3H); ^{13}C-NMR (101 MHz, DMSO-d_6) δ = 169.2 (q), 168.9 (q), 158.3 (q, quartet), 154.1 (q), 147.5 (q), 144.5 (q), 138.0 (q), 137.8 (q), 130.8 (+), 130.1 (q), 129.3 (+), 128.9 (+), 128.5 (+), 125.5 (+), 125.0 (+), 123.7 (+), 123.5 (+), 116.5 (q, quartet), 56.7 (−), 53.3 (−), 53.0 (−), 44.9 (−), 42.4 (+, 2C), 41.8 (−), 35.0 (+); IR (neat) ν = 3038, 2650, 2326, 1670, 1465, 1413, 1342, 1163, 1122, 969, 902, 831, 798, 705 cm^{-1}; HRMS (ESI) calcd. for $C_{30}H_{38}N_7O_3S$ M$^+$ m/z = 576.2751; found 576.2752.

(E)-2-((4-((4-(Diethylamino)phenyl)diazenyl)phenyl)(ethyl)amino)ethan-1-ol (40)

N,N-Diethyl-p-phenylenediamine was converted into its diazonium tetrafluoroborate using an adapted procedure from Abrahamian et $al.$[59] HBF$_4$ (48%, 1.7 mL) was added dropwise to a mixture of N,N-diethyl-p-phenylenediamine (559 mg, 3.40 mmol, 1.0 eq.) in water (1 mL) at 0 °C. After stirring for 30 min at 0 °C, a precooled aqueous solution (1 mL) of NaNO$_2$ (235 mg, 3.40 mmol, 1.0 eq.) was added dropwise within 15 min. The mixture was then stirred for 3 h at room temperature. The precipitate was collected by filtration, washed several times with a minimum amount of cold Et$_2$O and was dried in $vacuo$ at ambient temperature. The crude diazonium tetrafluoroborate (662 mg, 74%) was obtained as a brown yellowish solid and used without further purification.

2-(N-Ethylanilino)ethanol (681 mg, 4.56 mmol, 1.2 eq) and NaOAc trihydrate (181 mg, 1.33 mmol, 0.35 eq) were added to a solution of the previously prepared diazonium tetrafluoroborate (1.00 g, 3.80 mmol, 1.0 eq.) in MeOH (20 mL) and water (10 mL). After stirring the mixture for 3 d at room temperature, the precipitate was collected by filtration and purified by recrystallization from MeCN affording azo compound **40** (454 mg, 15%) as red solid. R$_f$ 0.12 (CH$_2$Cl$_2$/Et$_3$N 99:1); m.p. 166 °C; ^{1}H-NMR (300 MHz, DMSO-d_6) δ =7.65 (dd, J = 9.0, 1.8 Hz, 4H), 6.75 (t, J = 9.1 Hz, 4H), 4.80 (t, J = 5.4 Hz, 1H), 3.70 – 3.36 (m, 10H), 1.12 (t, J = 6.9 Hz, 9H); ^{13}C-NMR (75 MHz, DMSO-d_6) δ = 149.1 (q), 148.7 (q), 142.5 (q), 142.4 (q), 123.9 (+), 123.8 (+), 111.0 (+), 111.0 (+), 58.4 (−), 52.2 (−), 45.0 (−), 43.9 (−), 12.6 (+), 12.1 (+); IR (neat) ν = 3337, 2971, 2930, 2892, 1592, 1558, 1510, 1394, 1346, 1267, 1193, 1144, 1070, 999, 943, 820, 783, 731 cm^{-1}; HRMS (ESI) calcd. for $C_{20}H_{29}N_4O$ (M+H)$^+$ m/z = 341.2336; found 341.2343.

(*E*)-*N*,*N*,*N*-Triethyl-2-((4-((4-(ethyl(2-hydroxyethyl)amino)phenyl)diazenyl)phenyl) amino) -2-oxoethan-1-aminium (44)

Oxalyl chloride (123 µL, 1.43 mmol, 1.1 eq.) in anhydrous CH_2Cl_2 (0.7 mL) was added dropwise to 2-triethylammonio acetate (228 mg, 1.43 mmol, 1.1 eq.) in anhydrous MeCN (7 mL) and anhydrous DMF (50 µL). After stirring for 1 h at room temperature all volatiles were removed *in vacuo*. The residue was suspended in a mixture of anhydrous MeCN (3 mL) and anhydrous DMF (3 mL) and then added dropwise to a solution of azo compound **42** (370 mg, 1.30 mmol, 1.0 eq.) and DIPEA (2.26 mL, 13.00 mmol, 10.0 eq.) in anhydrous DMF (20 mL) at 0 °C. After stirring for 16 h at room temperature all volatiles were removed *in vacuo*. The residue was purified by automated flash column chromatography (CH_2Cl_2/MeOH, 3% - 25% MeOH) and subsequent preparative HPLC (3% - 75% MeCN in 10 min, t_R = 8.0 min) yielding compound **44** trifluoroacetate (235 mg, 33%) as dark purple glassy solid. R_f 0.20 (CH_2Cl_2/MeOH 9:1); m.p. 77 °C; ^{1}H-NMR (400 MHz, DMSO-d_6) δ = 10.98 (s, 1H), 7.84 − 7.70 (m, 6H), 6.82 (d, *J* = 9.3 Hz, 2H), 4.24 (s, 2H), 3.62 − 3.45 (m, 12H), 1.28 (t, *J* = 7.2 Hz, 9H), 1.14 (t, *J* = 7.0 Hz, 3H); ^{13}C-NMR (101 MHz, DMSO-d_6) δ = 162.1 (q), 158.3 (q, quartet), 150.5 (q), 149.0 (q), 142.2 (q), 138.7 (q), 124.9 (+), 122.6 (+), 120.1 (+), 116.1 (q, quartet) , 111.2 (+), 58.4 (−), 56.4 (−), 54.1 (−), 52.2 (−), 45.1 (−), 12.0 (+), 7.5 (+); IR (neat) ν = 3463, 3060, 2989, 1741, 1689, 1595, 1551, 1424, 1387, 1346, 1320, 1249, 1118, 1066, 1010, 910, 828, 705 cm^{-1}; HRMS (ESI) calcd. for $C_{24}H_{36}N_5O_2$ M$^+$ m/z = 426.2864; found 426.2872.

(*E*)-4-((4-(Ethyl(2-hydroxyethyl)amino)phenyl)diazenyl)-1-methylpyridin-1-ium (47)

A mixture of azo compound **46** (243 mg, 0.90 mmol, 1.0 eq.) and iodomethane (3.08 mL, 49.50 mmol, 55.0 eq.) in CH_2Cl_2 (10 mL) was stirred for 3 h at room temperature. The precipitate was collected by filtration, washed several times with a minimum amount of cold PE and was dried *in vacuo* affording compound **47** iodide (367 mg, 99%) as purple solid. R_f 0.25 (CH_2Cl_2/MeOH 9:1); m.p. 181 °C; ^{1}H-NMR (300 MHz, DMSO-d_6) δ = 8.88 (d, *J* = 7.1 Hz, 2H), 8.10 (d, *J* = 7.1 Hz, 2H), 7.90 (d, *J* = 9.3 Hz, 2H), 7.01 (d, *J* = 9.5 Hz, 2H), 6.55 (bs, 1H), 4.27 (s, 3H), 3.78 − 3.49 (m, 6H), 1.19 (t, *J* = 7.0 Hz, 3H); ^{13}C-NMR (75 MHz, DMSO-d_6) δ = 161.0 (q), 154.6 (q), 146.6 (+), 143.6 (q), 118.1 (+), 112.9 (+), 58.6 (−), 52.5 (−), 46.7 (+), 46.0 (−), 12.2 (+); IR (neat) ν = 3340, 3034, 2960, 2863, 1633, 1595, 1521, 1472, 1413,

1346, 1297, 1260, 1111, 988, 842, 775 cm^{-1}; HRMS (ESI) calcd. for $C_{16}H_{21}N_4O$ M$^+$ m/z = 285.1710; found 285.1714.

(E)-4-((4-(Ethyl(2-hydroxyethyl)amino)phenyl)diazenyl)-1-(3-(triethylammonio)propyl) pyridin-1-ium (48)

A solution of azo compound **46** (30 mg, 0.11 mmol, 1.0 eq.) and 3-bromopropyl triethylammonium bromide (100 mg, 0.33 mmol, 3.0 eq.) in anhydrous DMF (3 mL) was heated to 80 °C for 30 h in a crimp top vial under nitrogen atmosphere. After drying *in vacuo* the residue was purified by preparative HPLC (3% - 98% MeCN in 15 min, t_R = 6.2 min) yielding **48** bis-trifluoroacetate salt (40 mg, 56%) as purple highly hygroscopic solid. R_f 0.08 (CH$_2$Cl$_2$/MeOH 9:1); ^{1}H-NMR (300 MHz, D$_2$O) δ = 8.59 (d, *J* = 7.2 Hz, 2H), 7.88 (d, *J* = 7.0 Hz, 4H), 7.46 (d, *J* = 10.1 Hz, 2H), 4.51 (t, *J* = 7.5 Hz, 2H), 4.14 (t, *J* = 5.2 Hz, 2H), 4.10 − 3.92 (m, 4H), 3.29 (q, *J* = 7.2 Hz, 8H), 2.47 − 2.32 (m, 2H), 1.40 (t, *J* = 7.2 Hz, 3H), 1.23 (t, *J* = 7.2 Hz, 9H); ^{13}C-NMR (75 MHz, D$_2$O) δ = 162.9 (q, quartet), 161.8 (q), 154.3 (q), 144.6 (+), 141.9 (q), 116.3 (q, quartet), 113.0 (+), 59.1 (−), 56.2 (−), 55.3 (−), 53.0 (−), 52.7 (−), 50.1 (−), 23.1 (−), 12.7 (+), 6.6 (+); IR (neat) ν = 3314, 2989, 2706, 1677, 1636, 1595, 1502, 1409, 1301, 1264, 1197, 1103, 1025, 824, 716 cm^{-1}; HRMS (ESI) calcd. for $C_{24}H_{39}N_5O$ M^{2+} m/z = 206.6572; found 206.6583.

(E)-3-(2-((4-((4-(Diethylamino)phenyl)diazenyl)phenyl)(ethyl)amino)ethyl) 5-methyl 2,6-dimethyl-4-(3-nitrophenyl)-1,4-dihydropyridine-3,5-dicarboxylate (50)

Thionyl chloride (7 µL, 0.09 mmol, 1.1 eq.) was added to a suspension of carboxylic acid **49** (29 mg, 0.09 mmol, 1.0 eq.) in anhydrous CH$_2$Cl$_2$ (180 µL) and anhydrous DMF (50 µL) at 0°C under nitrogen atmosphere. After stirring the mixture for 1 h at 0 °C the solvent was removed *in vacuo*. Then a solution of azo compound **40** (30 mg, 0.09 mmol, 1.0 eq.) in anhydrous CH$_2$Cl$_2$ (50 µL) was added dropwise to the residue. The stirring was continued for 3 h at 0 °C and then for 24 h at room temperature. After addition of CH$_2$Cl$_2$ (10 mL) the organic solution was washed with a saturated aqueous solution of NaHCO$_3$ (10 mL) and brine (10 mL). The organic layer was separated, dried over Na$_2$SO$_4$, filtered and the solvent was removed under reduced pressure. The residue was purified by preparative HPLC (MilliQ water/MeCN, 75% - 98% MeCN in 9 min, 98% MeCN for further 6 min, t_R = 10.3 min) affording compound **50** (26 mg, 46%) as orange solid. R_f 0.09

(CH$_2$Cl$_2$/Et$_3$N 99:1); m.p. 78 °C; ^{1}H-NMR (400 MHz, DMSO-d_6) δ = 9.07 (s, 1H), 7.99 (ddd, J = 8.0, 2.4, 1.2 Hz, 1H), 7.96 (t, J = 1.8 Hz, 1H), 7.69 – 7.54 (m, 5H), 7.51 (t, J = 7.8 Hz, 1H), 6.75 (dd, J = 9.0, 5.1 Hz, 4H), 5.01 (s, 1H), 4.24 – 4.11 (m, 2H), 3.58 (t, J = 6.0 Hz, 2H), 3.54 (s, 3H), 3.42 (q, J = 7.1 Hz, 4H), 3.36 (dd, J = 7.3, 2.3 Hz, 2H), 2.27 (s, 6H), 1.13 (t, J = 7.0 Hz, 6H), 1.05 (t, J = 6.9 Hz, 3H); ^{13}C-NMR (101 MHz, DMSO-d_6) δ = 166.9 (q), 166.6 (q), 149.8 (q), 148.8 (q), 148.7 (q), 147.7 (q), 147.1 (q), 146.5 (q), 142.9 (q), 142.4 (q) 133.9 (+), 129.6 (+), 123.9 (+), 123.7 (+), 121.5 (+), 121.2 (+), 111.3 (+), 111.0 (+), 100.9 (q), 100.6 (q), 60.8 (−), 50.8 (+), 48.1 (−), 44.4 (−), 43.9 (−), 38.8 (+), 18.3 (+), 18.2 (+), 12.5 (+), 11.9 (+); IR (neat) ν = 3355, 3079, 2971, 2896, 1700, 1651, 1595, 1513, 1379, 1346, 1271, 1211, 1148, 1014, 824, 783, 746, 705 cm^{-1}; HRMS (ESI) calcd. for C$_{36}$H$_{43}$N$_6$O$_6$ (M+H)$^+$ m/z = 655.3239; found 655.3248.

(E)-N,N,N-Triethyl-2-((4-((4-(ethyl(2-((5-(methoxycarbonyl)-2,6-dimethyl-4-(3-nitro-phenyl)-1,4-dihydropyridine-3-carbonyl)oxy)ethyl)amino)phenyl)diazenyl)phenyl)amino)-2-oxoethan-1-aminium (51)

Thionyl chloride (16 µL, 0.22 mmol, 1.1 eq.) was added to a suspension of carboxylic acid **49** (67 mg, 0.20 mmol, 1.0 eq.) in anhydrous CH$_2$Cl$_2$ (500 µL) and anhydrous DMF (150 µL) at 0°C under nitrogen atmosphere. After stirring the mixture for 1 h at 0 °C and 1 h at room temperature the solvent was removed *in vacuo*. Then a solution of azo compound **44** (110 mg, 0.20 mmol, 1.0 eq.) in anhydrous DMF (2 mL) and DIPEA (104 µL) was added dropwise to the residue suspended in anhydrous CH$_2$Cl$_2$ (500 µL). The stirring was continued for 3 h at 0 °C and then for 20 h at room temperature. All volatiles were removed *in vacuo*. The residue was purified by automated flash column chromatography (CH$_2$Cl$_2$/MeOH, 3% - 100% MeOH) and subsequent preparative HPLC (3% - 98% MeCN in 25 min, t$_R$ = 16.8 min) yielding compound **51** trifluoroacetate salt (34 mg, 20%) as purple solid. R$_f$ 0.30 (CH$_2$Cl$_2$/MeOH 9:1); m.p. 88 °C; ^{1}H-NMR (400 MHz, DMSO-d_6) δ = 10.98 (s, 1H), 9.10 (s, 1H), 7.99 (ddd, J = 8.0, 2.4, 1.2 Hz, 1H), 7.94 (t, J = 2.0 Hz, 1H), 7.82 – 7.73 (m, 4H), 7.70 (d, J = 9.1 Hz, 2H), 7.56 (dt, J = 7.7, 1.4 Hz, 1H), 7.50 (t, J = 7.8 Hz, 1H), 6.80 (d, J = 9.3 Hz, 2H), 4.99 (s, 1H), 4.28 – 4.20 (m, 3H), 4.15 (dt, J = 11.5 Hz, 1H), 3.62 (t, J = 5.9 Hz, 2H), 3.59 – 3.51 (m, 9H), 3.39 (dq, J = 9.8, 4.9 Hz, 2H), 2.27 (s, 3H), 2.26 (s, 3H), 1.28 (t, J = 7.2 Hz, 9H), 1.07 (t, J = 7.0 Hz, 3H); ^{13}C-NMR (101 MHz, DMSO-d_6) δ = 166.9 (q), 166.6 (q),

162.1 (q), 158.1 (q, quartet), 150.2 (q), 149.8 (q), 148.9 (q), 147.6 (q), 147.2 (q), 146.5 (q), 142.5 (q), 138.8 (q), 133.9 (+), 129.6 (+), 124.7 (+), 122.7 (+), 121.5 (+), 121.2 (+), 120.1 (+), 111.3 (+), 100.9 (q), 100.5 (q), 60.8 (−), 56.4 (−), 54.1 (−), 50.8 (+), 48.1 (−), 44.5 (−), 38.7 (+), 18.3 (+), 18.2 (+), 11.9 (+), 7.5 (+); IR (neat) ν = 3273, 3071, 2982, 1674, 1595, 1528, 1424, 1383, 1349, 1249, 1200, 1133, 1018, 828, 719 cm^{-1}; HRMS (ESI) calcd. for $C_{40}H_{50}N_7O_7$ M$^+$ m/z = 740.3766; found 740.3770.

(*E*)-3-(2-(Ethyl(4-(pyridin-4-yldiazenyl)phenyl)amino)ethyl) 5-methyl 2,6-dimethyl-4-(3-nitrophenyl)-1,4-dihydropyridine-3,5-dicarboxylate (52)

Thionyl chloride (16 µL, 0.22 mmol, 1.1 eq.) was added to a suspension of carboxylic acid **49** (67 mg, 0.20 mmol, 1.0 eq.) in anhydrous CH_2Cl_2 (360 µL) and anhydrous DMF (100 µL) at 0°C under nitrogen atmosphere. After stirring the mixture for 1 h at 0 °C the solvent was removed *in vacuo*. Then a solution of azo compound **46** (55 mg, 0.20 mmol, 1.0 eq.) in anhydrous CH_2Cl_2 (100 µL) and Et$_3$N (50 µL) was added dropwise to the residue. The stirring was continued for 3 h at 0 °C and then for 24 h at room temperature. All volatiles were removed *in vacuo* and purification by preparative HPLC (MilliQ water/MeCN, 50% - 98% MeCN in 10 min, 98% MeCN for further 5 min, t_R = 9.9 min) afforded compound **52** (20 mg, 17%) as orange solid. R_f 0.15 (CH_2Cl_2/Et$_3$N 99:1); m.p. 83 °C (decomposition); ^{1}H-NMR (400 MHz, DMSO-*d$_6$*) δ = 9.07 (s, 1H), 8.76 − 8.66 (m, 2H), 7.98 (ddd, *J* = 8.0, 2.4, 1.2 Hz, 1H), 7.92 (t, *J* = 2.0 Hz, 1H), 7.81 − 7.71 (m, 2H), 7.68 − 7.61 (m, 2H), 7.55 (dt, *J* = 7.8, 1.5 Hz, 1H), 7.49 (t, *J* = 7.8 Hz, 1H), 6.84 (d, *J* = 9.3 Hz, 2H), 4.97 (s, 1H), 4.27 (dt, *J* = 11.4, 5.7 Hz, 1H), 4.17 (dt, *J* = 11.5, 5.8 Hz, 1H), 3.67 (t, *J* = 5.8 Hz, 2H), 3.53 (s, 3H), 3.43 (dq, *J* = 7.1, 3.4 Hz, 2H), 2.26 (s, 3H), 2.25 (s, 3H), 1.08 (t, *J* = 7.0 Hz, 3H); ^{13}C-NMR (101 MHz, DMSO-*d$_6$*) δ = 166.9 (q), 166.5 (q), 157.4 (q), 151.6 (q), 150.8 (+), 149.7 (q), 147.6 (q), 147.2 (q), 146.4 (q), 142.5 (q), 133.9 (+), 129.6 (+), 126.0 (+), 121.4 (+), 121.2 (+), 115.7 (+), 111.5 (+), 101.0 (q), 100.4 (q), 60.7 (−), 50.8 (+), 48.1 (−), 44.5 (−), 38.7 (+), 18.3 (+), 18.2 (+), 11.9 (+); IR (neat) ν = 3299, 3198, 3083, 2952, 1681, 1588, 1513, 1439, 1379, 1349, 1312, 1271, 1211, 1118, 1096, 1021, 828, 742, 705 cm^{-1}; HRMS (ESI) calcd. for $C_{31}H_{33}N_6O_6$ (M+H)$^+$ m/z = 585.2456; found 585.2459.

(*E*)-4-((4-(Ethyl(2-((5-(methoxycarbonyl)-2,6-dimethyl-4-(3-nitrophenyl)-1,4-dihydro-pyridine-3-carbonyl)oxy)ethyl)amino)phenyl)diazenyl)-1-methylpyridin-1-ium (53)

Thionyl chloride (8 μL, 0.10 mmol, 1.1 eq.) was added to a suspension of carboxylic acid **49** (33 mg, 0.10 mmol, 1.0 eq.) in anhydrous CH_2Cl_2 (150 μL) and anhydrous DMF (50 μL) at 0 °C under nitrogen atmosphere. After stirring the mixture for 1 h at 0 °C and 1 h at room temperature the solvent was removed *in vacuo*. Then a solution of azo compound **47** (42 mg, 0.10 mmol, 1.0 eq.) in anhydrous DMF (1 mL) and DIPEA (52 μL) was added dropwise to the residue suspended in anhydrous CH_2Cl_2 (150 μL). The stirring was continued for 3 h at 0 °C and then for 20 h at room temperature. All volatiles were removed *in vacuo* and purification by preparative HPLC (10% - 75% MeCN in 10 min, then 75% - 98% MeCN in 2 min, t_R = 9.1 min) afforded compound **53** trifluoroacetate salt (31 mg, 46%) as purple solid. R_f 0.09 (CH_2Cl_2/MeOH 9:1); m.p. 92 °C; ^{1}H-NMR (400 MHz, DMSO-d_6) δ = 9.13 (s, 1H), 8.92 (d, *J* = 7.1 Hz, 2H), 8.12 (d, *J* = 7.1 Hz, 2H), 7.95 (ddd, *J* = 7.8, 2.4, 1.4 Hz, 1H), 7.88 (t, *J* = 2.0 Hz, 1H), 7.82 (d, *J* = 9.3 Hz, 2H), 7.55 − 7.43 (m, 2H), 6.94 (d, *J* = 9.5 Hz, 2H), 4.93 (s, 1H), 4.43 − 4.12 (m, 5H), 3.79 (t, *J* = 5.7 Hz, 2H), 3.57 − 3.47 (m, 5H), 2.26 (s, 3H), 2.23 (s, 3H), 1.12 (t, *J* = 7.04 Hz, 3H); ^{13}C-NMR (75 MHz, DMSO-d_6) δ = 166.9 (q), 166.5 (q), 161.0 (q), 154.3 (q), 149.6 (q), 147.6 (q), 147.5 (q), 146.8 (+), 146.5 (q), 143.6 (q), 133.9 (+), 129.6 (+), 121.4 (+), 121.2 (+), 118.3 (+), 112.6 (+), 101.0 (q), 100.3 (q), 60.7 (−), 50.9 (+), 48.5 (−), 46.9 (+), 45.0 (−), 38.6 (+), 18.4 (+), 18.2 (+), 12.1 (+); IR (neat) ν = 3045, 2933, 1689, 1636, 1349, 1301, 1271, 1208, 1115, 1014, 846, 775, 738, 705 cm^{-1}; HRMS (ESI) calcd. for $C_{32}H_{35}N_6O_6$ M$^+$ m/z = 599.2613; found 599.2618; purity: 90% (254 nm), 93% (220 nm).

3-(2-(Ethyl(phenyl)amino)ethyl) 5-methyl 2,6-dimethyl-4-(3-nitrophenyl)-1,4-dihydro-pyridine-3,5-dicarboxylate (54)

Thionyl chloride (144 μL, 1.98 mmol, 1.1 eq.) was added to a suspension of carboxylic acid **49** (598 mg, 1.80 mmol, 1.0 eq.) in anhydrous CH_2Cl_2 (4 mL) and anhydrous DMF (1 mL) at 0°C under nitrogen atmosphere. After stirring the mixture for 1 h at 0 °C a solution of 2-*N*-ethylanilino ethanol (303 mg, 1.84 mmol, 1.0 eq.) in anhydrous CH_2Cl_2 (1 mL) was added dropwise. The stirring was continued for 3 h at 0 °C and then for 24 h at room temperature. The solvent was removed *in vacuo* and the residue dissolved in EtOAc (10 mL). The organic solution was washed with brine (10 mL) and a saturated aqueous

solution of NaHCO$_3$ (10 mL). The organic layer was separated, dried over Na$_2$SO$_4$, filtered and the solvent was removed under reduced pressure. The residue was purified by automated flash column chromatography (CH$_2$Cl$_2$ + 1% Et$_3$N /MeOH, 3% - 10% MeOH) and subsequent preparative HPLC (MilliQ water/MeCN, 75% - 98% MeCN in 9 min, t$_R$ = 6.7 min) yielding compound **54** (364 mg, 42%) as yellow solid. R$_f$ 0.11 (CH$_2$Cl$_2$/Et$_3$N 99:1); m.p. 121 °C; ^{1}H-NMR (400 MHz, DMSO-d_6) δ = 9.08 (s, 1H), 8.00 (ddd, J = 8.0, 2.4, 1.1 Hz, 1H), 7.96 (t, J = 2.0 Hz, 1H), 7.59 (dt, J = 7.7, 1.4 Hz, 1H), 7.51 (t, J = 7.9 Hz, 1H), 7.11 (dd, J = 8.7, 7.2 Hz, 2H), 6.69 – 6.61 (m, 2H), 6.56 (t, J = 7.2 Hz, 1H), 5.02 (s, 1H), 4.10 (td, J = 6.0, 4.4 Hz, 2H), 3.55 (s, 3H), 3.44 (t, J = 6.2 Hz, 2H), 3.27 (q, J = 6.9 Hz, 2H), 2.28 (s, 3H), 2.28 (s, 3H), 0.99 (t, J = 7.0 Hz, 3H); ^{13}C-NMR (101 MHz, DMSO-d_6) δ = 167.0 (q), 166.6 (q), 149.8 (q), 147.7 (q), 147.3 (q), 147.0 (q), 146.5 (q), 134.0 (+), 129.7 (+) , 129.1 (+), 121.5 (+), 121.2 (+), 115.5 (+), 111.6 (+), 100.9 (q), 100.7 (q), 60.8 (−), 50.9 (+), 48.1 (−), 44.3 (−), 38.8 (+), 18.3 (+), 18.3 (+), 11.8 (+); IR (neat) ν = 3355, 3094, 2952, 2885, 1703, 1648, 1595, 1528, 1507, 1484, 1379, 1346, 1290, 1215, 1122, 1044, 1014, 895, 828, 787, 742, 693 cm^{-1}; HRMS (ESI) calcd. for C$_{26}$H$_{30}$N$_3$O$_6$ (M+H)$^+$ m/z = 480.2129; found 480.2141.

3.4.2 X-ray Crystallography
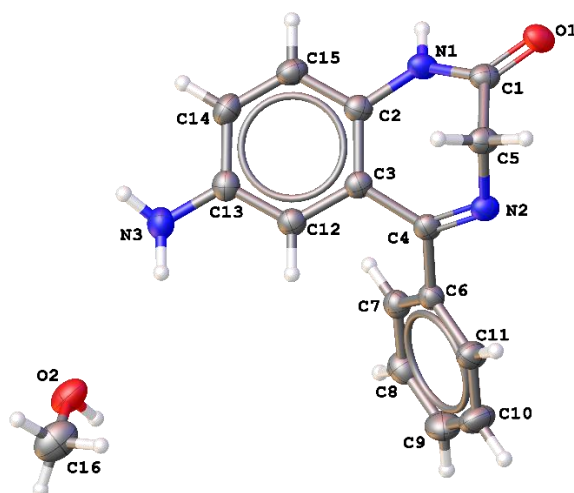
Crystallographic data of **6**.

Chemical formula	C$_{15}$H$_{13}$N$_3$O·CH$_4$O
M_r	283.32
Crystal system, space group	Monoclinic, $P2_1/c$

Temperature (K)	123
a, *b*, *c* (Å)	8.8058 (1), 15.9096 (2), 10.3309 (1)
β (°)	90.198 (1)
V (Å^3)	1447.32 (3)
Z	4
Radiation type	Cu *K*α
μ (mm^{-1})	0.71
Crystal size (mm)	0.17 × 0.16 × 0.13
Data collection	
Diffractometer	SuperNova, Single source at offset, Atlas
Absorption correction	Multi-scan *CrysAlis PRO*, Agilent Technologies, Version 1.171.37.31 (release 14-01-2014 CrysAlis171 .NET) (compiled Jan 14 2014,18:38:05) Empirical absorption correction using spherical harmonics, implemented in SCALE3 ABSPACK scaling algorithm. Empirical absorption correction using spherical harmonics, implemented in SCALE3 ABSPACK scaling algorithm.
T$_{min}$, *T*$_{max}$	0.838, 1.000
No. of measured, independent and observed [*I* > 2σ(*I*)] reflections	82319, 2915, 2679
R$_{int}$	0.031
(sin θ/λ)$_{max}$ (Å^{-1})	0.623
Refinement	
R[*F*^{2} > 2σ(*F*^{2})], *wR*(*F*^{2}), *S*	0.037, 0.102, 1.02
No. of reflections	2915
No. of parameters	197
H-atom treatment	H atoms treated by a mixture of independent and constrained refinement
Δρ$_{max}$, Δρ$_{min}$ (e Å^{-3})	0.25, −0.24

Computer programs: *CrysAlis PRO*, Agilent Technologies, Version 1.171.37.31 (release 14-01-2014 CrysAlis171 .NET) (compiled Jan 14 2014, 18:38:05), *SHELXS* (Sheldrick, 2008), *SHELXL* (Sheldrick, 2008), Olex2 (Dolomanov *et al.*, 2009).

Crystallographic data of **46**.

Chemical formula	$C_{15}H_{18}N_4O$
M_r	270.33
Crystal system, space group	Orthorhombic, $Pna2_1$
Temperature (K)	123
a, b, c (Å)	12.7730 (3), 14.7900 (3), 7.47602 (18)
V (Å^3)	1412.31 (6)
Z	4
Radiation type	Cu $K\alpha$
μ (mm^{-1})	0.67
Crystal size (mm)	0.15 × 0.06 × 0.04
Data collection	
Diffractometer	SuperNova, Single source at offset, Atlas
Absorption correction	Gaussian *CrysAlis PRO* 1.171.38.42b (Rigaku Oxford Diffraction, 2015) Numerical absorption correction based on gaussian integration over a multifaceted crystal model Empirical absorption correction using spherical harmonics, implemented in SCALE3 ABSPACK scaling algorithm.
T_{min}, T_{max}	0.988, 0.995
No. of measured, independent and observed [$I > 2\sigma(I)$] reflections	9497, 2721, 2510
R_{int}	0.032
$(\sin \theta/\lambda)_{max}$ (Å^{-1})	0.622

Refinement

$R[F^2 > 2\sigma(F^2)]$, $wR(F^2)$, S	0.033, 0.084, 1.05
No. of reflections	2721
No. of parameters	183
No. of restraints	1
H-atom treatment	H-atom parameters constrained
$\Delta\rho_{max}$, $\Delta\rho_{min}$ (e Å^{-3})	0.13, −0.14
Absolute structure	Flack x determined using 1030 quotients [(I+)-(I-)]/[(I+)+(I-)] (Parsons, Flack and Wagner, Acta Cryst. B69 (2013) 249-259).
Absolute structure parameter	−0.02 (18)

Computer programs: *CrysAlis PRO* 1.171.38.42b (Rigaku OD, 2015), *SHELXT* (Sheldrick, 2015), *SHELXL* (Sheldrick, 2015), Olex2 (Dolomanov *et al.*, 2009).

3.4.3 Electrophysiology[D]

Electrophysiological recordings in whole-cell configuration were conducted on CHO-K1 cells at room temperature (20 - 25°C) using an EPC-9 amplifier (HEKA Elektronic, Germany). Cells were continuously superfused with external solution containing (mM): NaCl 140, CaCl$_2$ 2, KCl 2.8, MgCl$_2$ 1, HEPES 20, glucose 10; pH 7.4; 320-330 mOsm. The patch pipette solution contained (mM): KCl 140, MgCl$_2$, MgATP 2, HEPES 10, BAPTA 2; pH 7.3; 290 mOsm. All recordings were performed at V$_{hold}$ -30 mV.

To express homomeric glycine-receptors cells were transfected with cDNA of one of its subunits: α_1 zebrafish, α_1 human, α_2 zebrafish, α_2 mouse, α_1 human G254A mutant or α_3 human; to express GABA$_A$-receptors cells were transfected with cDNA of α_1, β_2 and γ_2 subunits simultaneously. The Lipofectamine 3000 protocol (Life Technology, USA) was used for transfection. Activation of glycine and GABA$_A$-receptors was induced by application of agonists of different concentration (glycine and GABA, respectively). For rapid application of compounds a system of parallel rectangular tubes (100 µm in diameter), located at the distance of 40-50 µm from the tested cell, was used. The

---

[D] All electrophysiological investigations were performed in the group of Prof. Dr. Piotr Bregestovski by Galyna Maleeva at the Aix-Marseille University, France.

movement of the tubes was controlled by a computer-driven fast exchange system (SF77A Perfusion Fast-Step, Warner, USA).

UV illumination (365 nm) has been applied using a light emitting diode (Thorlabs).

3.4.4 Behavioral Tests in Zebrafish Larvae[E]

Zebrafish larvae (*Danio rerio*, Tupfel-long strain) at their 7th day post fertilization were habituated for 45 minutes inside the Zebrabox (ViewPoint high throughput monitoring system) under dark conditions into 200 µL of clean water. Continuously, 100 µL of water were extracted carefully from each well with a 12 multichannel pipette and rapidly substituted with 100 µL of a solution with a double final concentration of each treatment. To the wells with the control only 100 µL of clean water was added. The time between the first and last treatment addition never exceeded more than 40 seconds and experimental recording started as soon as all animals were refilled with their treatments.

In total, 96 larval zebrafish were recorded for 32 minutes and analysed into 6 treatment groups:

1. Control: 12 zebrafishes were kept as control animals swimming in 200 µL of clean water

2. DMSO: 12 zebrafishes were exposed to 200 µL of clean water with 1% of DMSO

3. Compound **26**: 12 zebrafishes were exposed to 100 µM of **26** in 200 µL of clean water with 1% of DMSO

4. Compound **27**: 12 zebrafishes were exposed to 100 µM of **27** in 200 µL of clean water with 1% of DMSO

5. Compound **29**: 12 zebrafishes were exposed to 100 µM of **29** in 200 µL of clean water with 1% of DMSO.

6. Compound **29**: 12 zebrafishes were exposed to 50 µM of **29** in 200 µL of clean water with 1% of DMSO

[E] All *in vivo* experiments were carried out in the group of Prof. Dr. Pau Gorostiza by Alexandre Gomila and Dr. Núria Camarero at the Institute of Bioengineering of Catalonia, Barcelona, Spain.

All photoswitchable azo benzodiazepines were initially used in their thermal equilibrium thus in their *trans* configuration.

Experimental procedure:

For the first 20 minutes (relaxation period) of the experiment, the animals were kept in dark conditions with no light changes or mechanic stimuli. After that the animals were exposed to UV/blue light cycles for in total 12 minutes with alternating continuous illumination for 2 minutes of 365 nm and 2 minutes of 455 nm. LEDs preinstalled in the Zebrabox were used as light sources.

For the figures a One-way ANOVA analysis was conducted with Dunnette's multiple comparisons test against the control animal group, establishing a p-value of 0'05 for significance. P-value > 0'05 (ns), p<0'05 (*), p<0'01 (**), p<0'001 (***) and p<0'0001 (****).

3.4.5 Molecular Docking[F]

All compounds were optimized with Gaussian09 (G09) software package[73] in B3LYP/6-31+G** level of theory. Used receptor structures: the GABA$_A$R homology model,[70] the available crystal structures of α_1 and α_3 GlyRs[15, 71] and a homology model of α_3 GlyR open state created using Modeller.[74] Hydrogens and missing atoms were added using psfgen[75] and MolProbity.[76] Rigid and flexible dockings were done using Autodock Vina.[77] All images were generated using VMD (version 1.9.2).[78]

[F] All *molecular docking* experiments were performed in the group of Prof. Dr. Carme Rovira by Alba Nin-Hill and Dr. Mercedes Alfonso-Prieto at the University of Barcelona, Spain.

3.5 Supporting Information

Photochromic data

Compound **26**
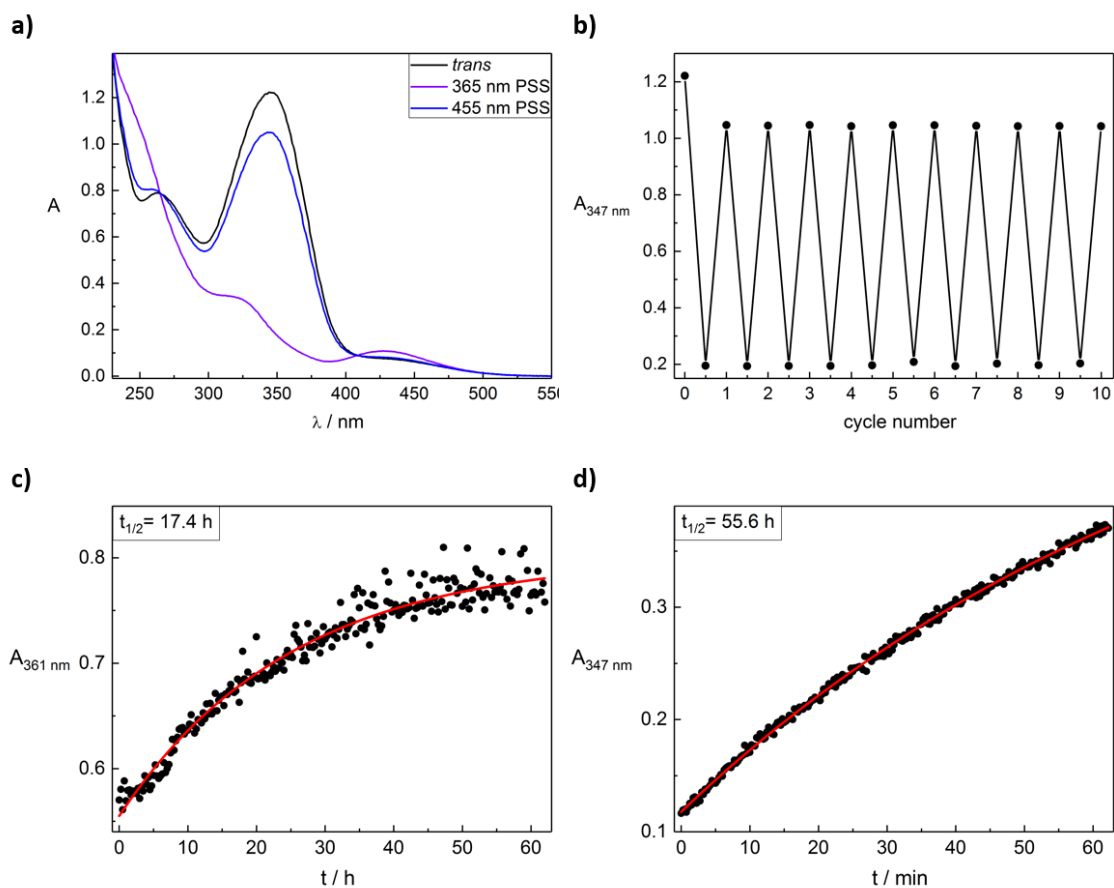
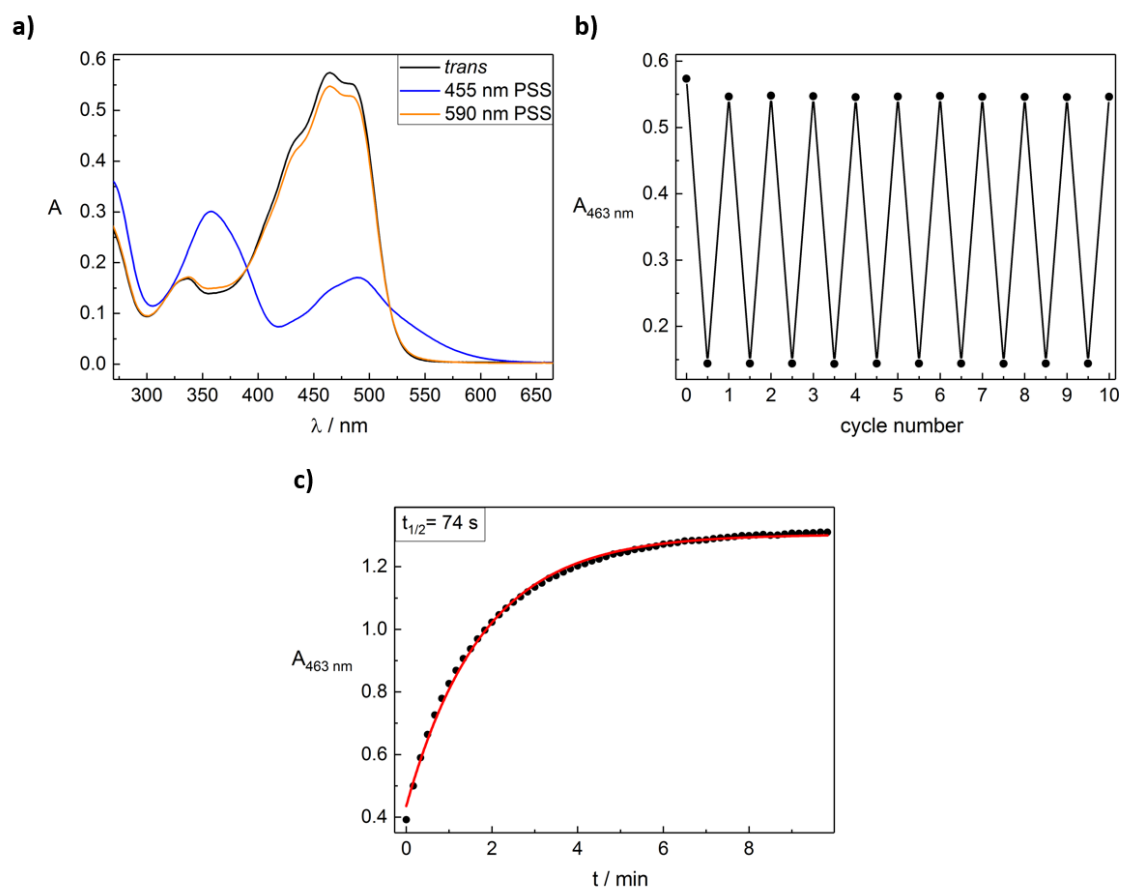

Figure S1. Photochromic data of compound **26**. **a)** UV-Vis spectra of azo benzodiazepine **26** (50 µM in PBS + 0.1% DMSO) from the *trans* isomer, the PSS at irradiation with UV-light of 365 nm and the PSS at irradiation with blue light of 455 nm. **b)** Cycle performance of azo benzodiazepine **26** (50 µM in PBS + 0.1% DMSO). Changes in absorption at λ_{max} of the *trans* isomer were measured during alternate irradiation with light of 365 nm and 455 nm. **c)**, **d)** Determination of the thermal half-lives of compound **26** at 25 °C (**c**: 50 µM in DMSO; **d**: 50 µM in PBS + 0.1% DMSO).
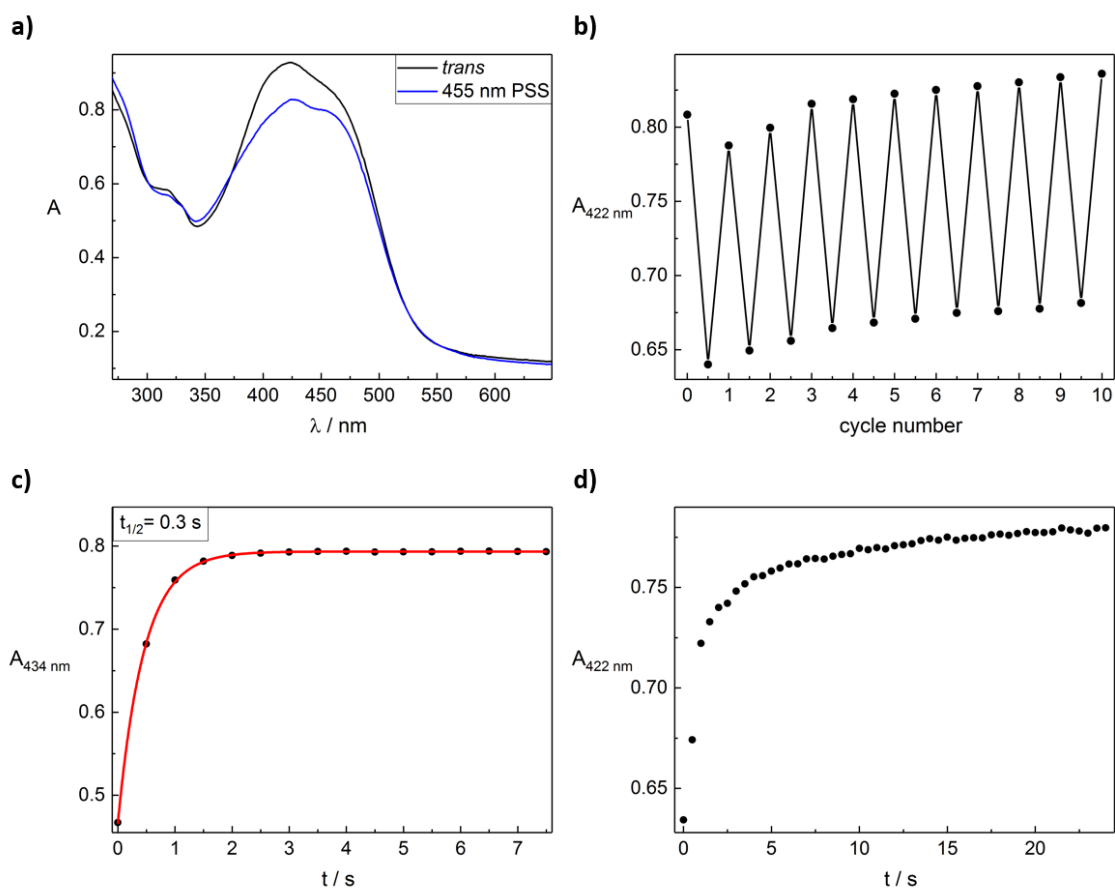
Compound **27**
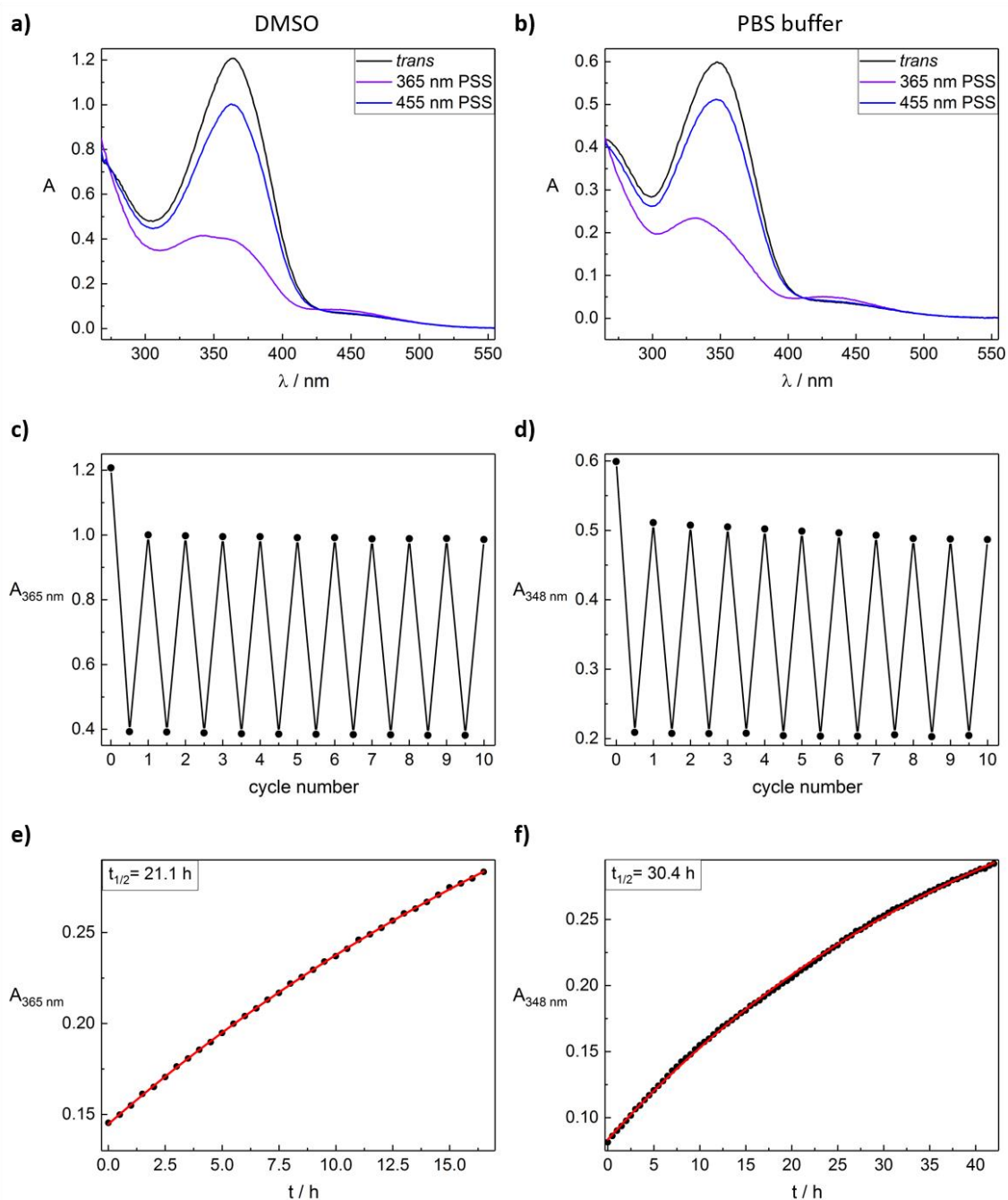
Figure S2. Photochromic data of compound **27**. **a)**, **b)** UV-Vis spectra of azo benzodiazepine **27** (**a**: 50 µM in DMSO; **b**: 30 µM in PBS + 3% DMSO) from the *trans* isomer, the PSS at irradiation with UV-light of 365 nm and the PSS at irradiation with blue light of 455 nm. **c)**, **d)** Cycle performance of azo benzodiazepine **27** (**c**: 50 µM in DMSO; **d**: 30 µM in PBS + 3% DMSO). Changes in absorption at λ$_{max}$ of the *trans* isomer were measured during alternate irradiation with light of 365 nm and 455 nm. **e)**, **f)** Determination of the thermal half-lives of compound **27** at 25 °C (**e**: 50 µM in DMSO; **f**: 30 µM in PBS + 3% DMSO).
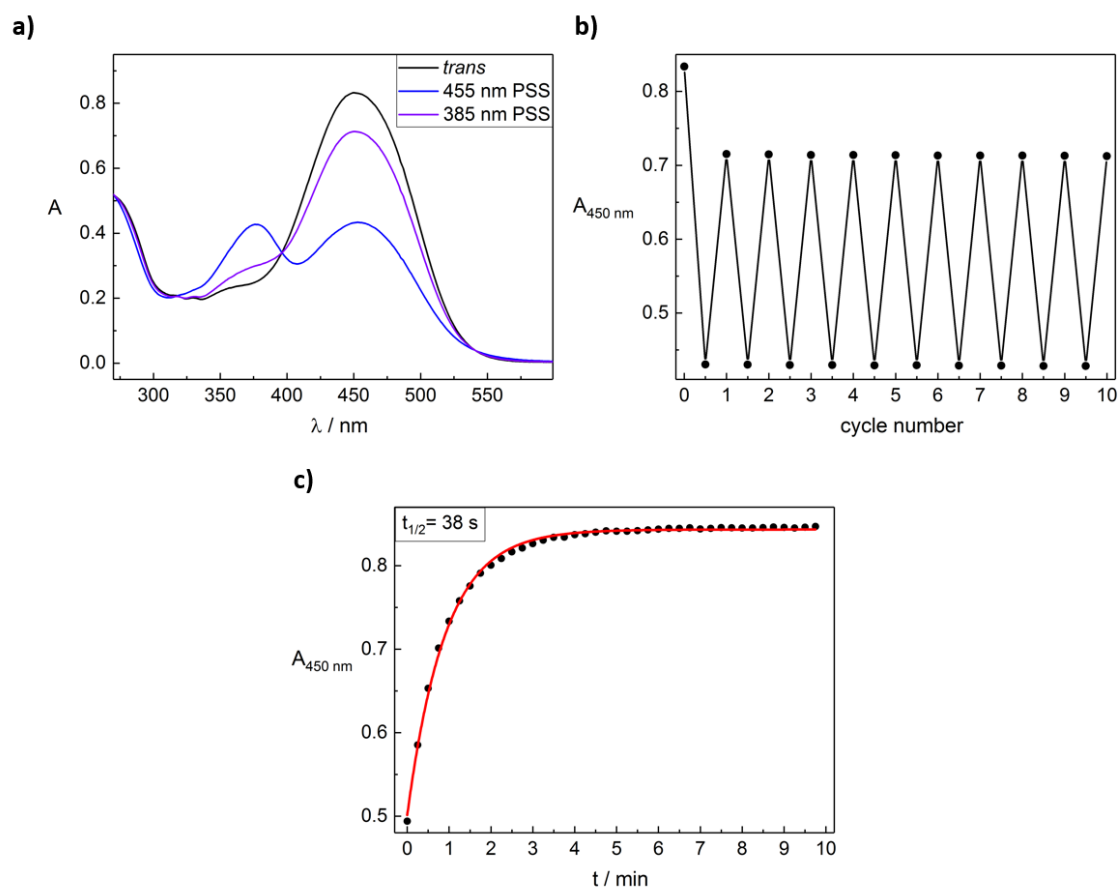
Compound **28**

a)

b)

c)
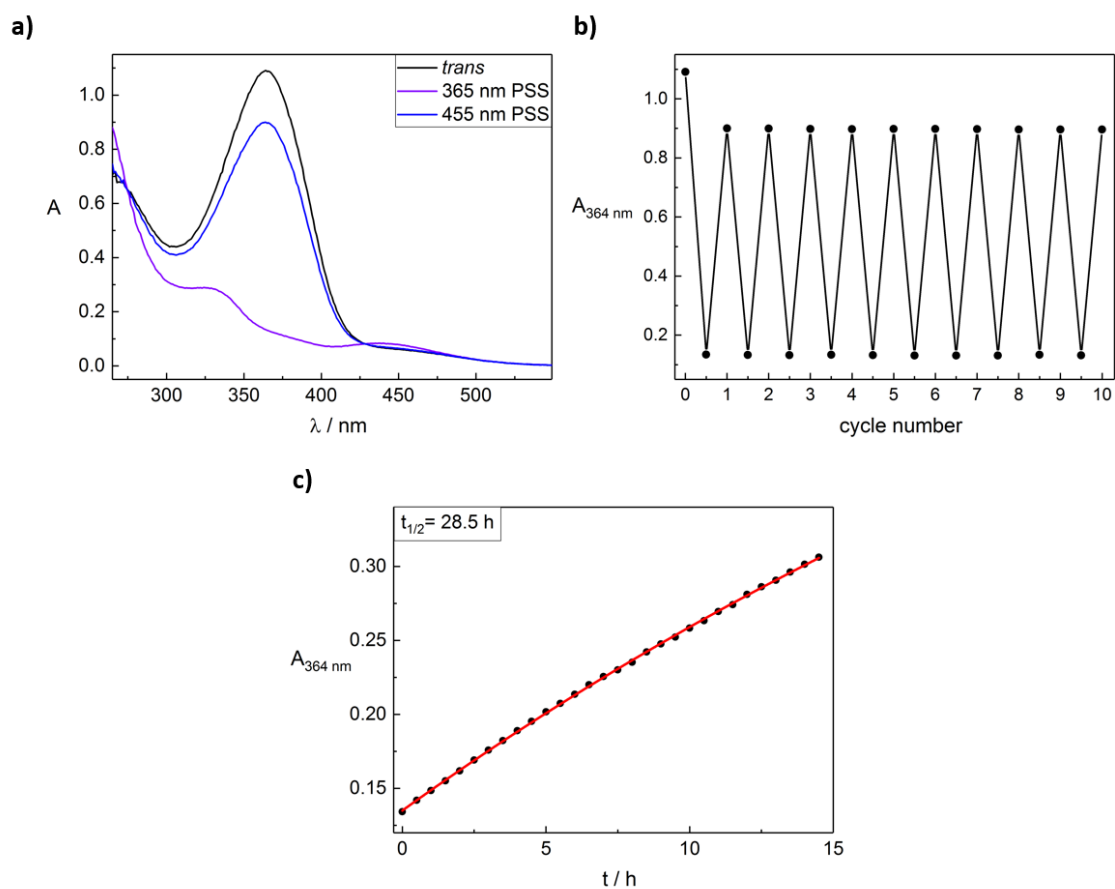
Figure S3. Photochromic data of compound **28**. **a)** UV-Vis spectra of azo benzodiazepine **28** (50 µM in DMSO) from the *trans* isomer, the PSS at irradiation with UV-light of 365 nm and the PSS at irradiation with blue light of 455 nm. **b)** Cycle performance of azo benzodiazepine **28** (50 µM in DMSO). Changes in absorption at λ_{max} of the *trans* isomer were measured during alternate irradiation with light of 365 nm and 455 nm. **c)** Determination of the thermal half-life of compound **28** at 25 °C (50 µM in DMSO).
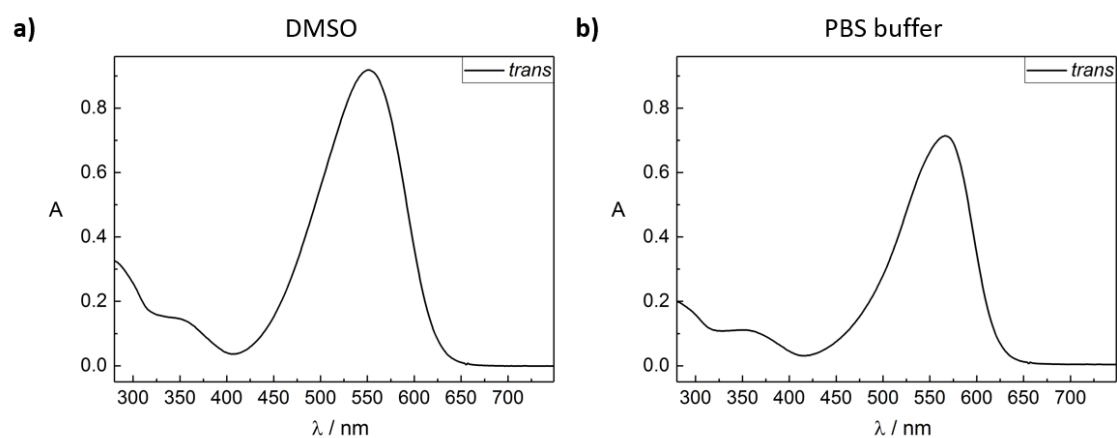
Compound **29**
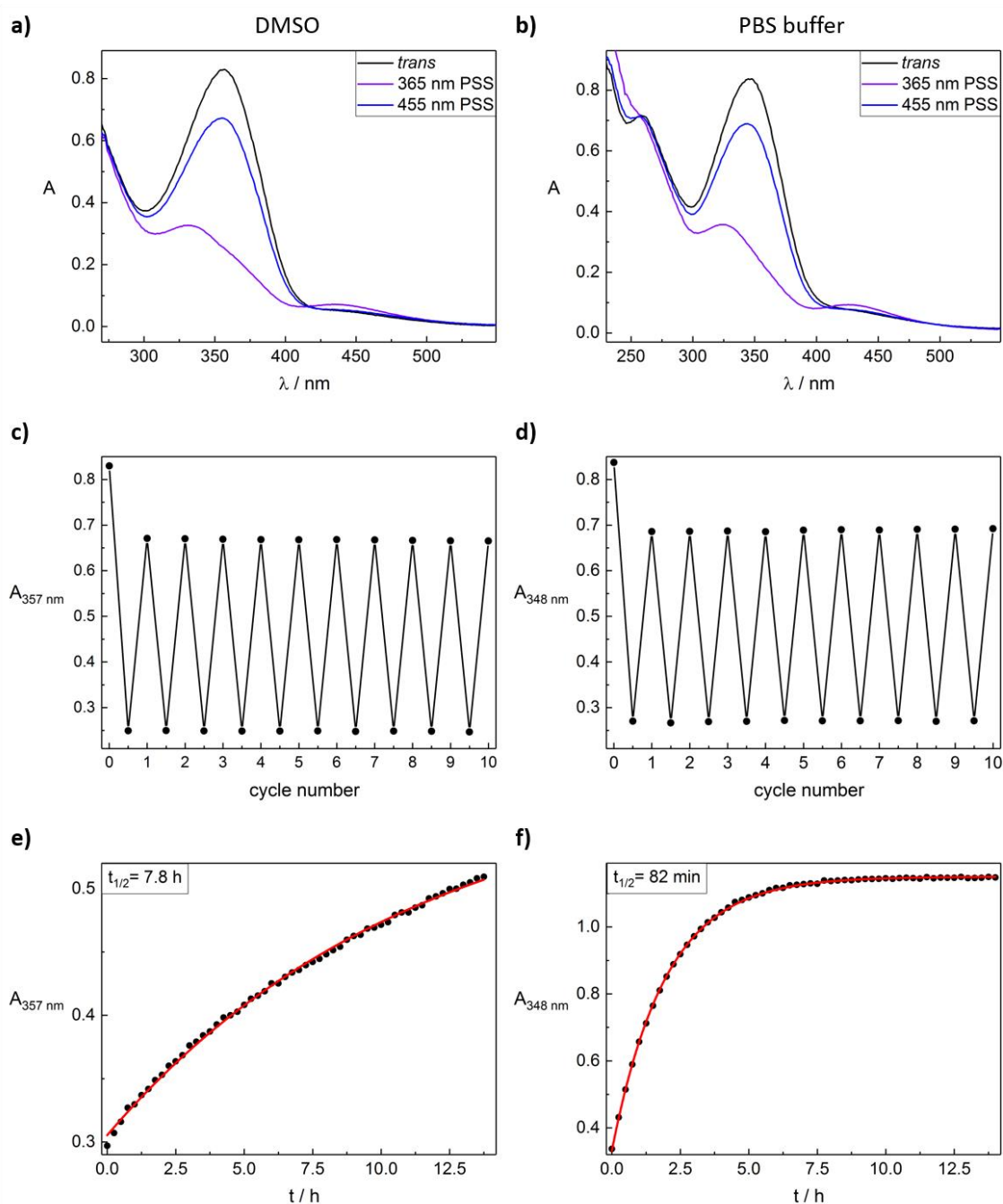
**Figure S4.** Photochromic data of compound **29**. **a)**, **b)** UV-Vis spectra of azo benzodiazepine **29** (**a**: 50 µM in DMSO; **b**: 50 µM in PBS + 0.1% DMSO) from the *trans* isomer, the PSS at irradiation with UV-light of 365 nm and the PSS at irradiation with blue light of 455 nm. **c)**, **d)** Cycle performance of azo benzodiazepine **29** (**c**: 50 µM in DMSO; **d**: 50 µM in PBS + 0.1% DMSO). Changes in absorption at λ_{max} of the *trans* isomer were measured during alternate irradiation with light of 365 nm and 455 nm. **e)**, **f)** Determination of the thermal half-lives of compound **29** at 25 °C (**e**: 50 µM in DMSO; **f**: 50 µM in PBS + 0.1% DMSO).

Compound **30**
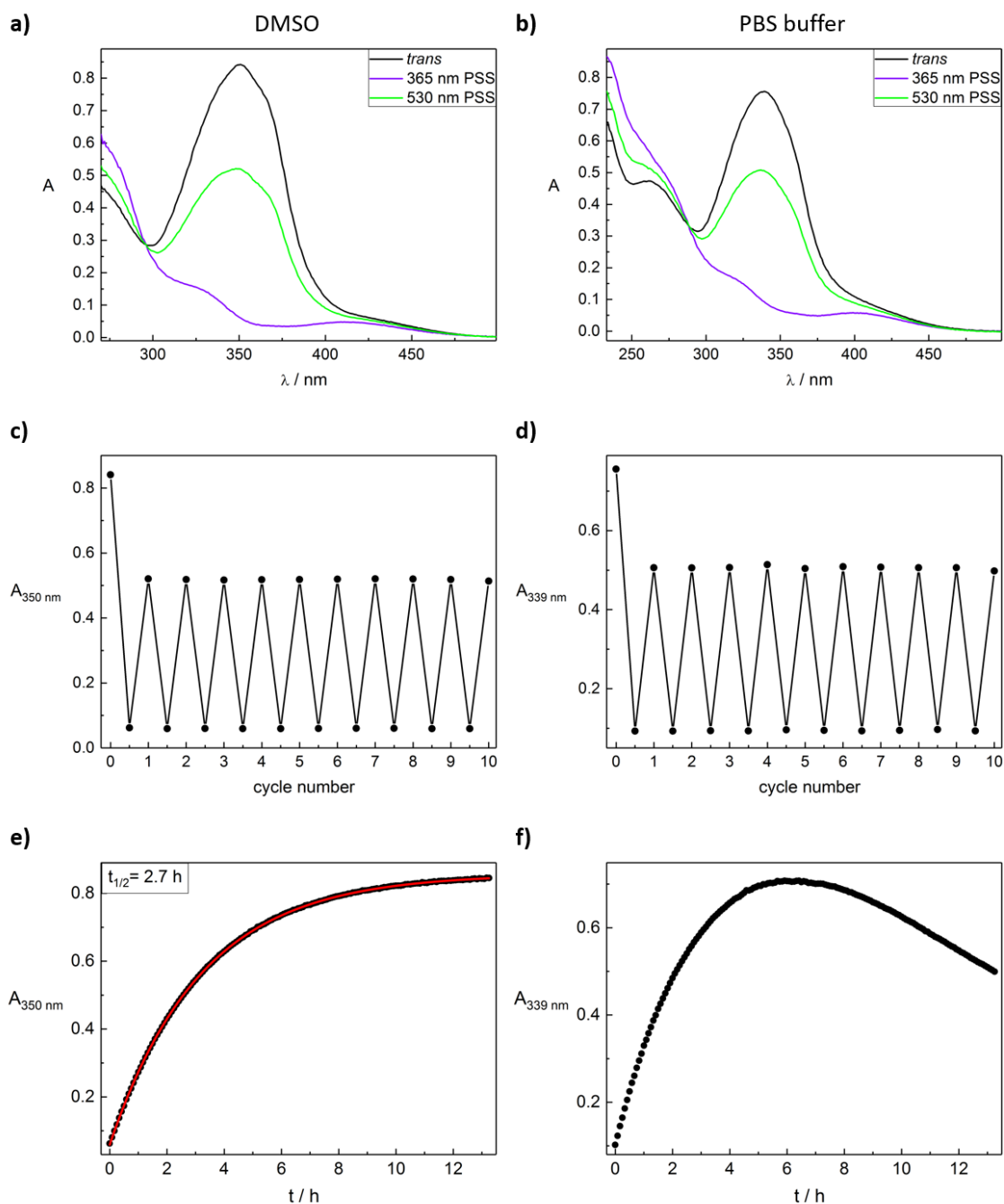
Figure S5. Photochromic data of compound **30**. **a)**, **b)** UV-Vis spectra of azo benzodiazepine **30** (**a**: 50 µM in DMSO; **b**: 50 µM in PBS + 0.1% DMSO) from the *trans* isomer, the PSS at irradiation with UV-light of 365 nm and the PSS at irradiation with blue light of 530 nm. **c)**, **d)** Cycle performance of azo benzodiazepine **30** (**c**: 50 µM in DMSO; **d**: 50 µM in PBS + 0.1% DMSO). Changes in absorption at λ_{max} of the *trans* isomer were measured during alternate irradiation with light of 365 nm and 530 nm. **e)**, **f)** Determination of the thermal half-lives of compound **30** at 25 °C (**e**: 50 µM in DMSO; **f**: 50 µM in PBS + 0.1% DMSO). Determination in PBS was not possible due to precipitation or decomposition.

Compound **31**
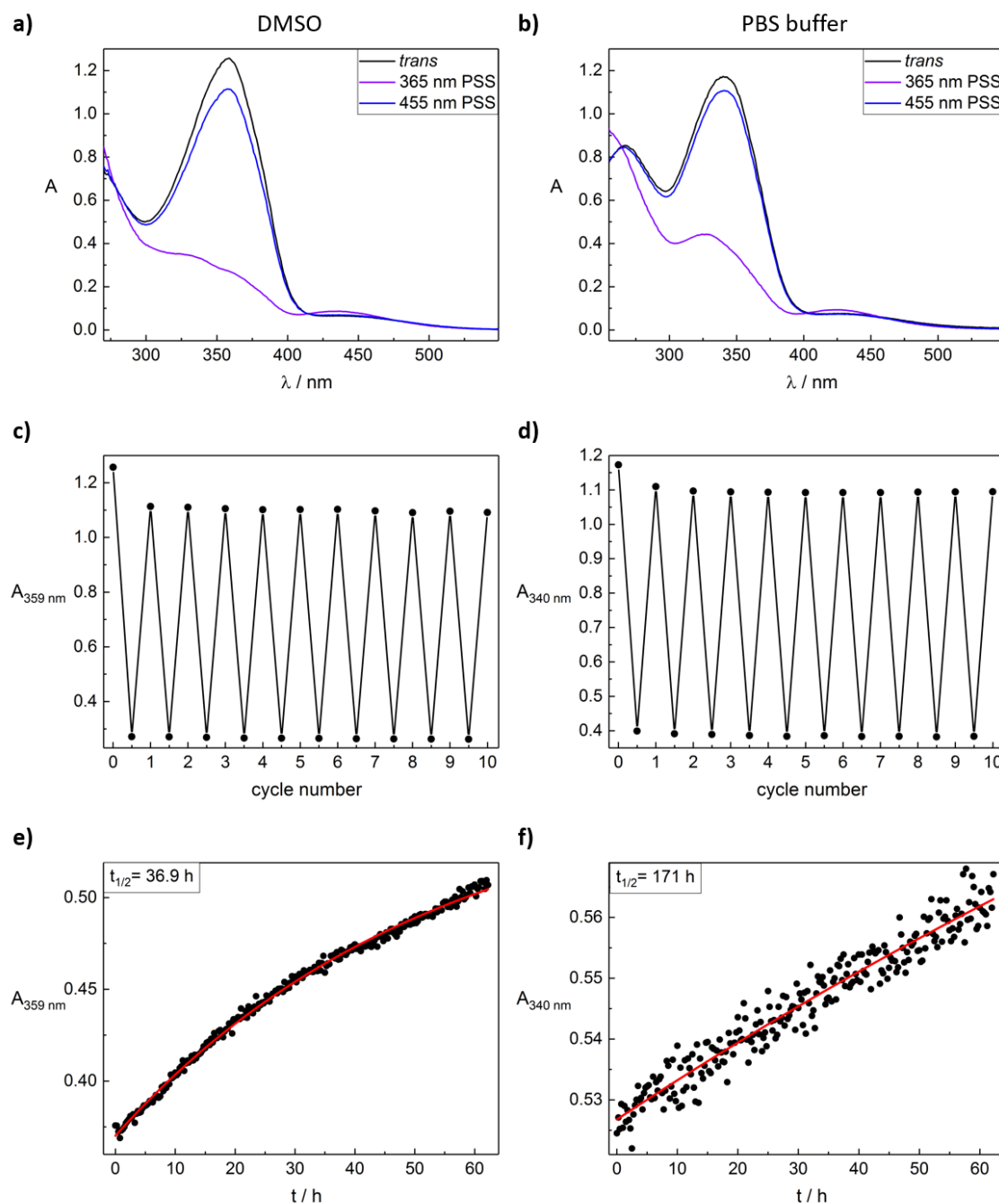
Figure S6. Photochromic data of compound **31**. **a), b)** UV-Vis spectra of azo benzodiazepine **31** (**a**: 50 µM in DMSO; **b**: 50 µM in PBS + 1% DMSO) from the *trans* isomer, the PSS at irradiation with UV-light of 365 nm and the PSS at irradiation with blue light of 455 nm. **c), d)** Cycle performance of azo benzodiazepine **31** (**c**: 50 µM in DMSO; **d**: 50 µM in PBS + 1% DMSO). Changes in absorption at λ_{max} of the *trans* isomer were measured during alternate irradiation with light of 365 nm and 455 nm. **e), f)** Determination of the thermal half-lives of compound **31** at 25 °C (**e**: 50 µM in DMSO; **f**: 50 µM in PBS + 1% DMSO).

Compound **32**
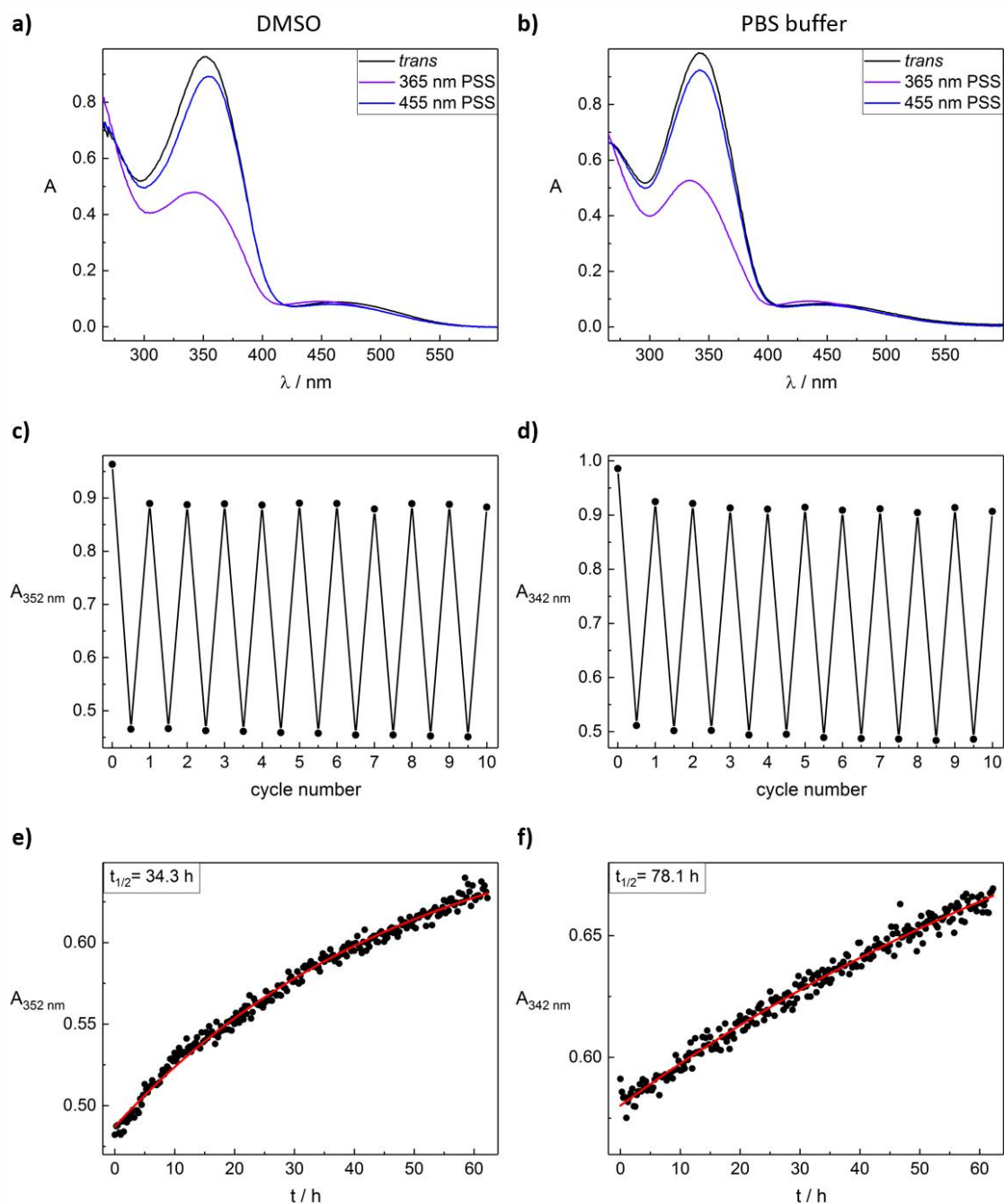
Figure S7. Photochromic data of compound **32**. **a), b)** UV-Vis spectra of azo benzodiazepine **32** (**a**: 50 µM in DMSO; **b**: 50 µM in PBS + 1% DMSO) from the *trans* isomer, the PSS at irradiation with UV-light of 365 nm and the PSS at irradiation with blue light of 455 nm. **c), d)** Cycle performance of azo benzodiazepine **32** (**c**: 50 µM in DMSO; **d**: 50 µM in PBS + 1% DMSO). Changes in absorption at λ_{max} of the *trans* isomer were measured during alternate irradiation with light of 365 nm and 455 nm. **e), f)** Determination of the thermal half-lives of compound **32** at 25 °C (**e**: 50 µM in DMSO; **f**: 50 µM in PBS + 1% DMSO).

Compound **50**

Figure S8. Photochromic data of compound **50**. **a)** UV-Vis spectra of azo nicardipine **50** (10 μM in DMSO) from the *trans* isomer, the PSS at irradiation with blue light of 455 nm and the PSS at irradiation with orange light of 590 nm. **b)** Cycle performance of azo nicardipine **50** (10 μM in DMSO). Changes in absorption at λ_{max} of the *trans* isomer were measured during alternate irradiation with light of 455 nm and 590 nm. **c)** Determination of the thermal half-life of compound **50** at 25 °C (10 μM in DMSO).

Compound **51**

Figure S9. Photochromic data of compound **51**. **a)** UV-Vis spectra of azo nicardipine **51** (25 µM in PBS + 1% DMSO) from the *trans* isomer and the PSS at irradiation with blue light of 455 nm. **b)** Cycle performance of azo nicardipine **51** (25 µM in PBS + 1% DMSO). Changes in absorption at λ_{max} of the *trans* isomer were measured during alternate irradiation with light of 455 nm and thermal relaxation **c), d)** Determination of the thermal half-lives of compound **51** at 25 °C (**c**: 25 µM in DMSO; **d**: 25 µM in PBS + 1% DMSO). The thermal half-life in PBS could not properly be determined due to the described aggregation effect and additionally a very short thermal half-life. By comparison to the measurement in DMSO the half-life in PBS has to be < 0.3 s.

Compound **52**

a)

b)

c)

Figure S10. Photochromic data of compound **52**. **a)** UV-Vis spectra of azo nicardipine **52** (25 µM in DMSO) from the *trans* isomer, the PSS at irradiation with blue light of 455 nm and the PSS at irradiation with UV-light of 385 nm. **b)** Cycle performance of azo nicardipine **52** (25 µM in DMSO). Changes in absorption at λ_{max} of the *trans* isomer were measured during alternate irradiation with light of 455 nm and 385 nm. **c)** Determination of the thermal half-life of compound **52** at 25 °C (25 µM in DMSO).

Compound **53**

Figure S11. a), **b)** UV-Vis spectra of the *trans* isomer of azo nicardipine **53** (**a**: 15 µM in DMSO; **b**: 15 µM in PBS + 1% DMSO).

^{1}H- and ^{13}C-NMR spectra

Compound **6**
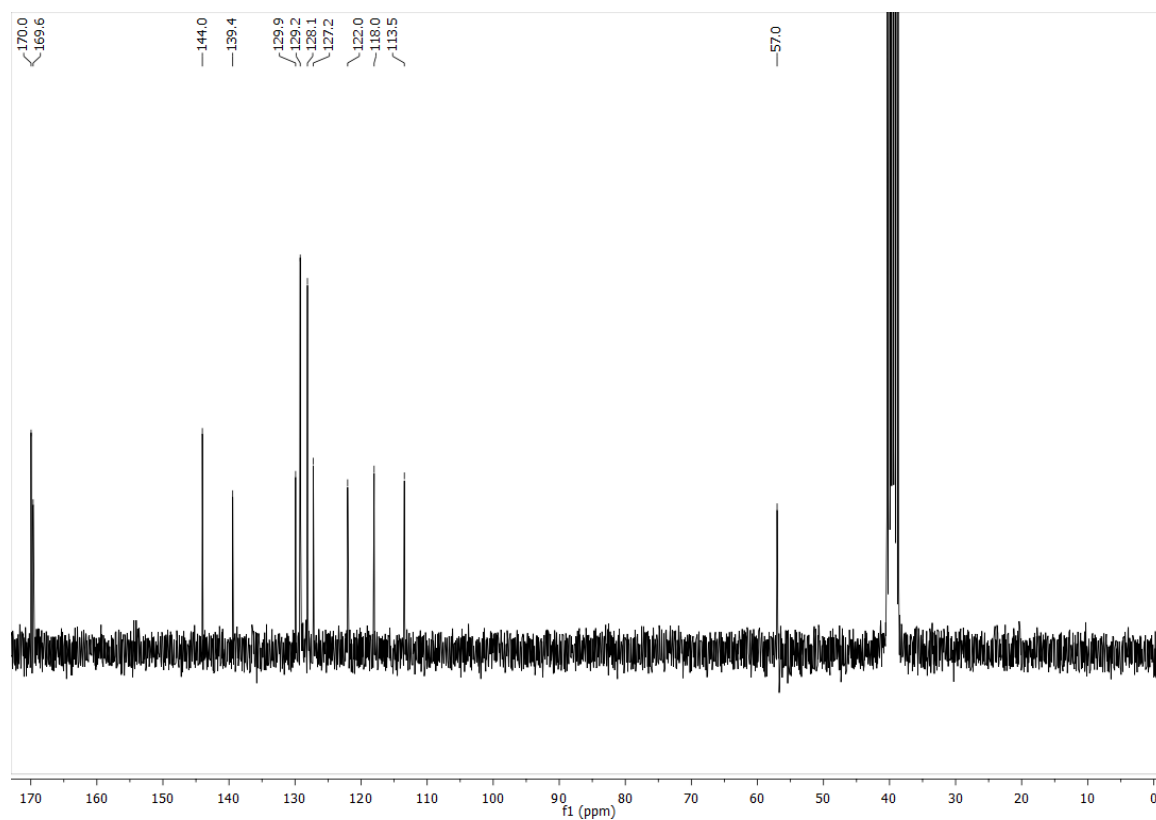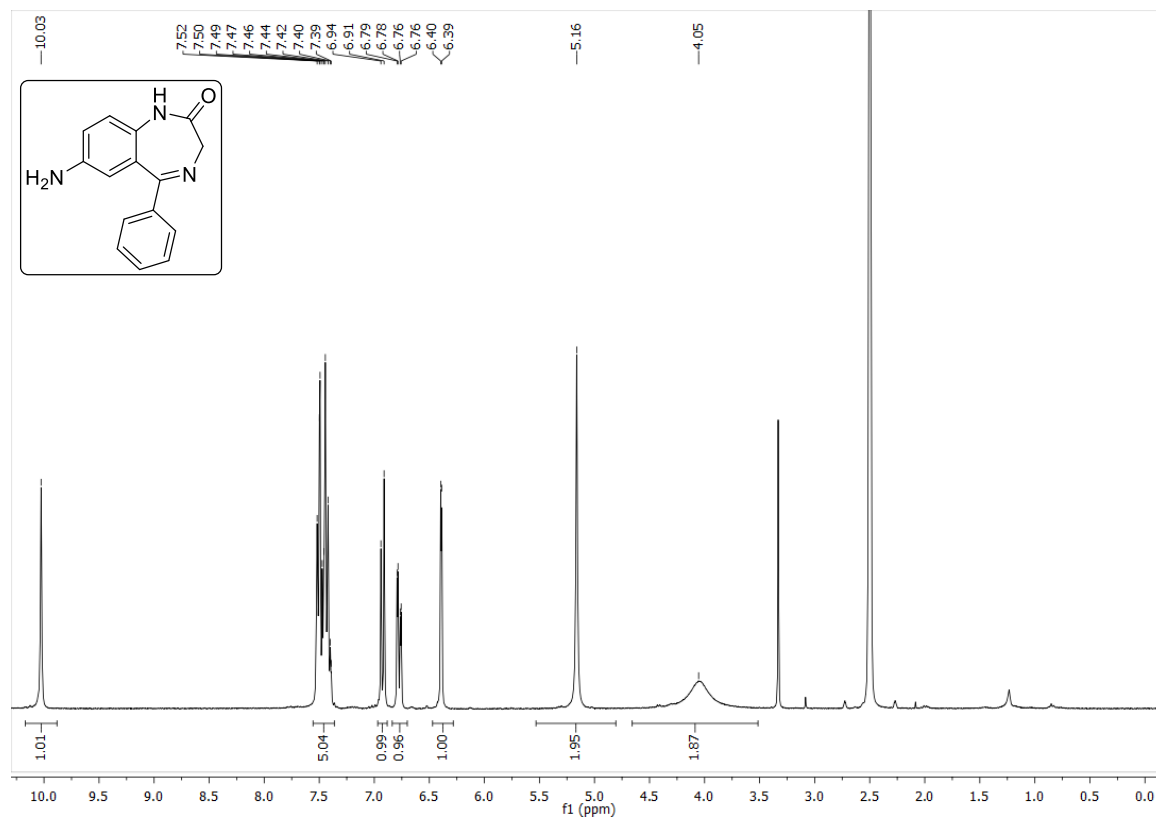
Compound **8**
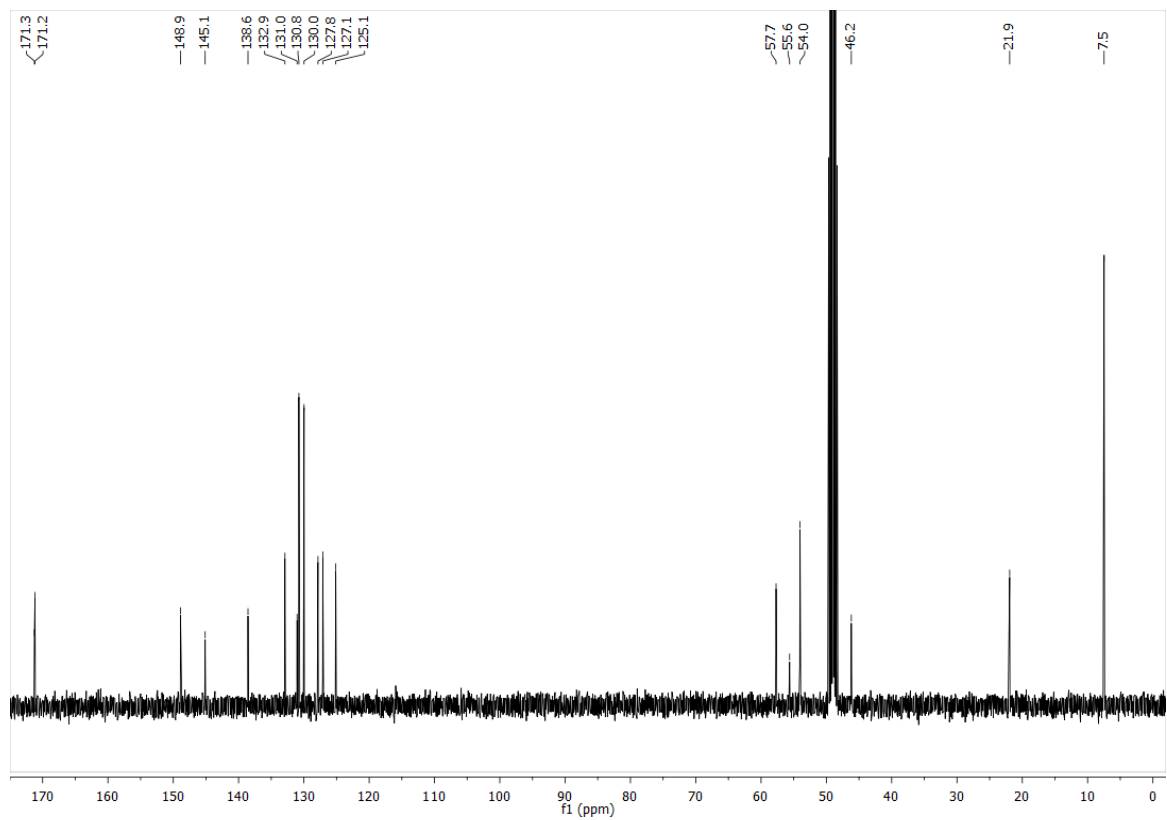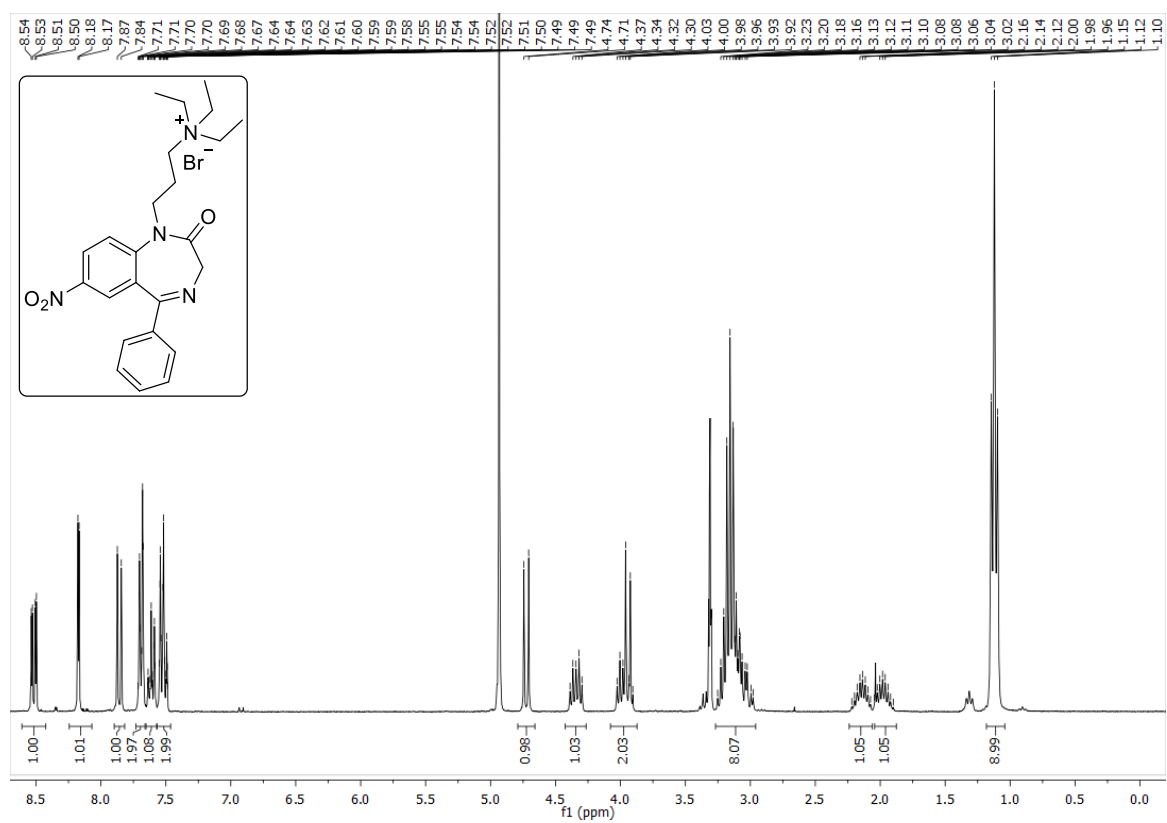
Compound **26**
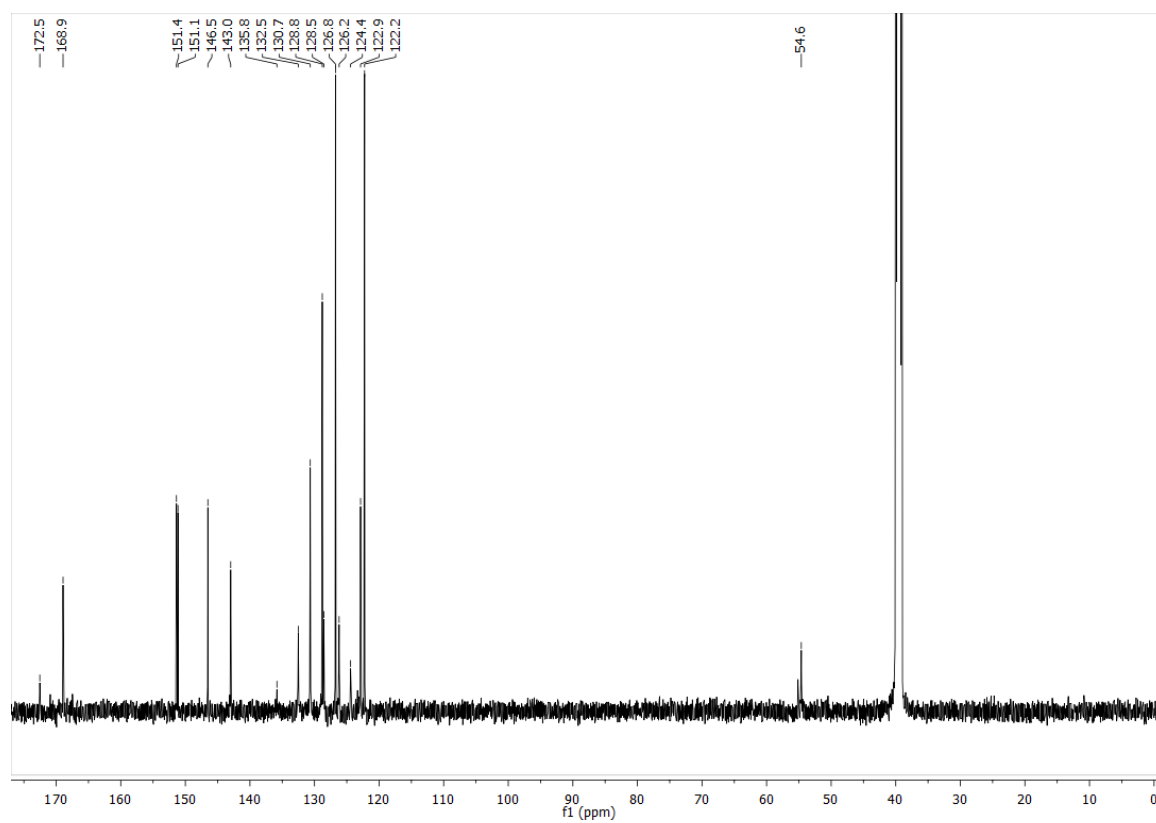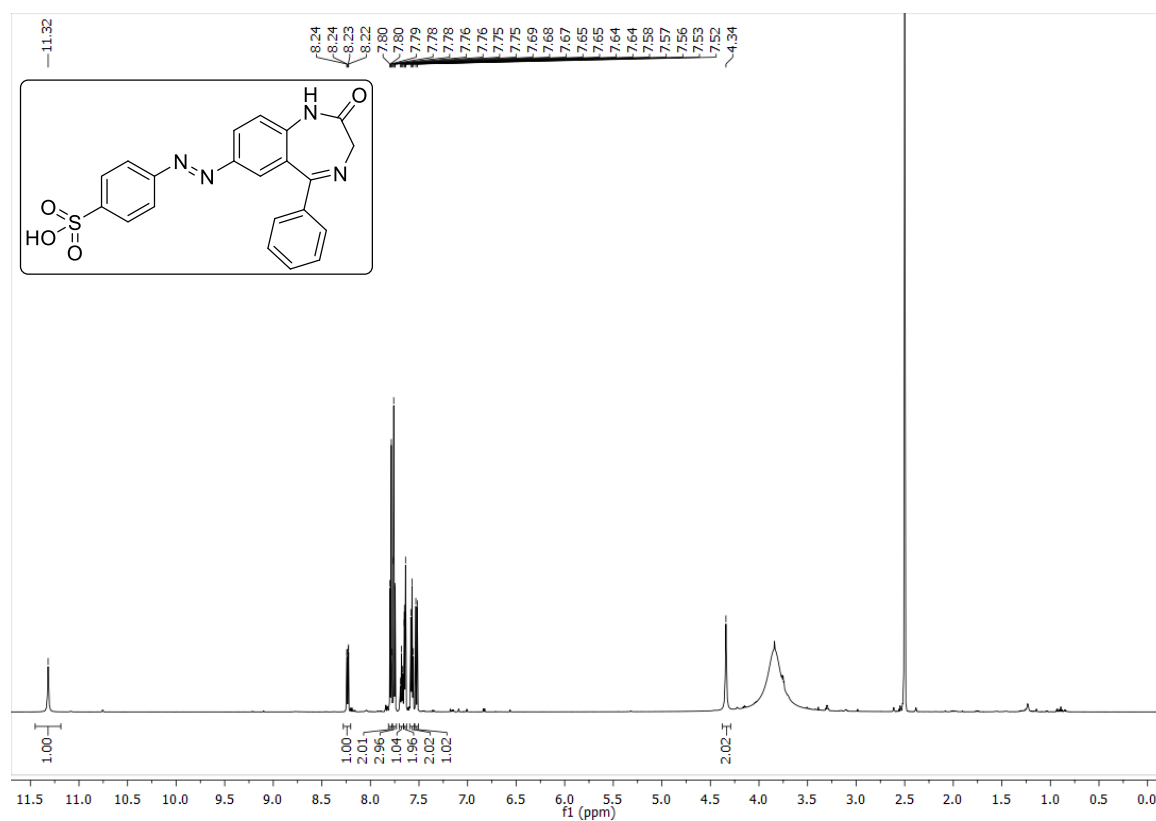
Compound **27**
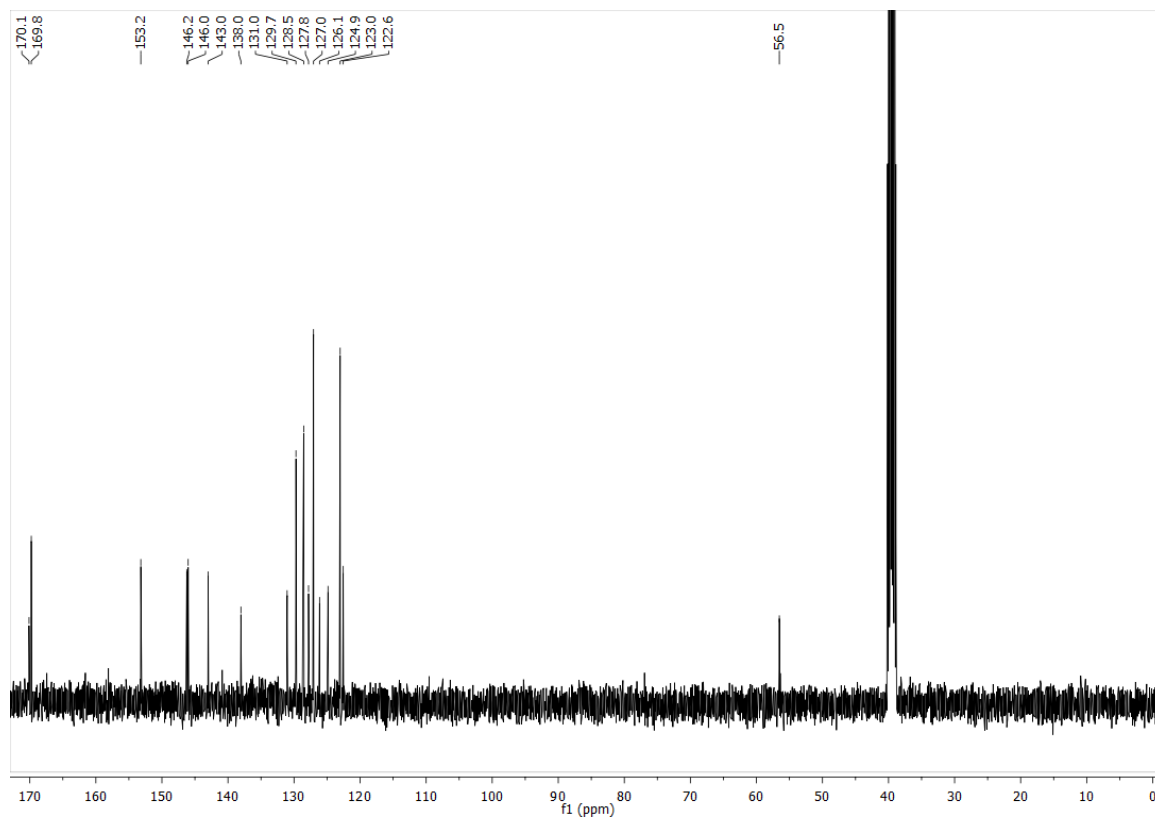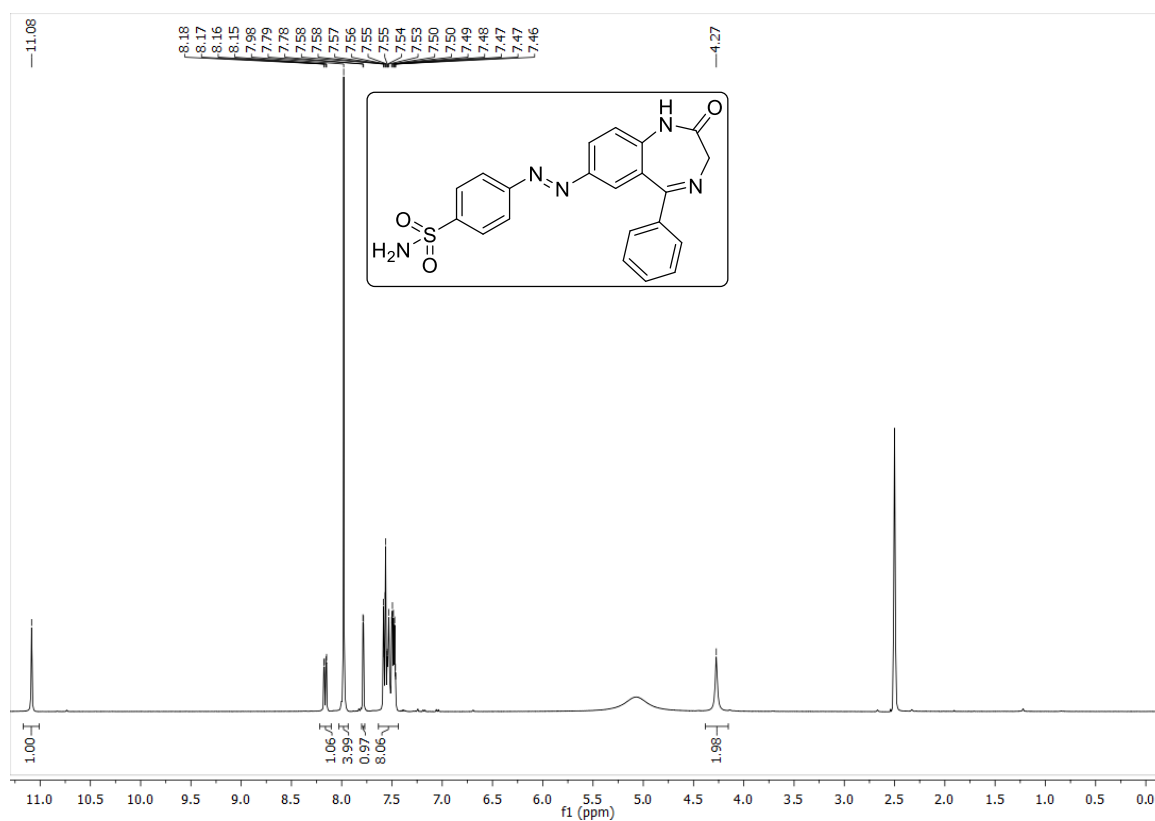
Compound **28**
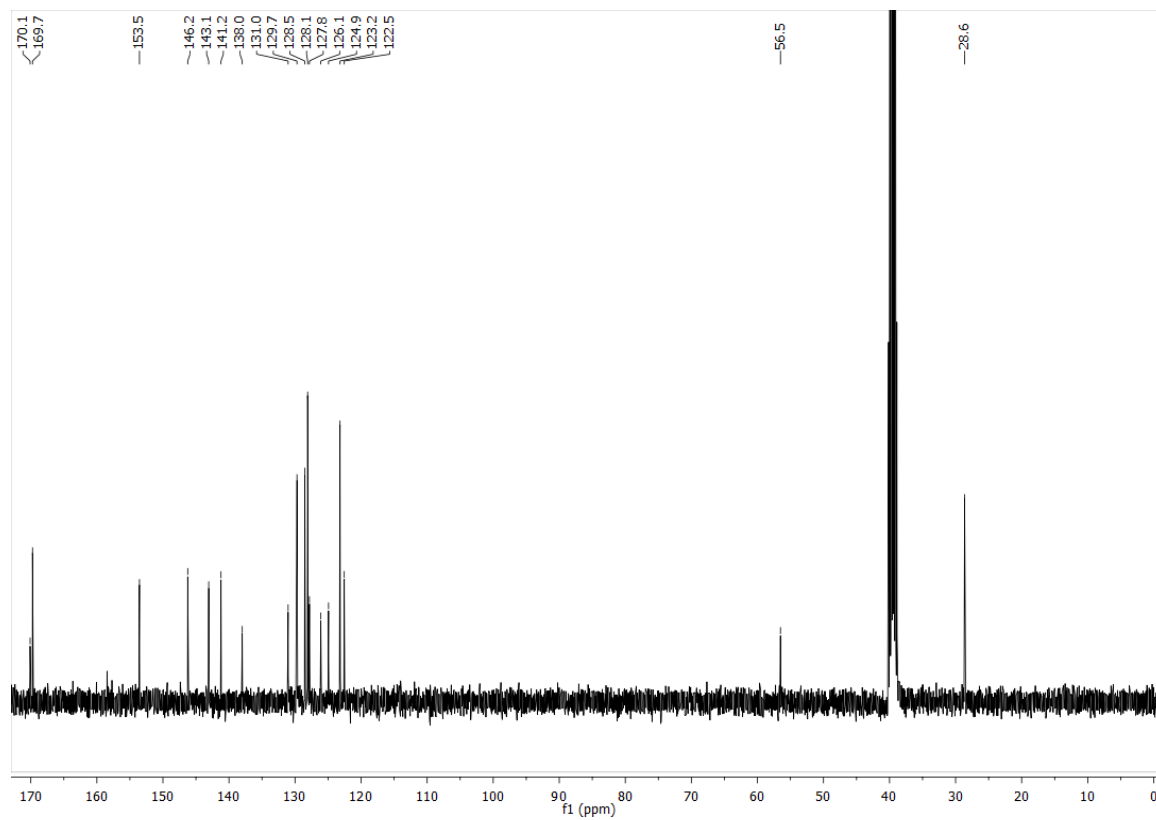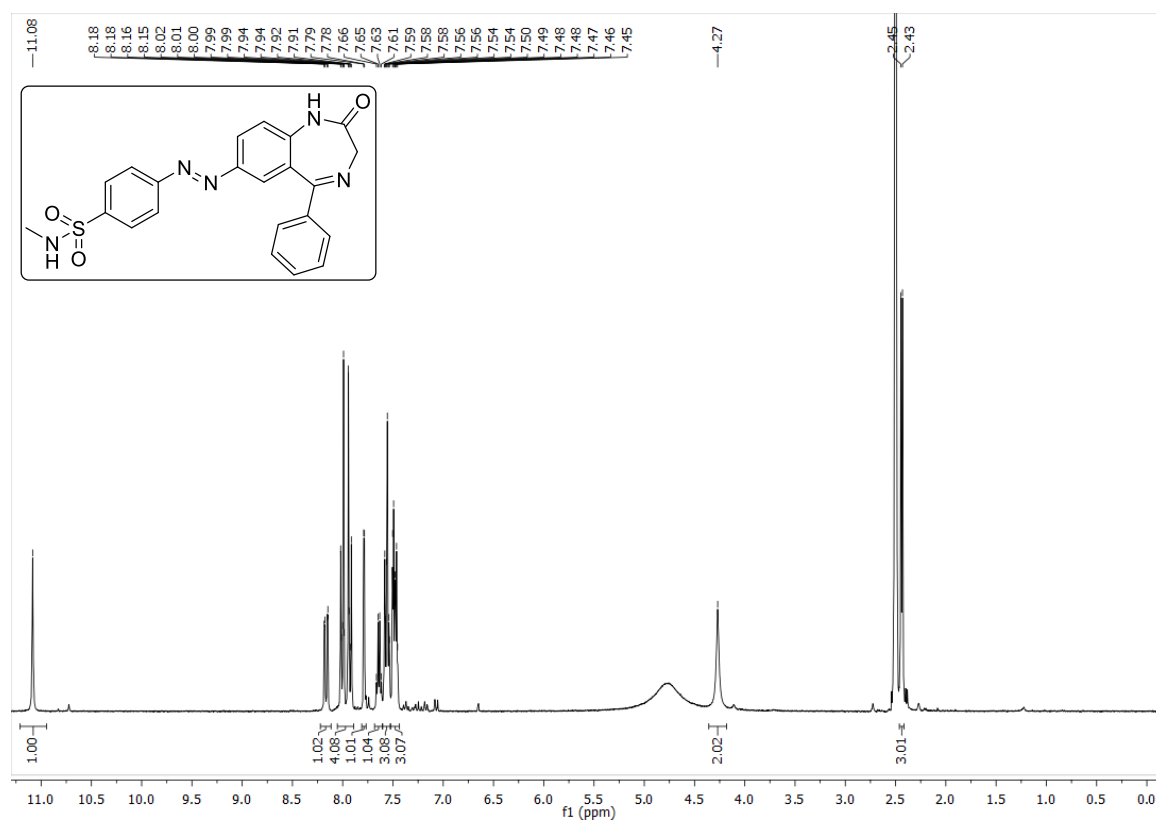
Compound 29
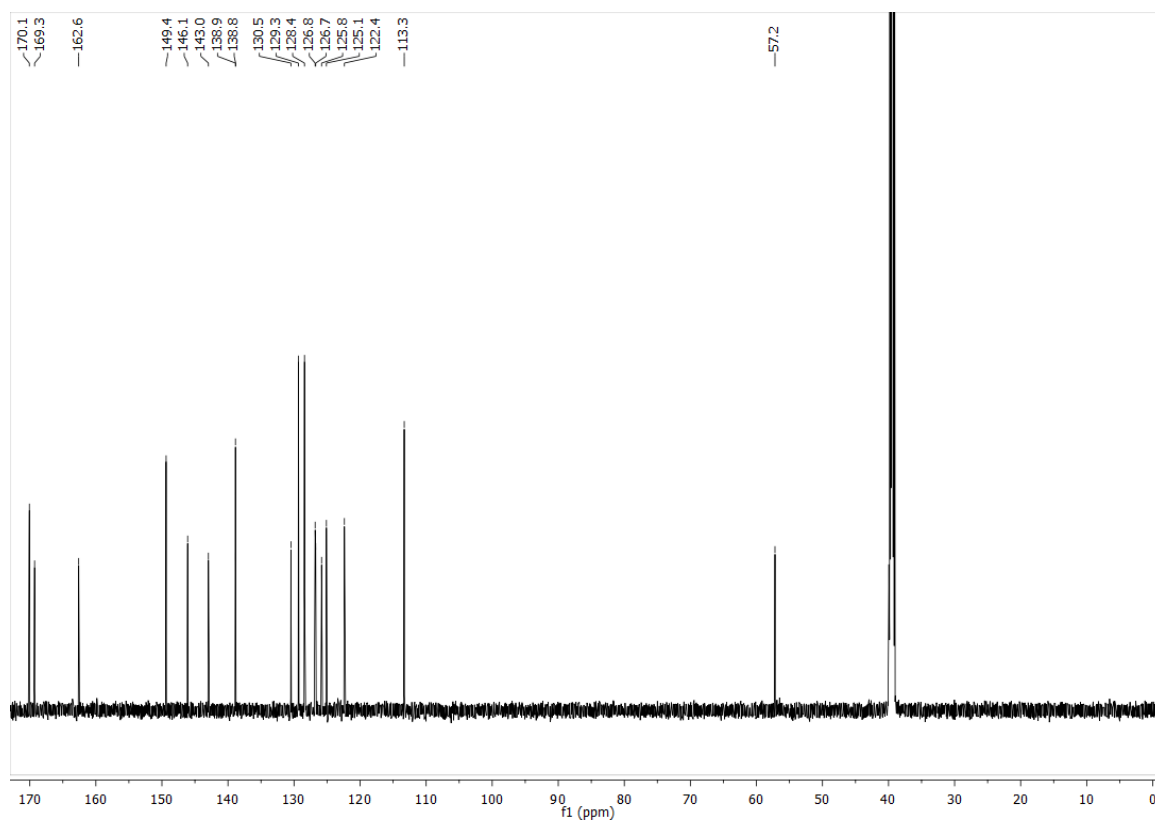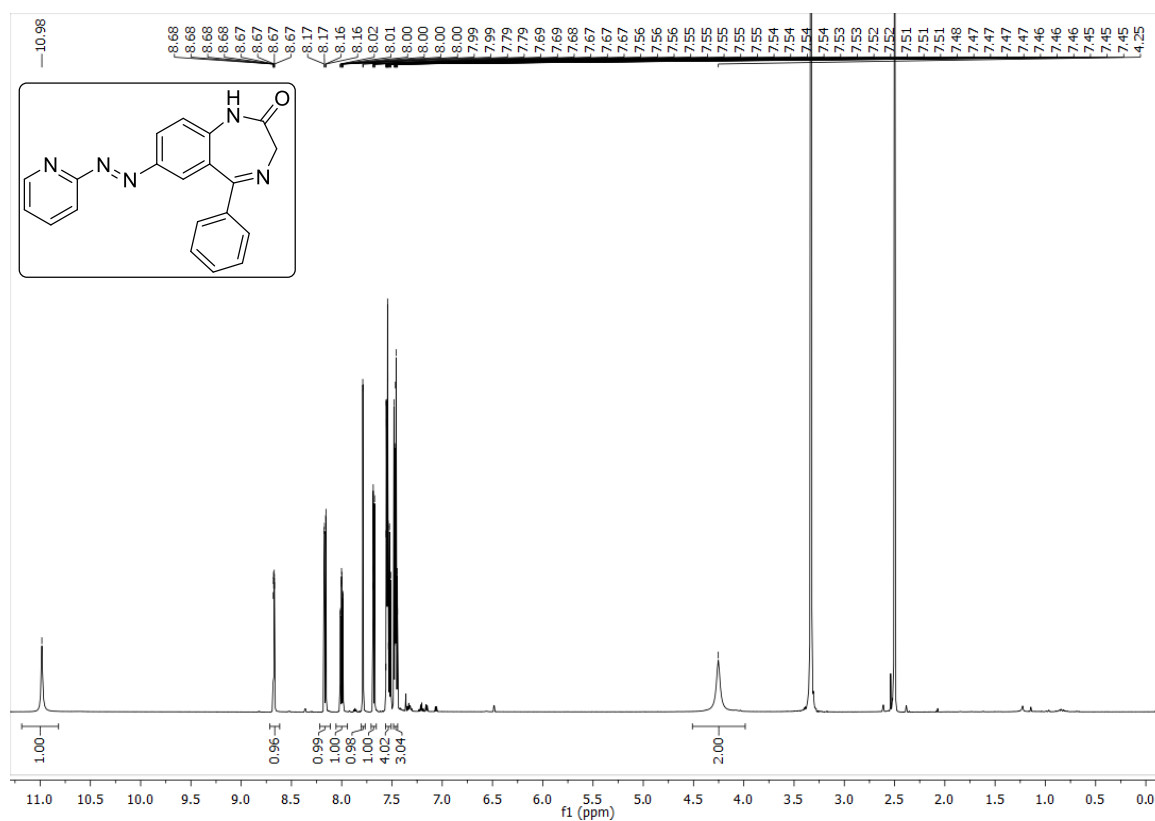
Compound **30**
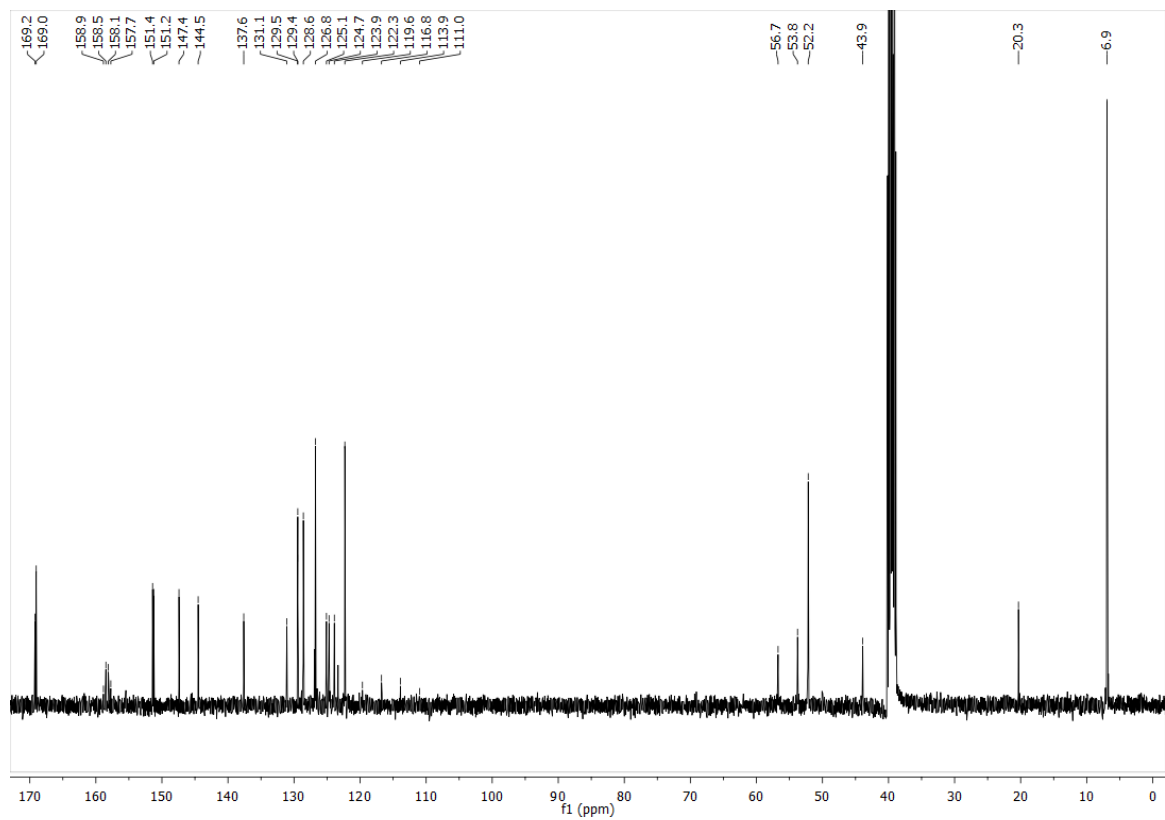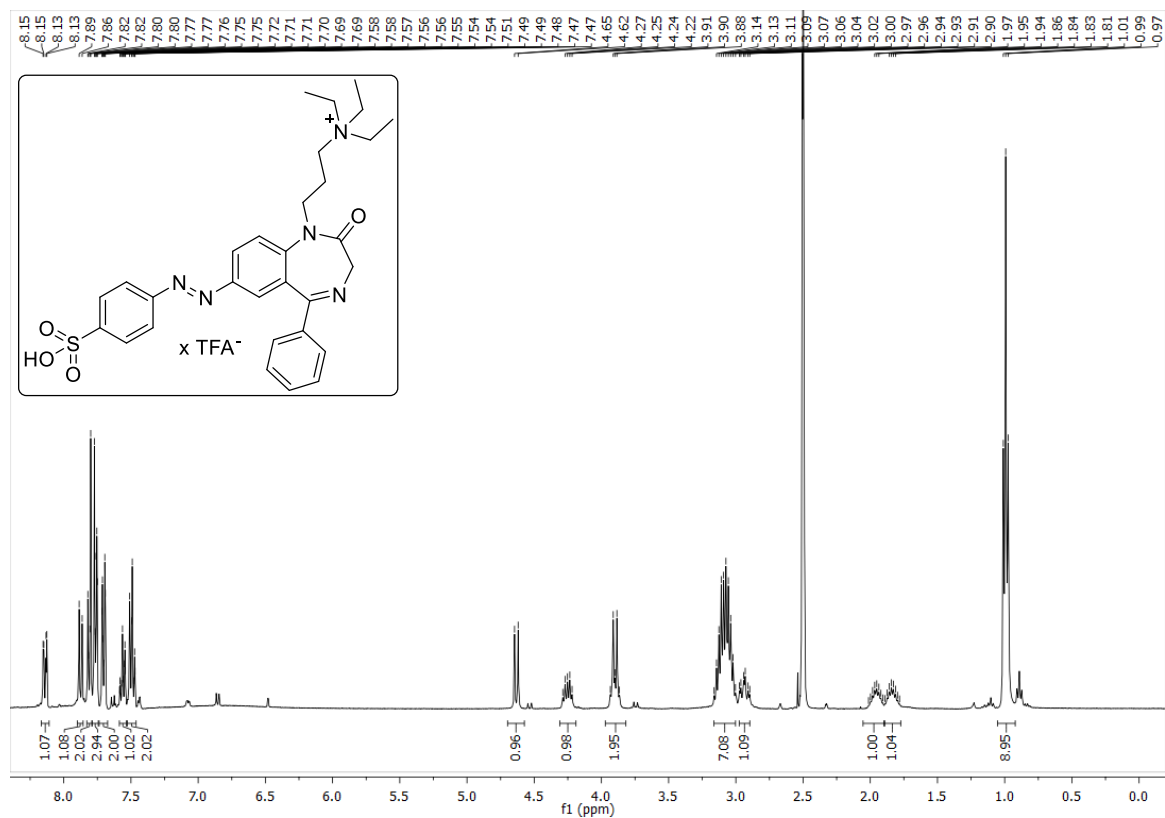
Compound **31**

Compound 32
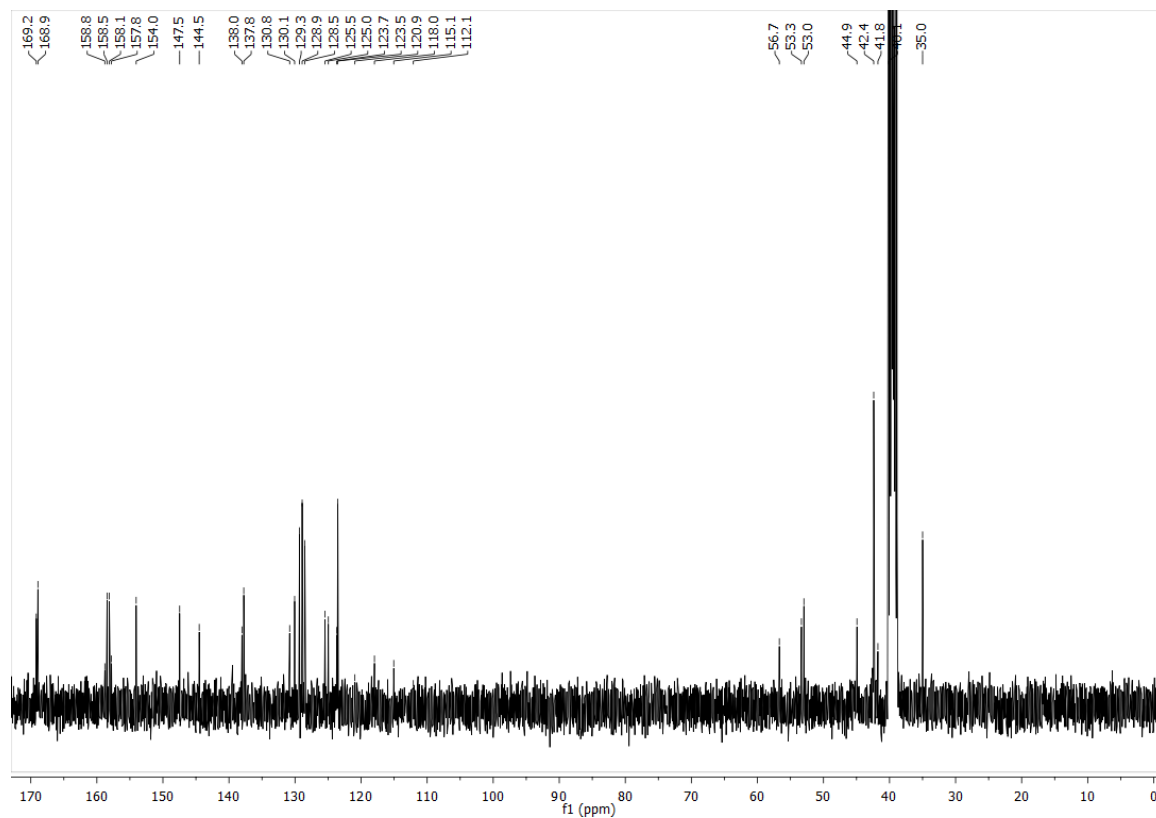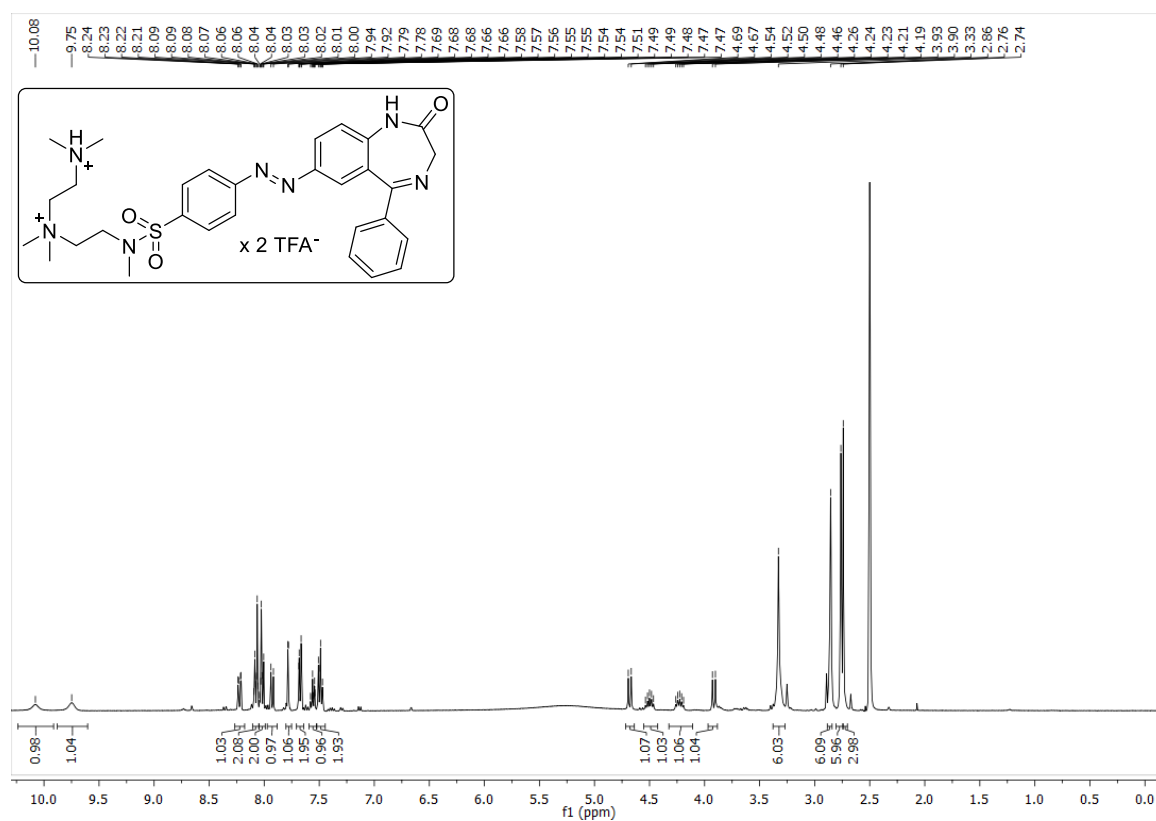
Compound **40**
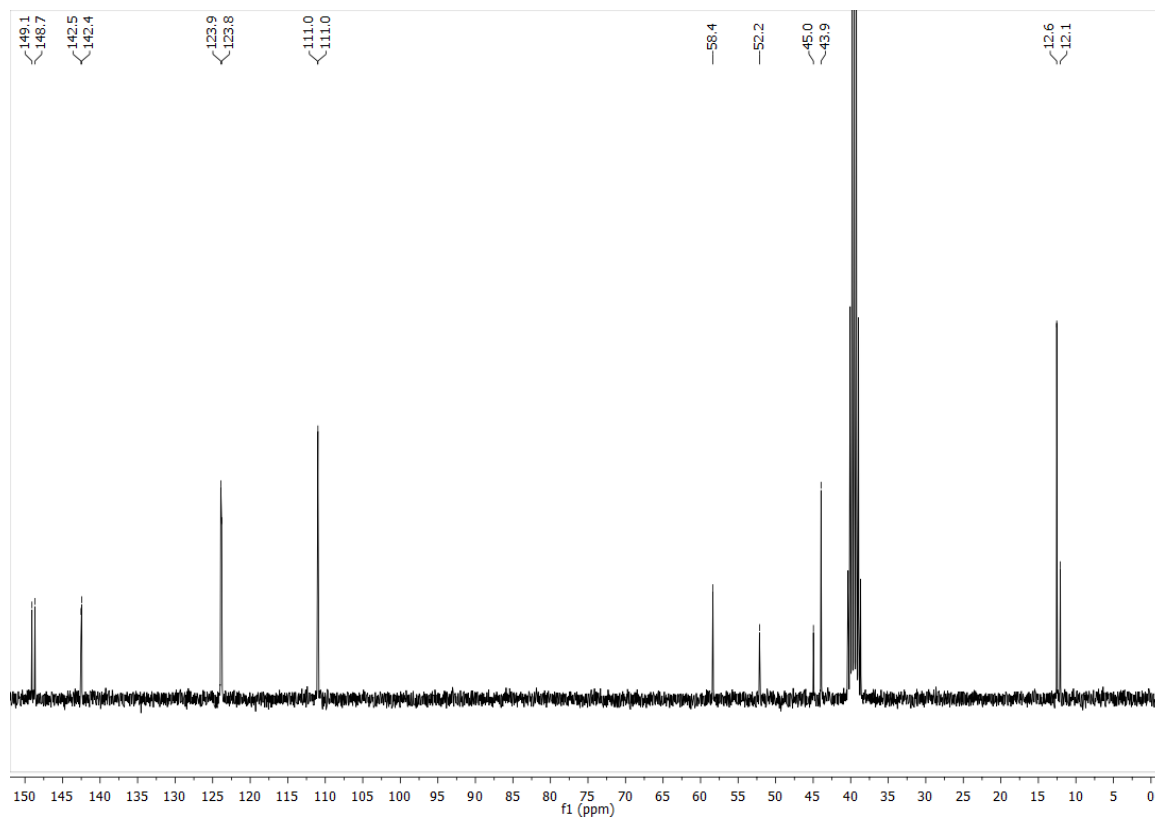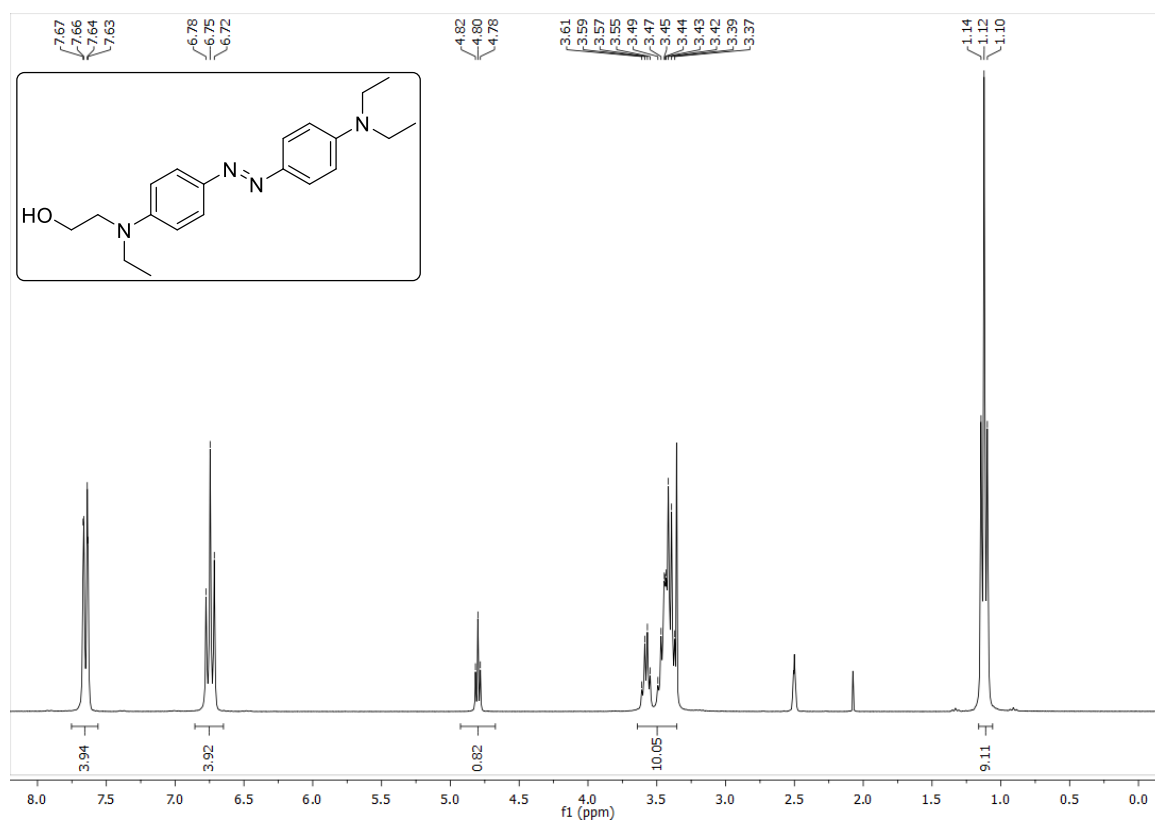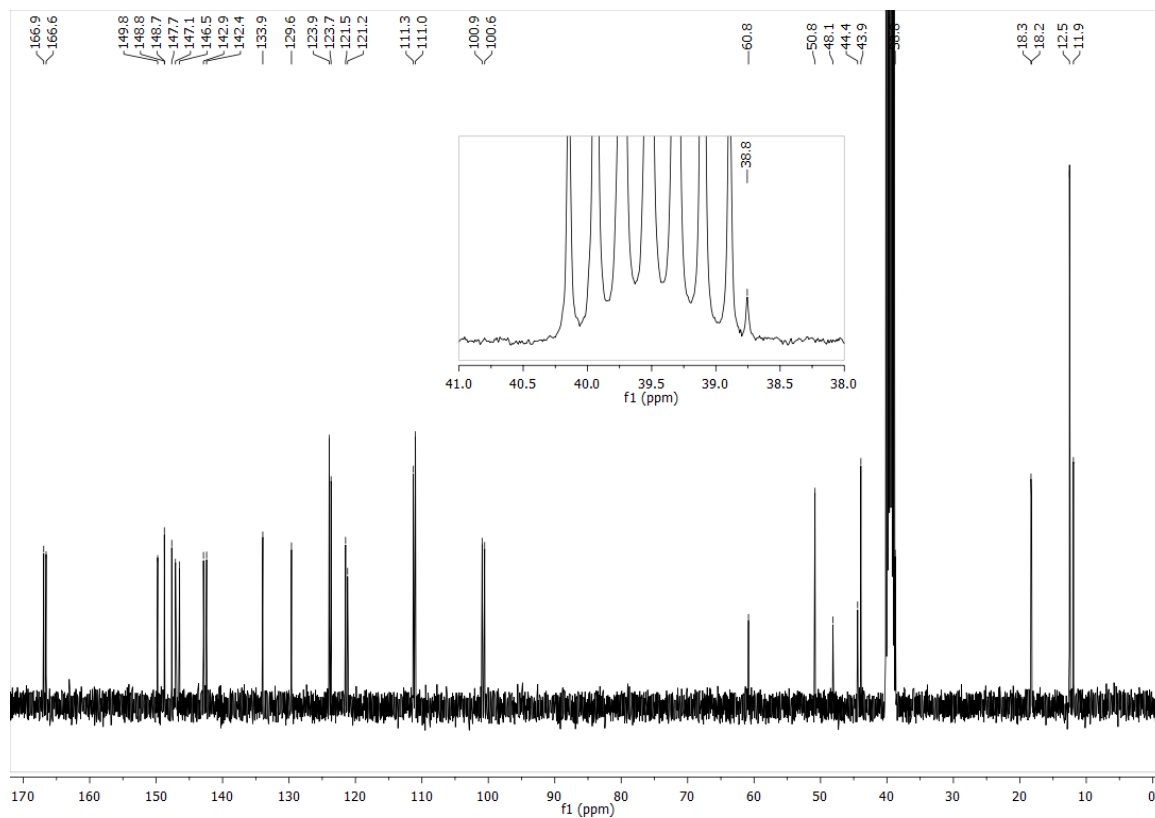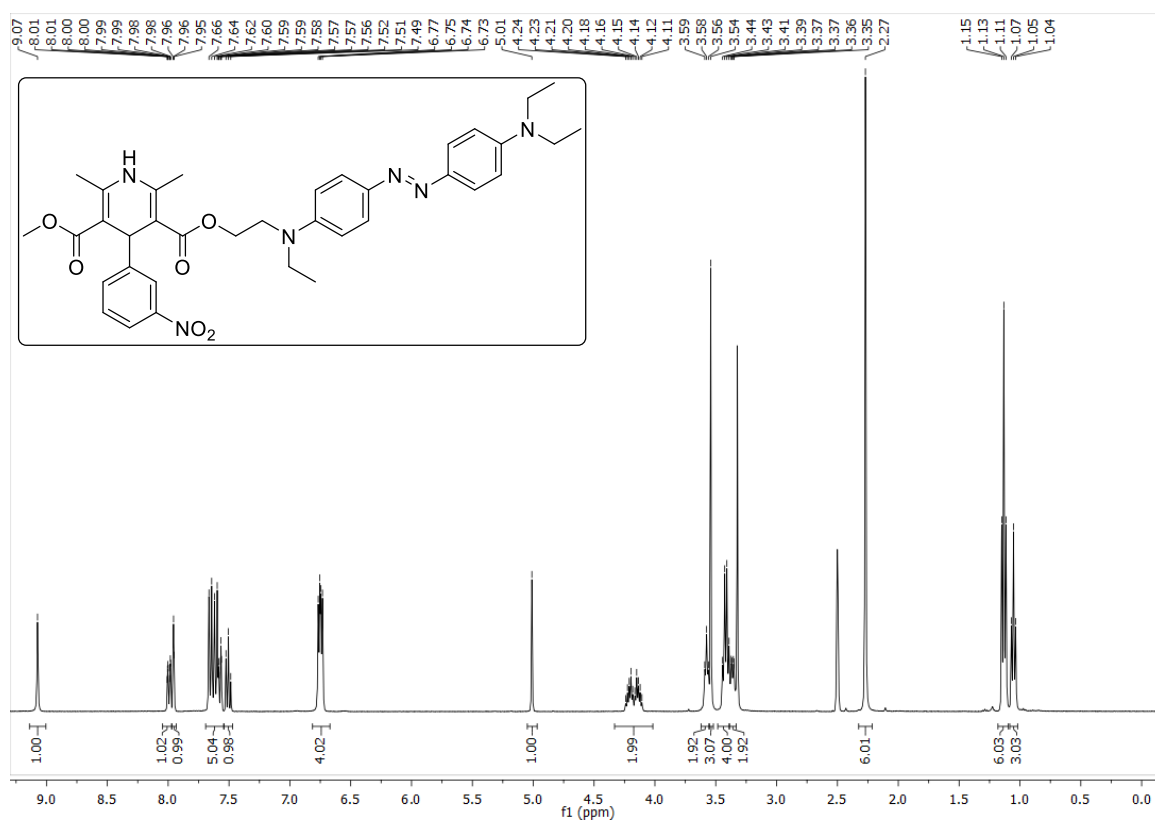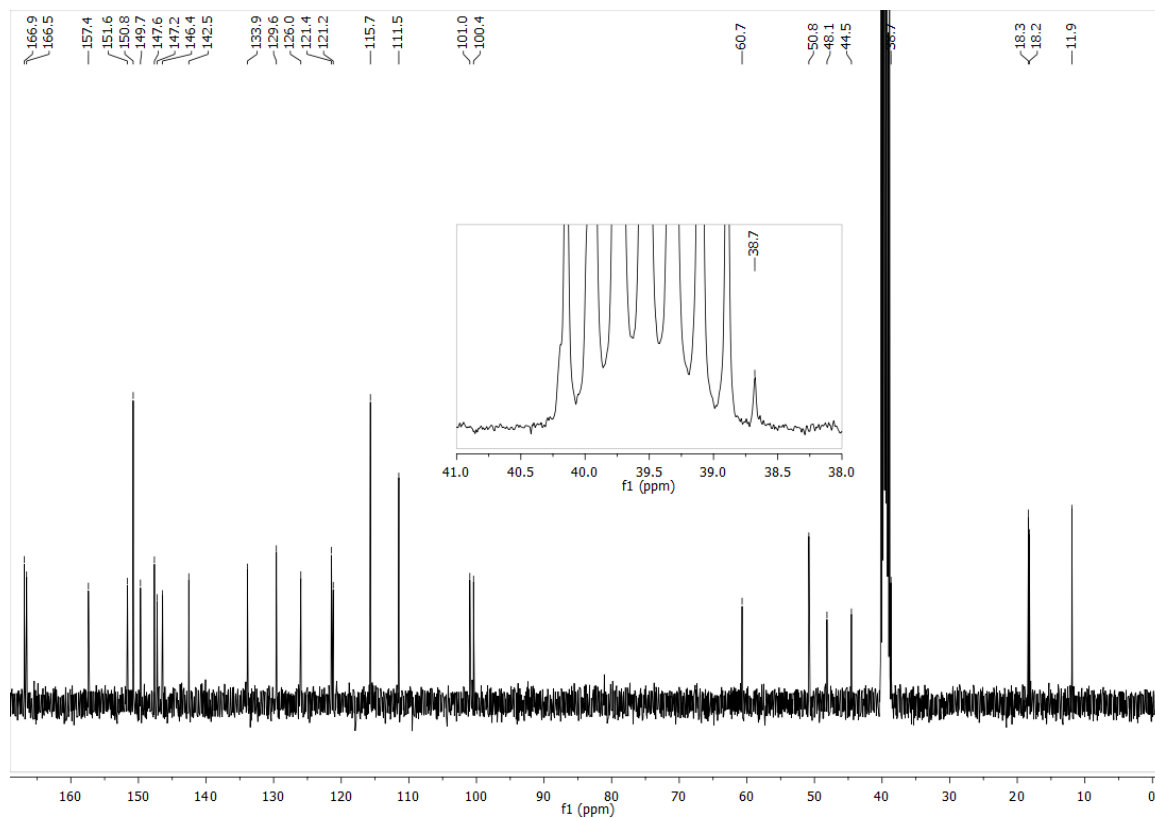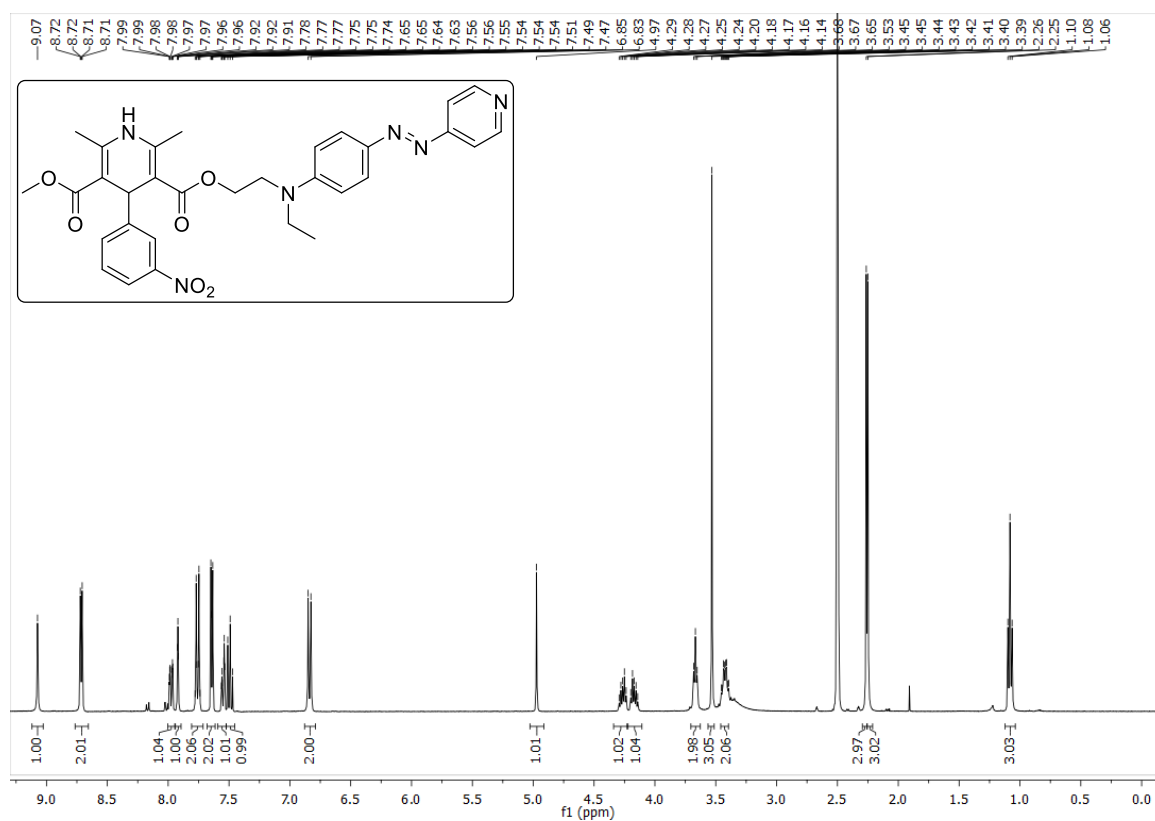
Compound **44**
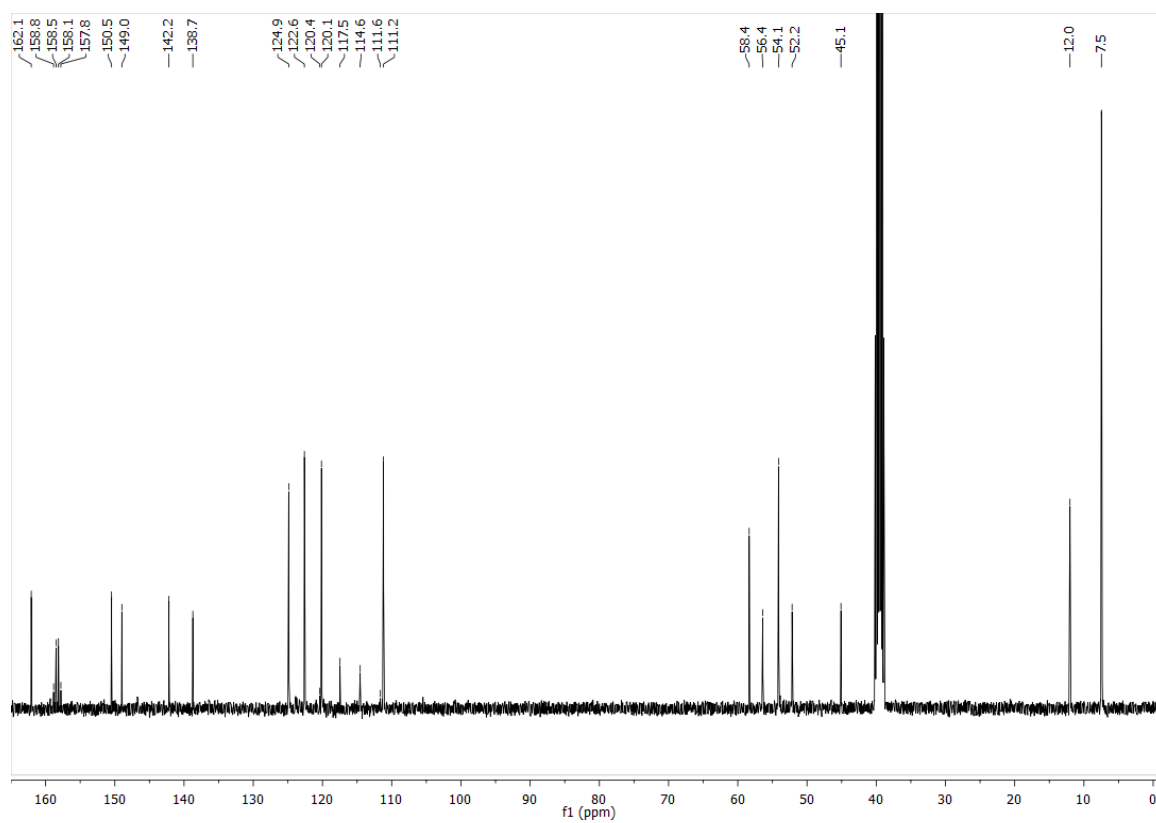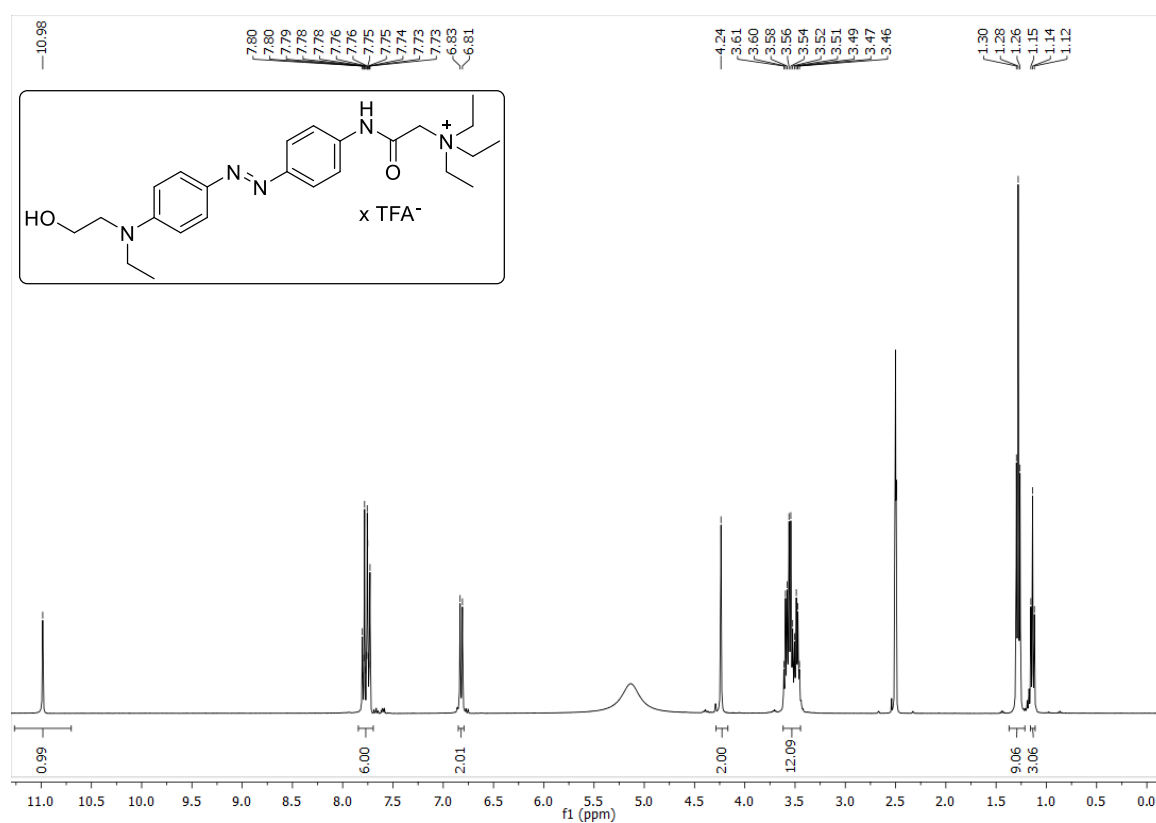
Compound **47**
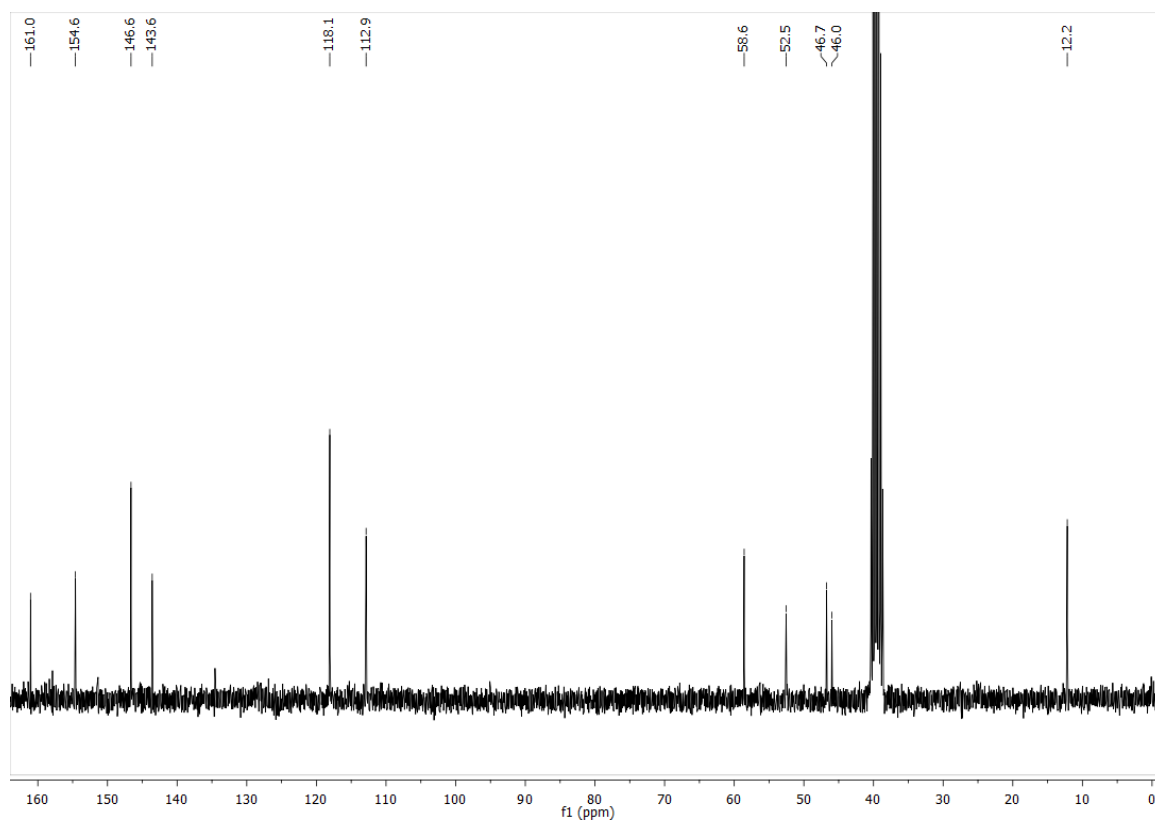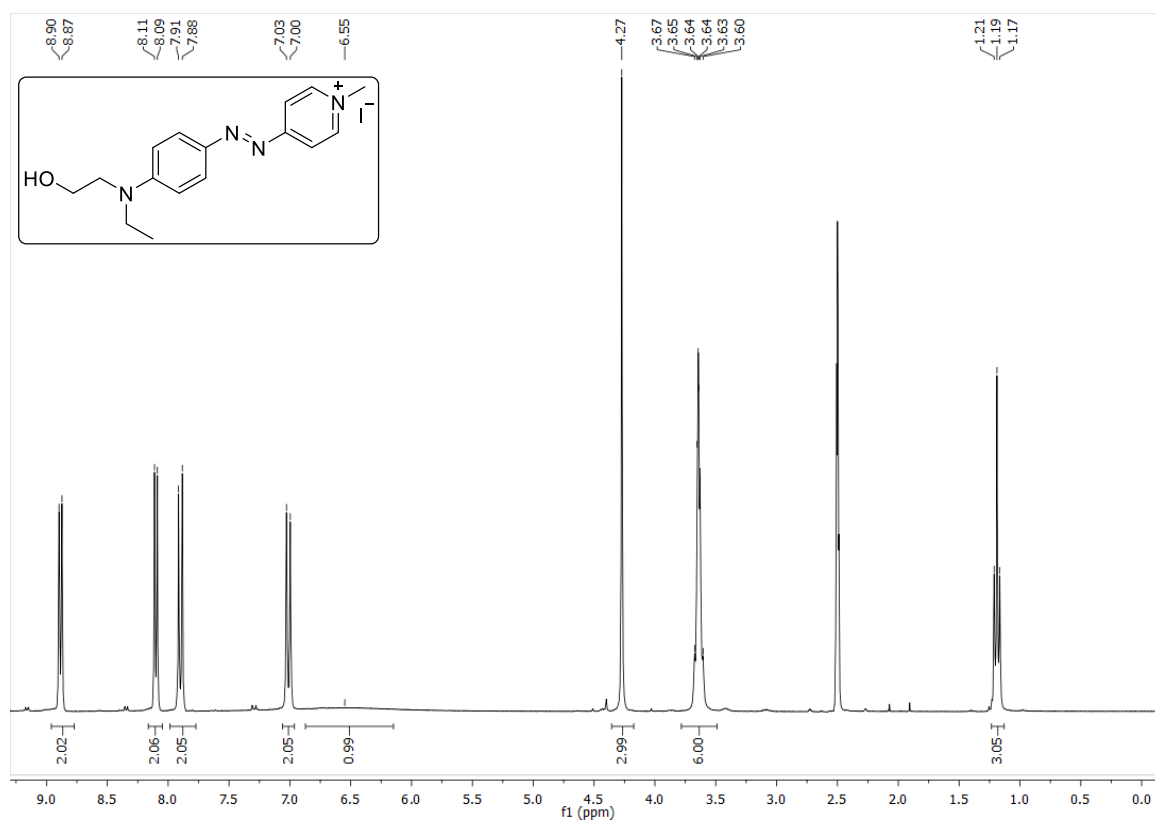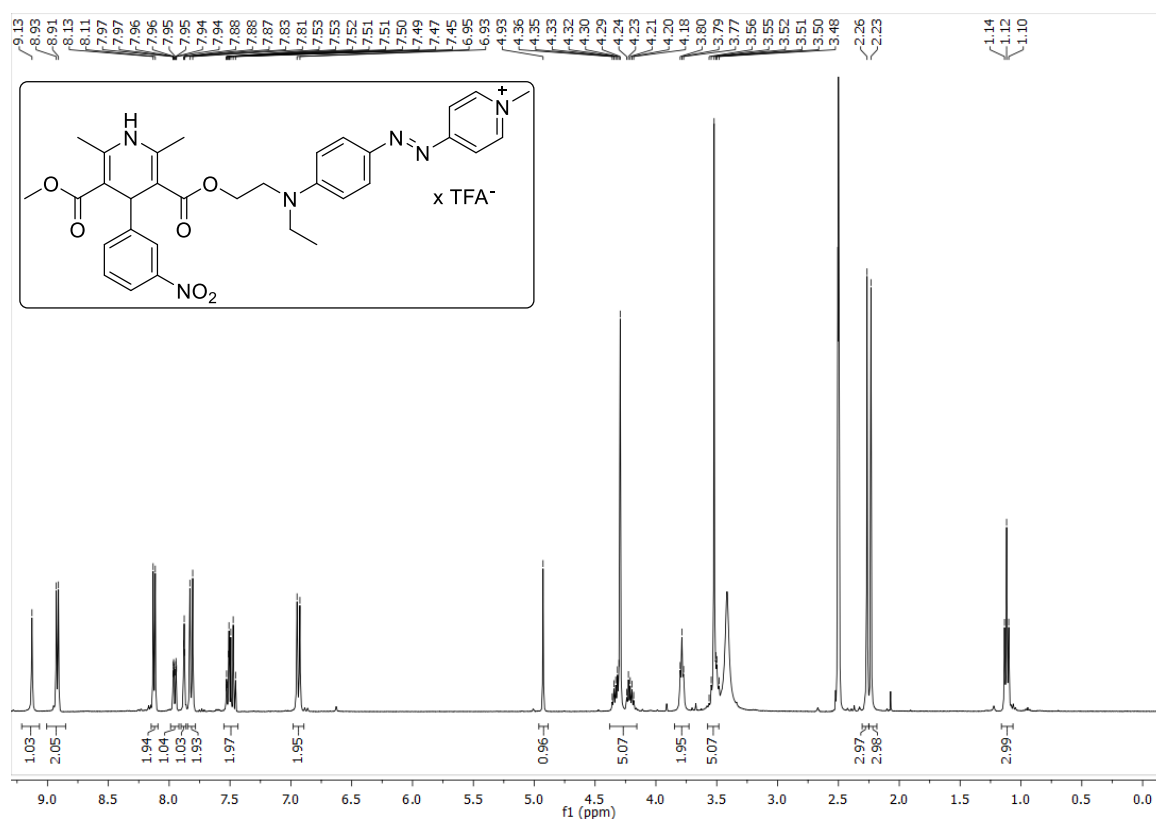
Compound **48**
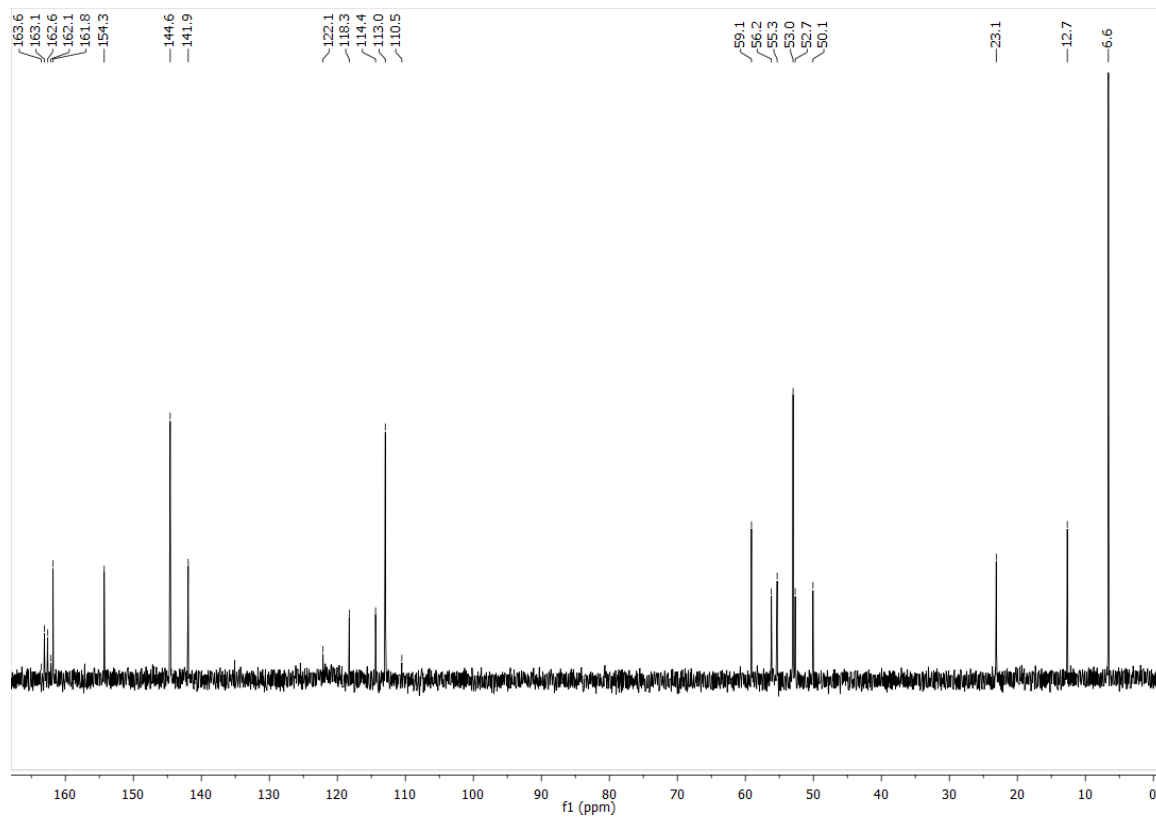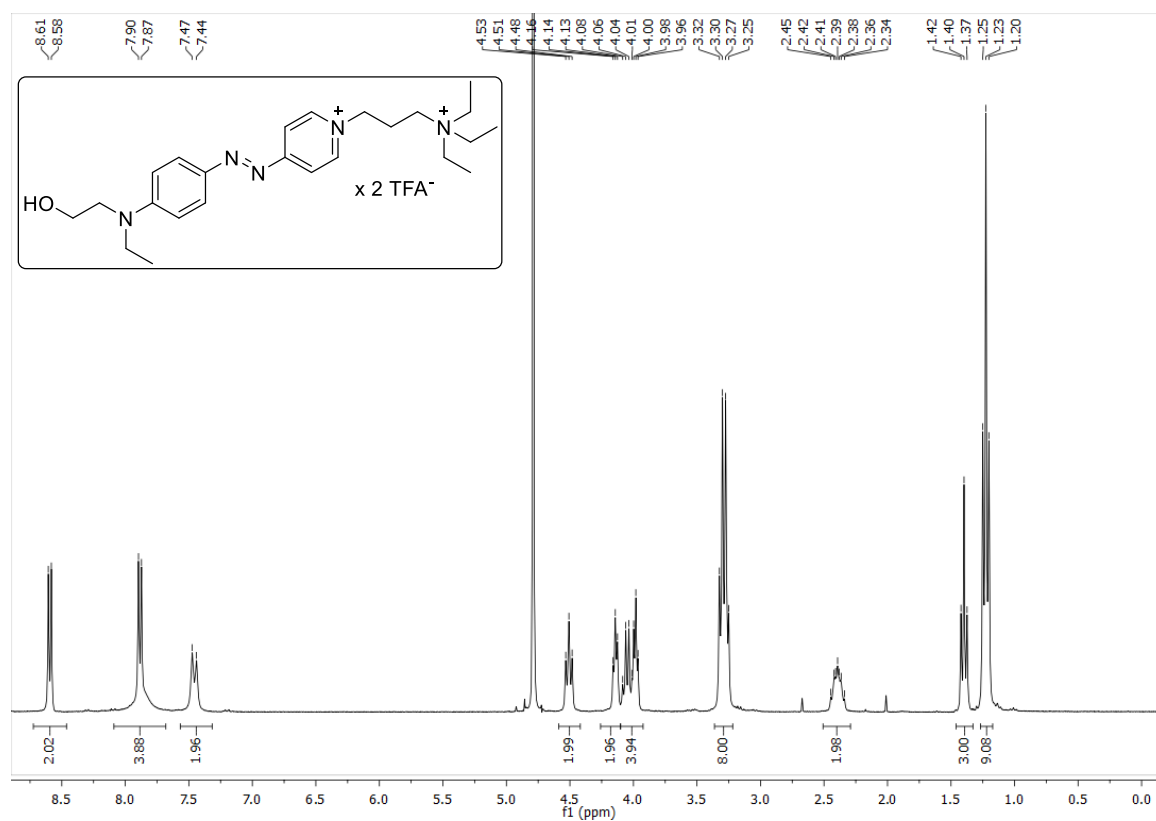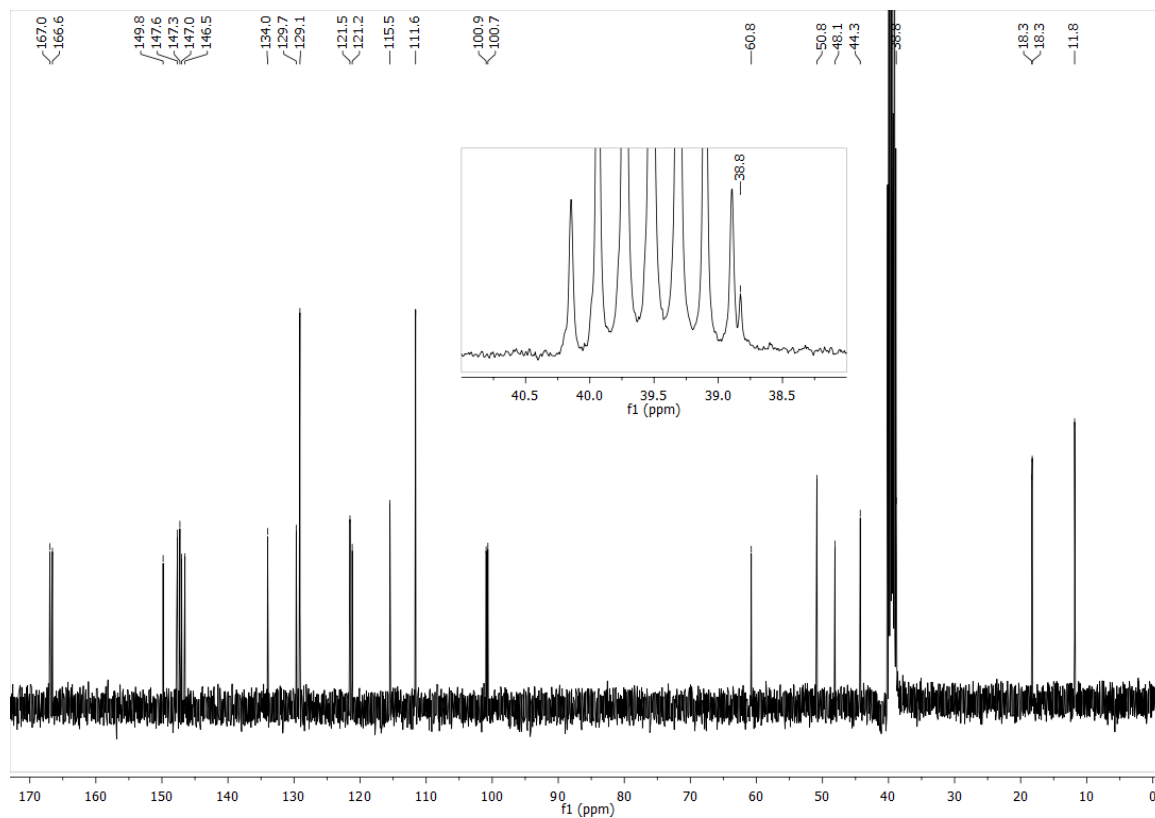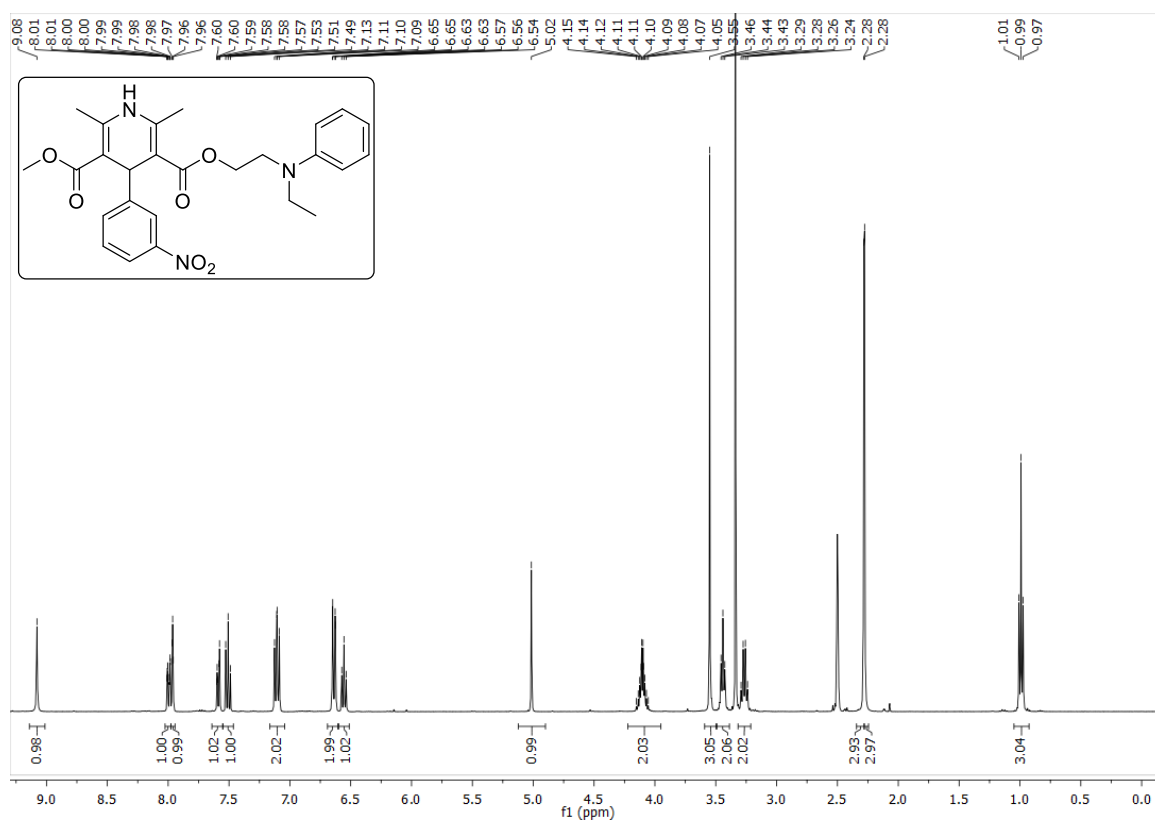
Compound **50**

Compound **51**
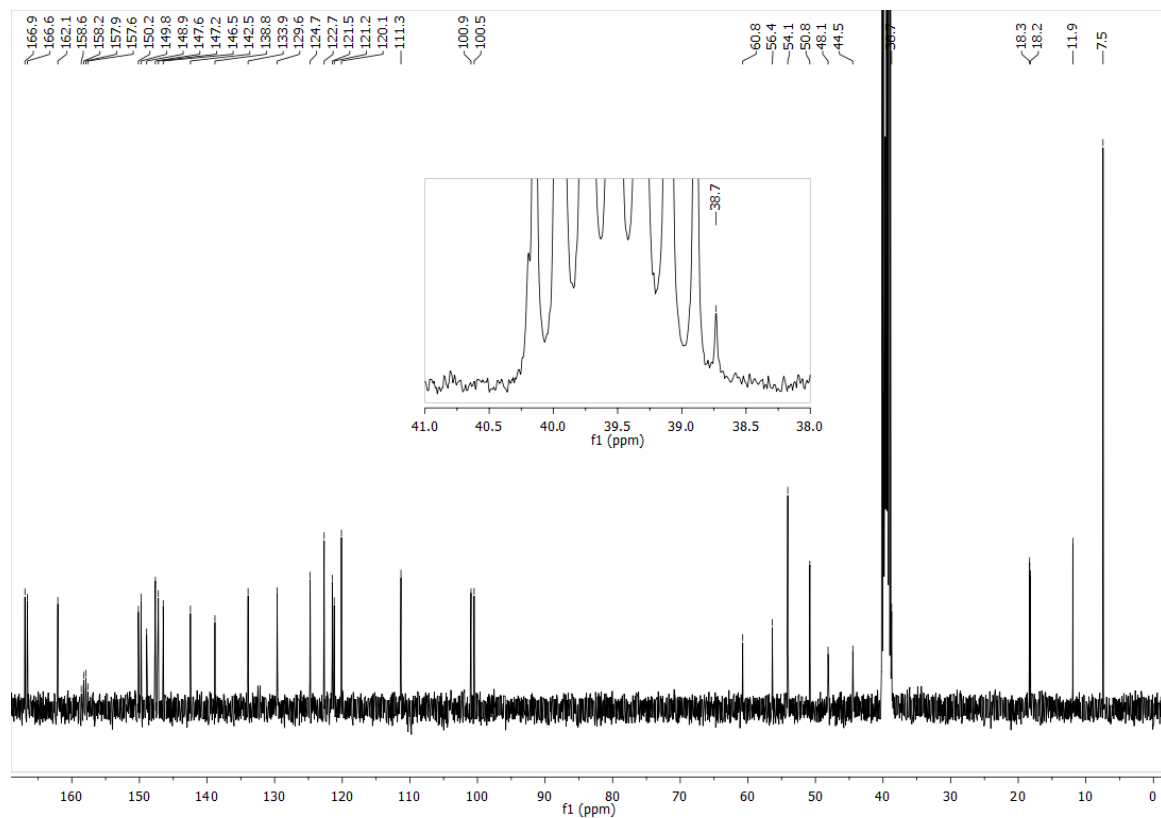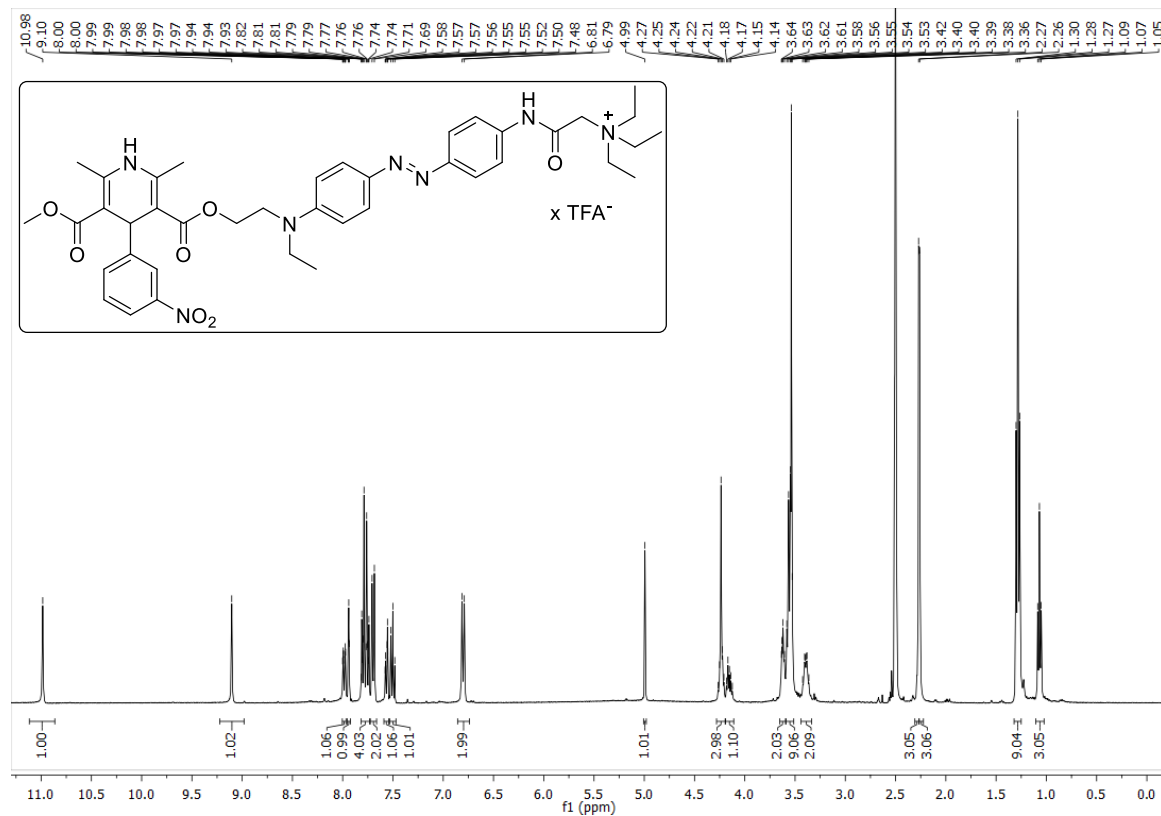
Compound **52**

Compound 53
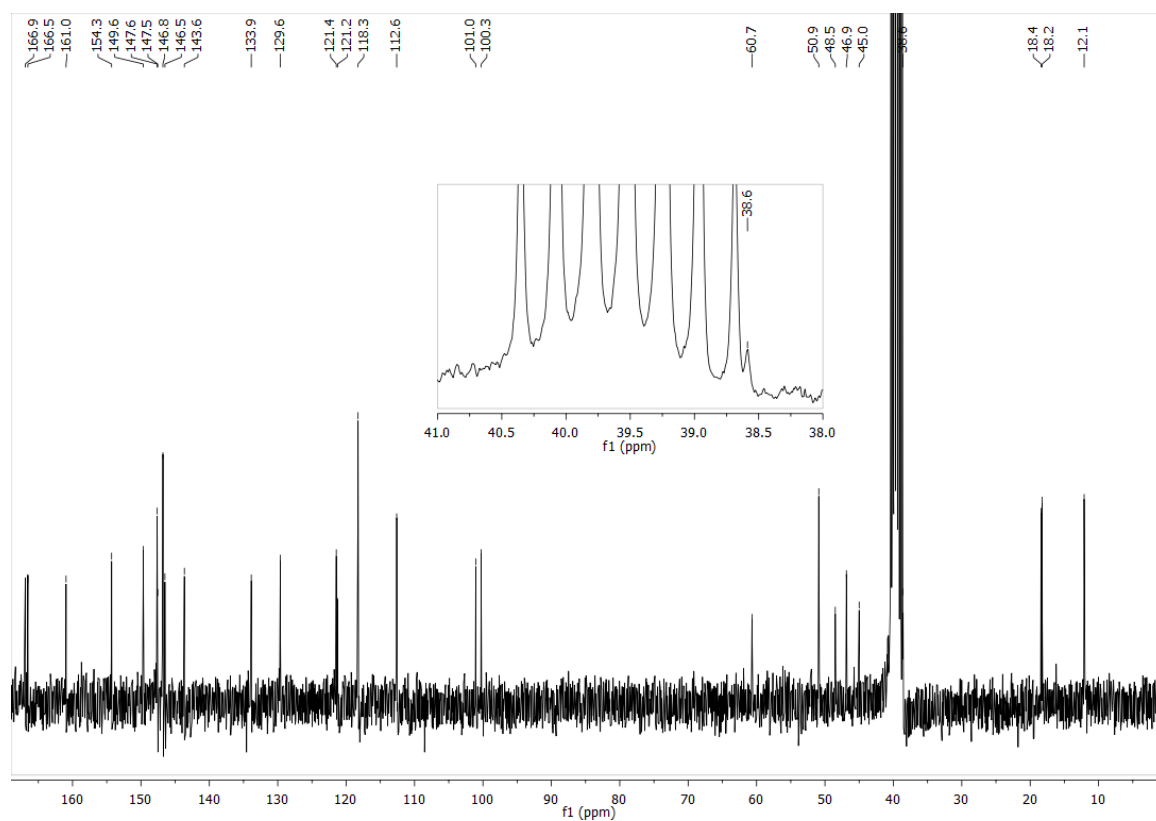
Compound **54**

3.6 References

[1]   P. Branchereau, D. Cattaert, A. Delpy, A.-E. Allain, E. Martin, P. Meyrand, *Scientific Reports* **2016**, *6*, 21753.

[2]   G. V. Maleeva, P. D. Brezhestovskii, *Neurosci. Behav. Physiol.* **2015**, *45*, 930-945.

[3]   B. S. Zhorov, P. D. Bregestovski, *Biophys. J.* **2000**, *78*, 1786-1803.

[4]   E. Sigel, R. Baur, N. Boulineau, F. Minier, *Biochem. Soc. Trans.* **2006**, *34*, 868-871.

[5]   M. Chebib, G. A. R. Johnston, *Clin. Exp. Pharmacol. Physiol.* **1999**, *26*, 937-940.

[6]   N. G. Bowery, T. G. Smart, *British Journal of Pharmacology* **2006**, *147*, S109-S119.

[7]   W. Sieghart, *Pharmacol. Rev.* **1995**, *47*, 181-234.

[8]   M. Lader, *CNS Drugs* **1994**, *1*, 377-387.

[9]   K. R. Tan, U. Rudolph, C. Lüscher, *Trends Neurosci.* **2011**, *34*, 188-197.

[10]   K. R. Tan, M. Brown, G. Labouèbe, C. Yvon, C. Creton, J.-M. Fritschy, U. Rudolph, C. Lüscher, *Nature* **2010**, *463*, 769-774.

[11]   J. H. Woods, J. L. Katz, G. Winger, *Pharmacol. Rev.* **1992**, *44*, 151-347.

[12]   A. B. Young, S. R. Zukin, S. H. Snyder, *PNAS* **1974**, *71*, 2246-2250.

[13]   A. Avila, L. Nguyen, J.-M. Rigo, *Front. Cell. Neurosci.* **2013**, *7*.

[14]   H. Betz, B. Laube, *J. Neurochem.* **2006**, *97*, 1600-1610.

[15]   J. Du, W. Lu, S. Wu, Y. Cheng, E. Gouaux, *Nature* **2015**, *526*, 224-229.

[16]   H. A. J. Struyker-Boudier, J. F. M. Smits, J. G. R. De Mey, *J. Cardiovasc. Pharmacol.* **1990**, *15*, 1-10..

[17]   X. Chen, B. Cromer, T. I. Webb, Z. Yang, J. Hantke, R. J. Harvey, M. W. Parker, J. W. Lynch, *Neuropharmacol.* **2009**, *56*, 318-327.

[18]   C. Brieke, F. Rohrbach, A. Gottschalk, G. Mayer, A. Heckel, *Angew. Chem. Int. Ed.* **2012**, *51*, 8446-8476.

[19]   A. Gupta, A. Kumar, *AIP Conference Proceedings* **2013**, *1536*, 1221-1222.

[20]   K. Deisseroth, *Nat. Methods* **2011**, *8*, 26-29.

[21]   M. Gascón-Moya, A. Pejoan, M. Izquierdo-Serra, S. Pittolo, G. Cabré, J. Hernando, R. Alibés, P. Gorostiza, F. Busqué, *J. Org. Chem.* **2015**, *80*, 9915-9925.

[22]   A. Rullo, A. Reiner, A. Reiter, D. Trauner, E. Y. Isacoff, G. A. Woolley, *Chem. Commun.* **2014**, *50*, 14613-14615.

[23]   W.-C. Lin, C. M. Davenport, A. Mourot, D. Vytla, C. M. Smith, K. A. Medeiros, J. J. Chambers, R. H. Kramer, *ACS Chem. Bio.* **2014**, *9*, 1414-1419.

[24]   M. A. Kienzler, A. Reiner, E. Trautman, S. Yoo, D. Trauner, E. Y. Isacoff, *J. Am. Chem. Soc.* **2013**, *135*, 17683-17686.

[25]   W. Szymański, J. M. Beierle, H. A. V. Kistemaker, W. A. Velema, B. L. Feringa, *Chem. Rev.* **2013**, *113*, 6114-6178.

[26]   M. M. Lerch, M. J. Hansen, G. M. van Dam, W. Szymanski, B. L. Feringa, *Angew. Chem. Int. Ed.* **2016**, *55*, 10978-10999.

[27]   J. Broichhagen, J. A. Frank, D. Trauner, *Acc. Chem. Res.* **2015**, *48*, 1947-1960.

[28]   W. A. Velema, W. Szymanski, B. L. Feringa, *J. Am. Chem. Soc.* **2014**, *136*, 2178-2191.

[29]   M. Irie, T. Fukaminato, K. Matsuda, S. Kobatake, *Chem. Rev.* **2014**, *114*, 12174-12277.

[30]   A. A. Beharry, G. A. Woolley, *Chem. Soc. Rev.* **2011**, *40*, 4422-4437.

[31]   E. Merino, *Chem. Soc. Rev.* **2011**, *40*, 3835-3853.

[32]   M. J. Hansen, M. M. Lerch, W. Szymanski, B. L. Feringa, *Angew. Chem. Int. Ed.* **2016**, *55*, 13514-13518.

[33]   M. Dong, A. Babalhavaeji, S. Samanta, A. A. Beharry, G. A. Woolley, *Acc. Chem. Res.* **2015**, *48*, 2662-2670.

[34]   J. B. Trads, J. Burgstaller, L. Laprell, D. B. Konrad, L. de la Osa de la Rosa, C. D. Weaver, H. Baier, D. Trauner, D. M. Barber, *Org. Bio. Chem.* **2017**, *15*, 76-81.

[35]   D. M. Barber, M. Schonberger, J. Burgstaller, J. Levitz, C. D. Weaver, E. Y. Isacoff, H. Baier, D. Trauner, *Chem. Sci.* **2016**, *7*, 2347-2352.

[36]   D. M. Barber, S.-A. Liu, K. Gottschling, M. Sumser, M. Hollmann, D. Trauner, *Chem. Sci.* **2017**, *8*, 611-615.

[37]   M. Schönberger, M. Althaus, M. Fronius, W. Clauss, D. Trauner, *Nat. Chem.* **2014**, *6*, 712-719.

[38]   M. Schönberger, D. Trauner, *Angew. Chem. Int. Ed.* **2014**, *53*, 3264-3267.

[39]   M. Izquierdo-Serra, D. Trauner, A. Llobet, P. Gorostiza, *Front. Mol. Neurosci.* **2013**, *6*.

[40]   A. Mourot, M. A. Kienzler, M. R. Banghart, T. Fehrentz, F. M. E. Huber, M. Stein, R. H. Kramer, D. Trauner, *ACS Chem. Neurosci.* **2011**, *2*, 536-543.

[41]   R. Huckvale, M. Mortensen, D. Pryde, T. G. Smart, J. R. Baker, *Org. Bio. Chem.* **2016**, *14*, 6676-6678.

[42]   M. Stein, S. J. Middendorp, V. Carta, E. Pejo, D. E. Raines, S. A. Forman, E. Sigel, D. Trauner, *Angew. Chem. Int. Ed.* **2012**, *51*, 10500-10504.

[43]   L. Yue, M. Pawlowski, S. S. Dellal, A. Xie, F. Feng, T. S. Otis, K. S. Bruzik, H. Qian, D. R. Pepperberg, *Nat. Commun.* **2012**, *3*, 1095.

[44]   V. N. Anikeev, A. I. Petrunin, M. T. Kilin, F. V. Guss, *Pharm. Chem. J.* **2004**, *38*, 261-263.

[45]   R. I. Fryer, B. Brust, L. H. Sternbach, *J. Chem. Soc.* **1964**, 3097-3101.

[46]   L. Guandalini, C. Cellai, A. Laurenzana, S. Scapecchi, F. Paoletti, M. N. Romanelli, *Bioorg. Med. Chem. Lett.* **2008**, *18*, 5071-5074.

[47]   M. Altenkämper, B. Bechem, J. Perruchon, S. Heinrich, A. Mädel, R. Ortmann, H.-M. Dahse, E. Freunscht, Y. Wang, J. Rath, A. Stich, M. Hitzler, P. Chiba, M. Lanzer, M. Schlitzer, *Biorg. Med. Chem.* **2009**, *17*, 7690-7697.

[48]   A. Escherich, J. Lutz, C. Escrieut, D. Fourmy, A. S. van Neuren, G. Müller, A. Schafferhans, G. Klebe, L. Moroder, *Biopolymers* **2000**, *56*, 55-76.

[49]   W. S. Jeon, E. Kim, Y. H. Ko, I. Hwang, J. W. Lee, S.-Y. Kim, H.-J. Kim, K. Kim, *Angew. Chem. Int. Ed.* **2005**, *44*, 87-91.

[50]   A. V. Turina, G. J. Quinteros, B. Caruso, E. L. Moyano, M. A. Perillo, *Org. Bio. Chem.* **2011**, *9*, 5737-5747.

[51]   B. Priewisch, K. Rück-Braun, *J. Org. Chem.* **2005**, *70*, 2350-2352.

[52]   L. S. Runtsch, D. M. Barber, P. Mayer, M. Groll, D. Trauner, J. Broichhagen, *Beilstein J. Org. Chem.* **2015**, *11*, 1129-1135.

[53]   K. S. Feldman, T. S. Folda, *J. Org. Chem.* **2016**, *81*, 4566-4575.

[54]   H. Kersten, P. Boldt, *J. Prakt. Chem.* **1996**, *338*, 129-139.

[55]   E. C. Taylor, C. P. Tseng, J. B. Rampal, *J. Org. Chem.* **1982**, *47*, 552-555.

[56]   I. Zrinski, M. Juribasic, M. Eckert-Maksic, *Heterocycles* **2006**, *68*, 1961-1967.

[57]   L. Birkofer, M. Franz, *Chem. Ber.* **1971**, *104*, 3062-3068.

[58]   H. Kim, J. Gao, D. J. Burgess, *Int. J. Pharm.* **2009**, *377*, 105-111.

[59]   I. Abrahamian, R. P. Hughes, Y. Yang, WO 2015031518 A1, **2015**.

[60]   L. Wagner, V. Raditoiu, A. Raditoiu, P. Ardeleanu, V. Amariutei, M. Radily, *Rev. Chim. (Bucaresti)* **2009**, *60*, 444-449.

[61]   K. Koumoto, H. Ochiai, N. Sugimoto, *Tetrahedron* **2008**, *64*, 168-174.

[62]   D. J. Dyer, J. R. Wolf, *Macromol. Res.* **2014**, *22*, 870-874.

[63]   D. R. C. Matazo, R. A. Ando, A. C. Borin, P. S. Santos, *J. Phys. Chem. A* **2008**, *112*, 4437-4443.

[64]   H. Mustroph, *Zeitschrift für Chemie* **1987**, *27*, 281-289.

[65]   T. Kamei, M. Kudo, H. Akiyama, M. Wada, J. i. Nagasawa, M. Funahashi, N. Tamaoki, T. Q. P. Uyeda, *Eur. J. Org. Chem.* **2007**, *2007*, 1846-1853.

[66]   D. G. Whitten, P. D. Wildes, J. G. Pacifici, G. Irick, *J. Am. Chem. Soc.* **1971**, *93*, 2004-2008.

[67]   T. Hayashita, T. Kurosawa, T. Miyata, K. Tanaka, M. Igawa, *Colloid. Polym. Sci.* **1994**, *272*, 1611-1619.

[68]   M. A. Rather, G. M. Rather, S. A. Pandit, S. A. Bhat, M. A. Bhat, *Talanta* **2015**, *131*, 55-58.

[69]   L. Richter, C. de Graaf, W. Sieghart, Z. Varagic, M. Mörzinger, I. J. P. de Esch, G. F. Ecker, M. Ernst, *Nat. Chem. Biol.* **2012**, *8*, 455-464.

[70]   R. Bergmann, K. Kongsbak, P. L. Sørensen, T. Sander, T. Balle, *PLOS ONE* **2013**, *8*, e52323.

[71]   X. Huang, H. Chen, K. Michelsen, S. Schneider, P. L. Shaffer, *Nature* **2015**, *526*, 277-280.

[72]   X. Huang, P. L. Shaffer, S. Ayube, H. Bregman, H. Chen, S. G. Lehto, J. A. Luther, D. J. Matson, S. I. McDonough, K. Michelsen, M. H. Plant, S. Schneider, J. R. Simard, Y. Teffera, S. Yi, M. Zhang, E. F. DiMauro, J. Gingras, *Nat Struct Mol Biol* **2017**, *24*, 108-113.

[73]   Gaussian 09, Revision D.01, M. J. Frisch, G. W. Trucks, H. B. Schlegel, G. E. Scuseria, M. A. Robb, J. R. Cheeseman, G. Scalmani, V. Barone, G. A. Petersson, H. Nakatsuji, X. Li, M. Caricato, A. Marenich, J. Bloino, B. G. Janesko, R. Gomperts, B. Mennucci, H. P. Hratchian, J. V. Ortiz, A. F. Izmaylov, J. L. Sonnenberg, D. Williams-Young, F. Ding, F. Lipparini, F. Egidi, J. Goings, B. Peng, A. Petrone, T. Henderson, D. Ranasinghe, V. G. Zakrzewski, J. Gao, N. Rega, G. Zheng, W. Liang, M. Hada, M. Ehara, K. Toyota, R. Fukuda, J. Hasegawa, M. Ishida, T. Nakajima, Y. Honda, O. Kitao, H. Nakai, T. Vreven, K. Throssell, J. A. Montgomery, Jr., J. E. Peralta, F. Ogliaro, M. Bearpark, J. J. Heyd, E. Brothers, K. N. Kudin, V. N. Staroverov, T. Keith,

R. Kobayashi, J. Normand, K. Raghavachari, A. Rendell, J. C. Burant, S. S. Iyengar, J. Tomasi, M. Cossi, J. M. Millam, M. Klene, C. Adamo, R. Cammi, J. W. Ochterski, R. L. Martin, K. Morokuma, O. Farkas, J. B. Foresman and D. J. Fox, Gaussian, Inc., Wallingford CT, 2013.

[74]   A. Šali, T. L. Blundell, *J. Mol. Biol.* **1993**, *234*, 779-815.

[75]   J. Gullingsrud, J. Saam and J. Phillips. "psfgen User's Guide, version 1.6.4" (2016) Theoretical and Computational Biophysics Group, University of Illinois University at Urbana-Champaign and Beckman Institute.

[76]   V. B. Chen, W. B. Arendall, III, J. J. Headd, D. A. Keedy, R. M. Immormino, G. J. Kapral, L. W. Murray, J. S. Richardson, D. C. Richardson, *Acta Cryst D* **2010**, *66*, 12-21.

[77]   O. Trott, A. J. Olson, *J. Comput. Chem.* **2010**, *31*, 455-461.

[78]   W. Humphrey, A. Dalke, K. Schulten, *J. Mol. Graph. Model.* **1996**, *14*, 33-38.

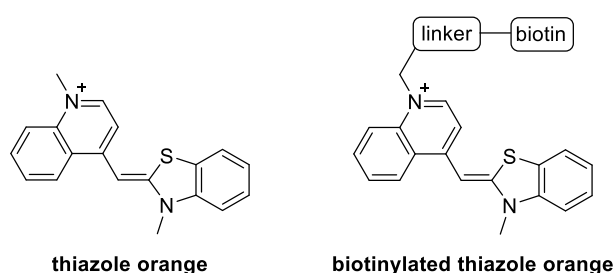# 4 Biotinylated Thiazole Orange for Purification of Triplex DNA

4.1 Introduction

Triplex DNA has recently received increasing attention in different fields of research due to its variety of biological activities including DNA damage, DNA repair, mutagenesis and even diseases.[1-2] The formation of triplex DNA was initially described in 1957.[3] Triplexes are formed by Hoogsteen or reverse Hoogsteen hydrogen bonds either intramolecularly whereby the third strand originates from the same DNA molecule or intermolecularly by binding of a separate triplex forming oligonucleotide (TFO) to the major groove of double stranded DNA (dsDNA) on the so called triplex target site (TTS).[4-5] Latter approach of a site-specific recognition of duplex DNA by TFOs was shown to be a useful approach for the modification of gene structure and functions both *in vitro* and *in vivo* providing a useful tool for gene-specific manipulation of DNA.[6]

The cyanine dye thiazole orange (TO) is very well-known for its interaction with DNA and nucleic acids in general.[7] The intrinsic fluorescence of TO is rather neglectable, but upon intercalation in DNA enhanced dramatically by a factor of more than 1000.[8] Therefore, it is commonly used to stain DNA in gels[9] and capillary electrophoresis[10] or to stain residual RNA in blood cells.[11] Recent investigations showed that thiazole orange exhibits an enhanced specific high-affinity binding to triplex DNA compared to dsDNA building stable complexes which do even not dissociate during chromatography and gel electrophoresis.[12] Hence, we envisioned that functionalizing thiazole orange with a biotin moiety *via* a linker could yield a specific probe for the isolation and purification of triplex DNA by utilizing the biotin/streptavidin or avidin affinity, respectively.

thiazole orange   biotinylated thiazole orange

Figure 1. Structure of the cyanine dye thiazole orange (TO) and common structure of the targeted biotinylated thiazole orange.

The interaction of biotinylated molecules with streptavidin or avidin is one of the most useful and applied tools for purification in biochemical and biomedical research due to

the high affinity and specificity of the vitamin biotin towards the proteins streptavidin and avidin.[13-14] For that reason the biotinylated thiazole orange should enable an isolation of only triplexes from complex mixtures of different oligonucleotides. It can also be used to finally extract specific dsDNA by adding a defined TFO to a mixture of dsDNA, which forms triplexes only with the targeted dsDNA bearing an appropriate TTS. Herein, we discuss the synthesis and preliminary biological evaluations of our biotinylated thiazole orange derivative (TO-Biotin).

4.2 Results and Discussion

4.2.1 Synthesis

Different approaches to functionalize TO with a biotin label were attempted. Thereby, the initial trial to directly attach the biotin moiety at the thiazole orange core *via* Friedel-Crafts acylation was not successful. Also the synthesis of a TO derivative bearing an amino group for functionalization with biotin by amide coupling was problematic due to occurring side reactions during condensation of the two aromatic precursors to the core scaffold of the dye. Finally, a biotinylated thiazole orange was successfully synthesized as depicted in Scheme 1.
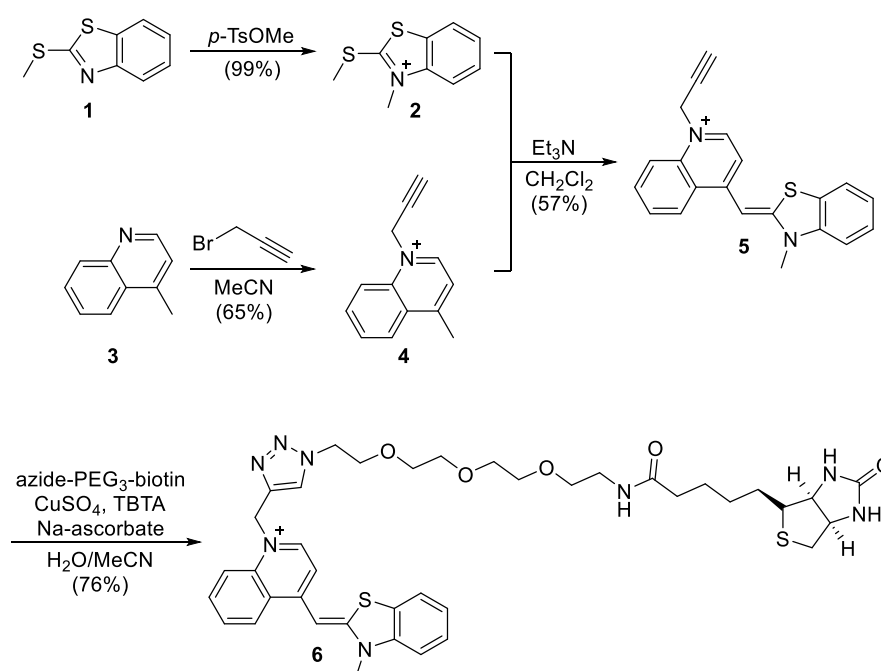
Scheme 1. Preparation of TO-Biotin **6**.

After methylation of benzothiazole **1** with methyl *p*-toluenesulfonate[15] and alkylation of lepidine (**3**) with propagyl bromide[16] thiazole orange derivative **5** was prepared by condensing the two afforded precursors **2** and **4** under basic conditions according to a reported procedure.[16] Subsequent copper catalyzed 1,3-dipolar cycloaddition of compound **5** with a commercially available azide-PEG$_3$-biotin conjugate yielded target structure **6** in good yield of 76%. The yield is based on a calculation with tosylate as quantitative counterion, which has the highest molecular weight of all possible counterions. However, we are aware that according to the proton NMR analysis only approximately 20% of the anions are tosylates. Due to the final purification by preparative HPLC with aqueous TFA as eluent we could also detect trifluoroacetate as counterion by fluorine NMR, but not quantify the overall amount. From the synthetic procedure, also bromide, sulfate or hydroxyl salts are conceivable, respectively, which all are not detectable by standard proton and carbon NMR measurements. Nevertheless, we used the obtained compound with mixed counterions for preliminary biological investigations using a molecular weight of 945.18 grams per mole (quantitative tosylate) for preparing stock solutions. By using the highest possible molecular weight we could obtain false higher affinity values (lower EC$_{50}$s) in the measurements, but in the first initial experiments we just wanted to check the influence of the modification we made on the dye structure and if the biotinylated thiazole still coordinates with higher selectivity to triplexes than dsDNA. Obtaining promising results in the initial biological investigations, we could convert the mixture of salts to a defined one by ion exchange chromatography.

4.2.2 Biological Investigations[A]

First, the ability of the investigated probes to form triplexes was verified by an electrophoretic mobility shift assay. Like depicted in Figure 2a the amount of triplexes is increasing with increasing concentration of the triplex forming oligonucleotide (TFO) up to 500 nM at which all TTS (dsDNA) is transformed into triplexes. The determination of the half-maximal effective concentrations (EC$_{50}$) of the TFO to the TTS, TO to TTS and triplexes as well as TO-Biotin to TTS and triplexes was accomplished by using microscale


[A] All biological investigations were performed in the group of Prof. Dr. Gernot Längst by Dr. Rodrigo Maldonado at the University of Regensburg, Germany.

thermophoresis (MST). This is an immobilization-free technology using the different mobility of fluorescent labeled biomolecules along a temperature gradient depending on a variety of molecular properties such as size, charge, hydration shell or conformation.[17] By plotting the fluorescent intensities against the different concentrations of unlabeled ligands the EC_{50} value as well as the unbound and bound states can be determined. Thus, an EC_{50} of 54.2 nM for the TFO binding to the TTS was measured (Figure 2b).
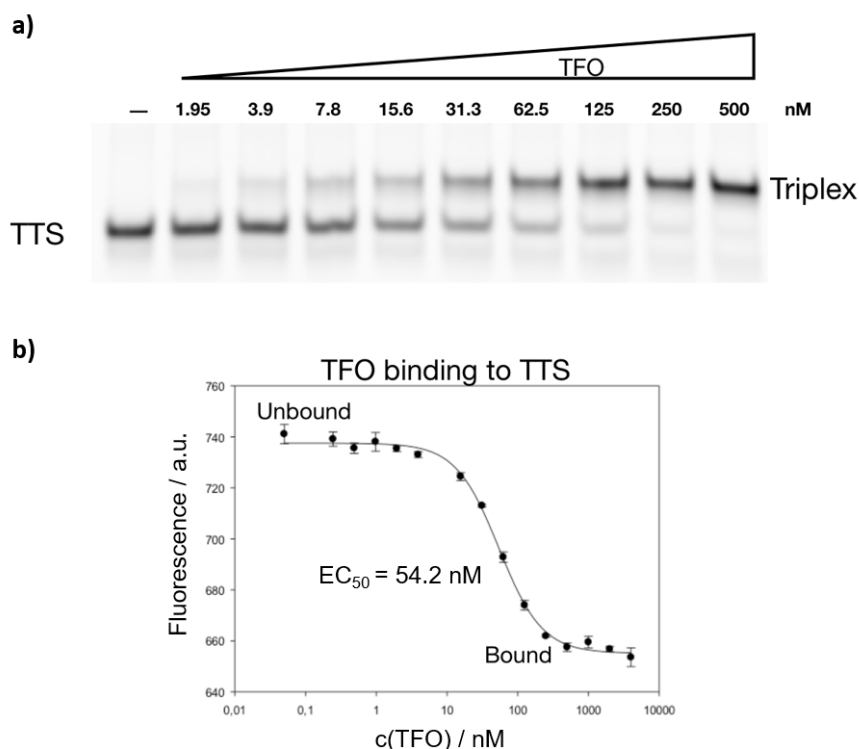

Figure 2. a) Triplex forming oligonucleotide (TFO, ssDNA of 29 bases) titration for triplex annealing. Increasing concentrations of non-labeled TFO (1.95 nM – 500 nM, specified above the gel image) were incubated with 20 nM of Cy5-labeled triplex targeting site (TTS, dsDNA of 29 base pairs) at 37 °C for 30 min. Then the samples were separated on a 15% polyacrylamide gel and visualized on a fluorescence scanner. As a control the TTS was incubated in the absence of the TFO (first lane –). **b)** Triplex formation analysis by microscale thermophoresis (MST). A fixed concentration of Cy5-labeled TTS (20 nM) was incubated with increasing amounts of non-labeled TFO (from 0.05 nM to 4 µM, 30 min at 37 °C) revealing an EC_{50} of 54.2 nM.

We could prove that TO exhibits a higher binding affinity to triplexes (EC_{50} = 0.87 µM, Figure 3b) compared to dsDNA (EC_{50} = 3.2 µM, Figure 3a). Prepared TO-Biotin **6** slightly lost affinity to dsDNA (EC_{50} = 4.8 µM, Figure 3c) but unfortunately also lost overall and relative affinity to triplexes (EC_{50} = 2.1 µM, Figure 3d). Therefore, we could not further utilize compound **6** for the purification of triplexes.
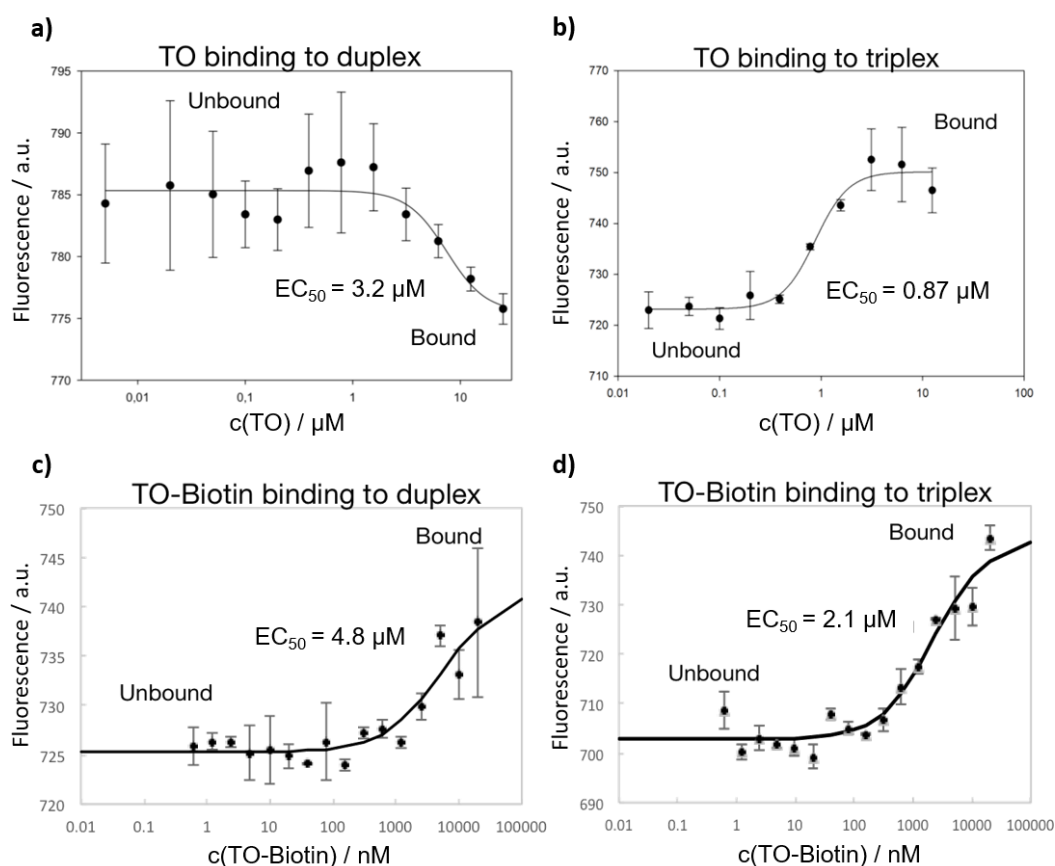
Figure 3. Analysis of thiazole orange (TO) and biotinylated thiazole orange (TO-Biotin) binding to dsDNA and triplex DNA by MST. **a)**, **b)** Fixed concentrations of Cy5-labeled TTS (20 nM, **a**) and Cy5-labeled triplex (20 nM Cy5-TTS + 2 μM TFO, **b**) were incubated with increasing amounts of TO (0.005 nM – 25 nM for **c**; 0.02 nM – 12.5 nM for **d**) revealing an EC_{50} of 3.2 μM for dsDNA and an EC_{50} of 0.87 μM for triplexes. **c)**, **d)** Fixed concentrations of Cy5-labeled TTS (20 nM, **c**) and Cy5-labeled triplex (20 nM Cy5-TTS + 2 μM TFO, **d**) were incubated with increasing amounts of TO-Biotin (0.061 nM – 20 μM) revealing an EC_{50} of 4.8 μM for dsDNA and an EC_{50} of 2.1 μM for triplexes.

Interestingly and in contrast to the loss of affinity, TO-Biotin **6** maintained the ability to stabilize triplexes known from thiazole orange as depicted in Figure 4. By adding a competitor oligonucleotide which is complementary to the TFO (anti_TFO) we could still detect triplexes in the lanes with TO-Biotin and TO, respectively. The lanes without any TO contained no triplexes any more, just duplexes consisting of TFO and anti_TFO.
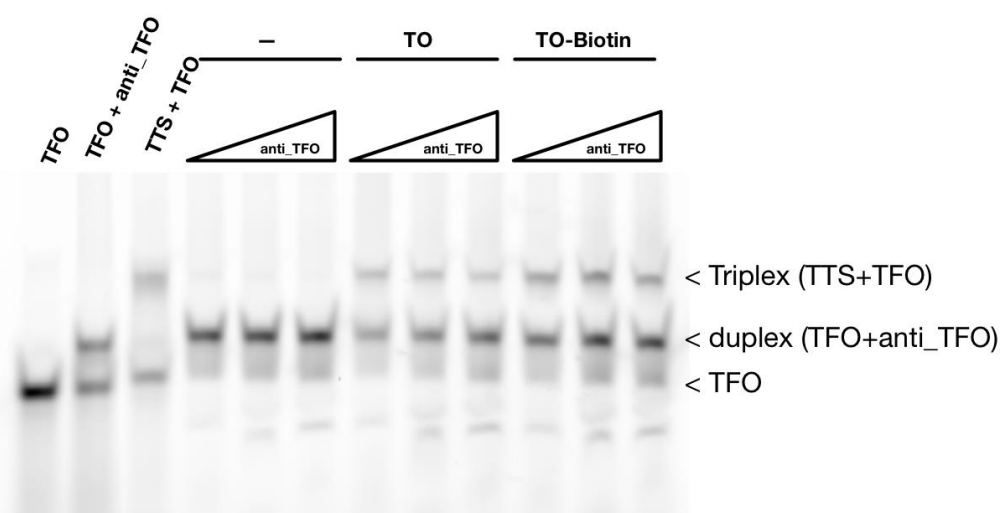
Figure 4. Stabilization of triplexes by TO and TO-Biotin. Triplexes were annealed by incubating a Cy5-labeled TFO and a non-labeled TTS using a ratio TTS:TFO of 1:4 (50 nM:200 nM) for 30 min at 37 °C (lane 3). In order to destabilize the triplexes a competitor oligonucleotide that is complementary to the TFO (anti_TFO, lane 2) was titrated after triplex annealing and incubated for 15 min at 37 °C (lane 4-6). To examine the stabilization of the triplexes by TO and TO-Biotin the triplexes were incubated with 50 µM of both compounds for 10 min at 25 °C prior to the titration of the anti_TFO. All samples were separated on a 12% polyacrylamide gel and visualized on a fluorescence scanner.

4.3 Conclusion

In summary, we designed a thiazole orange derivative functionalized with a biotin moiety for purification and isolation of triplex DNA. The target compound was synthesized connecting a thiazole orange derivative to a commercial biotin conjugate by azide-alkyne click chemistry in good yield. However, preliminary biological investigations showed that the prepared biotinylated thiazole orange lost overall affinity and specificity to triplex DNA compared to the non-functionalized thiazole orange. For this reason, our biotinylated thiazole orange could not be utilized for a selective purification of triplex DNA. In contrast, further investigations indicated that the prepared thiazole orange derivative kept the ability to stabilize triplexes against competitor oligonucleotides, which is a known feature for unfunctionalized thiazole orange.

4.4 Experimental

4.4.1 General Information

Compounds **2**,[15] **4**,[16] **5**,[16] were synthesized according to reported procedures. Commercial reagents and starting materials were purchased from Acros Organics, Alfa-Aesar, Fisher Scientific, Sigma Aldrich or VWR and used without any further purification. Solvents were used in p.a. quality. The melting point was measured with a Stanford Research Systems OptiMelt MPA 100 device and is uncorrected. NMR spectra were recorded on a Bruker Avance III 600 (^{1}H 600.25 MHz, ^{13}C 150.95 MHz) instrument. The spectra are referenced against the NMR-solvent (DMSO-d_6: δ_H = 2.50 ppm, δ_C = 39.52 ppm) and chemical shifts δ are reported in ppm. Abbreviations for resonance multiplicity: s (singlet), d (doublet), t (triplet), q (quartet) and m (multiplet). Carbon NMR signals are reported using a ^{1}H-^{13}C HSQC spectrum with (+) for primary/tertiary, (−) for secondary and (q) for quaternary carbons. An Agilent Q-TOF 6540 UHD (ESI-MS) instrument was used for measuring mass spectra. A Knauer system (two Knauer K-1001 pumps with a Knauer K-2600 UV-detector; column: Phenomenex Luna 10 µM C18(2) 100 Å, 250 x 21.2 mm; flow: 11.0 mL/min at room temperature; solvent A: MilliQ water with 0.05 % vol. TFA; solvent B: MeCN) was used for purification by preparative HPLC. Analytical HPLC measurements for reaction monitoring and a final purity test were performed on an Agilent 1220 Infinity LC (column: Phenomenex Luna 3 µM C18(2) 100 Å, 150 x 2.00 mm; flow: 0.3 mL/min at 30 °C; solvent A: MilliQ water with 0.05 % vol. TFA; solvent B: MeCN). A purity of 96% for biotinylated thiazole orange **6** (gradient: 10% - 98% MeCN in 25 min, 98% MeCN for further 5 min, t_R = 10.9 min) of 96% with detection at 254 nm was measured.

4.4.2 Synthesis and Characterization of TO-Biotin

4-((3-Methylbenzo[*d*]thiazol-2(3*H*)-ylidene)methyl)-1-((1-(13-oxo-17-((3a*S*,4*S*,6a*R*)-2-oxohexahydro-1*H*-thieno[3,4-*d*]imidazol-4-yl)-3,6,9-trioxa-12-azaheptadecyl)-1*H*-1,2,3-triazol-4-yl)methyl)quinolin-1-ium (6)

A reaction vessel was equipped with biotin-PEG$_3$-azide (105 mg, 0.24 mmol, 1.0 eq.), thiazole orange **5** (354 mg, 0.71 mmol, 3.0 eq.), CuSO$_4$ x 5 H$_2$O (177 mg, 0.71 mmol,

3.0 eq.), TBTA (438 mg, 0.83 mmol, 3.5 eq.) and sodium ascorbate (234 mg, 1.18 mmol, 5.0 eq.). Then a solution of H_2O/MeCN (1:1, 5 mL) was added and the mixture was stirred at room temperature for 3 d. After removal of the solvent by evaporation under reduced pressure and lyophilization the crude product was purified by preparative HPLC (10% - 95% MeCN in 25 min, t_R = 13.4 min) affording TO **6** (170 mg, 76%) as an orange-red fluffy solid. m.p. 188 °C; ^{1}H-NMR (600 MHz, MeOH-d_4) δ = 8.82 - 8.76 (m, 2H), 8.27 (s, 1H), 8.23 (d, J = 8.6 Hz, 1H), 8.08 (dd, J = 7.9, 0.8 Hz 1H), 7.94 (ddd, J = 8.5, 7.0, 1.2 Hz, 1H), 7.83 (d, J = 8.3 Hz, 1H), 7.80 (t, J = 5.6 Hz, 1H), 7.72 (ddd, J = 8.1, 7.4, 1.2 Hz, 1H), 7.64 (ddd, J = 8.4, 7.4, 1.2 Hz, 1H), 7.48 – 7.44 (m, 2H), 6.97 (s, 1H), 6.39 (s, 1H), 6.35 (s, 1H), 5.92 (s, 2H), 4.51 (t, J = 5.1 Hz, 2H), 4.29 (dd, J = 7.8, 5.0 Hz, 1H), 4.10 (ddd, J = 7.8, 4.5, 1.8 Hz, 1H), 4.05 (s, 3H), 3.77 (t, J = 5.2 Hz, 2H), 3.46 (dd, J = 5.9, 3.4 Hz, 2H), 3.43 – 3.40 (m, 6H), 3.37 – 3.36 (m, 2H), 3.16 (q, J = 5.9 Hz, 2H), 3.06 (ddd, J = 8.6, 6.2, 4.4 Hz, 1H), 2.80 (dd, J = 12.4, 5.1 Hz, 1H), 2.56 (d, J = 12.4 Hz, 1H), 2.04 (t, J = 7.4 Hz, 2H), 1.63 – 1.54 (m, 1H), 1.52 – 1.40 (m, 3H), 1.32 – 1.23 (m, 2H).; ^{13}C-NMR (151 MHz, MeOH-d_4) δ = 172.1 (q), 162.7 (q), 160.7 (q), 148.7 (q), 144.6 (+), 140.9 (q), 140.5 (q), 137.1 (q), 133.1 (+), 128.3 (+), 126.8 (+), 125.7 (+), 124.7 (+), 124.5 (+), 124.2 (q), 124.0 (q), 122.9 (+), 118.3 (+), 113.2 (+), 107.8 (+), 88.6 (+), 69.6 (−), 69.6 (−), 69.5 (−), 69.5 (−), 69.1 (−), 68.6 (−), 61.0 (+), 59.2 (+), 55.4 (+), 49.6 (−), 49.0 (−), 40.1 (−), 38.4 (−), 35.1 (−), 34.0 (+), 28.2 (−), 28.0 (−), 25.2 (−); HRMS (ESI) calcd. for $C_{39}H_{49}N_8O_5S_2$ M^+ m/z = 773.3262; found 773.3267.

4.5 Supporting Information

¹H- and ¹³C-NMR spectra of compound 6
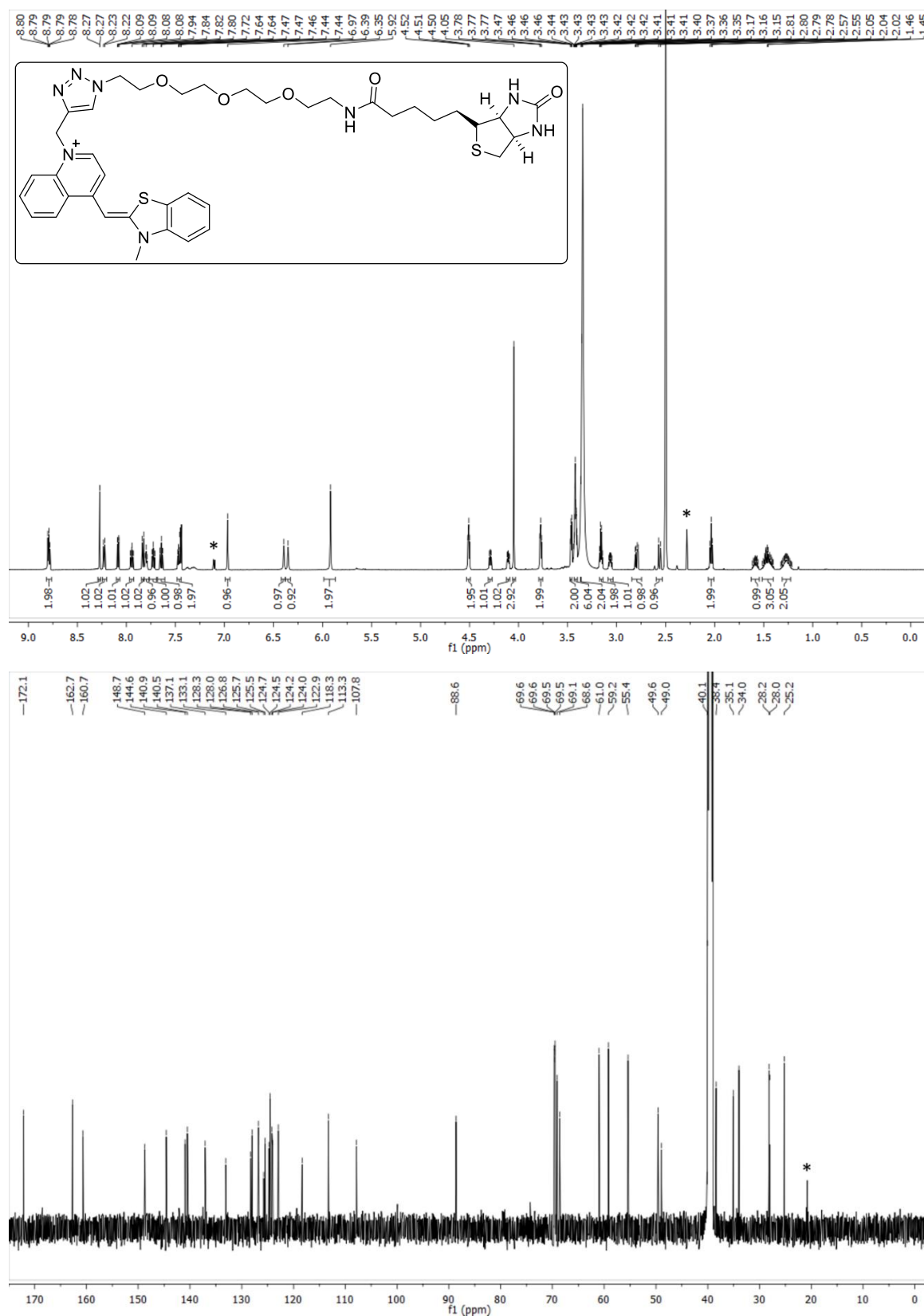
Signals marked with * result from tosylate as partial counterion.

4.6 References

[1]   A. Mukherjee, K. M. Vasquez, *Biochimie* **2011**, *93*, 1197-1208.

[2]   J. J. Bissler, *Front. Biosci., Landmark Ed.* **2007**, *12*, 4536–4546.

[3]   G. Felsenfeld, D. R. Davies, A. Rich, *J. Am. Chem. Soc.* **1957**, *79*, 2023-2024.

[4]   M. D. Frank-Kamenetskii, S. M. Mirkin, *Annu. Rev. Biochem* **1995**, *64*, 65-95.

[5]   a. S M Mirkin, M. D. Frank-Kamenetskii, *Annu. Rev. Biophys. Biomol. Struct.* **1994**, *23*, 541-576.

[6]   M. Duca, P. Vekhoff, K. Oussedik, L. Halby, P. B. Arimondo, *Nucleic Acids Res.* **2008**, *36*, 5123-5138.

[7]   J. Nygren, N. Svanvik, M. Kubista, *Biopolymers* **1998**, *46*, 39-51.

[8]   T. G. Deligeorgiev, N. I. Gadjev, K.-H. Drexhage, R. W. Sabnis, *Dyes Pigment.* **1995**, *29*, 315-322.

[9]   H. S. Rye, S. Yue, D. E. Wemmer, M. A. Quesada, R. P. Haugland, R. A. Mathies, A. N. Glazer, *Nucleic Acids Res.* **1992**, *20*, 2803-2812.

[10]   H. Zhu, S. M. Clark, S. C. Benson, H. S. Rye, A. N. Glazer, R. A. Mathies, *Anal. Chem.* **1994**, *66*, 1941-1948.

[11]   L. G. Lee, C.-H. Chen, L. A. Chiu, *Cytometry* **1986**, *7*, 508-517.

[12]   I. Lubitz, D. Zikich, A. Kotlyar, *Biochemistry* **2010**, *49*, 3567-3574.

[13]   J.-N. Rybak, S. B. Scheurer, D. Neri, G. Elia, *Proteomics* **2004**, *4*, 2296-2299.

[14]   E. P. Diamandis, T. K. Christopoulos, *Clin. Chem.* **1991**, *37*, 625-636.

[15]   S. Brenner, Y. N. Teo, F. Ghadessy, L. P. W. Goh, M. Y. Lee, WO2014/051521 A1, **2014**.

[16]   B. Ditmangklo, C. Boonlua, C. Suparpprom, T. Vilaivan, *Bioconjugate Chem.* **2013**, *24*, 614-625.

[17]   M. Jerabek-Willemsen, T. André, R. Wanner, H. M. Roth, S. Duhr, P. Baaske, D. Breitsprecher, *J. Mol. Struct.* **2014**, *1077*, 101-113.

5 Summary

The major part of this thesis (**Chapter 1 – 3**) focuses on the functionalization of different photochromic scaffolds for biological applications. **Chapter 4** deals with a modified dye for purification of triplex DNA.

Chapter 1 describes different synthetic routes to photochromic dithienylmaleimides functionalized either at each of the thiophene moieties or at the maleimide nitrogen. A Perkin-type condensation of two independently prepared thiophene precursors was successfully employed as the key step to assemble the maleimide core for non-symmetric diarylmaleimides. Thus, a photoswitchable amino acid was obtained and a variety of aromatic substituted dithienylmaleimides were synthesized by applying a Suzuki coupling strategy prior to the condensation. A different synthetic approach gave access to photochromic labeled natural amino acids as well as maleimide protected dithienylmaleimides by the reaction of a dithienylmaleic anhydride with amines or hydrazines. All prepared photoswitchable compounds exhibited reversible photochromism in polar organic solvents.

Photoswitchable histone deacetylase (HDAC) inhibitors are presented in **Chapter 2**. These inhibitors were gained by equipping dithienylethenes (DTEs) and fulgimides with hydroxamic acids to enable binding to zinc dependent HDACs. The control of these enzymes is of high biomedical interest in anticancer research and epigenetics due to their crucial role in numerous biological processes. While the photochromic performance of the two prepared classes of DTEs was only moderate in polar solvents the fulgimides featured excellent reversible photochromism even in aqueous buffer with very high photostationary states. All synthesized target compounds showed the anticipated inhibitory effect on the tested *h*HDAC1, *h*HDAC6, *h*HDAC8 and *sm*HDAC8 with best IC$_{50}$ values in the low nanomolar range. However, the corresponding photoisomers showed only a maximum four-fold difference in inhibitory ability. The differences in activity observed in the *in vitro* experiments could be rationalized by molecular dockings.

Chapter 3 reports the synthesis and biological evaluation of photochromic ligands for modulation of γ-aminobutyric acid (GABA) and glycine-receptors by light. Therefore, photochromic ligands were synthesized by merging structural elements of nitrazepam and nicardipine, which are well-known pharmacophores for ion channels, with photoswitchable azobenzenes. The photochromic properties of the ligands were outstanding with very good fatigue resistance and high photostationary states. Initial *in vitro* electrophysiological investigations identified one azo benzodiazepine as very promising ligand. This compound acted not only as a UV sensitive blocker of GABA$_A$-receptors, but also as subtype specific photoswitchable modulator of glycine-receptors. Preliminary molecular dockings could partly explain these experimental effects. Furthermore, *in vivo* investigations of the photochromic ligands were performed and another azo benzodiazepine showed photoswitchable influence on the activity of zebrafish larvae.

The attempt to purify triplex DNA with a biotinylated thiazole orange derivative, which was synthesized by azide-alkyne click chemistry, is described in **Chapter 4**. Biological investigations of the functionalized compound could prove that the prepared thiazole orange kept the ability to stabilize triplexes against competitor oligonucleotides. However, a loss of overall affinity and specificity to triplex DNA was observed, which disqualified the biotinylated thiazole orange for a utilization to purify triplexes.

Overall, this thesis presents functionalized synthetic compounds for biological applications. In particular, the contributions of this work are relevant for the future development of novel molecular tools to light-control cellular processes or living organisms.

6 Zusammenfassung

Der Großteil dieser Arbeit (**Kapitel 1 – 3**) befasst sich mit der Funktionalisierung photochromer Strukturen und deren biologischen Anwendungen. **Kapitel 4** diskutiert die Synthese und Eigenschaften eines modifizierten Farbstoffs für die Aufreinigung von Triplex-DNA.

In **Kapitel 1** werden verschiedene Syntheserouten zu photochromen Dithienylmaleimiden beschrieben, die entweder an jedem Thiophen oder am Maleimid-Stickstoff funktionalisiert sind. Eine Perkin-Kondensationsreaktion von zwei unabhängig voneinander hergestellten Thiophenvorstufen wurde als Schlüsselschritt zum Aufbau der Maleimid-Grundstruktur unsymmetrische Diarylmaleimde verwendet. Damit konnte eine photoschaltbare Aminosäure hergestellt werden, sowie verschiedene, aromatisch substituierte Dithienylmaleimide. Letzteres gelang durch eine Funktionalisierung der Vorstufen mittels Suzuki-Kupplung vor der Kondensation. Ein weiterer synthetischer Ansatz der Reaktion eines Dithienylmaleimidanhydrids mit Aminen oder Hydrazinen lieferte photochrom markierte natürliche Aminosäuren und Stickstoff-geschützte Dithienylmalemide. Alle hergestellten photoschaltbaren Verbindungen zeigten reversible Photochromie in polaren organischen Lösungsmitteln.

Kapitel 2 befasst sich mit photoschaltbaren Inhibitoren für Histon-Deacetylasen (HDACs). Diese Inhibitoren wurden durch Derivatisierung von Dithienylethenen (DTEs) und Fulgimiden mit Hydroxamsäuren erhalten, welche eine Bindung an HDACs mit einem Zinkion im katalytischen Zentrum ermöglichen. Die Kontrolle dieser Enzyme ist wegen ihrer entscheidenden Rolle in einer Vielzahl von biologischen Prozessen von hohem biomedizinischem Interesse in der Anti-Krebs-Forschung und auf dem Gebiet der Epigenetik. Während die photochromen Eigenschaften der zwei verschiedenen Klassen von verwendeten DTEs in polaren Lösungsmitteln nur mäßig waren, zeigten hingegen die Fulgimide sogar in wässrigen Puffersystemen ausgezeichnetes und reversibles photochromes Verhalten mit sehr hohen photostationären Zuständen. Alle

synthetisierten Zielstrukturen zeigten eine erwartete Inhibition der getesteten *h*HDAC1, *h*HDAC6, *h*HDAC8 und *sm*HDAC8 mit den besten IC_{50}-Werten im zweistelligen nanomolaren Bereich. Die entsprechenden Photoisomere unterschieden sich jedoch nur maximal vierfach in ihrer Inhibitionswirkung. Die beobachteten Inhibitionsunterschiede konnten durch molekulares Docking erklärt werden.

Die Synthese und biologische Untersuchung von photochromen Liganden für die Regulierung von γ-Aminobuttersäure- (GABA) und Glycinrezeptoren mittels Licht ist in **Kapitel 3** dargestellt. Für die Herstellung dieser Liganden wurden Strukturelemente von Nitrazepam und Nicardipin, die bekannte Pharmakophore für Ionenkanäle sind, mit der von Azobenzolen verschmolzen. Die photochromen Eigenschaften der Liganden waren herausragend mit sehr guter Stabilität und hohen photostationären Zuständen. Erste elektrophysiologische Untersuchungen *in vitro* identifizierten ein Azo-Benzodiazepin als vielversprechenden Liganden. Dieser wirkte nicht nur als UV-sensitiver Blocker von $GABA_A$-Kanälen, sondern auch als subtypspezifischer, photoschaltbarer Modulator an Glycinrezeptoren. Vorläufige molekulare Dockings konnten diese experimentellen Befunde teilweise erklären. Außerdem wurden die ersten photochromen Liganden auch *in vivo* untersucht und dabei zeigte ein weiteres Azo-Benzodiazepin photoschaltbaren Einfluss auf die Aktivität von Zebrafischlarven.

Kapitel 4 beschreibt den Versuch der Aufreinigung von Triplex-DNA mittels eines Thiazol Orange Derivats, das mit Hilfe einer Azid-Alkin-Cycloaddition mit Biotin funktionalisiert wurde. Biologische Untersuchungen zeigten, dass die hergestellte Verbindung zwar auch wie Thiazol Orange die Eigenschaft hat Triplex-DNA gegenüber konkurrierende Oligonucleotide zu stabilisieren, jedoch insgesamt nicht mehr so affin und spezifisch an Triplex-DNA bindet. Damit konnte das funktionalisierte Thiazol Orange nicht wie weiter angedacht zur Aufreinigung von Triplex-DNA verwendet werden.

Zusammengefasst beschreibt diese Arbeit synthetische, funktionalisierte Verbindungen für biologische Anwendungen. Die erzielten Erkenntnisse sind insbesondere für die zukünftige Entwicklung von neuen molekularen Werkzeugen relevant, um zelluläre Prozesse oder neurophysiologische Prozesse in Lebewesen mit Licht zu steuern.

7 Appendix

7.1 Abbreviations

A   absorbance

Alloc   allyloxycarbonyl

APCI   atmospheric pressure chemical ionization

Ar   aryl

BZD   benzodiazepine

calcd.   calculated

Cbz   carboxybenzyl

CDI   1,1'-carbonyldiimadazole

CMC   critical micelle concentration

conc.   concentration

dba   dibenzylideneacetone

DEPT   distortionless enhancement by polarization transfer

DIPEA   *N,N*-diisopropylethylamine

DMF   *N,N*-dimethylformamide

DMSO   dimethyl sulfoxide

DNA   deoxyribonucleic acid

dsDNA   double stranded deoxyribonucleic acid

DTE   dithienylethene

ε molar extinction coefficient

EC_{50} half-maximal effective concentration

eq.   equivalent(s)

ESI   electrospray ionization

Fmoc	fluorenylmethyloxycarbonyl
GABA	γ-aminobutyric acid
$GABA_AR$	γ-aminobutyric acid A-receptor
Gly	glycine
GlyR	glycine-receptor
HDAC	histone deacetylates
HDACi	histone deacetylates inhibitor
HPLC	high performance liquid chromatography
HR-MS	high-resolution mass spectrometry
HSQC	heteronuclear single-quantum correlation
IC_{50}	half-maximal inhibitory concentration
IR	infrared spectroscopy
J	coupling constant
λ	wavelength
LAH	lithium aluminum hydride
LC-MS	liquid chromatography–mass spectrometry
LED	light-emitting diode
Lys	lysine
m.p.	melting point
max	maximum
MCPBA	meta-chloroperoxybenzoic acid
MOE	Molecular Operating Environment
MST	MicroScale Thermophoresis
n.i.	no inhibition
NBS	N-bromosuccinimide
NMR	nuclear magnetic resonance
Oxone	potassium peroxysulfate
p.a.	pro analysi

PBS	phosphate-buffered saline
PCL	photochromic ligand
Pd/C	palladium on charcoal
PDB	Protein Data Bank
PE	petroleum ether
PEG	polyethylene glycol
PSS	photostationary state
PTL	photochromic tethered ligand
PyBOP	benzotriazol-1-yl-oxytripyrrolidinophosphonium hexafluorophosphate
R_f	retention factor
ssDNA	double stranded deoxyribonucleic acid
$t_{1/2}$	half-life
TBTA	tris[(1-benzyl-1*H*-1,2,3-triazol-4-yl)methyl]amin
TFA	trifluoroacetic acid
TFO	triplex forming oligonucleotide
THF	tetrahydrofuran
TICT	twisted intramolecular charge transfer
TO	thiazole orange
t_R	retention time
tra.	*trans*
TTN	thallium trinitrate
TTS	triplex target site
UV	ultraviolet
Vis	visible
WT	wild type
XPhos	2-dicyclohexylphosphino-2',4',6'-triisopropylbiphenyl
ZMAL	(S)-[5-acetylamino-1-(4-methyl-2-oxo-2H-chromen-7-ylcarbamoyl)-pentyl]-carbamic acid benzyl ester

7.2 Curriculum Vitae

PERSONAL DATA

Name:	Daniel Wutz
Date of birth:	25.03.1988
Place of birth:	Cham
Nationality:	German

EDUCATION

11/2013 – 04/2017   **Ph. D. thesis** at the Institute of Organic Chemistry, University of Regensburg (Supervisor: Prof. Dr. B. König)
"Functionalized Photochromic Scaffolds for Biological Applications"

10/2011 – 09/2013   **Master of Science** in Chemistry, University of Regensburg
Master thesis: *"Synthesis of Photoswitchable Amino Acids Based on Dithienylmaleimides"* (Supervisor: Prof. Dr. B. König)

10/2008 – 09/2011   **Bachelor of Science** in Chemistry, University of Regensburg
Bachelor thesis: *"Synthesis of Fluorescent Receptors Towards Multivalent Recognition"* (Supervisor: Prof. Dr. B. König)

09/1998 – 06/2007   **Allgemeine Hochschulreife** (general university entrance qualification) at the Joseph-von-Fraunhofer-Gymnasium Cham

WORK AND TEACHING EXPERIENCE

11/2013 – 05/2017   **Ph.D. research/research assistant** (scientific research, training of master and bachelor students in advanced laboratory courses, supervision of internship projects)

INTERNATIONAL EXPERIENCE

06/2016 – 08/2016   **Research stay** in the group of Prof. Dr. P. Gorostiza, Institute for Bioengineering of Catalonia, Barcelona, Spain
"In vivo characterization of photochromic ligands for $GABA_A$-receptors and glycine-receptors in freely behaving tadpoles and zebrafish larvae"

02/2017	**1st International Symposium on Photopharmacology**, Groningen, the Netherlands, poster presentation
09/2016	**6th EuCheMS Chemistry Congress**, Seville, Spain, poster presentation
06/2016	**2nd MODULIGHTOR Meeting**, Barcelona, Spain, oral presentation
07/2015	**19th European Symposium on Organic Chemistry**, Lisbon, Portugal, poster presentation
09/2014	**7th Summerschool "Medicinal Chemistry"**, Regensburg, Germany, poster presentation
09/2014	**Beilstein Symposium "Molecular Switches"**, Prien am Chiemsee, Germany

PUBLICATIONS

D. Wutz, C. Falenczyk, N. Kuzmanovic and B. König, *"Functionalization of photochromic dithienylmaleimides", RSC Advances* **2015**, *5*, 18075-18086.

D. Wutz, D. Gluhacevic, A. Chakrabarti, K. Schmidtkunz, F. Erdmann, C. Romier, W. Sippl, M. Jung and B. König, *"Photochromic HDAC Inhibitors based on DTEs and Fulgimides"*, *Org. Bio. Chem.* **2017**, DOI: 10.1039/C7OB00976C.

7.3 Danksagung

- DANKE -